Greener on the Other Side: Inequity and Tax Compliance*

Michael Carlos Best   Luigi Caloi   François Gerard   Evan Plous Kresch
Joana Naritomi   Laura Zoratto

July 31, 2026

Abstract

Governments frequently use observable tags as imperfect proxies to measure tax bases or household means, leading to inequities among equally-deserving individuals. This paper studies the efficiency effects of such misclassification in the context of the property tax in Manaus, Brazil. We leverage quasi-experimental variation in inequity generated by the boundaries of geographic sectors used to compute tax liabilities, as well as by a tax reform, in a series of augmented boundary discontinuity designs. Inequity significantly reduces tax compliance. The effect is concentrated among the overtaxed, and accounts for roughly 40% of the compliance change at sector boundaries. Combining our empirical results with a simple model of presumptive property taxation shows that optimal progressivity can be considerably lower once we account for inequity responses, and that investments in improving fiscal capacity to accurately assess properties can bolster progressivity.

*Best: michael.best@columbia.edu. Columbia University, BREAD, CEPR, IFS & NBER. Caloi: luigi.caloi@columbia.edu. Columbia University. Gerard: f.gerard@ucl.ac.uk. University College London, BREAD, CEPR, & IFS. Kresch: ekresch@oberlin.edu. Oberlin College. Naritomi: J.Naritomi@lse.ac.uk. London School of Economics, BREAD, CEPR, & IFS. Zoratto: lzoratto@worldbank.org. World Bank. We are grateful to Katarzyna Bilicka, Nadja Dwenger, Bill Hoyt, Henrik Kleven, Wojciech Kopczuk, Ilyana Kuziemko, Horacio Larreguy, Ben Lockwood, Karthik Muralidharan, Victor Pouliquen, Joel Slemrod, Johannes Spinnewijn, Jonathan Weigel and numerous seminar and conference participants at Berkeley, the CEPR Public Economics Symposium, Chicago Harris, Duke, FGV-EESP, Fordham, Georgetown, IFS-STICERD, Imperial College London, INSPER, ITAM, University of Kentucky, LACDev Conference, LACEA Annual Meeting, Mannheim, Münich, the National Tax Association Conference, NBER Public Economics Meetings, Northwestern, Oxford, Princeton, PUC-Rio, SITE, UFPE, University of Copenhagen, UC Chile, Universitat Pompeu Fabra, University of Toronto, and Wharton. We are grateful to Amanda Awadey, Carlota Loran Lopez, Malavika Mani, Samira Noronha, Maggie Shi, and Thaissa Sousa for excellent research assistance. We thank Zaheer Abbas, Angela Bayarmaa, Jonathan Chan, Cali Marie Dutta, Tingjun Huang, Nicole Li, Christian Lippmann, Lizzie Melashvili, Yunfeng Wu, Dongyang Zhang, Giovanni Ramos, and Sungjin Kim for their help with the Viva Real data. We thank *Secretaria Municipal de Finanças e Tecnologia da Informação* (SEMEF), who provided access anonymized administrative data. This project was funded with UK International Development Aid from the UK government, awarded through the J-PAL Governance Initiative. This study was also funded by the World Bank. All remaining errors are ours.

1 Introduction

Measuring the tax base is one of the most basic functions of the state. It requires investments in the capacity to "read" the rich complexity of taxpayers' economic activities and reduce them to standardized measures of the size of the tax base (Scott, 1998). Doing so successfully allows the modern state to differentiate tax and transfer policy between citizens with different abilities and needs. However, welfare-relevant attributes such as earning ability are hard, if not impossible, to observe directly. Thus, governments often rely on (coarse) proxies or "tags": observable attributes correlated with individuals' unobserved types, which can facilitate the implementation of policies intended to be progressive (Akerlof, 1978).

However, relying on imperfect proxies leads to misclassification. Individuals with the same welfare-relevant types, but different levels of a government policy's proxies, may be treated differently, creating (horizontal) inequity.[1] Citizens have strong views on this type of inequity, which has been shown to influence labor supply (Card *et al.*, 2012), policy preferences (Hvidberg *et al.*, 2023), subjective well-being (Luttmer, 2005), and even political stability (Keen & Slemrod, 2021). These challenges are especially severe in low- and middle-income countries, where the availability of reliable data to differentiate between individuals is more limited.

This paper studies the efficiency effects of such misclassification and their policy implications. Misclassification may generate resentment among those treated less favorably than others with the same welfare-relevant type, causing them to reduce compliance with a policy's mandates.[2] We focus on how inequities among equally deserving taxpayers – caused by the use of coarse tags in property taxation – affect tax compliance. We argue that inequities induced by mistagging reduce tax morale (Luttmer & Singhal, 2014; Slemrod, 2019). Consistent with this, we find that they generate large decreases in voluntary compliance. These effects exist over and above the standard response of compliance to the size of the tax bill. Our results have important implications for policy design: we show that inequity responses can considerably diminish the optimal progressivity of the tax schedule, and that investments in improving fiscal capacity to accurately assess properties can bolster progressivity.

We study these issues in the context of the property tax in Manaus, the capital of the Brazilian

[1]With imperfect tags, individuals with differing welfare-relevant types, but who share the same policy-relevant attributes will be treated equally, and individuals who have the same welfare-relevance but differing levels of the policy-relevant attributes will be treated differently. Adam Smith (1776) invokes this inequity in objection to the "Window Tax," an English presumptive property tax:

> "The principal objection to all such taxes is their inequality, an inequality of the worst kind, as they must frequently fall much heavier upon the poor than upon the rich. A house of ten pounds rent in a country town may sometimes have more windows than a house of five hundred pounds rent in London; and though the inhabitant of the former is likely to be a much poorer man than that of the latter, yet so far as his contribution is regulated by the window-tax, he must contribute more to the support of the state."

[2]In principle, those treated more advantageously than intended may increase their compliance in response, but as we show in section 5.3, we see no evidence for this type of response in our setting. Similarly, Dube *et al.* (2019) show that responses to peer wages are driven by comparisons with higher-paid peers.

state of Amazonas.[3] Like many other large cities around the world, Manaus' property tax is presumptive, based on properties' observable characteristics, rather than a direct assessment of their market value. The city is divided into 62 tax sectors used *exclusively* for the purposes of property taxation.[4] Each sector is tagged with an assessed land price, a key input into the formula that determines tax liabilities.[5] Properties within the same sector are evaluated at the same land price, and the price tags jump discretely across sectors. As a result, at the sector boundaries, otherwise similar properties on the same street can face different tax liabilities.[6]

The sector boundaries therefore also generate inequity: properties on one side of a boundary would face discretely different tax liabilities if they had happened to be located on the other side. In order to measure this inequity, for each property near a boundary, we construct the ratio of its actual liability to the counterfactual liability it would face if located in the neighboring tax sector, and hence tagged with a different land price. This measure captures inequity at the household level rather than at the group level, and thus does not require the analyst to take a stand on what reference group taxpayers compare themselves to when forming opinions about the (in)equity of their taxes (as in, e.g. Card *et al.*, 2012; Dube *et al.*, 2019; Hvidberg *et al.*, 2023; Ajzenman *et al.*, 2025). We exploit these discontinuities at tax sector boundaries, as well as a 2011 reform that updated values used in the presumptive formula, as sources of quasi-experimental variation in the extent of mistagging to study tax compliance responses to inequity.[7]

We introduce our empirical analysis by documenting a large change in compliance at the tax sector boundaries prior to the 2011 reform. Using a Boundary Discontinuity Design (BDD) (Black, 1999; Bayer *et al.*, 2007), we estimate that compliance is 8% lower on the side of the boundary with the higher land-price tag. This drop in compliance on the "high-tag" side, however, combines responses to two changes: (i) tax liabilities are on average 23% higher and (ii) inequity is 62% higher. We then develop a series of augmented BDDs to isolate tax compliance responses to inequity, while holding tax liabilities constant.

We begin by exploiting cross-sectional variation in properties' *exposure* to mistagging prior to the reform. Because the inequity we study is driven by mistagging of land prices, while the presumptive tax formula depends on proxies for both land and built structure, properties with

[3]Manaus has 2.3 million residents and the 5th largest GDP among Brazil's 5,570 municipalities (IBGE, 2022).

[4]Public goods and services are not dependent on which sector a property is located in. Importantly, tax collection and enforcement of unpaid tax bills are centralized and automated, so there is no door-to-door collection by tax officials that could induce differential enforcement or bribe opportunities across tax sectors.

[5]Table A.1 shows that many large cities around the world use presumptive property tax schemes, as opposed to schemes based on market value, and that a majority of these cities use geographic sectors in their assessment formula.

[6]These differences in tax burdens are unlikely to be dampened by capitalization into house prices. Manaus has a thin property market, and our empirical analysis suggests that there are no first-order effects of changes in property taxes on house prices (see appendix P) or mobility (see appendix Q). As we discuss in the next section, the property tax is salient when taxpayers receive their bills in the first quarter of each calendar year, and decide whether to comply. However, it may not be salient during the rest of the year, including when they purchase a property. In fact, about half of listings on a major real estate website do not include the property tax value. Nonetheless, mobility and capitalization responses may be meaningful in other settings, so we also highlight their potential effects in the paper.

[7]We focus on tax compliance because it is the primary behavioral margin in our setting. Households have little influence over their property's characteristics that feed into the presumptive formula. Filing a tax appeal (as in Nathan *et al.*, 2025) is also rare: even after the major tax reform in 2011, there were only about 30 appeals per year.

relatively more land and less built structure are more exposed to this source of inequity. This remains true even conditional on a property's tax liability, allowing us to hold tax liabilities fixed and compare discontinuities in compliance at tax sector boundaries across properties with differing levels of exposure. We show that such a *Difference* in Boundary Discontinuities Design (DBDD) identifies the elasticity of compliance with respect to inequity under the assumption that any selection into the high- versus low-tag side of the boundary is uncorrelated with exposure to inequity.[8] Using this empirical strategy, we obtain an elasticity around 0.26. Reassuringly, we find that these effects are concentrated among taxpayers for whom this source of inequity is more salient: those whose neighbors across the tax sector border are most similar to them.

While we present a placebo test supporting its plausibility, the key identification assumption of our DBDD remains arguably strong. Indeed, it requires comparing properties that are observably different, raising the possibility that they also differ in unobserved determinants of tax compliance in ways that are correlated with the inequity that they face.[9] In a second empirical strategy, we incorporate the 2011 reform of the property tax system to hold all time-invariant (unobserved) determinants of compliance fixed. The reform substantially changed the tax sectors' assessed land prices and other parameters of the presumptive tax formula, while keeping the map of the tax sectors fixed. As a result, households experienced large changes in their actual tax liabilities (the average tax bill roughly doubled), as well as in their counterfactual liabilities had they lived in the neighboring tax sector, and hence in the degree of inequity they face. We show how combining this reform with the previous approach identifies inequity effects by relating *changes* in compliance to *changes* in inequity, while controlling for changes in tax liabilities, holding fixed all time-invariant determinants of tax compliance, and allowing for different trends on the high- and low-tag sides of the boundary. This *dynamic* DBDD delivers our preferred estimates of the elasticity of compliance with respect to inequity, around 0.11.

In the final part of our empirical analysis, we use the 2011 reform to identify the impact of changes in inequity separately for the overtagged properties on the high-tag side of the sector boundaries and for the undertagged properties on the low-tag side. To do so, we invoke a "strong parallel trends" assumption (Callaway *et al.*, 2024) — requiring changes in potential compliance over time to be orthogonal to changes in inequity induced by the reform — for each side of the boundaries.[10] Standard pre-trend tests support the plausibility of these assumptions. We then show that the compliance responses to the changes in inequity after the 2011 reform are driven exclusively by households resenting being overtaxed on the high-tag side of the boundaries. We are unable to reject a null effect of changes in undertagging on the low-tag side.

In sum, our empirical analysis highlights that inequity responses can be an important driver of tax compliance decisions. To put magnitudes in perspective, we show that our preferred

[8]The formal derivation builds heavily on the methods developed by Frölich & Huber (2019) and Dong *et al.* (2023).

[9]For example, if properties on either side of the tax boundary share the same tax liability, the properties on the high-tag side must be smaller, and the extent to which they are smaller is in fact correlated with exposure.

[10]Our regressions include year-specific controls for properties' distance to the boundary and change in tax liability due to the reform.

estimate of the elasticity of compliance with respect to inequity implies that inequity responses can account for about 40% of the overall change in compliance at the tax sector boundaries.

To draw out the policy implications of our findings, we develop a stylized model of the optimal design of a presumptive property tax. Properties are of two types (market values), but the government only observes a *tag* that proxies for true types and uses these tags as the basis for the presumptive tax. Taxpayers, however, know their property type and, when they receive the incorrect tag this creates inequity. Households decide whether to pay the presumptive tax, trading off lower consumption and higher disutility from inequity if they pay against an idiosyncratic cost of delinquency — capturing both pecuniary and non-pecuniary costs — if they don't. We derive sufficient-statistics expressions for the optimal tax schedule and show that mistagging affects it through three channels. First, it alters the composition of taxpayers paying each tax: some taxpayers paying the high-tag tax have low-type houses. Second, compliance responses to inequity generate a novel source of efficiency costs of raising revenue. Third, mistagging raises the marginal utility of consumption of overtagged households, aggravating the welfare costs of taxation. Thus, greater mistagging and higher inequity responses push towards less differentiation between the taxes levied on low- and high-tag properties, while higher responses to the size of the tax liability actually push towards greater differentiation in our model.

A simple calibration of the model using our empirical results suggests that the strength of behavioral responses to inequity can have a considerable impact on the optimal tax schedule: it is roughly 40% less progressive than it would be if compliance responses were driven solely by the size of the tax liability. Our findings also imply that there could be large returns to investments in the capacity of the state to differentiate properties of different values more accurately. We explore the potential for data on property listings, now widely available on the internet, to undergird this additional capacity. Back-of-the-envelope calculations suggest that using available data on property asking prices to recalibrate Manaus' existing presumptive tax formula can yield a 20% reduction in mistagging and hence allow 8% more progressivity. Using standard machine-learning tools to predict properties' asking values — without being tied to the existing presumptive formula — and incorporating property attributes available in online property listings can further reduce mistagging by as much as 74%, allowing for 28% greater progressivity.

Our paper contributes to four strands of literature. First, we contribute to the literature on presumptive taxation and tagging in public finance. Akerlof (1978) and Nichols & Zeckhauser (1982) made seminal contributions showing how tagging can relax the incentive-compatibility constraints faced by redistributive policies. Despite these theoretical arguments, Mankiw & Weinzierl (2010) argue that tagging is not as prevalent a feature of real-world policy as one might expect, possibly due to equity considerations (Saez & Stantcheva, 2016). Subsequent work incorporates moral hazard into the tagging framework (Besley & Coate, 1992; Gaubert *et al.*, 2021). We explore an additional channel: efficiency effects of inequity from imperfect tagging.

Second, we contribute to the literature on fairness and tax compliance, and tax morale. Recent contributions include Cruces *et al.* (2013); Giaccobasso *et al.* (2025); Kuziemko *et al.* (2015);

Hvidberg *et al.* (2023); Knebelmann *et al.* (2026). In the context of property taxes, Cabral & Hoxby (2012) show that the more salient property taxes are, the lower governments set rates and limits. Nathan *et al.* (2026, 2025) study property tax appeals in Texas, showing experimentally that hassle costs and perceptions of the property tax system's fairness affect appeal behavior. In a related paper, Ajzenman *et al.* (2025) study the impacts of a different type of inequity. Through an information experiment, they study the effects of inequity that comes from the fact that taxpayers may care directly about how the tax system treats property types distinct from their own. By contrast, we study inequity that arises from the fact that the system features misclassification: it creates arbitrary differences in tax burdens between taxpayers with the same type. We contribute quasi-experimental estimates of the impact of inequity on compliance behavior and draw out the implications for policy design. Naturally, the two are highly complementary.

Third, we contribute to a growing literature on property taxation in low- and middle-income countries (Castro & Scartascini, 2015; Del Carpio, 2016; Weigel, 2020; Balan *et al.*, 2022; Okunogbe, 2023; Bergeron *et al.*, 2024a; Dzansi *et al.*, 2024; Bergeron *et al.*, 2024b; Kapon *et al.*, 2024). Brockmeyer *et al.* (2023) provide evidence on the impact of enforcement activities and tax rates on compliance with Mexico City's property tax, and explore the implications for how policy should trade off between the two instruments in the presence of liquidity constraints. Building on their work, we study a distinct channel: inequity, and draw out its implications for optimal policy.

Fourth, we contribute to the literature using boundary discontinuity designs to study public policy. Foundational contributions in this literature include Black (1999) and Bayer *et al.* (2007). More recent work has used augmented boundary discontinuity designs to study the valuation of local jurisdictions (Schönholzer, 2023) and the impacts of wealth taxation on saving (Ring, 2024). We show how the boundary discontinuity design can be augmented to incorporate cross-sectional differences in the intensity of treatment and changes in treatment over time.

Our paper proceeds as follows. Section 2 presents the context we study, the data we use, and how we use it to measure inequity. Section 3 lays out our presumptive property tax model, showing conceptually how mistagging and inequity affect the optimal tax schedule. Section 4 presents our Boundary Discontinuity Design (BDD) at the boundaries of Manaus' tax sectors and the identification strategies we develop to isolate the causal effects of inequity on tax compliance. Section 5 reports our empirical findings and Section 6 incorporates them into our model to highlight their potential implications for tax policy design. Section 7 concludes.

2 Context & Data

2.1 Property Tax (IPTU) in Manaus

The property tax (IPTU: *Imposto Predial e Territorial Urbano*) is one of the two main tax instruments assessed by municipal governments in Brazil.[11] Manaus' tax authority (SEMEF; *Secretaria*

[11] The other being the *Imposto Sobre Serviços* (ISS), a tax on services.

Municipal de Finanças e Tecnologia da Informação) informs households of their liability by letter in mid-January each year. Taxpayers can choose between making a single payment or paying their tax bill in installments and can do so either online or in person by visiting SEMEF's offices or an affiliated bank.[12] Failure to pay their property tax bill results in fines, interest, and ultimately, legal recourse. Fines and interest are automatically imposed, with no discretion by SEMEF to target penalties or enforcement on particular households.[13]

Unlike local governments in the United States, Manaus employs a presumptive formula to calculate property tax liabilities. In fact, most of the world's urban residents live in cities using presumptive property taxes. For instance, Table A.1 compares Manaus' property tax to those of 40 of the world's largest cities; 22 of the 38 cities with a property tax have presumptive systems.

Manaus' statutory property tax rate—the property tax liability as a percentage of a property's assessed value—is 0.9% (see, Lei No 1.628/2011, article 2).[14] However, the average *effective* property tax rate as a fraction of asking prices is 0.46%.[15] Using the 2010 census, we estimate that the average residential property tax bill in Manaus represents roughly 2.6% of annual household income.[16] This property tax burden as a share of annual income is similar to property taxes in the United States, which range from 1.5% to 5%, and is nearly identical to the burden faced by residents of California.[17] The estimated effective tax rate places Manaus among the lowest effective rates in the United States, which range from 0.4% to 3% (Twait & Langley, 2024).

The tax liability for residential property i in year y, T_{iy}, is calculated as follows:

$$T_{iy} = \alpha_y \left[b_{iy} + p_{s(i)} a_{iy} \right] = \alpha_y \left[f_{by}(\mathbf{B}_{iy}) + p_{s(i)} f_{ay}(\mathbf{A}_{iy}) \right] \tag{1}$$

where the property's assessed value (*valor venal*) is multiplied by the statutory tax rate (α_y; *aliquota*) according to a schedule based on the type of property (0.9% for residential properties). The property's assessed value is the sum of the assessed value of the built structure (b_{iy}; *valor da edificação*) and the assessed value of the land (*valor do terreno*), which is itself the product of an adjusted land area a_{iy} and a sector-specific price per unit of land $p_{s(i)}$ to account for differences in property values across the city. The values a_{iy} and b_{iy} are based on easily observable characteristics of the land ($\mathbf{A}_{iy}$) and built structure ($\mathbf{B}_{iy}$), such as the type of construction and the materials (see Table A.2 for details on the formula).

[12]Contrary to other developing countries, there is no face to face interaction between the taxpayer and a tax collection agent. Payment collection is centralized and automated (e.g. SEMEF lists payment location options on its website `https://semefatende.manaus.am.gov.br/inventario.php?id=3663`)

[13]See `https://www.manaus.am.gov.br/pgm/divida-ativa-servico/`. A detailed discussion on enforcement and an empirical test examining differential enforcement across boundaries is provided in Appendix O.

[14]The 0.9% rate is applicable for all residential properties in the city. Other types of property are evaluated with a different rate (for example, 3% for non-residential real estate with built area less than one-ninth the total land area).

[15]In appendix P, we present a dataset of asking prices scraped from Viva Real, a Brazilian real estate platform, and matched to our cadaster, from which we draw this statistic. Nearly 43% of the scraped listings include the IPTU.

[16]This figure is calculated using the average household income in Manaus from the 2010 census tracts. Note that this figure is likely to be an upper bound, as we are likely underestimating household income.

[17]See `https://usafacts.org/articles/where-do-people-pay-the-most-and-least-in-property-taxes/`

Figure 1 displays a map of Manaus' 62 tax sectors, $s(i)$.[18] Crucially for our identification, they are not used for other policy or administrative purposes, and only a few of the sector boundaries overlap with neighborhood boundaries (see Figure A.1). The use of geography is ubiquitous in presumptive property taxes around the world. For instance, 16 of the 22 cities with a presumptive system in Table A.1 use geography as an input to the tax formula, and Manaus is not unique in having tax sectors that do not align with municipal administrative divisions. All properties within a sector are assigned the same square meter value, which was initially set in 1983 when the tax authority first created the tax sectors, based roughly on estimated property valuations at the time. Despite the rapid growth of the city, the boundaries of these sectors have not changed and the prices $p_{s(i)}$ remained unchanged for almost 30 years until the reform described in section 2.2, leading to arbitrary changes in square-meter values for very similar neighboring properties separated by a tax sector boundary (see Figure 2).

The IPTU becomes very salient to households at the time they make payment decisions. Like all property taxes, it is a direct tax on households that makes it inherently more salient to taxpayers (Cabral & Hoxby, 2012). Google search activity in Manaus show a cyclical interest in the IPTU, which peaks in January just after residents first receive their property tax bills and around the March/April deadline to make the first payment (see appendix A, figure A.5). This is in stark contrast to the other main municipal tax, which is an indirect tax on services (ISS), and has virtually no search activity (despite it being levied on many more transactions). Moreover, articles related to the IPTU appear frequently in the local newspaper, including an annual announcement in January outlining how and when residents can pay their bills.[19]

2.2 2011 Tax Reform

Manaus passed a major reform to its property tax system in 2011 (Law 1.628/2011), which came into force in 2012, updating the parameters used to estimate land and building values. An inability to revise the square meter values $p_{s(i)}$ and the value of the parameters for a_{iy} and b_{iy} — all set to target higher-value properties in 1983 — had led to a deterioration in the usefulness of these tags and severe inequities. The sector-specific prices were particularly outdated, as the socioeconomic geography of the city shifted dramatically over time.[20] For instance, Figure B.3a shows that, although households in wealthier census tracts still had larger tax bills in 2010, the slope of this relationship flattened considerably between 2000 and 2010.

The reform raised tax liabilities for almost every property, with the average property experiencing a doubling of its property tax, and striking heterogeneity in the size of the tax increase across properties (see Figure B.2). Given the large increases, the reform was phased in between

[18]While SEMEF plotted 65 tax sectors, the three northern and westernmost sectors are *Zona de Transição* - comprised of rain forest with virtually no buildings - and are thus excluded from our analysis.

[19]For example, the 2014 announcement in the Diário do Amazonas found here.

[20]The 1983 population was only 38 percent of the 2011 population, and Manaus' remarkable growth created new housing developments in previously uninhabited forest (see Figure B.1). These areas were assigned their 1983 sector and square-meter value, resulting in areas where the formula dramatically failed to capture market values of land.

2012 and 2016; each year, 20% of the additional amount was added to the tax bill.[21]

The 2012 property tax system was still based on presumptive estimates, and thus did not eliminate the potential for mistagging, especially for otherwise identical households on sector boundaries, which we use as our main source of identification throughout the rest of the paper. However, it was considered more fair by the municipal government as the improvement in targeting resulted in assessed property values more aligned with contemporaneous property values than those based on the 1983 parameters.[22] For instance, Figure B.3b illustrates this improvement in targeting: not only did the reform increase the average property tax bill across census tracts, it also led to a larger change in tax bills for richer households.

2.3 Data

Through a collaboration with SEMEF, we have access to de-identified cadaster information for 613,131 properties that includes a snapshot of the building characteristics, lot size and land characteristics in 2018. This data is geo-referenced and matched to the road network of the city. We also have GIS maps for all relevant boundaries (tax sector, neighborhood, city block, parcel), which we use to measure a household's distance to a tax sector boundary, and hence to the discontinuity in the square-meter value. We also have data on property tax liabilities and payments from 2004–2019 for the universe of taxpayers, including fines and legal follow-up due to delinquency. We thus directly observe both the household's tax liability in a given year and whether a given property was compliant with its tax payments. Finally, we have data on property transfers and sales from the property transfer tax system (ITBI; *Imposto sobre transmissão de bens imóveis*).

Our main outcome when studying the behavioral response to mistagging is compliance,[23] which we define as the share of a household's liability paid within 18 months of receiving their bill.[24] Figure A.3 shows that compliance is relatively low in Manaus, around 65%, and stable over time. It also shows that compliance is driven primarily by the extensive margin: most households either pay their tax bill in full or not at all. Compared to other large Brazilian cities, the compliance rate is lower in Manaus than in richer cities like São Paulo, but it is comparable to poorer cities like Salvador (see Figure A.4). The 65% compliance rate in Manaus is nearly identical to that in Mexico City (Brockmeyer *et al.*, 2024) and Montevideo (Dunning *et al.*, 2017), and much higher than the 12% rate in Kananga (Weigel, 2020) and Accra (Jensen *et al.*, 2026).

[21] This phase-in was meant to avoid backlash from the sharp increases in the property tax bill. An earlier attempt to update the parameters of the property tax system in 2006 failed and was never implemented.

[22] The online portal of one of the main Brazilian newspaper *O Globo (G1)* highlighted that the updated property value estimates were more fair given how outdated the 1983 values were (link to article).

[23] Since a household's tax bill is mechanically determined by its characteristics in the cadaster, there is no self-declaration of the tax base. Thus, we study the compliance response of households *after* receiving their bill, and not the moral hazard response of households attempting to change their "tags." There is a mechanism for households to petition SEMEF to update the cadaster, but this is almost never used. SEMEF can also update the cadaster (and did so in 2011), but this is generally done city-wide and so it is exogenous from the households' point of view.

[24] In Appendix L we repeat the main exercises using alternative definitions of compliance and find the same results.

2.4 Boundary Sample

Our empirical analysis exploits the discontinuous changes in square-meter rates across the tax sector boundaries. We thus restrict our sample of interest to properties close to a tax sector boundary. Concretely, we use a cutoff distance of 300 meters, measured as the closest point of a given lot to the boundary line, where properties on the boundary are defined as having a distance of zero (see Appendix C for more details on the construction of the distance measure).

Our analysis sample further excludes properties that are exempt from property taxes, as well as lots that are vacant or not designated as residential. For our cross-sectional analysis, we also exclude properties on sector boundaries that overlap with neighborhood (*"bairro"*) boundaries since these boundaries may be perceived as relevant for other purposes, even if nothing about the provision of public goods or the enforcement of taxes varies by neighborhood. For the tax reform analysis, we do not exclude these properties since our design is able to hold fixed any changes at the boundaries that don't change over time, such as differences between neighborhoods. After these adjustments, our cross-sectional and tax reform analyses center on 25,097 and 53,685 properties, respectively, resulting in 382,229 and 825,853 property-year observations from 2004 to 2018. Appendix K provides more details on the sample selection process.

2.5 Measuring Inequity

The inequity that we study arises from the discrepancy between properties' assessed property values and their market values. While the property tax formula described in section 2.1 is complex, it is only a rough proxy for market values.[25] Misspecification of any of the components of the formula creates misclassification of properties and hence potential inequity. However, this misclassification varies sharply at the boundaries of the tax sectors, and so we focus on a measure of inequity based on the jumps in tax liabilities at the tax sector boundaries.

For a given property i, we identify the nearest neighboring tax sector $\hat{s}(i)$ and label households as being on the "high-tag" side of the boundary if $p_{s(i)}$ is higher than $p_{\hat{s}(i)}$. We then define our inequity measure as $\sigma_{iy} = \frac{T_{iy}}{\hat{T}_{iy}}$, where the counterfactual tax liability $\hat{T}_{iy} := \alpha \left[b_{iy} + p_{\hat{s}(i)} a_{iy}\right]$ is the tax liability property i would have received had it been located on the other side of the tax sector boundary, with all other land (a_{iy}) and building (b_{iy}) characteristics held fixed.

Defining inequity in this way has two key advantages. First, since we are computing the counterfactual tax bill using the household's own characteristics, we are able to construct our measure of inequity for every property in our data at the individual property level. Second, our measure is based only on how the taxpayer is treated relative to how they would have been treated had they lived in their neighboring tax sector, allowing us to be agnostic about what peer group(s) taxpayers compare themselves to in forming their opinions about inequity. This is in contrast to papers that define the peer group needed for comparisons of inequity (Dube *et al.*,

[25]Figure P.2 presents a scatter plot comparing properties' log tax liabilities to their log asking prices. While they are correlated, the R^2 is only 0.20, demonstrating that assessed values only roughly approximate true market values.

2019; Card *et al.*, 2012; Hvidberg *et al.*, 2023; Ajzenman *et al.*, 2025).[26] Our measure of inequity is therefore a "selfish" measure, capturing whether households feel that *they* have been treated unfairly by the system, not whether they care about whether *other* people are treated fairly.[27] We further investigate the salience of our inequity measure in appendix M.

Capitalization of property taxes into house prices may dampen the inequity felt by taxpayers when making tax compliance decisions if they paid lower prices for higher-tax properties. However, such capitalization is unlikely to be a meaningful factor in our context. First, Manaus' property market is relatively thin. Using data from the property transfer tax system, we estimate that only around 1.4% of properties are sold each year, compared to around 3.1–5.6% in U.S. cities and 4% in the UK.[28] Second, as described in appendix P, we gathered data from a large online property listing platform, and linked it to the property tax cadaster. With this data we run both hedonic regressions and a version of our boundary discontinuity design, neither of which show evidence of any meaningful capitalization of the IPTU into asking prices, consistent with null findings in other, more developed, real-estate markets (Nielsson *et al.*, 2024). Indeed only 43% of listings include the property's IPTU liability. In section 3.3.2, we extend our conceptual framework to clarify how house price capitalization affects the optimal policy design.

3 Conceptual Framework

This section presents a simple model of the welfare effects of property taxation. There is a mass 1 of each of two *types* of houses: $\theta \in \{H, L\}$. These houses generate flows of housing consumption $y_H > y_L$. Actual house types θ are not observable to the government. Instead, the government observes a *tag* ϕ: either h or l for each house. When houses are correctly tagged, the H-type houses receive the tag $\phi = \phi(H) = h$ and the L-type houses receive the tag $\phi = \phi(L) = l$. However, when a house receives the incorrect tag ($\phi \neq \phi(\theta)$) this generates inequity. We model this inequity as $\sigma_{\theta\phi} = T_\phi / T_{\phi(\theta)}$. Whenever $\sigma_{\theta\phi} > 1$ the house is said to be *overtagged*, while if $\sigma_{\theta\phi} < 1$ the house is *undertagged*. Households have a distaste for paying an inequitable tax $d(\sigma_{\theta\phi})$.[29] We assume that when they are correctly tagged they have no distaste for inequity:

[26] As we show in appendix D, our inequity measure also varies substantially in our sample. There is significant variation in σ across the city (see Figure D.1), implying that households respond to a markedly different counterfactual of what their property tax bill would have been if taxed on the other side of the sector boundary. Moreover, the counterfactual and true tax liabilities are not collinear (see Figure D.2), so we can estimate the behavioral response to inequity (σ_{iy}) while holding households' tax liabilities (T_{iy}) fixed.

[27] This can be seen in residents' posts on social media complaining about their increase in property tax bill relative to their neighbors (see Figure D.3), and the government's response that highlights how the IPTU is calculated and how the 2011 reform was implemented (see Figure D.4).

[28] Statistics for the United States are calculated by taking the ratio of existing home sales to the number of housing units nationally. The numbers for the whole country are similar to the estimated 3.2–6.5% of residential homes for sale annually in the Chicago metropolitan area (Institute for Housing Studies).

[29] As discussed in section 2.5, the notion of inequity that we focus on here is one that focuses on the taxpayer's own "selfish" experience of the amount they are asked to pay relative to what they consider equitable, not on broader notions of equity that include judgements of whether other taxpayers' liabilities are equitable.

$d(1) = 0$ and that $d(\cdot)$ is continuous and weakly monotonic in $\sigma_{\theta\phi}$.[30]

Households decide whether to pay their property tax T_ϕ. If they pay, this reduces their consumption and they bear the disutility of inequity. If they don't pay, they face an idiosyncratic cost of being a tax delinquent γ with distribution in the population $F(\gamma)$.[31] A household will pay taxes whenever their cost of delinquency is high enough:

$$u_{\theta\phi}^{\text{pay}} > u_{\theta}^{\text{evade}} \leftrightarrow u(y_\theta - T_\phi) - d(\sigma_{\theta\phi}) > u(y_\theta) - \gamma \leftrightarrow \gamma > u(y_\theta) - u(y_\theta - T_\phi) + d(\sigma_{\theta\phi}) = \gamma_{\theta\phi}^{\star}$$

and as a result, compliance among households of type θ with tag ϕ is $c_{\theta\phi} = 1 - F\left(\gamma_{\theta\phi}^{\star}\right)$.

For simplicity, we will start by assuming that there is only overtagging: all H-type houses are correctly tagged with $\phi = h$, but a fraction ψ of the L-type houses are incorrectly given the $\phi = h$ tag. In section 3.3.1 and appendix G we present an extension that incorporates undertagging.

Tax revenue $r = \psi c_{Lh} T_h + (1-\psi) c_{Ll} T_l + c_{Hh} T_h$ is used to finance the provision of local public goods with social benefits of $B(r)$ and marginal benefits $b(r)$. Social welfare combines the welfare of a unit mass of each type of household and the benefits of the public good:

$$W = \psi \omega_L V_{Lh} + (1-\psi)\omega_L V_{Ll} + \omega_H V_{Hh} + B(r)$$

where ω_θ are Pareto weights on the welfare of the two types of households, and

$$V_{\theta\phi} = \int_{-\infty}^{\gamma_{\theta\phi}^{\star}} \left[u(y_\theta) - \gamma\right] dF(\gamma) + \int_{\gamma_{\theta\phi}^{\star}}^{\infty} \left[u(y_\theta - T_\phi) - d(\sigma_{\theta\phi})\right] dF(\gamma)$$

is the private welfare of θ-type houses with the ϕ tag.

3.1 Benchmark: Perfect Tagging, No Inequity

First, consider the case in which tagging is perfect ($\psi = 0$ and $\phi = \phi(\theta)$ for all houses). In this case, there is no inequity, so households' compliance behavior is driven only by the level of taxation they face. Changes in compliance in response to marginal changes in taxes generate fiscal externalities, so that the increase in tax revenue from marginal increases in the l-tag tax is $dr/dT_l = c_{Ll}(1-\varepsilon)$, where $\varepsilon \equiv -\frac{\partial c}{\partial T}\frac{T}{c} \geq 0$ is the elasticity of compliance with respect to the tax liability. Analogously, the effect of a marginal increase in the h-tag tax is $dr/dT_h = c_{Hh}(1-\varepsilon)$.

The optimal property tax trades off the benefits of additional revenue for public goods against the costs of reducing private welfare as characterized in the following proposition:

[30] Households may have different distaste for inequity depending on whether they are undertagged ($\sigma_{\theta\phi} < 1$) or overtagged ($\sigma_{\theta\phi} > 1$), analogously to Dube *et al.* (2019). For example, we might use a piecewise linear function $d(\sigma_{\theta\phi}) = (\sigma_{\theta\phi} - 1)(d_1 + (\delta - d_1)\mathbf{1}[\sigma_{\theta\phi} > 1])$ where $\delta > d_1 \geq 0$.

[31] This cost can represent a variety of sources of tax morale, including trust in the state, distaste for the government, expected penalties, or the real costs of justifying failure to pay taxes (Luttmer & Singhal, 2014; Slemrod, 2019).

Proposition 1 (Property Taxes Under Perfect Tagging)**.** *The optimal property tax schedule satisfies*

$$\frac{T_l}{y_L} = \frac{1-\varepsilon-g_L}{\rho g_L} \qquad \frac{T_h}{y_H} = \frac{1-\varepsilon-g_H}{\rho g_H} \tag{2}$$

where $g_\theta = \omega_\theta u'(y_\theta)/b(r)$ is the generalized social marginal welfare weight of type θ (Saez & Stantcheva, 2016) and $\rho \equiv -u''(y)\,y/u'(y)$ is the coefficient of relative risk aversion.

The optimal level of taxation is lower the stronger are behavioral responses to the tax liability: $\partial T_\phi/\partial\varepsilon < 0$. Moreover, the optimal property tax' progressivity $\frac{T_h}{y_H}/\frac{T_l}{y_L}$ is higher the stronger society's preference for redistribution g_L/g_H, and the larger the elasticity of compliance with respect to the tax liability ε.

Proof. See appendix E ☐

These expressions relate taxes to the parameters in intuitive ways. The larger are the utility costs of reducing consumption (governed by the g_θ and the curvature of utility ρ), the lower are taxes; the larger are the behavioral responses and the corresponding fiscal externalities (governed by the elasticity of compliance ε) the lower are taxes. Perhaps less obviously, in this model, the progressivity of the tax is steeper the stronger are behavioral responses. While both taxes are decreasing in ε, the proportional decrease in T_l/y_L is larger, leading to higher progressivity.[32]

3.2 Imperfect Tagging and Inequity Aversion

We now consider a model that also features the key force we seek to study: households are mistagged ($\psi > 0$) and they have a distaste for the resulting inequity ($d(\sigma)$). This creates a third group of households: L-type houses incorrectly tagged with the h tag. These Lh households experience first-order welfare losses from both a higher tax liability and inequity $\sigma_{Lh} > 1$. Moreover, their compliance decisions depend not only on their tax liability T_h but also on the inequity they face $\sigma = T_h/T_l$. This creates a new source of fiscal externalities governed by the strength of the elasticity of compliance with respect to inequity $\eta \equiv -\frac{\partial c}{\partial \sigma}\frac{\sigma}{c} \geq 0$. As a result, the elasticity of compliance by Lh households with respect to the h tax is $\frac{dc_{Lh}}{dT_h}\frac{T_h}{c_{Lh}} = -\varepsilon - \eta \leq 0$ and with respect to the l tax (which they do not face but which affects inequity) is $\frac{dc_{Lh}}{dT_l}\frac{T_l}{c_{Lh}} = \eta \geq 0$.[33]

The following proposition characterizes the optimal tax schedule and how the presence of mistagging and inequity aversion affect the optimal policy:

Proposition 2 (Property Taxes with Imperfect Tagging and Inequity Aversion)**.** *The optimal property tax schedule satisfies*

$$\frac{T_l}{y_L} = \frac{1-\varepsilon-g_L+\varphi_l\frac{\eta}{\varepsilon}\sigma\left(g_L+\varepsilon\right)}{\rho g_L\left(1-\varphi_l\frac{\eta}{\varepsilon}\sigma^2\right)} \qquad \frac{T_h}{y_H} = \frac{1-\varepsilon-\bar{g}_h-\varphi_h\frac{\eta}{\varepsilon}\left(g_L+\varepsilon\right)}{\rho\left[\bar{g}_h+\varphi_h g_L\left(\frac{y_H}{y_L}\left(1+\frac{\eta}{\varepsilon}\right)-1\right)\right]} \tag{3}$$

[32] Similarly, in the classic many-person Ramsey rule (Feldstein, 1972; Diamond, 1975), the sensitivity of commodity tax rates to the covariance between consumption of the good and social marginal welfare weights is stronger when the price elasticity of demand is larger.

[33] To see these, note that $\frac{dc_{Lh}}{dT_h}\frac{T_h}{c_{Lh}} = \left(\frac{\partial c_{Lh}}{\partial T_h} + \frac{\partial c_{Lh}}{\partial \sigma}\frac{\partial \sigma}{\partial T_h}\right)\frac{T_h}{c_{Lh}} = \frac{\partial c_{Lh}}{\partial T_h}\frac{T_h}{c_{Lh}} + \frac{\partial c_{Lh}}{\partial \sigma}\frac{\sigma}{c_{Lh}}\frac{\partial \sigma}{\partial T_h}\frac{T_h}{\sigma} = -\varepsilon-\eta$ and, analogously, that $\frac{dc_{Lh}}{dT_l}\frac{T_l}{c_{Lh}} = \frac{\partial c_{Lh}}{\partial \sigma}\frac{\sigma}{c_{Lh}}\frac{\partial \sigma}{\partial T_l}\frac{T_l}{\sigma} = \eta$.

where $\sigma = \sigma_{Lh} = T_h/T_l$; $\varphi_l = \psi c_{Lh}/(1-\psi)c_{Ll}$ is the number of mistagged L taxpayers relative to the number of l-tag taxpayers; $\varphi_h = \psi c_{Lh}/\left(\psi c_{Lh} + c_{Hh}\right)$ is the number of mistagged L taxpayers relative to the number of h-tag taxpayers, and $\bar{g}_h = \varphi_h g_L + \left(1-\varphi_h\right) g_H$ is the average social marginal welfare weight of h-tag taxpayers.

Relative to the benchmark of perfect tagging, imperfect tagging reduces optimal property tax revenues and the progressivity of the optimal tax schedule. In particular, revenues are decreasing in the extent of mistagging ψ; the elasticity of compliance with respect to inequity η; and the elasticity of compliance with respect to the tax liability ε. Progressivity $\frac{T_h}{y_H}/\frac{T_l}{y_L}$ is decreasing in ψ and η; and increasing in ε.

Proof. See appendix F □

Comparing the optimal tax schedules in equations (2) and (3), imperfect tagging and inequity aversion adds three new effects. First, a fraction φ_h of the households paying the h tax are not H-types (T_h's intended targets) but rather mistagged L-types. This raises the average social marginal welfare weight of the h-taxpayers from g_H to $\bar{g}_h$, lowering T_h and making the tax schedule less progressive. Second, inequity aversion $d(\sigma)$ reduces the utility of mistagged taxpayers, increases the fiscal externality of compliance responses to T_h, and decreases that of compliance responses to T_l. The $\varphi_\phi \frac{\eta}{\varepsilon}$ terms in the numerators in equation (3) account for these effects, which increase T_l and reduce T_h. Third, mistagged L households pay a higher tax than their correctly tagged counterparts, raising the marginal utility at which their consumption losses are evaluated. The φ_ϕ terms in the denominators in equation (3) account for these effects, which also increase T_l and reduce T_h. All three effects make the tax system less progressive.

Proposition 2 shows the intuitive effects of mistagging and inequity aversion η on optimal policy. It also shows that these effects can have opposite implications for progressivity than responses to the level of the tax liability ε. In practice, empirical estimates of behavioral responses to taxes may reflect a mixture of these two channels, complicating the mapping from estimated responses to policy implications. In section 4.1, we show how this affects the interpretation of estimates from a standard boundary discontinuity design. In sections 4.2 and 4.3, we then show how we can identify and estimate the response to inequity η we are interested in. Section 6 then uses our estimates to calibrate our model and provide quantitative insights into the implications of mistagging for policy design. Before turning to the empirics, however, we present some model extensions to highlight the robustness of the qualitative conclusions in proposition 2.

3.3 Extensions

3.3.1 Mistagging of Both House Types

Appendix G presents an extension to the baseline model in which both L- and H-type houses can be mistagged. It incorporates two changes to the baseline model. First, a fraction $\psi_{Hl} \geq 0$ of H-type houses is undertagged with the l tag. Second, the elasticity of compliance with respect to inequity of the undertagged, η_{Hl}, need not equal the elasticity of the overtagged, η_{Lh}.

The three effects of mistagging on the optimal tax schedule with only overtagged households in proposition 2 are now also present for undertagging. First, a share of the households with the l tag are undertagged H-types, and a larger share of the households with the h tag are overtagged L-types. This lowers the average social marginal welfare weight of the l-taxpayers, raising T_l, and raises the average social marginal welfare weight of the h-taxpayers, lowering T_h. Second, inequity makes undertagged households better off ($d(\sigma) \leq 0$). Therefore, increases in inequity from higher T_h dampen their compliance responses, reducing fiscal externalities from T_h, and reductions in inequity from increasing T_l raises the fiscal externality of their compliance responses. Third, undertagged H households pay lower taxes than their correctly tagged counterparts, lowering the marginal utility at which their consumption losses are evaluated.

While the first effect of undertagging reinforces the effects of overtagging, further pushing towards less progressivity, the other two forces of undertagging can counteract those. However, for reasonable parameter values, the effects of undertagging are smaller than the effects of overtagging, so that the overall effect of mistagging is still to lower progressivity. Moreover, our empirical evidence in section 5.3 suggests that the elasticity of compliance with respect to undertagging, η_{Hl} is zero, in which case the net effect is unambiguously towards less progressivity.

3.3.2 Location Choice and House-Price Capitalization

Appendix H presents an extension to the baseline model in which inequity in property taxes can be capitalized into house prices. Specifically, L-type households can choose to live in L-type houses located in areas with l and h tags. For simplicity, we assume that the H-type households all live in houses with h tags, so that there is again only overtagging in this model.

Households take house prices $p_{L\phi}$ for L-type houses taxed at T_ϕ as given and choose where to live, anticipating their tax compliance decision. Prices adjust to equilibrate housing demand and an exogenous supply of houses in each location. The disutility from inequity now reflects only the portion of inequity that is not capitalized into prices, $d(\tilde{\sigma})$ where $\tilde{\sigma} = (T_h + p_{Lh} - p_{Ll})/T_l$. In the extreme, when tax differences are fully capitalized, households no longer experience inequity ($\tilde{\sigma} = 1$) and the impacts of mistagging on optimal policy disappear. As is common in spatial models (Redding & Rossi-Hansberg, 2017), however, households can have idiosyncratic preferences for locations ξ_ϕ. Heterogeneity of these tastes ($\mathsf{Var}(\xi_\phi) > 0$) leads to incomplete capitalization, so that mistagging still generates inequity and shapes optimal policy.

Marginal changes in property taxes now also affect households' location decision. By the envelope theorem, this has no first-order effect on the utility of marginal households (those who make a different location decision).[34] However, mobility responses can affect compliance rates in the two areas through a composition effect, and the fiscal externality now include composition elasticities μ, alongside the elasticities from households changing their compliance decision (ε and η). Welfare and optimal policy are also affected by an additional sufficient statistic: $\kappa \equiv$

[34]Tax-induced changes in house prices also imply transfers between buyers and sellers. To the extent that buyers and sellers have different welfare weights, this can have implications for optimal policy.

$-\partial p_{L\phi}/\partial T_{\phi}$, which governs the extent to which property taxes are capitalized into house prices.

The modified optimal tax formulas still feature the three channels through which mistagging reduces progressivity. The first channel (higher welfare weight of h-tag taxpayers) is unaffected. The second and third channels are dampened — but not eliminated — by capitalization and the decrease in effective inequity. The quantitative impacts will depend on the extent of house price capitalization, but the qualitative impacts of mistagging remain as in the baseline model. Finally, as household location changes may create fiscal externalities, the composition elasticities also enter the numerator of the tax formulas to account for these effects.

Our empirical analysis suggests that there are no first-order effects of changes in property taxes on house prices (see appendix P) or mobility (see appendix Q). Moreover, our preferred specification studies *within*-property changes in compliance to highlight the potential implications of mistagging. Yet, mobility and capitalization responses may be meaningful in other settings, so we also highlight their potential impacts in our simulation exercise in Appendix R.

4 Identifying Behavioral Responses to Inequity

We now present the empirical methods we use to identify behavioral responses to inequity in our setting. We exploit four sources of quasi-experimental variation. Section 4.1 introduces a standard Boundary Discontinuity Design (BDD) (Black, 1999; Bayer *et al.*, 2007) studying tax compliance around the boundaries of the tax sectors (see Section 2.1). Since both tax liabilities and inequity change at these boundaries, the BDD identifies a combination of the households' behavioral responses to tax liabilities and the behavioral responses to inequity that we seek to isolate. Section 4.2 then combines the BDD with variation in properties' *exposure* to mistagging. Since the inequity we seek to isolate is driven by mistagging of land prices, properties whose assessed value is driven predominantly by land — rather than the built structure — are more exposed to mistagging and the resultant inequity. We develop a *difference* in boundary discontinuities design that recovers the behavioral response to inequity by studying differences in BDDs between properties with high and low exposure. Section 4.3 incorporates quasi-experimental variation from the 2011 tax reform (see Section 2.2) to develop a *dynamic difference* in boundary discontinuities design, which relaxes some of the (arguably strong) identifying assumptions in Section 4.2 (i.e., netting out time-invariant determinants of tax compliance). Section 4.3 therefore yields our preferred estimates of the elasticity of compliance with respect to mistagging. Finally, Section 4.4 shows that we can separately estimate the impacts of undertagging and overtagging with an additional "strong parallel trends" assumption (Callaway *et al.*, 2024).

4.1 Boundary Discontinuity Design

Figure 2 illustrates the source of quasi-experimental variation used by our BDD to study impacts on tax compliance. It shows a street view of a boundary between two of the tax sectors shown in the map in Figure 1, with seemingly similar properties on either side. However, the tag for land value in the tax formula (1) changes discretely at that boundary, leading to differential taxation of identical properties across the boundary.[35] The tax sector boundaries are used exclusively to determine the tax base (see Section 2.1). They do not determine tax enforcement efforts, access to public goods or which level of government delivers them.[36] Moreover, our boundary sample excludes boundaries that overlap with neighborhood boundaries (see Section 2.4).

Still, because both tax liabilities and inequity change discontinuously at the boundaries, our BDD estimates should be interpreted as capturing the causal effects of joint changes in these determinants of (non-)compliance. In addition, Section 3.3.2 highlights that differences in tax incentives may induce house-price capitalization and sorting responses, which may contribute to observed compliance gaps at the tax boundaries. Using the same BDD, we find no first-order effects of property taxes on house prices (see appendix P). We also find no evidence of mobility responses to the tax changes induced by the 2011 reform (see appendix Q), so that we can rule out any major selection concern for the empirical approach developed in Section 4.3. However, even small mobility responses may accumulate over time. For these reasons, the static BDD presented here should be viewed as a first step towards a more credible empirical strategy.

To build towards our preferred empirical strategy, we focus on compliance in 2010, the year immediately preceding the 2011 reform, when mistagging was most pronounced.[37] For each taxpayer, we compute compliance as the fraction of their tax liability paid within 18 months of receiving the tax bill. Our results are similar using longer time windows or considering whether taxpayers made any tax payment (see appendix L). We then estimate the following specification:

$$c_i = \lambda_{r(i)} + f_0\left(d_i\right) + \beta_0 HTS_i + f_1\left(d_i\right) \times HTS_i + \mathbf{X}_i \boldsymbol{\beta} + \varepsilon_i \tag{4}$$

where c_i measures the compliance of taxpayer i and $\lambda_{r(i)}$ are fixed effects for each 500-meter road segment $r(i)$ to ensure that we are comparing properties close to each other; HTS_i is an indicator for being on the high-tag side of the boundary ($d_i > 0$); $f_0\left(d_i\right)$ and $f_1\left(d_i\right)$ control for distance to the boundary on the low- and high-tag sides of the boundary, respectively; $\mathbf{X}_i$ are the properties' effective land area a_i and assessed built structure value b_i; and ε_i is the residual.[38]

Figure 3 shows the results in the subsample of our boundary sample where properties face a non-trivial degree of inequity ($|\log\left(\sigma_i\right)| > 0.05$).[39] The figure displays our point estimate of the change in compliance at the boundary, computed using local linear controls for distance,

[35]Figure 2 shows the boundary between sectors 40 and 54. The square-meter price of sector 40 is 800% higher than the square-meter price in sector 54 before the reform, and is still 25% higher after the reform.

[36]The interpretation of the BDD could differ if the tax authority internalized inequity concerns and diverted enforcement efforts away from the high-tag side. Tax collection and enforcement of unpaid liabilities, however, are centralized and automated. Appendix O discusses enforcement procedures and shows that there is no evidence that enforcement is weaker on the high-tag side.

[37]In appendix K we provide evidence that the estimates are robust to our sample selection decisions.

[38]For context, 500 meter segments is the length of between three and six city blocks in Manaus, depending on the orientation of the street grid.

[39]Focusing on properties that would experience at least a 5% difference in their tax liability on the other side of the boundary drops about half of the boundary sample, as shown in Appendix figure K.6. The same figure shows that the results are unchanged if we use thresholds between 0.02 and 0.2

the MSE-minimizing bandwidth, and triangular weighting kernels (Calonico *et al.*, 2014, 2020). To help visualize the design, the figure also shows the conditional expectation of compliance using decile-spaced bins of distance from the boundary weighted with the same triangular kernel used to compute the point estimate, but censoring the kernel at its tenth percentile to give positive weights to observations outside the MSE-optimal bandwidth (bins outside the optimal bandwidth are shown in gray). We also plot an estimate of (4) with cubic distance controls f_0 and f_1 estimated over the full ± 300–meter window with the same triangular weighting kernel.

Three findings emerge. First, panel A shows that there is a sharp drop in compliance on the high-tag side precisely at the boundary, suggesting that compliance behavior is responsive to the tax system. Second, the drop in compliance — 5.6%-pts — is economically meaningful. Since average compliance reaches 69% just on the low-tag side of the boundary, this amounts to an 8.1% drop in compliance. Third, as panels B and C make clear, the boundaries generate quasi-experimental variation in two distinct first-stages. Tax liabilities are 23% higher on the high-tag side, but inequity is also 62% higher, so that the compliance effect combines responses to both incentives. The next section thus turn to isolating the response to inequity.

4.2 Exposure to Inequity: A Difference in Boundary Discontinuities Design

To isolate the effect of inequity, we augment our BDD by comparing properties on the low- and the high-tag side of the boundary while holding their tax liability fixed (Frölich & Huber, 2019). This is possible because even properties with the same tax liability can face different levels of inequity due to differences in their *exposure* to inequity. Indeed, the inequity we seek to exploit is driven by mistagging of land prices, whereas tax liabilities depend on both the assessed value of the land and the assessed value of the built structure on that land. A property with a small house on a large lot has a liability that is primarily driven by its land value, whereas a property with the same liability but featuring a large house on a small lot has its liability driven primarily by the built structure. Hence, the two properties will be exposed to different degrees of inequity.

Formally, we can use the presumptive tax formula (1) to express the counterfactual tax liability for a property in sector $s(i)$ had it been on the other side of the boundary in sector $\hat{s}(i)$:

$$\hat{T}_i = \frac{1 + p_{\hat{s}(i)} e_i}{1 + p_{s(i)} e_i} \times T_i$$

where $e_i = a_i / b_i$ is the ratio of property's IPTU contribution from land characteristics to building characteristics, and $p_{s(i)}$ and $p_{\hat{s}(i)}$ are the land prices in the property's own and counterfactual tax sectors as defined in Section 2.5.[40] The ratio e_i governs a property's *exposure* to mistagging: properties with high e_i will be more exposed to the inequity coming from the difference in assessed land prices $p_{s(i)} - p_{\hat{s}(i)}$ than properties with low e_i, even if they share the same tax liability. Comparing properties with the same tax liability on different sides of the tax sector boundaries,

[40]By holding $p_{s(i)}$ and $p_{\hat{s}(i)}$ fixed, we implicitly condition on properties at a particular boundary.

necessarily implies comparing properties that differ in observable ways. In particular, properties on the high-tag side must feature less land a_i and/or a smaller built structure b_i.[41] These differences may also be correlated with unobserved determinants of compliance.[42]

Our Difference in Boundary Discontinuities Design (DBDD) allows for properties' unobserved determinants of compliance to be different on the high- and low-tag sides of the boundary, but requires that this gap is unrelated to exposure e_i. We sketch out the formal identification argument below, but this assumption essentially allows us to recover the impact of inequity by comparing changes in compliance at the tax sector boundary between properties at the bottom and at the top of the exposure distribution. This assumption is arguably strong. However, we can test it empirically by combining sector boundaries at which the assessed land price, and hence inequity, does not change. To do this, we take pairs of boundaries at which the land tags do not change — one pair with a high tag and one pair with a low tag — and use them to construct placebo boundaries. The placebo boundary's high-tag side comes from the boundary with a high tag and the placebo boundary's low-tag side comes from the boundary with a low tag. Reassuringly, running our DBDD analysis on these placebo boundaries, we find no evidence of treatment effects (see Appendix N), providing support for our identifying assumption.

Sketch of formal derivation. The formal derivation of our estimator is a relatively straightforward application of existing results. Specifically, we build heavily on the methods developed by Frölich & Huber (2019) to incorporate covariates into Regression Discontinuity Designs (RDD), and by Dong *et al.* (2023) to adapt the RDD to settings with continuous treatments. Therefore, we only present the full formal derivation in Appendix J, and provide a brief exposition of the identification argument here.

The setup is as follows. We denote the distance to the tax sector boundary — the running variable — as $D \in \mathcal{D} \subset \mathbb{R}$. Potential compliance is given by $C = G(\sigma, \tau, D, \nu) = G_0(\tau, D, \nu_0) + G_1(\sigma, \tau, D, \nu_1)$ where inequity $\sigma = \frac{\hat{T}_i}{T_i} \in \mathbb{R}^+$ is our treatment of interest, τ is the (log) tax liability, and ν are other, potentially unobserved, determinants of compliance. We separate the potential outcomes into an untreated component G_0 capturing potential compliance at different tax liabilities τ in the absence of inequity, and a treatment effect G_1 capturing the impact of inequity on compliance. We partition the unobserved determinants of compliance ν into those that influence the treatment effect ν_1 and those that only affect the untreated potential outcomes ν_0.

The identification result rests on three assumptions. The first one allows us to map one-to-one between quantiles u of exposure to mistagging e and inequity σ. The second assumption

[41] To see this, assume the contrary, that there are properties on either side of the boundary with the same tax liability $T_H = T_L$, but that the property on the high-tag side has both more land, $a_H > a_L$ and more built structure, $b_H > b_L$. Rearranging the tax formula (1), we can write the difference in tax liabilities as $T_H - T_L = b_H - b_L + a_H(p_H - p_L) + (a_H - a_L)p_L$. $a_H > a_L$ and $b_H > b_L$ imply that all the terms on the right hand side are positive and so we have contradicted the assumption that the two properties have the same tax liability. Hence either $b_H < b_L$ or $a_H < a_L$.

[42] Notwithstanding this, in appendix I we formalize the assumptions required for a BDD that is augmented to hold properties' tax liabilities fixed to identify the impact of compliance and present the results following this design. We find results that are very much in line with our more credible research design in this section and section 4.3.

requires that inequity, taxes, distance, and unobservables ν_1 all generate smooth impacts on the G_1 component of potential outcomes. However, it allows for taxes, distance, and the unobservables ν_0 to have a discontinuous effect on compliance at the boundary through G_0, but only for reasons that are unrelated to inequity. The third assumption maintains that properties' ranks in the inequity distribution and the ν_1 component of their unobservables are uncorrelated locally at the boundary. In other words, it implies that a property would be at roughly the same rank in the distribution of exposure to mistagging if it were exogenously moved across the boundary.[43]

With these, our main proposition shows that we can identify the *difference* in the LATE of inequity at the boundary experienced by properties at any pair of exposure to mistagging ranks $\underline{u}$ and $\bar{u}$ — and hence any pair of levels of inequity ranks since there is a one-to-one mapping between quantiles of e and σ. Since we permit discontinuities in compliance at the boundary through G_0, neither of the LATEs experienced by properties at each level of exposure are identified. However, the difference between the two, and hence the shape of the relationship between inequity and LATEs, is identified. We present these DBDD estimates in section 5.1.

4.3 Dynamic DBDD Using the 2011 Reform

While the placebo test presented before the sketch of the formal derivation of our DBDD estimator supports the validity of its identifying assumptions, we may still be concerned that there are unobserved confounders of the treatment effect of inequity. For example, if properties on either side of the tax boundary share the same tax liability, the properties on the high-tag side must be smaller, and the extent to which they are smaller is in fact correlated with exposure.[44] However, while property size may correlate with compliance behaviors (e.g. through attitudes towards government), it is unlikely to change over time, at least not over short time spans, and so we will use the 2011 reform to hold all time-invariant, unobserved determinants of compliance fixed. As discussed in section 2.2, the 2011 reform created large increases in tax liabilities, and also in the counterfactual liabilities that households would face if their properties were located in the tax sector adjoining theirs. This allows us to compare changes in compliance over time on the high-tag and low-tag sides of the sector boundaries and relate them to changes in inequity, holding fixed changes in tax liability and any time-invariant determinants of compliance.

Our identification argument mirrors that of the DBDD above except that the outcomes of interest become *changes* in compliance over time, which we relate to changes in inequity. Our design allows compliance on the low- and high-tag sides of the boundaries to be on different trends, but analogously to the approach in section 4.2, we require that whatever difference

[43] This does not require properties to have the same potential exposure to mistagging on either side of the boundary. The relative after-tax price of land a is higher on the high-tag side of the boundary and so we might expect property owners to substitute towards built structure. Our assumption allows this, but requires that the unobservables are not correlated with the elasticity of substitution between land a and built structure b in such a way that it would reverse ranks in the exposure distribution when crossing the boundary.

[44] To see this formally, consider two properties on either side of the boundary that share the same tax liability $b_L + a_L p_L = b_H + a_H p_H$ and exposure level $a_L/b_L = a_H/b_H = E$. Rearranging we see that $a_L/a_H = b_L/b_H = (1 + p_H E)/(1 + p_L E) > 1$ and note that $\partial(b_L/b_H)/\partial E = (p_H - p_L)/(1 + p_L E)^2 \neq 0$.

in trends there is between the two sides of the boundary, it is orthogonal to properties' exposure to mistagging, akin to a triple-differences design. Formally, we assume that potential compliance outcomes in year y are given by $C_y = G(\sigma_y, \tau_y, D, \mu, \nu_{0y}, \nu_{1y})$. As before, compliance depends on inequity σ, tax liability τ, and distance to the boundary D. We augment the potential outcomes to depend on a set of time-invariant unobservables μ, and time-varying unobservables ν_{0y} and ν_{1y}. We assume that the difference between potential compliance in 2010 (before the reform) and 2016 (after the reform is fully phased in) can be written as $\Delta C = \Delta G_0\left(\Delta\tau, D, \Delta\nu_0\right) + \Delta G_1\left(\Delta\sigma, \Delta\tau, D, \Delta\nu_1\right)$ where, critically, by taking differences over time, we eliminate the dependence of the potential outcomes on the time-invariant unobservables μ. From here, the formal derivation proceeds as that of the DBDD estimator, replacing the level of compliance C with the change in compliance ΔC, and the levels of τ and σ with their changes $\Delta\tau$ and $\Delta\sigma$ (see Appendix J). Applying the same proposition, we are now able to identify the differences in the causal effects of *changes in inequity* on *changes in compliance* between any two pairs of exposure ranks. We present these dynamic DBDD estimates in section 5.2.

4.4 Responses to Undertagging vs Overtagging

The sources of inequity we exploit at the sector boundary generate both overtagging $\sigma > 1$ and undertagging $\sigma < 1$. Our final design is therefore aimed at distinguishing the effects of the two. It also permits us to evaluate the dynamics of the causal effects and the plausibility of our parallel trends assumptions by studying trends in compliance leading up to the 2011 reform. Formally, we make the following additional assumption (building on Callaway *et al.*, 2024):

Assumption (Strong Parallel Trends)

$$\begin{aligned}
&\mathbb{E}\left[G\left(s_y, t_y, d, \mu, \nu_y\right) - G\left(s_0, t_0, d, \mu, \nu_0\right)|\sigma_y = s_y, \sigma_0 = s_0, \tau_y = t_y, \tau_0 = t_0, D = d\right] \\
&\quad = \mathbb{E}\left[G\left(s_y, t_y, d, \mu, \nu_y\right) - G\left(s_0, t_0, d, \mu, \nu_0\right)|\tau_y = t_y, \tau_0 = t_0, D = d\right] \quad \forall y
\end{aligned} \tag{5}$$

where $G\left(\sigma_y, \tau_y, D, \mu, \nu_y\right)$ are the compliance potential outcomes, and the base year $y = 0$ is 2010.

This assumption requires that changes in compliance over time at different distances from the boundary are orthogonal to changes in the inequity that those properties experience over time. Applying this assumption to properties on the high-tag side of the boundary — predominantly overtagged before the reform — permits Difference-in-Differences designs such as those we present in section 5.3 to identify the effects of reducing overtagging. Similarly, it allows us to identify the effect of reducing undertagging on the low-tag side of the boundaries.

5 The Effects of Inequity on Tax Compliance

This section presents our main estimates of inequity effects using the empirical strategies developed in the previous section. We show that our estimates are robust to sample inclusion decisions and definitions of compliance in appendices K and L, respectively.

5.1 Difference in Boundary Discontinuities Design Using Exposure to Inequity

We start by presenting the results of the Difference in Boundary Discontinuities Design (DBDD, see section 4.2), which holds tax liabilities fixed and examines whether the discontinuous jump in compliance at tax sector boundaries is larger for properties with greater exposure to inequity.

We proceed in two steps. First, we highlight the variation underlying the identification of inequity effects with this design, by comparing two groups of properties experiencing very different exposure to inequity. Specifically, we take properties in the top quartile of $|\sigma|$ as our high exposure group, and the remaining properties in our boundary sample as our low exposure group. We then estimate the following regression for the two groups separately:

$$c_i = \lambda_{r(i)} + g(\tau_i, e_i) + f_0(d_i) + \beta_0 HTS_i + f_1(d_i) \times HTS_i + \varepsilon_i \tag{6}$$

where we add flexible controls for property i's (log) tax liability τ_i and exposure to mistagging e_i in the term $g(\tau_i, e_i)$ to the specification in equation (4). As mentioned earlier, we focus on 2010, the year immediately preceding the 2011 reform, when mistagging was most pronounced.

Figure 4 reports estimates using our preferred functional form for $g(\tau_i, e_i)$, namely cubic splines of τ and fifty quantiles of exposure fixed effects (we consider alternative functional forms below). Panels A and B show that the two groups experience markedly different increases in inequity at the tax sector boundaries. In the low exposure group, we see only a small average increase of 4.9%-pts, while the inequity jump is much larger in the high exposure group at 73.9%-pts. Next, we turn to compliance effects. In Panel C, we see that compliance changes very little at the tax sector boundaries in the low exposure group; if anything, the point estimate is even slightly positive at 3.3%-pts. Recall that the estimator developed in section 4.2 allows compliance to differ systematically between the two sides of the boundary, and identifies inequity effects entirely from differences in exposure to inequity. The key result is therefore that Panel D shows a large decrease in compliance at the boundary in the high exposure group, which experience a much larger jump in inequity at the boundary. We estimate a drop in compliance of 8.9%-pts in Panel D, implying a differential change in compliance between the two groups of 12.2%-pts.

In a second step, we use the full variation in exposure to inequity in our boundary sample, and estimate inequity effects using the following linear specification:

$$c_i = \lambda_{r(i)} + g_0(\tau_i, e_i) + f_0(d_i) + HTS_i \times [\beta_0 + \tilde{\eta} \log(\sigma) + f_1(d_i) + g_1(\tau_i, e_i)] + \varepsilon_i \tag{7}$$

where we now also permit the controls $g(\tau_i, e_i)$ to be different on each side of the boundary.

The results are presented in Table 1. In column (1), we control for cubic splines of the tax liability and fixed effects for fifty quantiles of the exposure distribution, as in Figure 4. In column (2) we control separately for the tax liability and exposure to mistagging on either side of the boundary. Column (3) replaces the exposure quantiles with cubic splines in exposure while column (4) replaces the cubic splines in tax liability with fifty quantiles fixed effects. Columns (5)–(7) replicate the specifications in columns (2)–(4), respectively, but additionally include interactions between the tax liability controls and the exposure controls. The estimated $\tilde{\eta}$ are highly significant and robust across the different columns of Table 1. The point estimates range from $-.19$ to $-.14$, which is in line with the results in Figure 4 where we obtain a value of $(-.089 - .033)/(.739 - .049) = -.177$. The elasticities of compliance with respect to inequity implied by our estimates — dividing $|\tilde{\eta}|$ by the average compliance level — range between 0.21 and 0.29.

The identification of inequity effects in this section relies on rather strong assumptions, but in light of the supporting evidence from the placebo exercise discussed in section 4.2, we see the results in Figure 4 and Table 1 as our first evidence that tax inequity reduces compliance.

Salience. Before turning to the results from our preferred identification strategy developed in section 4.3, we provide support for a key contextual assumption of our analysis: that property owners are aware of their counterfactual tax liability, $\hat{T}_i$, and hence of the inequity they face.

This awareness is plausibly stronger when inequity is more salient — for example, when comparable properties are located just across the boundary. We thus explore heterogeneous treatment effects along two measures of the salience of inequity (see Appendix M for details on their construction). Our first *density* measure builds on the notion of similarity used in Auerbach & Hassett (2002). For each property i, we compute the density of its counterfactual tax liability $\hat{T}_i$ within the distribution of observed tax liabilities on the opposite side of the boundary.[45] Intuitively, inequity is more salient when a property's counterfactual liability closely matches the liability of nearby properties. For our second *type* measure, we calculate the share of properties on the opposite side of the boundary that are of the same type as property i, where type is defined as apartment versus house. We then split our sample into disjoint groups based on each salience measure and estimate equation (7) separately within each group.

Figure 5 reports the implied inequity elasticities, showing that responses are concentrated among taxpayers for whom inequity is more salient. In Panel A, the estimated elasticity of compliance with respect to inequity is close to zero in the lowest quartile of the density measure, but becomes positive (indicating that inequity reduces tax compliance) in higher salience quartiles. Panel B shows that the elasticity is larger for properties whose neighbors across the boundary are predominantly of the same type. To the extent that some taxpayers do not perceive the inequity they face, and therefore do not respond to it, our estimates will capture lower bounds on the behavioral response to *salient* inequity.

[45] Note that this would not be hard for taxpayers to do, they can look up the IPTU of any property in the city via the government's open access geodata portal: `https://wsgeo.manaus.am.gov.br/ConsultaPreviaCidadao/`.

5.2 Dynamic DBDD Using the 2011 Reform

We now turn to the results of the dynamic DBDD developed in section 4.3, which holds all time-invariant determinants of compliance fixed and examines whether the *change* in the compliance discontinuity at tax sector boundaries is larger where the 2011 reform reduced inequity by more.

We start again by highlighting the variation underlying the identification of inequity effects with this design. For each property, we measure the extent to which the 2011 reform reduced inequity, either by reducing overtagging or by reducing undertagging. We then estimate the following regression separately for properties in the top quartile of this measure — the high-treatment group — and for the remaining properties — the low-treatment group:[46]

$$\Delta c_i = \lambda_{r(i)} + g\left(\Delta\tau_i, e_i\right) + f_0\left(d_i\right) + HTS_i \times \left[\beta_0 + f_1\left(d_i\right)\right] + \varepsilon_i \tag{8}$$

This specification is analogous to the one in equation (6), but it studies changes in compliance over time controlling for baseline exposure e_i and for changes in tax liability. As mentioned in section 4.3, we focus on the change between 2010 (just before the reform, when mistagging was most pronounced) and 2016 (after the reform is fully phased in).

The results are presented in Figure 6, where our preferred functional form for $g\left(\Delta\tau_i, e_i\right)$ now uses cubic splines of $\Delta\tau_i$ (and fifty quantiles of exposure fixed effects). Panels A and B show that the 2011 reform led to very different reductions in inequity between the two groups of properties. In the low-treatment group, the difference in the average change in inequity between the two sides of the tax sector boundaries is 11.9%-pts, while the same figure reaches 45.0 %-pts in the high-treatment group, driven mostly by a large reduction in over-tagging on the high-tag side.[47] Panel C then shows that the change in compliance is similar on the two sides of the tax sector boundaries in the low-treatment group. The difference is very close to zero and insignificant. By contrast, in Panel D, we see that the change in compliance is 5.2%-pts higher on the high-tag side than on the low-tag side (the difference is precisely estimated), where properties experienced very different changes in inequity on the two sides of the boundaries following the 2011 reform. In sum, households' tax compliance appears to respond strongly to reductions in inequity.

Next, we pool all properties together and estimate the impact of reducing inequity using the full variation induced by the 2011 reform through the following linear regression:

$$\Delta c_i = \lambda_{r(i)} + g_0\left(\Delta\tau_i, e_i\right) + f_0\left(d_i\right) + HTS_i \times \left[\delta_0 + \tilde{\eta}\Delta\log\left(\sigma_i\right) + g_1\left(\Delta\tau_i, e_i\right) + f_1\left(d_i\right)\right] + \varepsilon_i \tag{9}$$

where all terms are as defined previously. The results are presented in Table 2, where the specifications in columns (1)-(7) mirror those in columns (1)-(7) in Table 1. The estimated $\tilde{\eta}$ are highly

[46]Our inequity-reduction measure corresponds to $\Delta\sigma$ for properties on the high-tag side and $-1\times\Delta\sigma$ for properties on the low-tag side. We note that, as explained in section 2.4, we re-incorporate tax sector boundaries that overlap with neighborhood boundaries in our estimation sample in this subsection and the one below.

[47]We note that, in Figure 6, a reduction in inequity implies a positive change in $\log(\sigma)$ for undertagged properties on the low-tag side of the boundary and a negative change in $\log(\sigma)$ for overtagged properties on the high-tag side.

significant and robust across specifications at around -0.07. Converting this to an elasticity of compliance with respect to inequity yields an elasticity of 0.11 with our preferred specification in column (1). This design requires the weakest assumptions and so we interpret it as our most robust, and hence preferred, estimate of the elasticity of compliance with respect to inequity.

5.3 Responses to Undertagging vs Overtagging

Our final design is aimed at distinguishing between the effects of overtagging $\sigma > 1$ and the effects of undertagging $\sigma < 1$. By invoking the "strong" parallel trends assumption in section 4.4, we are able to estimate the impact of changes in inequity separately for the overtagged properties on the high-tag side of the boundary and the undertagged properties on the low-tag side of the boundary. Specifically, we estimate the following regression:

$$c_{iy} = \alpha_i + \lambda_{r(i)y} + \sum_{j \neq 2010} D_j \times \Big[f_{0j}(d_i) + \beta_{0j} \Delta \tau_i + \tilde{\eta}_{0j} \Delta \log(\sigma_i) + HTS_i \times \big(\delta_j + f_{1j}(d_i) + \beta_{1j} \Delta \tau_i + \tilde{\eta}_{1j} \Delta \log(\sigma_i) \big) \Big] + \varepsilon_{iy} \quad (10)$$

where $\lambda_{r(i)y}$ are segment-year fixed effects, $D_j \equiv \mathbf{1}[y = j]$ are year dummies, and we include year-specific distance controls —$f_{0j}(d_i)$ and $f_{1j}(d_i)$— and year-specific controls for property i's tax liability change due to the reform. We use the balanced panel subsample of our tax reform sample (described in Section 2.4), resulting in 41,197 properties per year.

Figure 7 presents the results. Panel A shows the impacts on the high-tag side, plotting the estimated combination of coefficients $\tilde{\eta}_{0j} + \tilde{\eta}_{1j}$ (along with their 95% confidence intervals). Prior to the reform, the estimates are all indistinguishable from zero, consistent with our strong parallel trends assumption on the high-tag side. They become negative after the reform, indicating that compliance improves for properties experiencing larger reductions in inequity relative to properties experiencing smaller reductions. This suggests that the inequity generated by overtagging has strong effects on compliance. Perhaps surprisingly, the effects emerge immediately following the reform's enactment in 2011 despite the fact that the reform was phased in over 5 years. This is likely due to the high salience of the reform as it was being implemented.

Panel B shows the impacts on the low-tag side. The estimated $\tilde{\eta}_{0j}$ are not as closely clustered around zero prior to the reform as the estimated $\tilde{\eta}_{1j}$. Still, we do not find any clear evidence against our strong parallel trends assumption. If the effects of undertagging were symmetric to the effects of overtagging, we would expect households that experience larger reductions in undertagging following the 2011 reform to become relatively *less* compliant, leading to a similar pattern as in Panel A.[48] The post-reform coefficients in panel B, however, are all indistinguishable from zero. Therefore, we cannot reject the hypothesis that undertagging has no effect on compliance. This is consistent with the findings in Dube *et al.* (2019) studying inequity in the

[48] Reductions in overtagging imply negative changes in σ leading to increases in compliance and hence negative post-reform coefficients. Similarly, reductions in undertagging imply positive changes in σ and so reductions in compliance would also lead to negative post-reform coefficients.

workplace: quit behavior is responsive to wage rises for workers' higher-paid peers (the analog of overtagging in our setting) but not to wage increases for their lower-paid peers.

In sum, across a range of augmented BDD designs, we find consistent evidence that inequity matters for tax compliance. To put the magnitude of our estimated elasticity of compliance with respect to inequity in perspective, it is useful to go back to the overall change in compliance at the tax sector boundaries documented in Figure 3, a drop of 8.1%. As highlighted in the same figure, this is associated with a 62% increase in inequity. However, since we find no response to undertagging, we can treat the effective change in inequity as resulting solely from the increase in overtagging — a change of $62/2 = 31\%$ in σ. In that case, our preferred estimate of the elasticity of compliance with respect to inequity implies that inequity responses can account for $\frac{.11 \times .31}{.081} = 42\%$ of the overall change in compliance at the tax sector boundaries.

6 Implications for Tax Policy Design

The elasticity of compliance with respect to inequity can have important implications for policy design, which we now explore through the lens of our conceptual framework. As discussed in section 3, the extent to which compliance responses are driven by behavioral responses to inequity, as opposed to standard responses to tax liabilities, can have very different implications for the optimal tax schedule. Figure 8 presents a simple calibration of our stylized model to illustrate this point. The overall compliance response can be decomposed into the two underlying behavioral mechanisms using $-dc/c = \eta d\sigma/\sigma + \varepsilon dT/T$. In figure 8, we hold fixed the size of the overall compliance response, and show how optimal tax burdens (T_l/y_L and T_h/y_H) and progressivity ($\frac{T_h}{y_H}/\frac{T_l}{y_L}$) vary with the share of the response attributed to the inequity elasticity.

We proceed as follows. We start with the 8.1% drop in compliance at tax sector boundaries in figure 3 and assume that it is entirely driven by the 23% increase in tax liability and the 62% increase in inequity highlighted in the same figure. As discussed above, we treat the effective change in inequity as resulting solely from the change in overtagging, so we have $d\sigma/\sigma = 31\%$. With these in place, using our preferred estimate of the inequity elasticity implies that responses to inequity and tax liability account for 42% and 58% of the overall change in compliance, respectively.[49] We then use this calibration to simulate the optimal tax schedule with mistagging of both house types (see section 3.3.1), assuming no behavioral responses to undertagging. This baseline calibration is marked by a dashed vertical line in panel A of Figure 8. As the relative size of inequity responses may differ in other settings, we also present simulation results varying the share of the overall response attributed to inequity from 0% to more than 75%.[50]

Our baseline calibration implies a markedly less progressive tax schedule than if compliance

[49] This calibration implies an underlying elasticity of compliance with respect to the tax liability of $\varepsilon = \frac{.58 \times .081}{.23} = 0.2$. This is in line with the results in Brockmeyer *et al.* (2023), who estimate overall compliance elasticities between 0.24 and 0.46 in Mexico City using a range of difference-in-differences and regression discontinuity approaches.

[50] In all our simulations, we set the parameters of the model as follows: mistagging of both types $\psi_{Hl} = \psi_{Lh} = 0.05$, no behavioral responses to undertagging $\eta_{Hl} = 0$, $\rho = 2$, $y_H = 6,630.8$ Reais, $y_L = 4,911.5$ Reais, $b(r) = 1$, $g_H/g_L = 1.6$. See Appendix R for full details.

responses were only driven by direct responses to the tax liability. Absent responses to inequity, the optimal tax schedule sets the rate on high-value properties 3 times as large as the rate on low-value properties. This drops to 1.83 in our baseline calibration, or only 61% of the progressivity without inequity responses. This comes about because the comparative statics of the optimal tax schedule with respect to ε and η have opposite signs: more responsiveness to the tax liability implies a more progressive tax schedule while greater responsiveness to inequity implies a *less* progressive schedule. In fact, the optimal tax schedule is no longer progressive ($\frac{T_h}{y_H}/\frac{T_l}{y_L} = 1$) in our simulations once inequity responses account for 78% of the overall response (the optimal tax rates on high- and low-value properties are 40% and 320% larger, respectively, than when inequity responses are absent). In sum, panel A of Figure 8 illustrates that the strength of behavioral responses to inequity can have a considerable impact on the optimal tax schedule.

In appendix R we also explore how these conclusions change as we change the parameters of the model and incorporate extensions to the model. Overall, the comparative statics are intuitive and the qualitative findings are robust to changes in the parameter values. Three comparative static results bear mentioning. First, more mistagging of either type (undertagging ψ_{Hl} or overtagging ψ_{Lh}) reduces progressivity, but with a greater impact of overtagging ψ_{Lh}. Second, introducing behavioral responses to undertagging η_{Hl} has very little impact on optimal progressivity. Third, substantial amounts of house price capitalization and/or mobility responses would be required to have meaningful impacts on the results.

Our findings that taxpayers respond strongly to the presence of inequity in the tax schedule also imply that there are potentially large returns to investments in the capacity of the state to assess properties' values more accurately. One promising avenue for such improvements is to leverage the fact that, as the property market thickens and moves online, there are large datasets of property asking prices available on the internet. To explore this, we bring to bear a dataset of property listings from Viva Real, a property listing platform, as discussed in appendix P.

We begin by computing the effective tax rate for each property in our merged dataset. These rates vary dramatically, with a coefficient of variation of 2.5. Moreover, the Root Mean Squared Error (RMSE) of the assessed values as predictions of the asking prices is large, at 1.36 million Reais, exceeding the standard deviation of the asking prices (1.17 million Reais; see appendix S for the full details of this calculation and the exercises that follow). We then consider a simple improvement: how much better would it be possible to do by using data on asking prices to recalibrate the coefficients in the existing property tax formula? By optimizing these coefficients, we estimate that the RMSE can be reduced by 20%, to 1.09 million Reais.

This exercise has the advantage of being transparent and not requiring any legislative change to the existing formula, but it does not fully exploit the richness of the data available in the government's cadaster since the formula itself is likely to be misspecified. As a second exercise, we thus consider how much better it might be possible to do by using only the data already available in the cadaster, but with a more complex estimation of properties' assessed values. In particular, we train a random forest model to predict properties' asking values using the property features contained in the cadaster. This brings the RMSE down to 798,225 Reais, indicating that the current property assessment formula is significantly misspecified (on top of using sub-optimal coefficients). Finally, we consider what could be done if we also incorporate additional property attributes available in the Viva Real data but not in the cadaster (e.g., number of rooms). This third exercise further reduces the RMSE down to 350,186 Reais. In summary, these exercises suggest that by leveraging more recently available property listing data and standard machine-learning tools, the government may be able to reduce misclassification by up to 74%.

In our stylized model, the government's ability to correctly differentiate between property types is captured by ψ_{Lh}, the fraction of L-type houses that are erroneously given the h tag and ψ_{Hl}, the fraction of H-type houses given the l tag. We set these probability to 5% for the simulations presented in panel A of figure 8. In panel B, we explore how reducing the extent of mistagging, holding all other parameters fixed, affects the optimal tax schedule, starting from the baseline calibration in panel A. Eliminating mistagging (ψ=0) would allow the progressivity of the tax schedule to increase by 42% from 1.83 to 2.6. More circumspectly, the reductions in misclassification suggested by the three exercises discussed above — which we model as a proportional reduction in ψ of the same size as the reduction in the RMSE — would allow the government to increase progressivity by 8% (to 1.97), 15% (to 2.1), and 28% (to 2.35), respectively. These results highlight the potentially large returns to improving the fiscal capacity to differentiate between properties of different market values.

7 Conclusion

Property taxes are an important source of government revenues, particularly for local governments, but they are seldom based on direct evaluations of market prices. Rather, they are overwhelmingly based on presumptive formulas that approximate properties' values using a limited set of observable characteristics. More generally, observable tags are used throughout tax codes, especially in low- and middle- income countries where presumptive taxes are ubiquitous and eligibility for benefits is commonly based on proxy-means tests. A large literature has emphasized the consequences of the limited statistical precision of imperfect tags for eligibility (Besley & Kanbur, 1988) and the moral hazard presumptive taxes induce (Oates & Schwab, 2015; Gaubert *et al.*, 2021). We introduce a novel force into this discussion — behavioral responses to the inevitable inequity that imperfect tagging generates. Our conceptual framework shows how imperfect tagging for property taxation can lead to both lower tax revenues and less progressive tax schedules, and our empirical analysis that these behavioral responses can be sizable.

Given the ubiquity of presumptive taxes throughout the world, these findings have profound implications for the design of tax systems. Imperfect tagging places severe constraints on governments' ability to raise revenues, and on their ability to redistribute through the tax code. As a result, our findings suggest that there are large returns to investments in the capacity of the state to use more precise tags, reducing the extent of mistagging, the resulting inequity, and the consequent behavioral responses that raise the efficiency cost of taxation.

Our measure of inequity is "selfish" in the sense that it captures the extent to which an individual may feel that they are over/under-taxed. This has the advantage of being easily and precisely operationalized, but it does not capture the extent to which taxpayers may care about how much *others* have to pay. In particular, it cannot capture traditional notions of vertical equity regarding preferences over how the burden of taxation is distributed across groups of taxpayers with different abilities to pay. A more comprehensive evaluation of these effects, incorporating both horizontal and vertical elements of inequity is a promising direction for future research.

References

AJZENMAN, NICOLAS, CRUCES, GUILLERMO, PEREZ-TRUGLIA, RICARDO, TORTAROLO, DARÍO, & VAZQUEZ-BARE, GONZALO. 2025. *From Flat to Fair? The Effects of a Progressive Tax Reform*. NBER Working Paper No. 33286. 2, 5, 10

AKERLOF, GEORGE A. 1978. The Economics of "Tagging" as Applied to the Optimal Income Tax, Welfare Programs, and Manpower Planning. *American Economic Review*, **68**(1), 8–19. 1, 4

ALLCOTT, HUNT, & TAUBINSKY, DMITRY. 2015. Evaluating Behaviorally Motivated Policy: Experimental Evidence from the Lightbulb Market. *American Economic Review*, **105**, 2501–2538. 18

AUERBACH, ALAN J., & HASSETT, KEVIN A. 2002. A New Measure of Horizontal Equity. *American Economic Review*, **92**(4), 1116–1125. 22, 72

BALAN, PABLO, BERGERON, AUGUSTIN, TOUREK, GABRIEL, & WEIGEL, JONATHAN. 2022. Local Elites as State Capacity: How City Chiefs use Local Information to Increase Tax Compliance in D.R. Congo. *American Economic Review*, **112**, 1–36. 5

BAYER, PATRICK, FERREIRA, FERNANDO, & MCMILLAN, ROBERT. 2007. A Unified Framework for Measuring Preferences for Schools and Neighborhoods. *Journal of Political Economy*, **115**(4). 2, 5, 15, 11

BERGERON, AUGUSTIN, TOUREK, GABRIEL, & WEIGEL, JONATHAN. 2024a. The State Capacity Ceiling on Tax Rates: Evidence from Randomized Tax Abatements in the DRC. *Econometrica*, **92**, 1163–1193. 5

BERGERON, AUGUSTIN, BESSONE, P, KABEYA, JK, TOUREK, GABRIEL, & WEIGEL, JONATHAN. 2024b. *Supermodular Bureaucrats: Evidence from Randomly Assigned Tax Collectors in the DRC*. forthcoming, American Economic Review. 5

BESLEY, TIMOTHY, & COATE, STEPHEN. 1992. Workfare versus Welfare: Incentive Arguments for Work Requirements in Poverty-Alleviation Programs. *American Economic Review*, **82**, 249–261. 4

BESLEY, TIMOTHY, & KANBUR, RAVI. 1988. Food Subsidies and Poverty Alleviation. *Economic Journal*, **98**, 701–719. 27

BLACK, SANDRA E. 1999. Do Better Schools Matter? Parental Valuation of Elementary Education. *Quarterly Journal of Economics*, **114**(2), 577–599. 2, 5, 15, 11

BROCKMEYER, ANNE, ESTEFAN, ALEJANDRO, ARRAS, KARINA RAMÍREZ, & SERRATO, JUAN CARLOS SUÁREZ. 2023. *Taxing property in developing countries: theory and evidence from Mexico*.

National Bureau of Economic Research Working Paper. 5, 25, 18

Brockmeyer, Anne, Garfias, Francisco, & Serrato, Juan Carlos Suárez. 2024. *The fiscal contract up close: Experimental evidence from Mexico City*. Tech. rept. National Bureau of Economic Research. 8

Cabral, Marika, & Hoxby, Caroline. 2012. *The hated property tax: salience, tax rates, and tax revolts*. Tech. rept. National Bureau of Economic Research. 5, 7

Callaway, Brantly, Goodman-Bacon, Andrew, & Sant'Anna, Pedro H.C. 2024. *Difference-in-Differences with a Continuous Treatment*. Mimeo: Emory University: `https://doi.org/10.48550/arXiv.2107.02637`. 3, 15, 20

Calonico, Sebastian, Cattaneo, Matias D., & Titiunik, Rocio. 2014. Robust Nonparametric Confidence Intervals for Regression-Discontinuity Designs. *Econometrica*, **82**(6), 2295–2326. 17, 78, 80

Calonico, Sebastian, Cattaneo, Matias D., & Farrell, Max H. 2020. Optimal Bandwidth Choice for Robust Bias-Corrected Inference in Regression Discontinuity Designs. *Econometrics Journal*, **23**, 192–210. 17, 78, 80

Card, David, Mas, Alexandre, Moretti, Enrico, & Saez, Emmanuel. 2012. Inequality at work: The effect of peer salaries on job satisfaction. *American Economic Review*, **102**(6), 2981–3003. 1, 2, 10

Carvalho Junior, Pedro Humberto Bruno. 2017. *Property tax performance and potential in Brazil*. Ph.D. thesis, University of Pretoria. 6

Castro, Lucia, & Scartascini, Carlos. 2015. Tax Compliance and Enforcement in the Pampas: Evidence from a Field Experiment. *Journal of Economic Behavior & Organization*, 65–82. 5

Chenozhukov, Victor, & Hansen, Christian. 2005. An IV Model of Quantile Treatment Effects. *Econometrica*, **73**, 245–261. 34, 41

Chetty, Raj. 2006. A General Formula for the Optimal Level of Social Insurance. *Journal of Public Economics*, **90**, 1879–1901. 16

Cruces, Guillermo, Perez-Truglia, Ricardo, & Tetaz, Martin. 2013. Biased perceptions of income distribution and preferences for redistribution: Evidence from a survey experiment. *Journal of Public Economics*, **98**, 100 – 112. 4

Del Carpio, Lucia. 2016. *Are the Neighbors Cheating? Evidence from a Social Norm Experiment on Property Taxes in Peru*. mimeo: INSEAD. 5

Diamond, Peter A. 1975. A Many-person Ramsey Tax Rule. *Journal of Public Economics*, **4**, 335–342. 12

Dong, Yingying, Lee, Ying-Ying, & Gou, Michael. 2023. Regression Discontinuity Designs With a Continuous Treatment. *Journal of the American Statistical Association*, **118**, 208–221. 3, 18, 33, 34, 35, 40, 41

Dube, Arindrajit, Giuliano, Laura, & Leonard, Jonathan. 2019. Fairness and frictions: The impact of unequal raises on quit behavior. *American Economic Review*, **109**(2), 620–663. 1, 2, 9, 11, 24

Dunning, Thad, Monestier, Felipe, Pineiro, Rafael, Rosenblatt, Fernando, & Tuñón, Guadalupe. 2017. Is paying taxes habit forming? Theory and evidence from Uruguay. 8

DZANSI, JAMES, JENSEN, ANDERS, LAGAKOS, DAVID, & TELLI, HENRY. 2024. *Technology and Tax Capacity: Evidence from Local Governments in Ghana*. NBER Working Paper No. 29923. 5

ELMINEJAD, ALI, HAVRANEK, TOMAS, & IRSOVA, ZUZANA. 2025. Relative risk aversion: A meta-analysis. *Journal of Economic Surveys*, **39**(5), 2315–2333. 89

FACK, GABRIELLE, & GRENET, JULIEN. 2010. When do better schools raise housing prices? Evidence from Paris public and private schools. *Journal of Public Economics*, **94**(1-2), 59–77. 11

FELDSTEIN, MARTIN S. 1972. Distributional Equity and the Optimal Structure of Public Prices. *American Economic Review*, **62**, 32–36. 12

FRÖLICH, MARKUS, & HUBER, MARTIN. 2019. Including Covariates in the Regression Discontinuity Design. *Journal of Business & Economic Statistics*, **37**, 736–748. 3, 17, 18, 33, 40

GAUBERT, CECILE, KLINE, PATRICK, VERGARA, DAMIEN, & YAGAN, DANNY. 2021. *Place-Based Redistribution*. Mimeo: UC Berkeley. 4, 27

GIACCOBASSO, MATIAS, NATHAN, BRAD, PEREZ-TRUGLIA, RICARDO, & ZENTNER, ALEJANDRO. 2025. Where do my Tax Dollars Go? Tax Morale Effects of Perceived Government Spending. *American Economic Journal: Applied Economics*, **17**(4), 223–259. 4

GIBBONS, STEPHEN, MACHIN, STEPHEN, & SILVA, OLMO. 2013. Valuing school quality using boundary discontinuities. *Journal of Urban Economics*, **75**, 15–28. 11

HVIDBERG, KRISTOFFER B, KREINER, CLAUS T, & STANTCHEVA, STEFANIE. 2023. Social positions and fairness views on inequality. *Review of Economic Studies*, **90**(6), 3083–3118. 1, 2, 5, 10

IBGE. 2022. *Cidades@: Manaus (AM)*. Instituto Brasileiro de Geografia e Estatística (IBGE). Accessed: 4 December 2025. 2

IMBENS, GUIDO, & NEWEY, WHITNEY. 2009. Identification and Estimation of Triangular Simultaneous Equations Models Without Additivity. *Econometrica*, **77**, 1481–1512. 34

JENSEN, ANDERS, KUMAR, NIKHIL, & POENSGEN, KONSTANTIN. 2026. *Tax Knowledge in Equilibrium: Evidence from an Education Program in Ghana*. 8

KAPON, SAMUEL, DEL CARPIO, LUCIA, & CHASSANG, SYLVAIN. 2024. Using Divide-and-Conquer to Improve Tax Collection. *Quarterly Journal of Economics*, **139**(4), 2475–2523. 5

KEELE, LUKE J, & TITIUNIK, ROCIO. 2015. Geographic boundaries as regression discontinuities. *Political Analysis*, **23**(1), 127–155. 11

KEEN, MICHAEL, & SLEMROD, JOEL. 2021. *Rebellion, Rascals, and Revenue: Tax Follies and Wisdom Through the Ages*. Princeton University Press. 1

KNEBELMANN, JUSTINE, POULIQUEN, VICTOR, & SARR, BASSIROU. 2026. *Discretion Versus Algorithms: Bureaucrats, Tax Equity and Acceptability*. Mimeo: Sciences Po. 5

KUZIEMKO, ILYANA, NORTON, MICHAEL, SAEZ, EMMANUEL, & STANTCHEVA, STEFANIE. 2015. How Elastic are Preferences for Redistribution? Evidence from Randomized Survey Experiments. *American Economic Review*, **105**, 1478–1508. 4

LIVY, MITCHELL R. 2018. Intra-school district capitalization of property tax rates. *Journal of Housing Economics*, **41**, 227–236. 11

LUTTMER, ERZO, & SINGHAL, MONICA. 2014. Tax Morale. *Journal of Economic Perspectives*, **28**, 149–168. 1, 11

LUTTMER, ERZO F. P. 2005. Neighbors as Negatives: Relative Earnings and Well-Being. *Quar-*

terly Journal of Economics, **120**(3), 963–1002. 1

MANKIW, N GREGORY, & WEINZIERL, MATTHEW. 2010. The optimal taxation of height: A case study of utilitarian income redistribution. *American Economic Journal: Economic Policy*, **2**(1), 155–176. 4

NATHAN, BRAD, PEREZ-TRUGLIA, RICARDO, & ZENTNER, ALEJANDRO. 2025. My Taxes are Too Darn High: Why do Households Protest Their Taxes? *American Economic Journal: Economic Policy*, **17**(1), 273–310. 2, 5

NATHAN, BRAD, PEREZ-TRUGLIA, RICARDO, & ZENTNER, ALEJANDRO. 2026. Paying your fair share perceived fairness and tax compliance. *Journal of Accounting and Economics*, **81**(2), 101838. 5

NICHOLS, ALBERT L, & ZECKHAUSER, RICHARD J. 1982. Targeting Transfers through Restrictions on Recipients. *American Economic Review*, **72**, 372–377. 4

NIELSSON, ULF, WROBLEWSKI, CALEB, & YDING, ANDERS. 2024. *The Incidence and Efficiency of Land Value Taxation*. Mimeo: UC Berkeley. 10

OATES, WALLACE E, & SCHWAB, ROBERT M. 2015. The window tax: A case study in excess burden. *Journal of Economic Perspectives*, **29**(1), 163–180. 27

OKUNOGBE, OYEBOLA. 2023. *Becoming Legible to the State: The Role of Detection and Enforcement Capacity on Tax Compliance*. mimeo: World Bank. 5

REDDING, STEPHEN J., & ROSSI-HANSBERG, ESTEBAN. 2017. Quantitative Spatial Economics. *Annual Review of Economics*, **9**, 21–58. 14

RING, MARIUS AK. 2024. Wealth taxation and household saving: Evidence from assessment discontinuities in Norway. *Review of Economic Studies*, rdae100. 5, 11

SAEZ, EMMANUEL, & STANTCHEVA, STEFANIE. 2016. Generalized Social Marginal Welfare Weights for Optimal Tax Theory. *American Economic Review*, **106**, 24–45. 4, 12

SCHÖNHOLZER, DAVID. 2023. *Measuring Preferences for Local Governments*. Working Paper. 5, 11

SCOTT, JAMES C. 1998. *Seeing Like a State*. Yale University Press. 1

SLEMROD, JOEL. 2019. Tax Compliance and Enforcement. *Journal of Economic Literature*, **57**, 904–954. 1, 11

SMITH, ADAM. 1776. *An Inquiry into the Nature and Causes of the Wealth of Nations*. London: W. Strahan and T. Cadell. Chap. Book V, Chapter 2: Of the Sources of the General or Public Revenue of the Society. 1

TURNER, MATTHEW A, HAUGHWOUT, ANDREW, & VAN DER KLAAUW, WILBERT. 2014. Land use regulation and welfare. *Econometrica*, **82**(4), 1341–1403. 11

TWAIT, AARON, & LANGLEY, ADAM. 2024. *50-State Property Tax Comparison Study*. Lincoln Institute of Land Policy. 6

WEIGEL, JONATHAN. 2020. The Participation Dividend of Taxation: How Citizens in Congo Engage More with the State When it Tries to Tax Them. *Quarterly Journal of Economics*, **135**, 1849–1903. 5, 8

Figures & Tables

FIGURE 1: TAX SECTOR BOUNDARIES

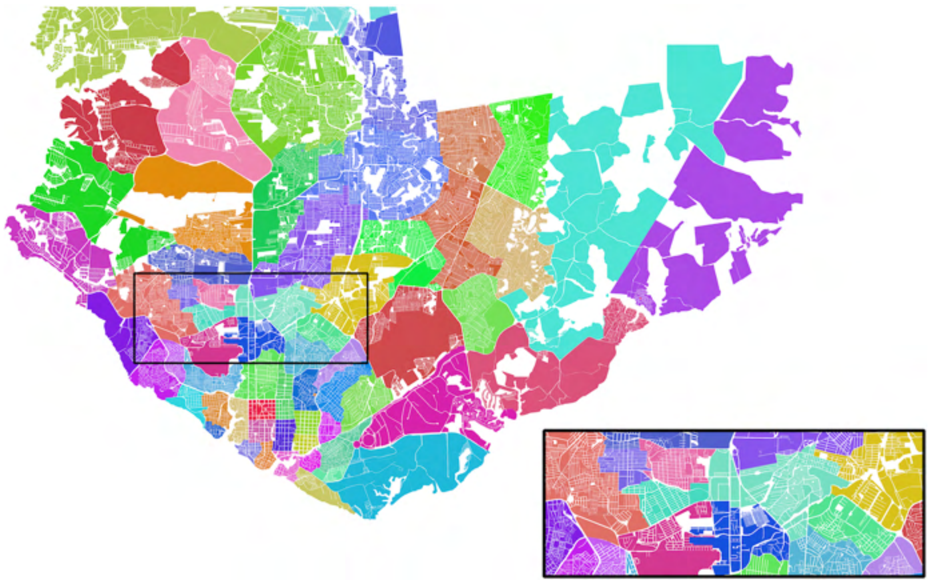

Notes: The figure shows a map of the city of Manaus, with colors highlighting the different tax sectors created by SEMEF in 1983. Within each sector, properties are assigned the same square meter land value. The rectangle zooms in on an area of the city to show the tax sector boundaries more clearly.

FIGURE 2: SECTORS CREATE ARBITRARY BOUNDARIES

Notes: Tax sectors can create arbitrary boundaries where similar houses are assigned different tax bills. This photo shows one of the sector boundaries from Figure 1. The street Rua Visconde de Santa Cruz forms part of the boundary between sector 40 (left) and sector 54 (right). The figure also displays the sector-specific square meter rate initially set by SEMEF in 1983 (p_{1983}) and after the reform (p_{2011}), with the rate higher in sector 40. Map data: © 2025 Google.

FIGURE 3: DIFFERENTIAL TAXATION REDUCES COMPLIANCE

PANEL A: OVERALL CHANGE IN COMPLIANCE AT TAX SECTOR BOUNDARIES

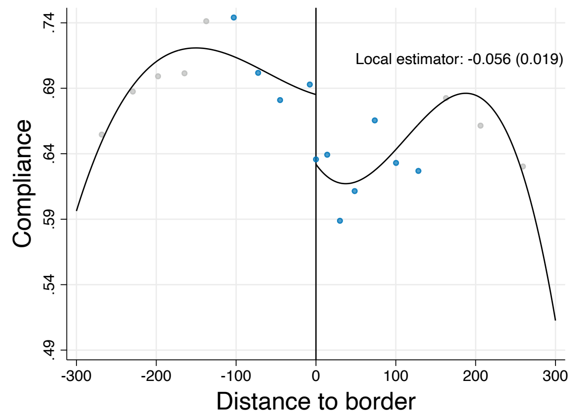

PANEL B: CHANGE IN LOG TAX LIABILITY

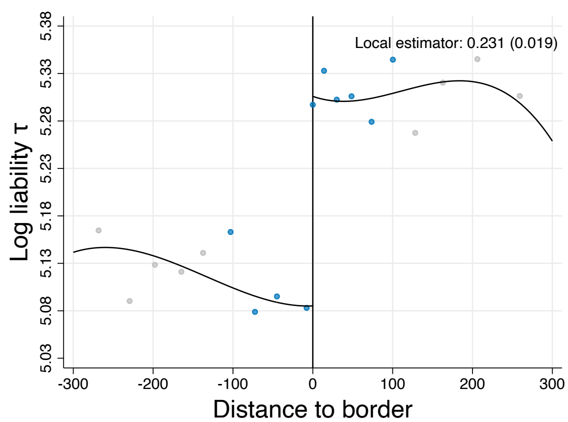

PANEL C: CHANGE IN LOG INEQUITY

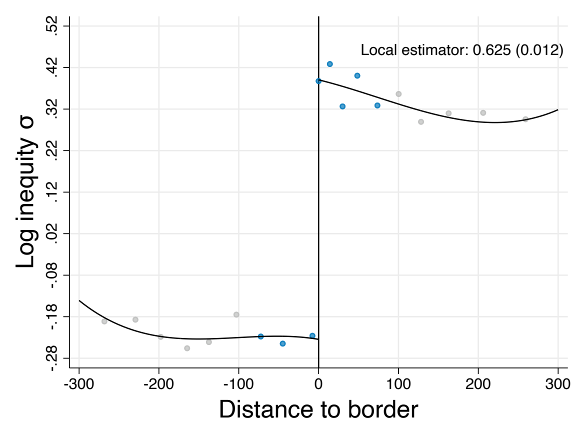

Notes: The figure shows the overall effects of differential taxation at tax sector boundaries discussed in section 4.1. Specifically, we show the results of estimating equation (4) for outcome y_i by taxpayer i: $y_i = \lambda_{r(i)} + f_0(d_i) + \beta_0 HTS_i + f_1(d_i) \times HTS_i + \mathbf{X}_i\boldsymbol{\beta} + \varepsilon_i$ where $\lambda_{r(i)}$ are boundary-segment fixed effects, HTS_i is an indicator for being on the high-tag side of the boundary ($d_i > 0$); $f_0(d_i)$ and $f_1(d_i)$ control for distance to the boundary on the low- and high-tag sides of the boundary, respectively; $\mathbf{X}_i$ are the properties' effective land area a_i and assessed built structure value b_i; and ε_i is the residual. The outcome variable y_i is compliance in panel A, log liability τ in panel B, and log inequity $\log(\sigma)$ in panel C. Overlaid on the figure, we show the point estimate of the discontinuity in compliance estimated using local linear distance controls, the MSE-minimizing bandwidth, and triangular kernel weights in distance. The dots in the figure show the coefficients from estimating (4) with fixed effects for decile-spaced bins of distance, using the same triangular kernel weights but censoring them at their tenth percentile to give non-zero weights to distances outside the optimal bandwidth. The bins in the optimal bandwidth are shown in blue while those outside are shown in gray. The black line is a global cubic polynomial fit in the same way.

Figure 4: Difference in Boundary Discontinuities Design

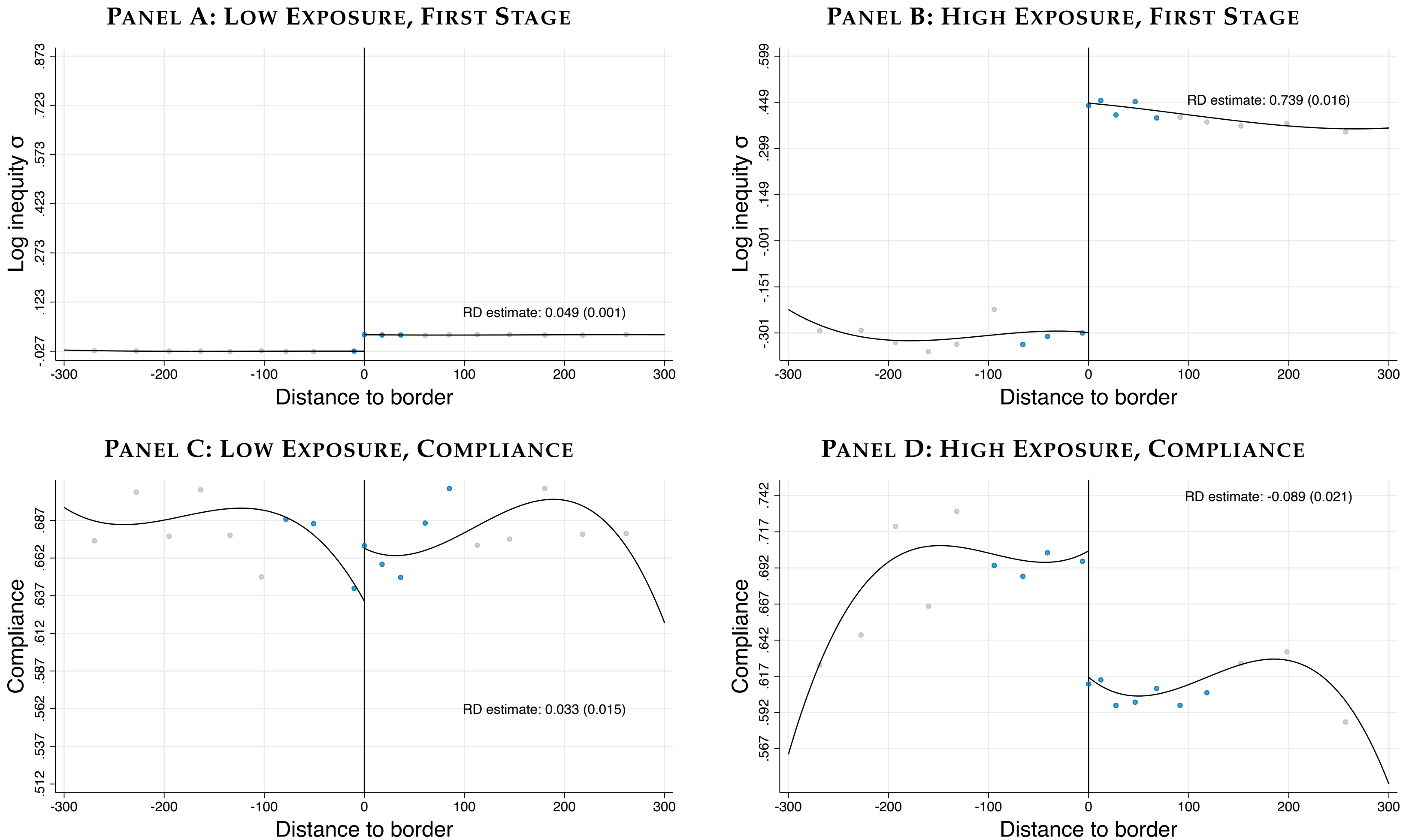

Notes: The figure shows the results of estimating equation (6) discussed in section 5.1: $y_i = \lambda_{r(i)} + g(\tau_i, e_i) + f_0(d_i) + \beta_0 HTS_i + f_1(d_i) \times HTS_i + \varepsilon_i$, where terms are as defined in the notes to figure 3 but with the addition of the $g(\tau_i, e_i)$ term to control flexibly for the tax liability τ_i (using a cubic spline) and exposure e_i (using fifty quantiles of exposure fixed effects). In panels A and B the outcome variable is inequity $\log(\sigma_i)$, and in panels C and D the outcome variable is compliance c_i. Panels A and C show estimates in the subsample of properties with low exposure (defined as being in the bottom 3 quartiles of inequity) while panels B and D show the estimates in the subsample of properties with high exposure (defined as being in the top quartile of inequity).

FIGURE 5: HETEROGENEITY OF THE INEQUITY ELASTICITY BY SALIENCE GROUPS

A: DENSITY-MEASURE OF SALIENCE

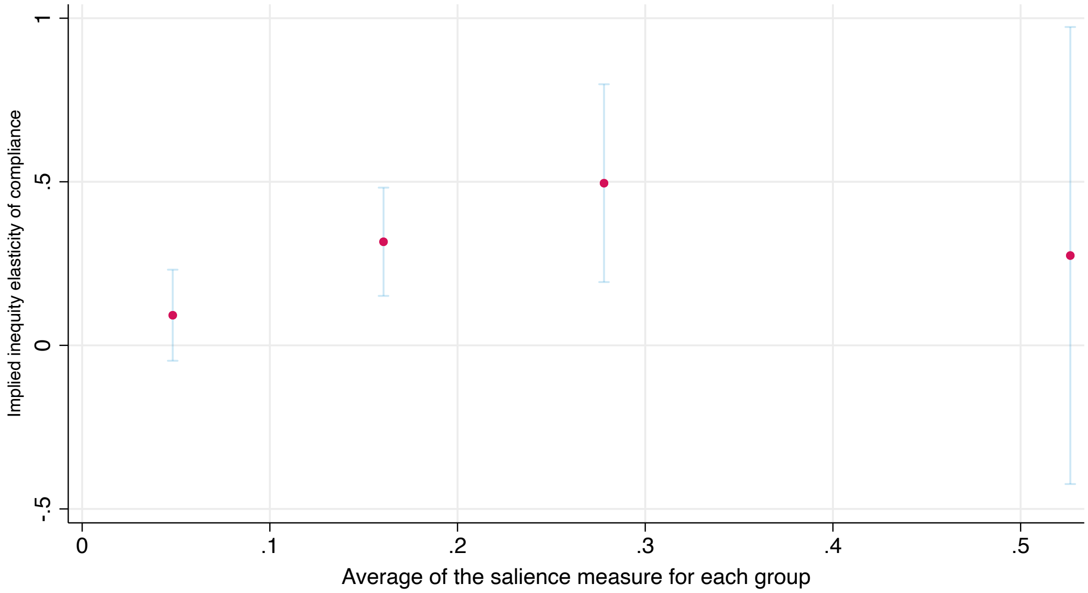

B: TYPE-MEASURE OF SALIENCE

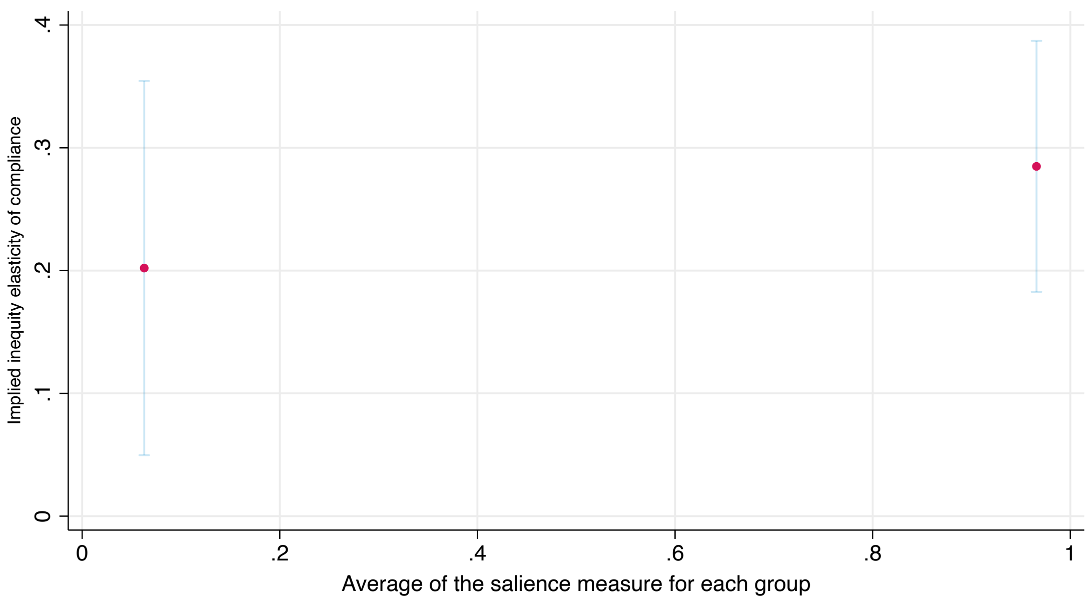

Notes: The figure shows the compliance elasticity by groups of our salience measure. Specifically, we split our sample into disjoint groups using the salience measures and estimate the difference in boundary discontinuities design from regression (7). Panel A splits the data using quartiles of our density measure of salience. Panel B splits the data using the type measure of salience. Appendix figure M.2 shows that the type measure of salience is concentrated around 0 and 1. Thus, we split the data into two groups: above and below 0.5. Both measures are described in more detail in Appendix M. For each group, we show on the y-axis the inequity elasticity ($|\tilde{\eta}|$) implied by estimating equation (7), along with their 95% confidence intervals. On the x-axis, we show the average salience for each group. The figure shows that our results are strongly increasing in the salience of the property tax.

FIGURE 6: DYNAMIC DIFFERENCE IN BOUNDARY DISCONTINUITIES DESIGN

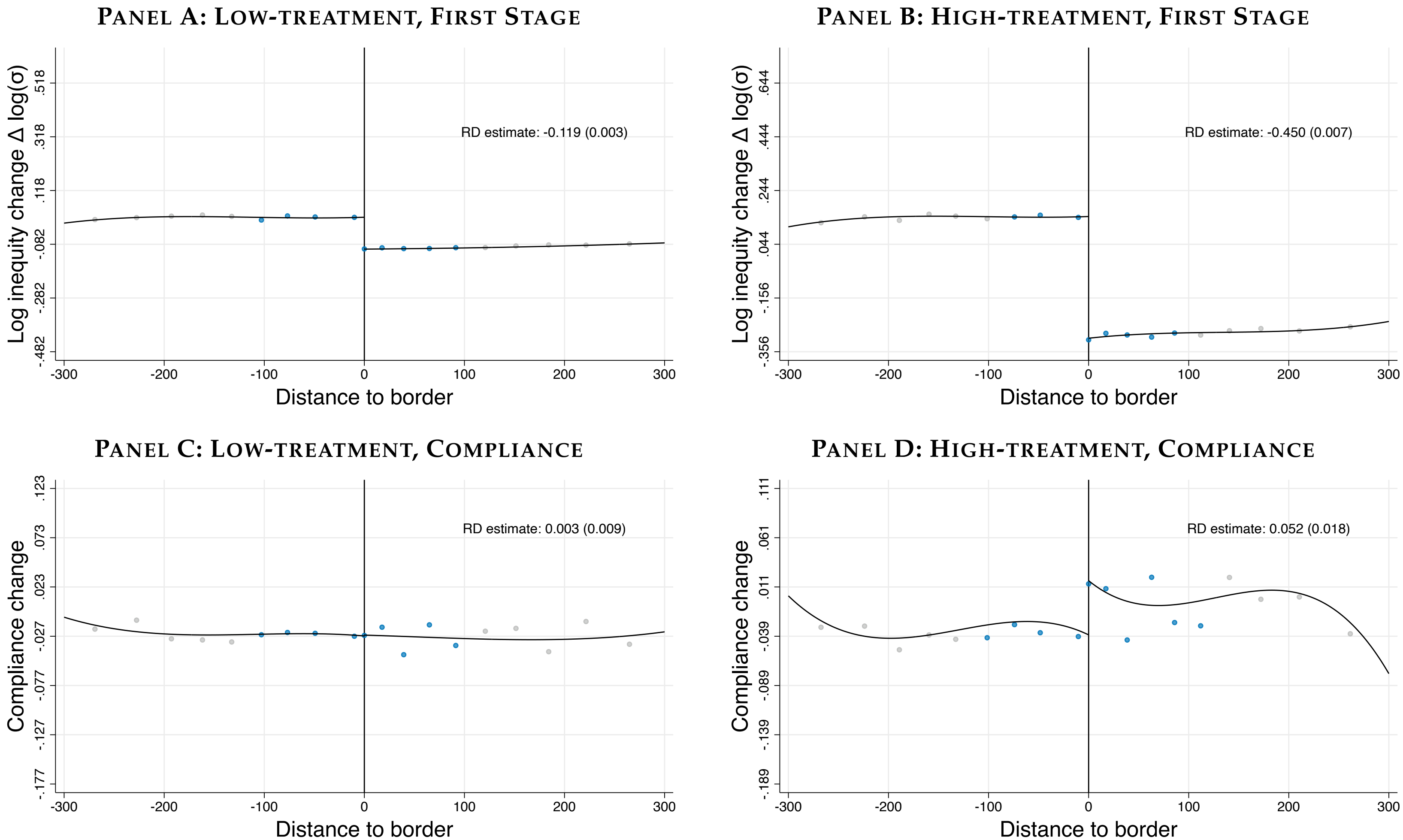

Notes: The figure shows the results of estimating equation (8): $\Delta y_i = \lambda_{r(i)} + g(\Delta\tau_i, e_i) + f_0(d_i) + HTS_i \times [\beta_0 + f_1(d_i)] + \varepsilon_i$ where $\lambda_{r(i)}$ are boundary-segment fixed effects, HTS_i is an indicator for being on the high-tag side of the boundary ($d_i > 0$); $f_0(d_i)$ and $f_1(d_i)$ control for distance to the boundary on the low- and high-tag sides of the boundary, respectively; and ε_i is the residual. $g(\Delta\tau_i, e_i)$ controls flexibly for changes in log tax liability, τ_i and exposure e_i. Specifically, we control for splines of $\Delta\tau_i$ and fifty quantiles of exposure fixed effects. Panels A and C show the estimates for the low-treatment group, the subsample of properties for whom the reform led to a moderate reduction in inequity following the 2011 reform. Panels B and D shows the estimates for the high-treatment group, the subsample of properties that experienced larger reductions in inequity. Panels A and B show estimates of the first-stage effect on changes in inequity (a reduction in inequity implies a positive change in $log(\sigma)$ on the low-tag side and a negative change on the high-tag side). Panels C and D show estimates of the effects on changes in compliance.

FIGURE 7: DIFFERENCE IN DIFFERENCE ESTIMATES OF OVERTAGGING AND UNDERTAGGING EFFECTS

A: OVER-TAGGED

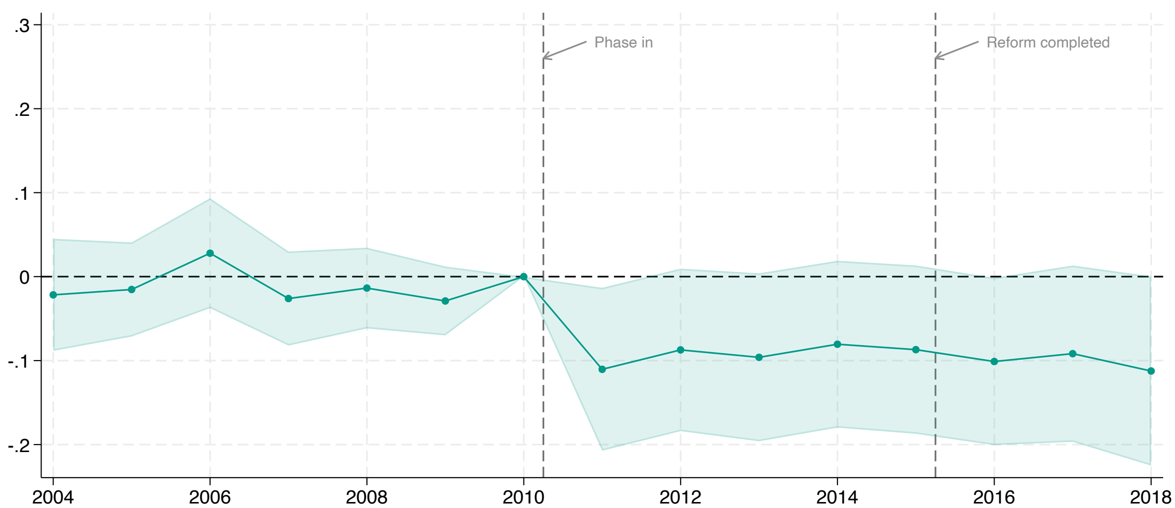

B: UNDER-TAGGED

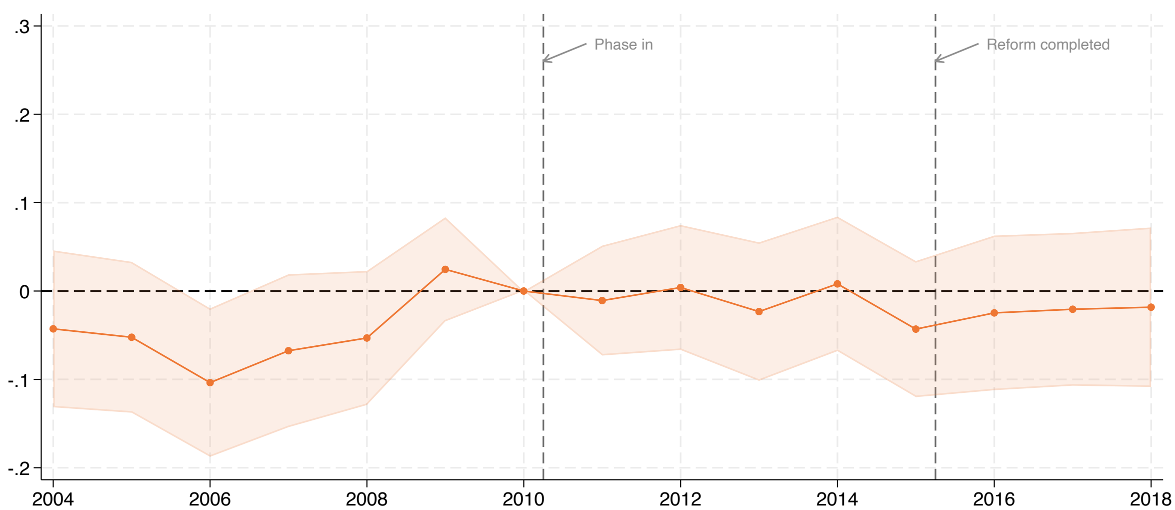

Notes: The figure shows the results of the estimation of equation (10) as discussed in section 5.3: $c_{iy} = \alpha_i + \lambda_{r(i)y} + \sum_{j \neq 2010} D_{jy} \times \left[f_{0j}(d_i) + \beta_{0j}\Delta\tau_i + \tilde{\eta}_{0j}\Delta\sigma_i + HTS_i \times \left(\delta_j + f_{1j}(d_i) + \beta_{1j}\Delta\tau_i + \tilde{\eta}_{1j}\Delta\sigma_i\right)\right] + \varepsilon_{iy}$, where $\lambda_{r(i)y}$ are segment-year fixed effects, $D_{jy} \equiv \mathbf{1}[y = j]$ are year dummies, and we include year-specific distance controls $f_{0j}(d_i)$ and $f_{1j}(d_i)$; and year-specific controls for property i's tax liability change due to the reform. Panel A shows the estimated $\eta_{0j} + \eta_{1j}$ coefficients along with their 95% confidence intervals. Panel B shows the estimated η_{0j} coefficients along with their 95% confidence intervals.

Figure 8: Optimal Tax Calibration and Fiscal Capacity Counterfactuals

Panel A: Share of Overall Response Due to Inequity Responses

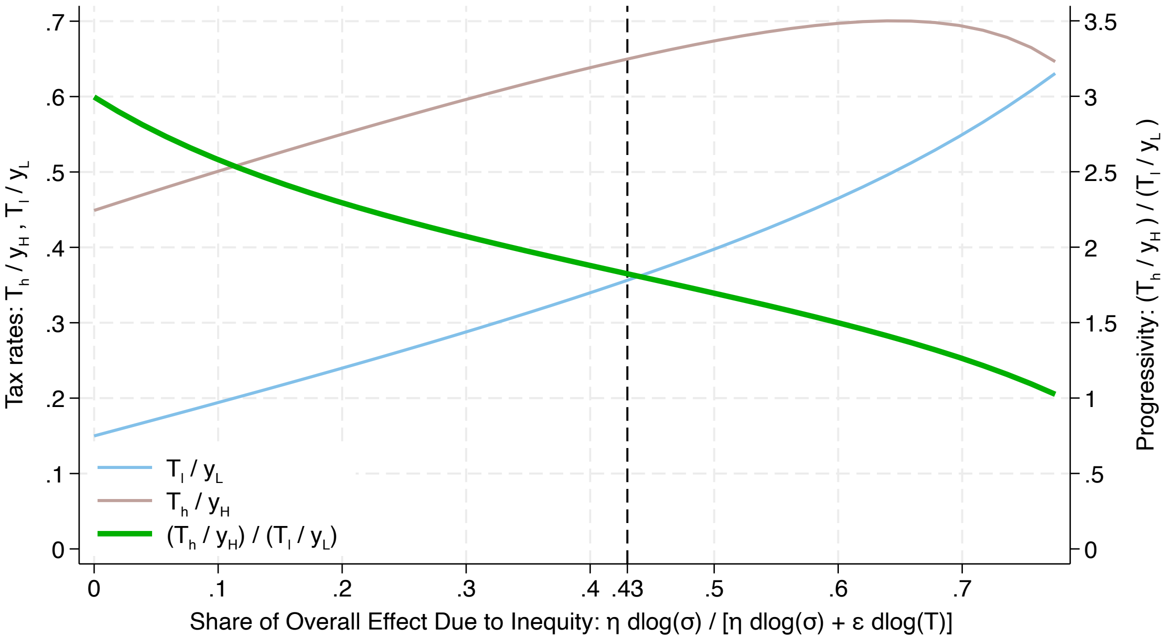

Panel B: Fiscal Capacity Counterfactuals

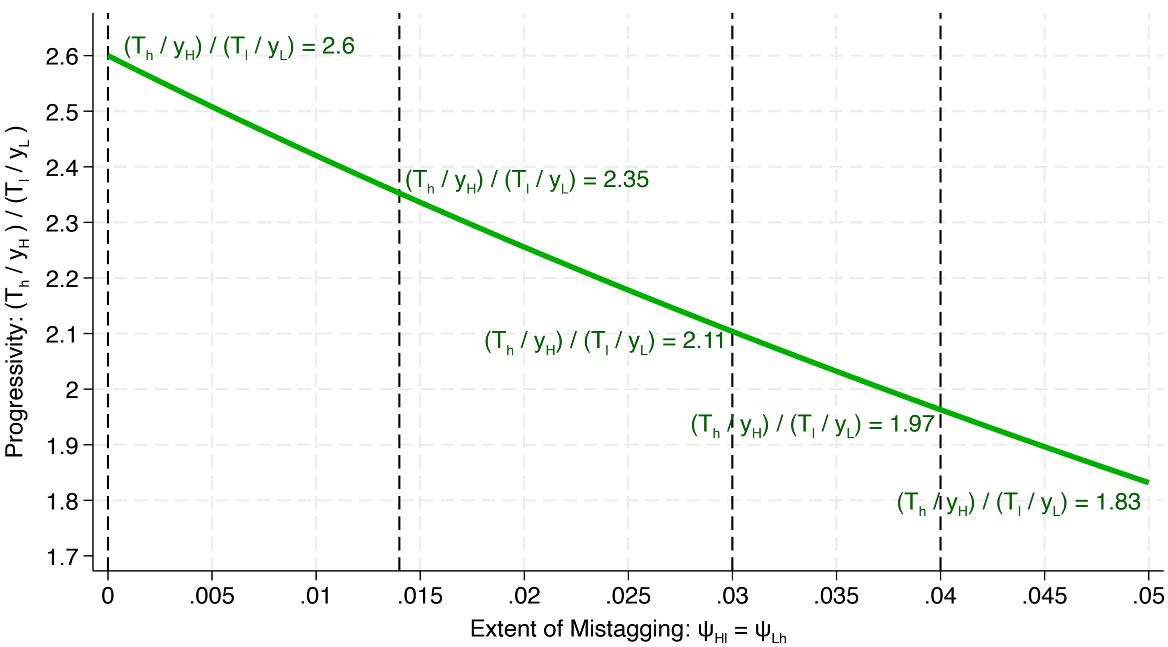

Notes: The figure shows calibrations of the optimal tax schedule discussed in section 3.3.1. We set the parameters as follows: $\psi_{Hl} = \psi_{Lh} = 0.05$, $\eta_{Hl} = 0$, $\rho = 2$, $y_H = Rs.6,630$ $y_L = Rs.4,911.5$ $b(r) = 1$ $g_H/g_L = 1.6$. In panel A, we hold the overall compliance response at the tax sector boundaries fixed and vary the share we attribute to responses to inequity. We show the two optimal tax rates and the ratio of the two: the progressivity of the tax schedule. Our preferred estimate of $\eta = 0.11$ implies 42% of the overall response coming from inequity. See section 6 and Appendix R for full details. In Panel B we perform counterfactual reductions in the extent of mistagging due to investments in fiscal capacity as described in section 6 and appendix S, and show the implications for the progressivity of the optimal tax schedule.

TABLE 1: DIFFERENCE IN BOUNDARY DISCONTINUITY DESIGN: COMPLIANCE EFFECTS

	(1)	(2)	(3)	(4)	(5)	(6)	(7)
1(high tag side) $\times \lvert \log(\sigma) \rvert$	-0.16***	-0.14***	-0.18***	-0.14***	-0.16***	-0.19***	-0.14***
	(0.03)	(0.03)	(0.03)	(0.03)	(0.03)	(0.03)	(0.03)
R^2	0.132	0.135	0.130	0.138	0.150	0.132	0.295
Distance controls	✓	✓	✓	✓	✓	✓	✓
Segment fixed effects	✓	✓	✓	✓	✓	✓	✓
τ splines	✓	✓	✓	✗	✓	✓	✗
τ deciles	✗	✗	✗	✓	✗	✗	✓
Exposure deciles	✓	✓	✗	✓	✓	✗	✓
Exposure splines	✗	✗	✓	✗	✗	✓	✗
τ splines $\times$ HTS	✗	✓	✓	✗	✓	✓	✗
τ deciles $\times$ HTS	✗	✗	✗	✓	✗	✗	✓
Exposure deciles $\times$ HTS	✗	✓	✗	✓	✓	✗	✓
Exposure splines $\times$ HTS	✗	✗	✓	✗	✗	✓	✗
τ splines $\times$ exp deciles	✗	✗	✗	✗	✓	✗	✗
τ splines $\times$ exp splines	✗	✗	✗	✗	✗	✓	✗
τ deciles $\times$ exp deciles	✗	✗	✗	✗	✗	✗	✓
τ splines $\times$ HTS $\times$ exp deciles	✗	✗	✗	✗	✓	✗	✗
τ splines $\times$ HTS $\times$ exp splines	✗	✗	✗	✗	✗	✓	✗
τ deciles $\times$ HTS $\times$ exp deciles	✗	✗	✗	✗	✗	✗	✓
Elasticity η	0.244***	0.218***	0.286***	0.225***	0.245***	0.290***	0.214***
	0.040	0.044	0.041	0.044	0.047	0.043	0.054
N	25061	25061	25061	25061	25061	25061	24515

Notes: The table shows the results of estimation of equation (7) derived in section 4.2 and discussed in section 5.1: $c_i = \lambda_{r(i)} + g_0(\tau_i, e_i) + f_0(d_i) + HTS_i \times [\beta_0 + \tilde{\eta}\log(\sigma) + f_1(d_i) + g_1(\tau_i, e_i)] + \varepsilon_i$ where $\lambda_{r(i)}$ are boundary segment fixed effects, HTS_i is an indicator for being on the high-tag side of the boundary ($d_i > 0$); $f_0(d_i)$ and $f_1(d_i)$ control for distance to the boundary on the low- and high-tag sides of the boundary, respectively; $g_0(\tau_i, e_i)$ and $g_1(\tau_i, e_i)$ control for the tax liability and exposure on the low- and high-tag sides of the boundary, respectively; and ε_i is the residual. In column (1), we control for cubic splines of the tax liability and fifty quantiles of exposure fixed effects. In column (2) we control separately for the tax liability and exposure to mistagging on either side of the boundary. Column (3) replaces the exposure quantiles with cubic splines in exposure while column (4) replaces the tax liability cubic splines with fifty quantiles fixed effects. Columns (5)–(7) replicate the specifications in columns (2)–(4), respectively, but additionally include interactions between the tax liability controls and the exposure controls.

Table 2: Dynamic Difference in Boundary Discontinuity Design

	(1)	(2)	(3)	(4)	(5)	(6)	(7)
1(high tag side) X $\Delta \log(\sigma)$	-0.071***	-0.071**	-0.071***	-0.070**	-0.075***	-0.074***	-0.073**
	(0.026)	(0.028)	(0.027)	(0.028)	(0.028)	(0.028)	(0.030)
R^2	0.027	0.028	0.026	0.029	0.035	0.026	0.118
Distance controls	✓	✓	✓	✓	✓	✓	✓
Segment FEs	✓	✓	✓	✓	✓	✓	✓
$\Delta\tau$ splines	✓	✓	✓	✗	✓	✓	✗
$\Delta\tau$ deciles	✗	✗	✗	✓	✗	✗	✓
Exposure deciles	✓	✓	✗	✓	✓	✗	✓
Exposure splines	✗	✗	✓	✗	✗	✓	✗
$\Delta\tau$ splines $\times$ HTS	✗	✓	✓	✗	✓	✓	✗
$\Delta\tau$ deciles $\times$ HTS	✗	✗	✗	✓	✗	✗	✓
Exposure deciles $\times$ HTS	✗	✓	✗	✓	✓	✗	✓
Exposure splines $\times$ HTS	✗	✗	✓	✗	✗	✓	✗
$\Delta\tau$ splines $\times$ exp deciles	✗	✗	✗	✗	✓	✗	✗
$\Delta\tau$ splines $\times$ exp splines	✗	✗	✗	✗	✗	✓	✗
$\Delta\tau$ deciles $\times$ exp deciles	✗	✗	✗	✗	✗	✗	✓
$\Delta\tau$ splines $\times$ HTS $\times$ exp deciles	✗	✗	✗	✗	✓	✗	✗
$\Delta\tau$ splines $\times$ HTS $\times$ exp splines	✗	✗	✗	✗	✗	✓	✗
$\Delta\tau$ deciles $\times$ HTS $\times$ exp deciles	✗	✗	✗	✗	✗	✗	✓
Elasticity η	0.111***	0.112**	0.110***	0.110**	0.117***	0.116***	0.114**
	(0.041)	(0.044)	(0.042)	(0.044)	(0.044)	(0.044)	(0.047)
N	53267	53267	53267	53267	53267	53267	53137

Notes: This table shows the results of estimating equation (9) derived in section 4.3 and discussed in section 5.2: $\Delta c_i = \lambda_{r(i)} + g_0(\Delta\tau_i, e_i) + f_0(d_i) + HTS_i \times [\delta_0 + \tilde{\eta}\Delta\log(\sigma_i) + g_1(\Delta\tau_i, e_i) + f_1(d_i)] + \varepsilon_i$ where all terms are as defined above in the notes to table 1. Column (1) controls for cubic splines of the changes in tax liability and fixed effects for fifty quantiles of exposure. Column (2) controls separately for the changes in tax liability and exposure to mistagging on either side of the boundary. Column (3) replaces the exposure quantiles with splines, while column (4) replaces the changes in tax liability splines with fixed effects for fifty quantiles of the changes in tax liability. Columns (5)–(7) replicate the specifications in columns (2)–(4), respectively, but additionally include interactions between the changes in tax liability controls and the exposure controls.

Online Appendix: Not for Publication

A Additional Background on Property Tax (IPTU) in Manaus

SEMEF utilizes a presumptive formula based on house and building characteristics to calculate the property tax bill, as opposed to basing the tax on a proportion of the fair market value of the property. The presumptive method is commonly used throughout the world (see table A.1), and SEMEF's use of geography in the presumptive formula is not atypical.

TABLE A.1: PROPERTY TAXES AROUND THE WORLD

City	Property Tax Assessment	Does geography enter into the assessment?	Do assessment zones align with administrative divisions?
Addis Ababa (ET)	Presumptive	No	-
Amsterdam (NL)	Market value	No	-
Bangkok (TH)	Presumptive	Yes	Yes
Beijing (CN)	No property tax	-	-
Berlin (DE)	Presumptive	No	-
Bogota (CO)	Market value	No	-
Buenos Aires (AR)	Market value	No	-
Cairo (EG)	Presumptive	Yes	Yes
Chicago (US)	Market value	No	-
Delhi (IN)	Presumptive	No	-
Dhaka (BD)	Presumptive	Yes	No
Hong Kong (HK)	Market value	No	-
Istanbul (TR)	Presumptive	Yes	No
Jakarta (ID)	Market value	Yes	No
Johannesburg (ZA)	Market value	No	-
Karachi (PK)	Presumptive	Yes	No
Lagos (NG)	Market value	No	-
Lahore (PK)	Presumptive	Yes	No
Lima (PE)	Presumptive	Yes	No
London (UK)	Market value	No	-
Los Angeles (US)	Market value	No	-
Madrid (ES)	Presumptive	Yes	Yes
Manaus (BR)	**Presumptive**	**Yes**	**No**
Manilla (PH)	Market Value	No	-
Maputo (MZ)	Presumptive	Yes	No
Mexico City (MX)	Presumptive	Yes	Yes
Moscow (RU)	Presumptive	No	-
Mumbai (IN)	Presumptive	Yes	No
New York City (US)	Market value	No	-
Paris (FR)	Presumptive	Yes	Yes
Rio de Janeiro (BR)	Presumptive	Yes	No
Rome (IT)	Presumptive	No	-
Sao Paulo (BR)	Presumptive	Yes	No
Seoul (KR)	Presumptive	Yes	Yes
Shanghai (CN)	No property tax	-	-
Singapore (SG)	Market value	No	-
Sydney (AU)	Market value	No	-
Taipei (TW)	Presumptive	Yes	No
Tehran (IR)	Market value	No	-
Tokyo (JP)	Presumptive	No	No
Toronto (CA)	Market value	No	-

Notes: This table shows the method of property tax valuation for large urban areas across the world. Presumptive assessment uses a formula that takes observable characteristics of the property as its inputs. Market value assessment assigns a property tax based proportionally on the estimated value of the property in the real estate market. Note that China does not impose a property tax.

Every year, SEMEF calculates a property's tax bill (IPTU) as a function of a small number of easily observable characteristics of the land and any built structures on the property. Table A.2 lists the categories for each characteristic used in the calculation of the land value (VT) and building value (VE).

TABLE A.2: PROPERTY TAX (IPTU) CALCULATION FACTORS

$$IPTU = (VE + VT) \times aliquot$$

$VE = Value(m^2) \times Area \times (CAT/100) \times Alignment \times Construction \times Position$			$VT = Value(m^2) \times Area \times Situation \times Typography \times Pedology$		
Alignment	Construction	Position	Situation	Topography	Pedology
• Aligned • Backtracked	• Isolated • Combined • Detached	• Front • Back • Superimposed Front • Superimposed Back • Mezzanine • Gallery • Village	• Corner • Middle of Block • Village • Enclave • Horizontal Condo • Favela/Stilit	• Flat • Uphill • Downhill • Irregular	• Floodable + 50% • Floodable - 50% • Firm

Notes: This table shows the equation used by SEMEF to calculate a household's property tax bill. CAT is defined as the sum of building components points, and factors in the construction material used in a household's roof, exterior walls, structure, and building height.

To calculate the per-square meter rate in the tax calculation, SEMEF divided Manaus into 65 tax sectors in 1983. Importantly, this division is only used in the property tax calculation; the smallest official administrative division of the city is the neighborhood (*Bairro*). As the tax sectors were created in 1983, before much of the city was built out, it is not conterminous with the bairro boundaries. Similarly, tax sectors do not factor into the division of Manaus into voting precincts (*Zonas eleitorais*). Figure A.1 shows the overlay between the tax sector boundaries and the bairro boundaries (in blue), and the zonas eleitorais boundaries (in pink).

RY OVERLAYS

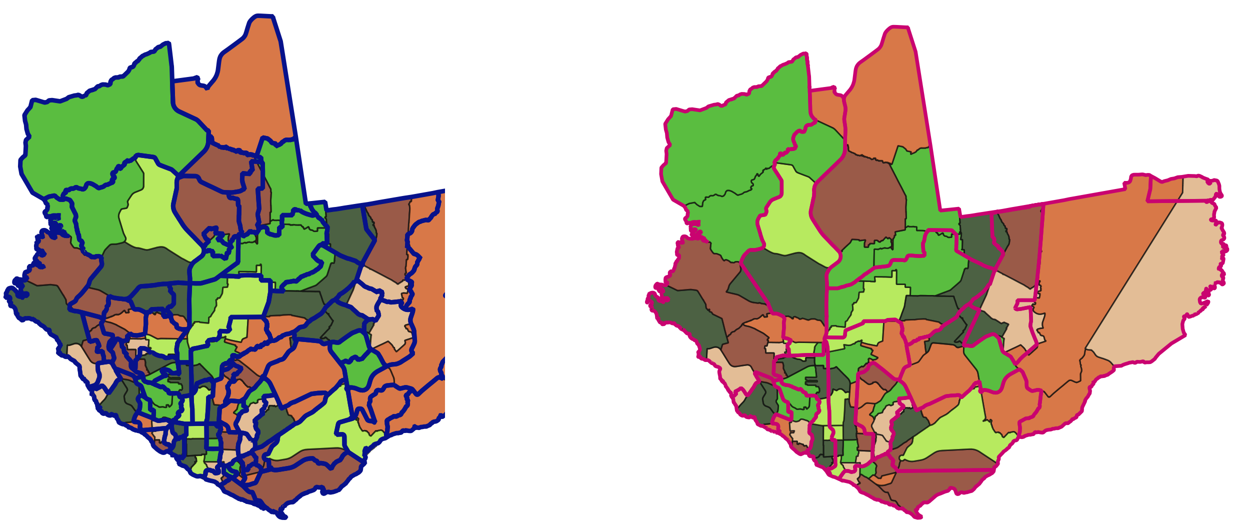

Notes: This figure shows the boundaries of tax sectors overlaid by the boundaries of municipal neighborhoods (Panel A, in blue) and voting precincts (Panel B, in pink) in Manaus.

After a household receives its property tax bill in January (see figure A.2), it has the option to pay it in one installment by March (at a discounted rate) or to pay the bill in ten equal monthly installments. Failure to pay the complete property tax bill by December 31 results in automatic interest and fines applied in the next billing cycle, with the property being placed on the *divida ativa* registry until the remaining balance is paid off. Despite the penalty for nonpayment, we find that compliance rates in Manaus are relatively low. Figure A.3 shows the compliance rate from 2004 through 2019 for three definitions of compliance. The series in orange circles shows the fraction of properties that make any tax payment. The series in green squares computes the ratio of tax paid to tax owed for each property and then averages it across taxpayers. The series in purple triangles shows the fraction of properties that pay their tax in full. Despite a slight increase in compliance after 2008, the fraction of (nonexempt) households in the city that pay their property tax bill in a given year is between 60 and 65 percent. However, as seen in the figure, compliance appears to be driven at the extensive margin, with the large majority of households who pay their property tax choosing to pay the full amount owed to SEMEF that year.

FIGURE A.2: EXAMPLE OF A 2018 IPTU BILL

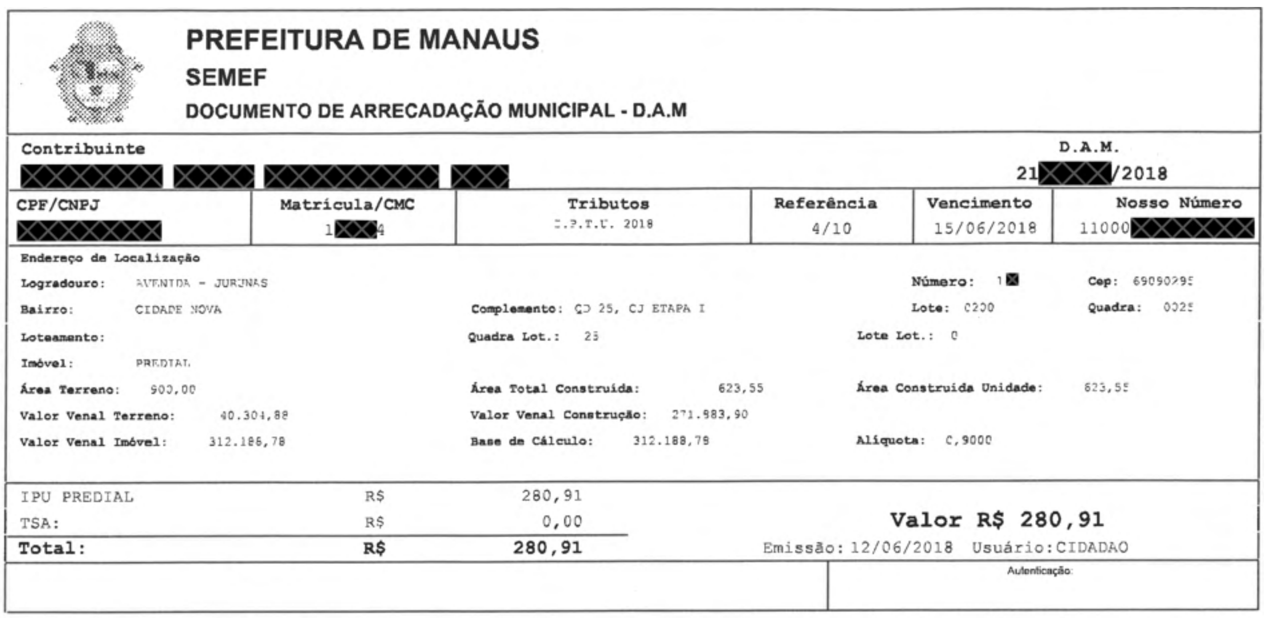
PREFEITURA DE MANAUS
SEMEF
DOCUMENTO DE ARRECADAÇÃO MUNICIPAL - D.A.M

Contribuinte [redacted]
D.A.M. 21[redacted]/2018

CPF/CNPJ	Matrícula/CMC	Tributos	Referência	Vencimento	Nosso Número
[redacted]	1[redacted]4	I.P.T.U. 2018	4/10	15/06/2018	11000[redacted]

Endereço de Localização
Logradouro: AVENIDA - JURUNAS   Número: 1[redacted]   Cep: 69090295
Bairro: CIDADE NOVA   Complemento: CD 25, CJ ETAPA I   Lote: 0200   Quadra: 0025
Loteamento: Quadra Lot.: 25   Lote Lot.: 0
Imóvel: PREDIAL
Área Terreno: 900,00   Área Total Construida: 623,55   Área Construida Unidade: 623,55
Valor Venal Terreno: 40.304,88   Valor Venal Construção: 271.883,90
Valor Venal Imóvel: 312.188,78   Base de Cálculo: 312.188,78   Aliquota: 0,9000

IPU PREDIAL	R$	280,91
TSA:	R$	0,00
Total:	**R$**	**280,91**

Valor R$ 280,91
Emissão: 12/06/2018 Usuário: CIDADAO
Autenticação:

Notes: This is an example of an property tax bill received by a household in 2018.

Although we do not have the data necessary to compute the compliance rate in other Brazilian municipalities, we can use publicly available data on municipal finances to calculate the property tax collection rate. This rate is defined as the ratio of total revenue collected to the total amount of property tax bills issued in a given city in a given year and can be used as a proxy for the compliance rate assuming that the distribution of property values is similar across Brazil. Figure A.4 shows the collection rates for property tax bills in large Brazilian municipalities in 2021. Two features of the figure stand out: relative to other large cities-particularly in the south-Manaus has a relatively low collection rate. However, its low collection rate is consistent with lower collection rates in much of the northern states of Brazil.

Figure A.3: Compliance is driven by the extensive margin

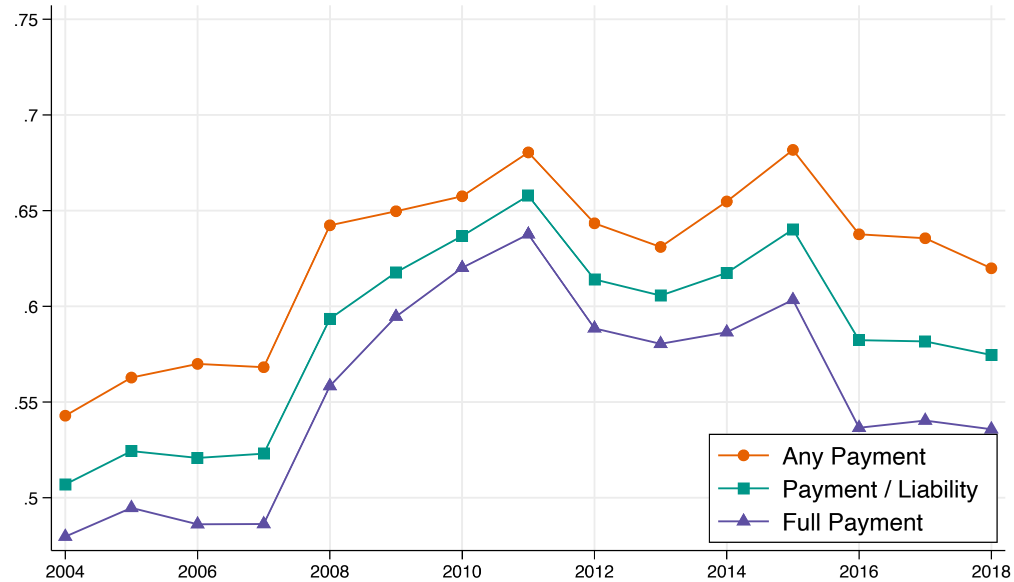

Notes: The figure shows the compliance rate by all non-exempt residential households in Manaus. The orange line depicts the fraction of households in a given year that paid at least a portion of their property tax bill. The purple line shows the fraction of households that paid the full amount of their property tax bill in a given year.

Figure A.4: Property tax collection rate among large Brazilian cities

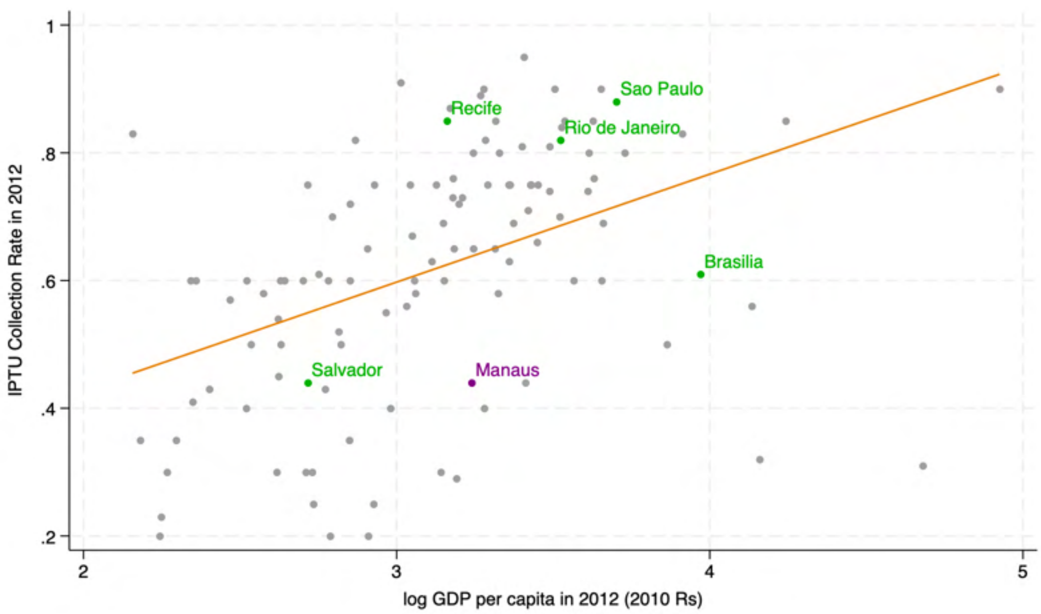

Notes: The figure shows the 2012 property tax (IPTU) collection rate for cities in Brazil with more than 200,000 residents. The collection rate is defined as the ratio of collected tax revenue to total property tax bills issued that year. Data on municipal GDP comes from the IBGE, and data on collection rates is from Carvalho Junior (2017).

Like property tax in other settings,[51] the IPTU is very salient to residents of Manaus. Of the two main taxes that can be levied by Brazilian municipalities, there is a stark contrast in citizen interest, as proxied by Google searches (see figure A.5). Whereas searches for the property tax (IPTU) are cyclical, with searches peeking at the beginning of the year when bills are sent out, there is very little search activity on the municipal tax on services (ISS).

FIGURE A.5: GOOGLE SEARCHES IN MANAUS - PROPERTY VERSUS SERVICE TAX

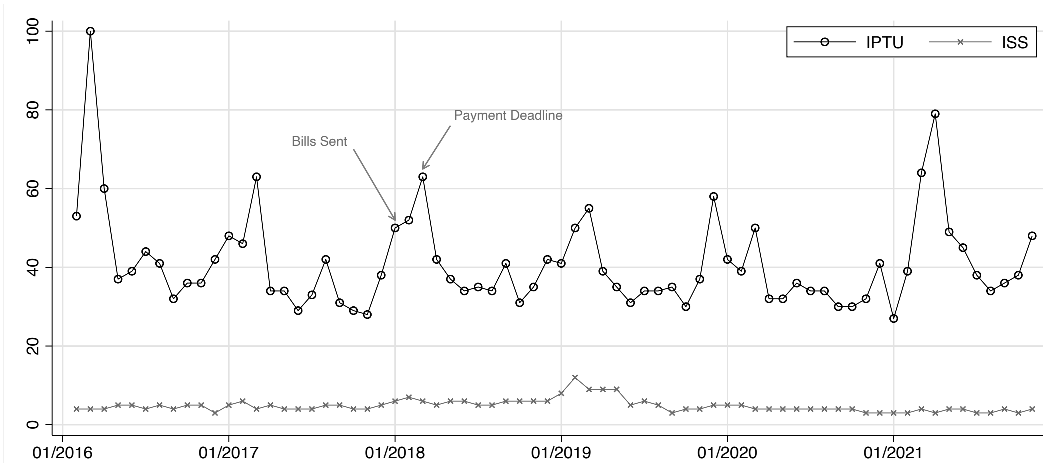

Notes: This figure shows the Google searched for two municipal tax: property tax (IPTU) and service tax (ISS). Data is restricted between two dates that have consistent measurement according to Google trends. Data query is from the state of Amazonas, Brazil, with 100% of searches from the city of Manaus.

[51]For example, Cabral & Hoxby (2012).

B Additional Background on the 2011 Reform

In 2011 the government of Manaus passed Law 1.628/2011, which implemented a reform to the property tax system by altering the calculation of both the building and land value for a given property. The impetus of this reform was to better reflect the (presumptive) property values in light of the significant growth in Manaus since the property tax was first implemented in 1983. Figure B.1 shows a timeline of satellite images of Manaus since 1984. Although the downtown core was already developed when the property tax was created, much of the growth in the city during the past 40 years took place in the northern section of the city. Many of the tax sectors that determine the square-meter rate were sparsely populated until the late 1990s, with rates that did not reflect the increasing real estate density, activity, and value.

Figure B.1: Growth of Manaus over 40 years through satellite imagery

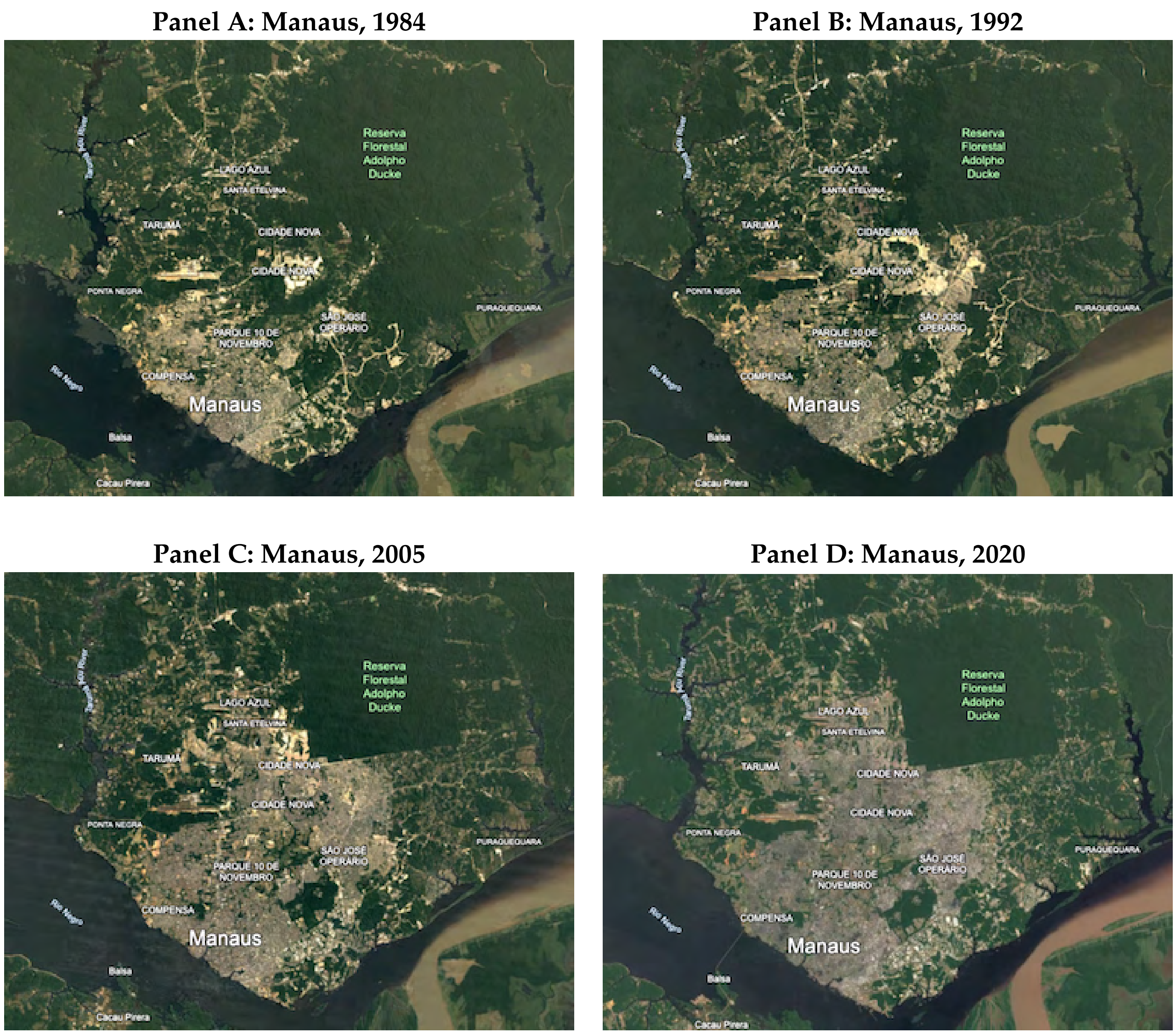

Notes: This figure shows the growth of Manaus from 1984 to 2020 using a time lapse of satellite images. Map data: © 2023 Google / Maxar Technologies, AirbusCNES, Airbus.

The reform was not designed to be a complete overhaul of the system, but rather an update to the existing presumptive formula. The formula used to calculate the property tax (equation 1) was unchanged, but the values for the land factors in $f_{ay}(\cdot)$ and building factors in $f_{by}(\cdot)$ were updated. Importantly for our empirical strategies, the reform included updates to the square-meter prices (p_s), with changes in the difference in rates across sector boundaries. Figure B.2 shows that for most residential properties in the city, the reform led to an increase in their tax bill.

FIGURE B.2: DISTRIBUTION OF CHANGES IN LOG TAX BILLS DUE TO THE 2011 REFORM

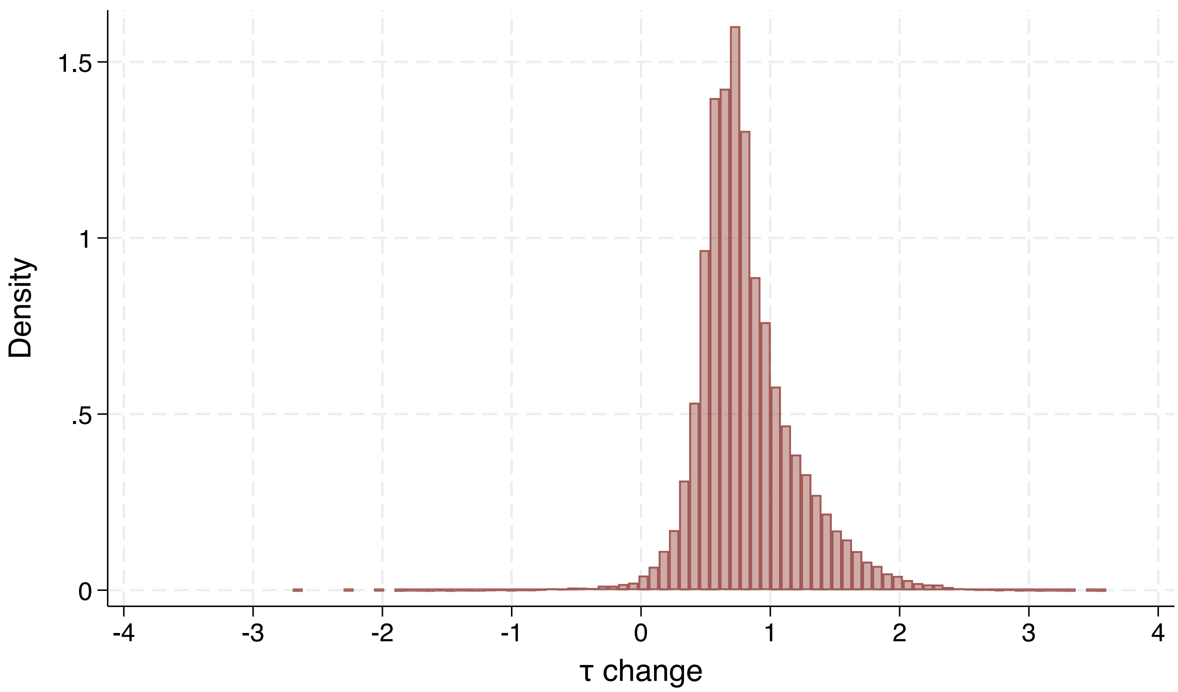

Notes: This figure shows the distribution of changes in the property tax bill for households in our study sample.

In addition to reflecting the growth of the city since 1983, the changes implemented through the reform were meant to improve progressivity in property taxes. Without updates to the relative rates paid by households across the city, richer households would face increasingly smaller tax burdens as their property values increased, but they did not face higher property tax bills. Figure B.3 panel A shows a weakening of tax progressivity in Manaus between the 2000 and 2010 census rounds, with a significant weakening of the relationship between the average tax bill and household income in a census tract.

However, the 2011 reform was partially successful in strengthening the progressivity of the property tax system. Panel B of figure B.3 shows the relationship between the tax bill and average household income across census tracts in Manaus for the last pre-reform tax year (2010) and the first year when the new tax bills were fully implemented (2016). Two features are worth noting: there is an upward shift in the curves, implying that tax bills increased for almost all households in the city. However, there is also a rotation of the curve, with a steeper relationship between income and the property tax in 2016, meaning that richer households faced a greater increase in their property taxes as a result of the reform.

Figure B.3: 2011 Reform Improves Targeting of Property Tax

Panel A: Liability-Income Gradient Pre-reform

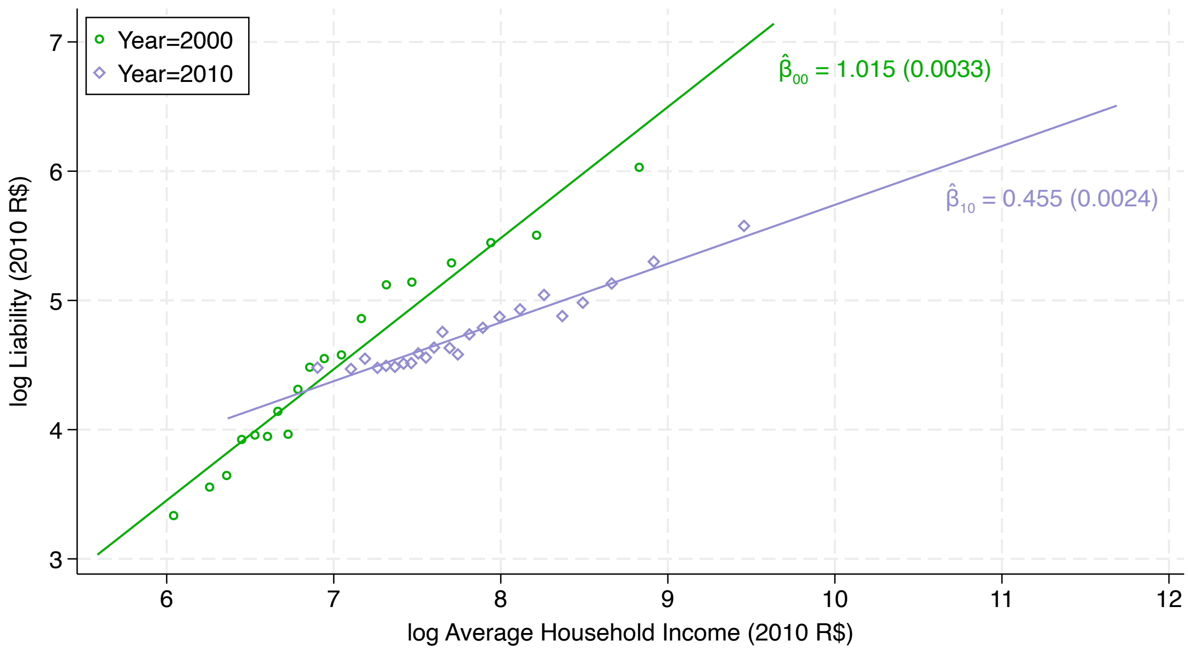

Panel B: Liability-Income Gradient Post-reform

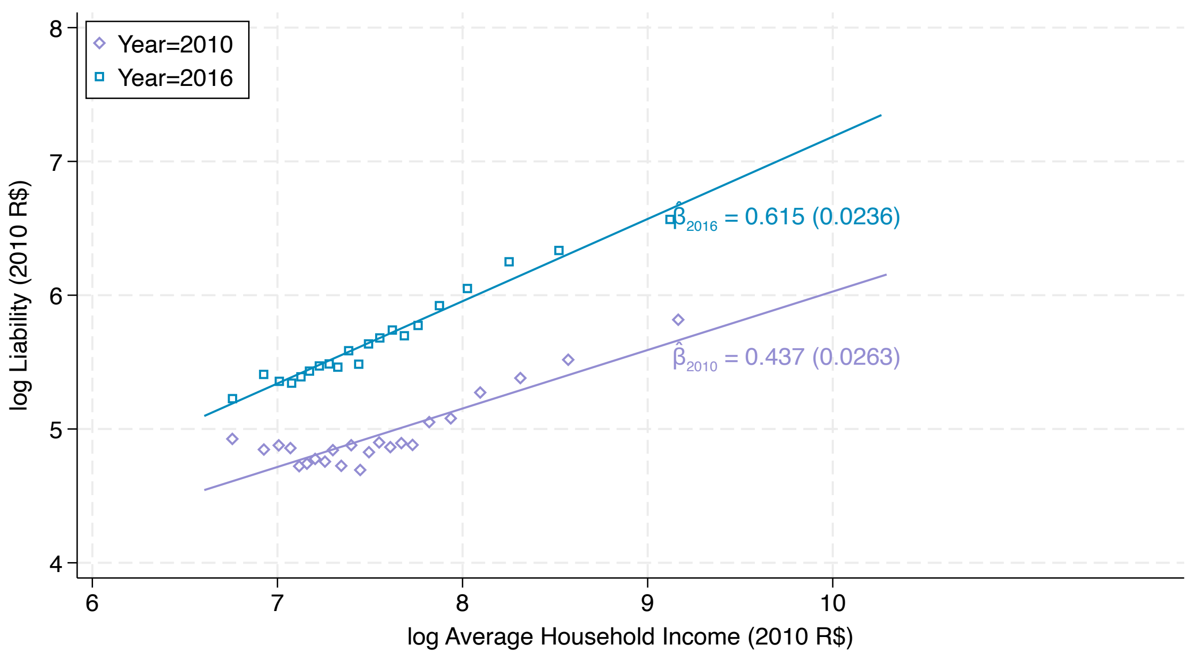

Notes: This figure plots the association between property tax liabilities and household income at the census-tract level. Data on census tract average income for 2010 and 2016 comes form the 2010 census, while data on 2000 household income coming from tracts from the 2000 census. We merge the census tracts to the IPTU administrative data geographically and compute average property tax liabilities for each census tract. For the 2000 liability we use the 2010 liability (adjusted for inflation) since the tax law was constant between 1983 and 2011.

C Creation of Distance Measure

In this section, we provide additional details on the construction of the distance measure employed in our Boundary Discontinuity Designs (BDD). Despite the numerous recent studies employing spatial discontinuities (Ring, 2024; Bayer *et al.*, 2007; Black, 1999; Livy, 2018; Gibbons *et al.*, 2013; Fack & Grenet, 2010; Turner *et al.*, 2014; Schönholzer, 2023; Keele & Titiunik, 2015), there is no consensus on the creation of the running variable (e.g. distance), especially in an urban setting.

Several features of our setting inform our decisions about the calculation of the distance measure. First, our level of observation is the property lot, which is often quite small relative to the tax sectors and Manaus as a whole. Second, property lots vary in size and are not uniform in their orientation to the sector boundaries; some sectors have lots that are oriented so that the short side of the lot is closest to the boundary, while other sectors have the long side of the lots running parallel to the boundary. Therefore, if one were to measure the distance of the lot to the boundary by taking the distance from the centroid of the lot polygon, there would be variation in the running variable that is not caused by the "true" distance of the property to the sector boundary, but is rather an artifact of the irregular shape and orientation of the lots relative to the street grid.

In addition to issues related to lot sizes across the city, the creation of the tax sector boundary requires careful consideration in our distance calculation. SEMEF defined the sector boundaries as (almost always) running through various streets in Manaus. However, street width varies throughout the city, with some streets used in the sector boundaries being wide avenues and others quite narrow side streets or alleys. Using the full width of the street would result in borders with varying thicknesses. Moreover, the shapefiles provided by SEMEF do not place the sector boundaries in the middle of the street, which means that the distance to households on different sides of the sector will depend on how accurately the government "drew" the polygons for the tax sectors.

To address these issues, we take the approach of constructing many transects along the sector boundaries to simulate an individual "walking" into a given sector. For each of these "walks" we record both which properties we run in to, as well as its distance along the walk. Given the shapefiles identifying the property lots and tax sector polygons, we take the following steps to estimate the distance to the boundary:

1. Remove all corners where three or more tax sectors intersect (*Note: this ensures that the transects are not generated at the edge case of a boundary*)

2. Divide sector boundaries into 500 meter long segments

3. Along the entire boundary, seed "nodes" every 10 meters

4. From each node, create a transect that is perpendicular to the boundary and has a distance of 300 meters into each sector

5. Identify points where a transect intersects the polygon of a lot (*Note: this usually generates two points per lot per transect – where the transect "enters" the lot, and where it "exits" the lot*)

6. Calculate the distance of each of these intersections to the transect node

FIGURE C.1: TRANSECT CREATION ACROSS SECTOR BOUNDARIES

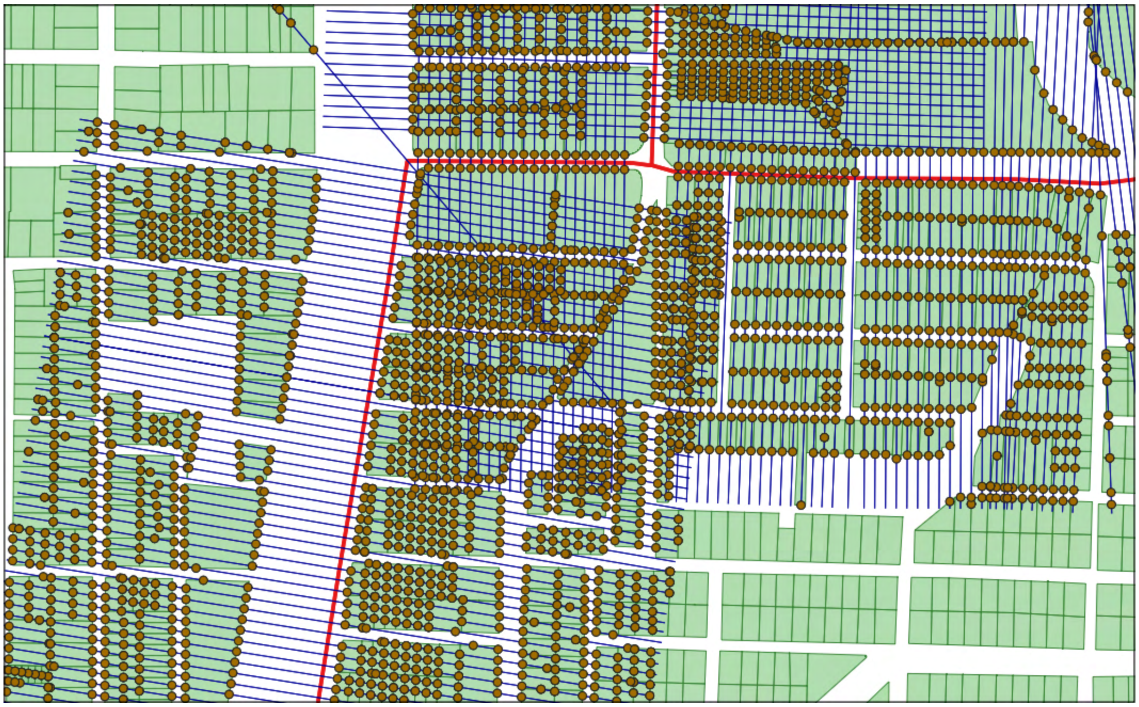

Notes: This figure depicts the calculation of the distance measure to the boundary used in our regression discontinuity analysis for a small section of Manaus. The red line denotes the tax sector boundary, the blue lines denote the transects generated perpendicular to the boundary, and the green polygons depict the lot lines for the properties. Transect lines are generated along the sector boundary in 10 meter intervals, with each transect extending perpendicularly into each side of the boundary for 300 meters. The yellow dots denote places where the transect intersect a lot–either through "entering" or "exiting" the lot.

Figure C.1 shows a small portion of the SEMEF shapefile after the above process is completed. It is important to note that since the transects were seeded every 10 meters along the boundary, there may be multiple transects that intersect a given property lot. Moreover, the sector boundary on the left side of the figure is drawn very close to one side of the (wide) street; without correcting this in the distance calculation, we would interpret the properties in the left sector as being farther away from the boundary, even though the properties on both sides of the boundary are on the street. To correct for this, we make the following post-calculation adjustments:

1. For each intersection point along the transect, remove the distance from the transect node to the first intersection point (*Note: this will "force" all properties nearest to the boundary to have a distance of zero to the boundary*)

2. For each lot, keep the smallest distance to the boundary

This creates a file of distances for 178,767 properties that are within 300 meters of a tax sector boundary, which we use as the base for our sample selection outlined in appendix K.

D Additional Background on Inequity Measure (σ)

In this section, we provide additional evidence for our measurement of inequity (σ) and its relationship to the direct tax paid by the household (τ). Figure D.1 shows the distribution of the inequity measure for households in our sample. The histogram shows a large amount of variation in the level of inequity faced by households of different sides of the tax sectors.

FIGURE D.1: DISTRIBUTION OF σ_i

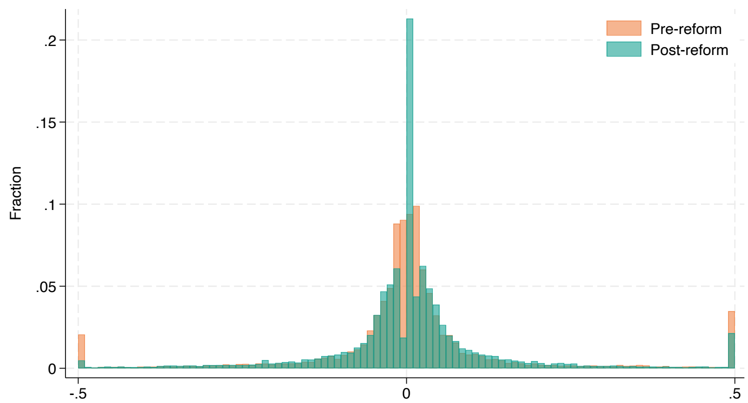

Although our measure of inequity is relative to a household's own tax liability, it is not collinear with it (figure D.2). The fact that households with the same tax liability face different levels of inequity allows us to isolate the effect of inequity in section 4.2.

FIGURE D.2: τ_i AND σ_i ARE NOT COLLINEAR

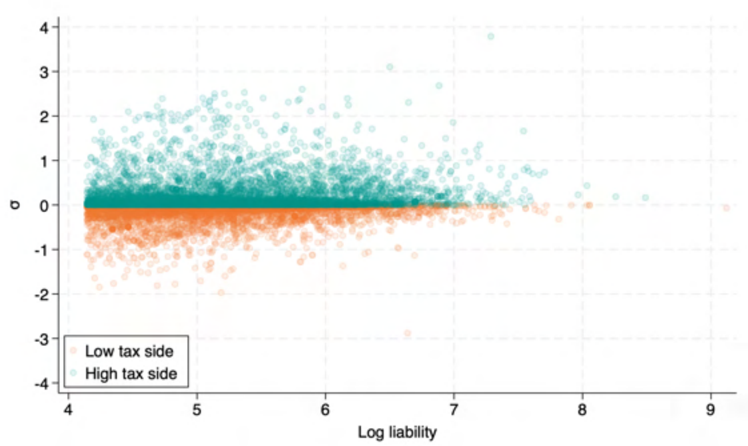

Note: This figure plots a household's (log) tax liability against its inequity value (σ). Properties in a sector with a higher square-meter price than the neighboring sector are defined as being on the "high tag side".

Our measure of inequity is partly driven by the observation that a household's response to its property tax bill is driven by whether it feels like they have been treated unfairly by the system, and does not capture whether a household cares about whether other people are treated fairly. Figure D.3 shows a typical post on social media of a household complaining about their tax bill. In the post, the resident highlights the inequity of the system in that she pays nearly double the property tax than her downstairs neighbor, even though they have similar apartments. This elicits a response from the government explaining that the 2011 reform caused property tax bills to increase throughout the city, and it is not targeted at specific individuals.

FIGURE D.3: EXAMPLE OF SOCIAL MEDIA POST HIGHLIGHTING INEQUITY IN IPTU BILLS

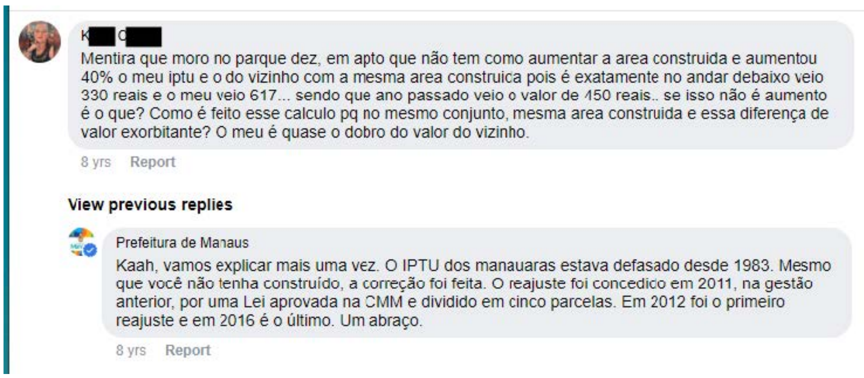

Notes: This is a social media post from a Manaus resident responding to a thread concerning the IPTU. The city directly responded to her post to explain the 2011 reform. Translated to English:

> **K C:** It's a lie that I live in Parque Dez, in an apartment where it's impossible to increase the built area, and my property tax (IPTU) increased by 40%, and so did my neighbor's, who has the same built area – it's exactly the apartment below mine – theirs came to 330 reais and mine came to 617... considering that last year the value was 150 reais... if that's not an increase, what is it? How is this calculation done because in the same complex, with the same built area, there's this exorbitant difference in value? Mine is almost double the value of my neighbor's.
>
> **Manaus City Hall:** Kaah, let's explain once again. The property tax for Manaus residents had been outdated since 1983. Even if you haven't built anything, the correction was made. The readjustment was granted in 2011, during the previous administration, by a Law approved in the City Council and divided into five installments. 2012 was the first readjustment and 2016 is the last. Best regards.

The reform generated so many disinformation posts that the government felt it necessary to make a post clarifying the rationale and implementation of the reform (figure D.4). It highlights that the increase in 2016 was part of the 2011 reform and was not targeted at individuals.

Figure D.4: Example of Social Media Response by the Government

Prefeitura de Manaus
Esclarecimentos sobre o IPTU

A Prefeitura de Manaus, por meio desta nota, esclarece, expressamente, que NÃO DECRETOU aumento nos valores do IPTU em 2016, como assinalam alguns blogs e páginas do Facebook, criadas nitidamente para disseminar informações falsas. O reajuste foi concedido em 2011 com a aprovação da Lei n.º 1.628, discutida, inclusive, na Câmara Municipal de Manaus (CMM), para ajustar o valor de metro quadrado de terrenos e construções e corrigir distorções no cálculo do Valor Venal dos imóveis. À época, o assunto foi bastante divulgado. Ou seja, a correção começou há quatro anos e foi feito em cinco parcelas.

Antes da lei, a última atualização da PGV da capital foi aplicada no ano de 1983. Com a planta defasada, além da renúncia de receita, havia graves distorções no cálculo.

Com a atualização, aproximadamente 75% dos contribuintes tributáveis, tiveram reajustes de 0% a 30%. Os outros imóveis sofreram reajustes de 30 a 100%.

Numericamente, apenas 986 contribuintes tiveram aumento acima dos padrões. Eram imóveis de alto padrão localizados na Ponta Negra e Tarumã que pagavam IPTU de aproximadamente R$ 100. A base era calculada pela PGV de 1983 que, na época, considerava essa área de Manaus como a menos valorizada.

A Prefeitura de Manaus está cumprindo uma decisão que foi tomada em 2011, na gestão passada, sob pena de sofrer sanções na Justiça. A primeira parcela da correção aconteceu em 2012 e em 2016 ocorre a última. Compartilhe.

Ajude a combater falsas informações.

Timeline photos · 7 Mar 2016 ·

View full size

Notes: A social media post on the city of Manaus's official social media page that attempts to address the spread of misinformation on the 2011 property tax reform. Translated to English:

> **Manaus City Hall:** Manaus Clarifications regarding Property Tax (IPTU) The Manaus City Hall, through this statement, expressly clarifies that it DID NOT DECREE an increase in property tax values in 2016, as indicated by some blogs and Facebook pages, clearly created to spread false information. The adjustment was granted in 2011 with the approval of Law No. 1,628, which was even discussed in the Manaus City Council (CMM), to adjust the value per square meter of land and buildings and correct distortions in the calculation of the market value of properties. At the time, the matter was widely publicized. That is, the correction began four years ago and was done in five installments.
>
> Before the law, the last update of the capital's General Property Valuation (PGV) was applied in 1983. With the outdated valuation, in addition to revenue loss, there were serious distortions in the calculation.
>
> With the update, approximately 75% of taxable taxpayers had adjustments of 0% to 30%. The other properties underwent adjustments of 30 to 100%.
>
> Numerically, only 986 taxpayers had increases above the standards. These were high-end properties located in Ponta Negra and Tarumã that paid approximately R$ 100 in property tax. The base was calculated using the 1983 PGV, which at the time considered this area of Manaus as the least valued.
>
> The Manaus City Hall is complying with a decision that was made in 2011, during the previous administration, under penalty of facing sanctions in court. The first installment of the correction occurred in 2012 and the last one will occur in 2016. Share
>
> Help combat false information.

E Proof of Proposition 1

Proof. To see that the optimal property tax satisfies (2), note that without mistagging, social welfare is

$$W = \omega_L V_{Ll} + \omega_H V_{Hh} + B(r) \tag{E.1}$$

The government chooses T_l and T_h to maximize W subject to its constraint that $r = c_L T_l + c_H T_h$. Without inequity, household compliance decisions depend only on the tax that they face and so the (normalized) social marginal welfare effects of changes in the two taxes are

$$\frac{dW}{dT_l}\frac{1}{b(r)} = \frac{\omega_L}{b(r)}\frac{\partial V_{Ll}}{\partial T_l} + \frac{dr}{dT_l} = 0$$
$$\frac{dW}{dT_h}\frac{1}{b(r)} = \frac{\omega_H}{b(r)}\frac{\partial V_H}{\partial T_h} + \frac{dr}{dT_h} = 0$$

with marginal revenue effects

$$\frac{dr}{dT_l} = c_{Ll} + \frac{dc_{Ll}}{dT_l}T_l = c_{Ll}(1-\varepsilon)$$
$$\frac{dr}{dT_h} = c_{Hh} + \frac{dc_{Hh}}{dT_h}T_h = c_{Hh}(1-\varepsilon)$$

The marginal private welfare effects are

$$\frac{\partial V_{\theta\phi}}{\partial T_\phi} = -c_{\theta\phi}u'(y_\theta - T_\phi) \simeq -c_{\theta\phi}u'(y_\theta)\left(1+\rho\frac{T_\phi}{y_\theta}\right) \tag{E.2}$$

where we approximate marginal utility using $u'(y_\theta - T_\phi) \simeq u'(y_\theta)(1+\rho T_\phi/y_\theta)$, where $\rho \equiv -u''(x)\,x/u'(x)$ is the coefficient of relative risk aversion (Chetty, 2006). Combining these elements, the optimal property taxes satisfy the first order conditions

$$\frac{dW}{dT_l}\frac{1}{b(r)} = -g_L\left(1+\rho\frac{T_l}{y_L}\right)c_L + c_L(1-\varepsilon) = 0 \tag{E.3}$$
$$\frac{dW}{dT_h}\frac{1}{b(r)} = -g_H\left(1+\rho\frac{T_h}{y_H}\right)c_H + c_H(1-\varepsilon) = 0 \tag{E.4}$$

Solving equations (E.3) and (E.4) yields the expressions in (2) in Lemma 1.

To see that the level of taxation is lower the stronger are behavioral responses, note that differentiation of (2) shows that both taxes are lower when ε is higher. Since the private marginal welfare effects are strictly negative, the optimum is on the increasing side of the Laffer curve and so tax revenues also decrease.

To see that the progressivity of the tax is increasing in the relative welfare weights, combine the two expressions in (2) and rearrange so that we can relate the progressivity of the tax schedule to the ratio of the welfare weights:

$$\frac{g_L}{g_H} = \frac{1+\rho T_h/y_H}{1+\rho T_l/y_L}$$

Similarly, we can combine the two expressions in (2) to relate the progressivity of the tax schedule to the compliance elasticity:

$$\frac{T_h/y_H}{T_l/y_L} = 1 + \frac{\left(\frac{g_L}{g_H} - 1\right)(1-\varepsilon)}{1-\varepsilon-g_L}$$

Differentiating with respect to ε shows that the progressivity of the optimal tax schedule is increasing in the compliance elasticity. $\square$

F Proof of Proposition 2

Proof. Social welfare with mistagging is

$$W = \psi\omega_L V_{Lh} + (1-\psi)\,\omega_L V_{Ll} + \omega_H V_{Hh} + B(r) \tag{F.1}$$

where the private welfare of the θ-types with the ϕ tag is

$$V_{\theta\phi} = \int_{-\infty}^{\gamma^\star_{\theta\phi}} \big(u(y_\theta) - \gamma\big) dF(\gamma) + \int_{\gamma^\star_{\theta\phi}}^{\infty} \big(u(y_\theta - T_\phi) - d(\sigma)\big) dF(\gamma) \tag{F.2}$$

The optimal tax schedule satisfies $dW/dT_l = dW/dT_h = 0$.

Starting with the government's budget, total revenue is

$$r = \psi c_{L,h} T_h + (1-\psi)\, c_{L,l} T_l + c_{H,h} T_h$$

and the effects of changes in taxes on tax revenue are:

$$\begin{aligned}
\frac{dr}{dT_h} &= \psi\left(c_{L,h} + \frac{dc_{L,h}}{dT_h}T_h\right) + c_{H,h} + \frac{dc_{H,h}}{dT_h}T_h \\
&= \psi c_{L,h}(1-\varepsilon-\eta) + c_{H,h}(1-\varepsilon) \\
\frac{dr}{dT_l} &= \psi\frac{dc_{L,h}}{dT_l}T_h + (1-\psi)\left(c_{L,l} + \frac{dc_{L,l}}{dT_l}T_l\right) \\
&= \psi c_{L,h}\eta\sigma + (1-\psi)\, c_{L,l}(1-\varepsilon)
\end{aligned}$$

For the $\{Ll\}$ and the $\{Hh\}$ types, the marginal private welfare effects of a small change in the tax liability are as in equation (E.2) in the the proof of lemma 1 in appendix E. However, for the $\{Lh\}$ types we now have marginal welfare effects

$$\begin{aligned}
\frac{dV_{Lh}}{dT_l} &= \int_{\gamma^\star_{Lh}}^{\infty} -d'(\sigma)\frac{\partial\sigma}{\partial T_l} dF = c_{L,h} d'(\sigma)\frac{T_h}{T_l^2} \\
&\simeq c_{L,h} u'(y_L - T_h)\frac{\eta}{\varepsilon}\frac{T_h}{T_l} \simeq c_{L,h} u'(y_L)\left[1 + \rho\frac{T_h}{y_L}\right]\frac{\eta}{\varepsilon}\sigma \qquad \text{(F.3)} \\
\frac{dV_{Lh}}{dT_h} &= \int_{\gamma^\star_{Lh}}^{\infty}\left[-u'(y_L - T_h) - d'(\sigma)\frac{\partial\sigma}{\partial T_h}\right] = -c_{Lh}\left[u'(y_L - T_h) + d'(\sigma)\frac{\partial\sigma}{\partial T_h}\right] \\
&\simeq -c_{Lh} u'(y_L - T_h)\left(1 + \frac{\eta}{\varepsilon}\right) \simeq -c_{L,h} u'(y_L)\left[1 + \rho\frac{T_h}{y_L}\right]\left(1 + \frac{\eta}{\varepsilon}\right) \qquad \text{(F.4)}
\end{aligned}$$

where we have approximated marginal utility around y_L using $u'(y) \simeq u'(y_L)\left(1 - \rho\frac{y-y_L}{y_L}\right)$. We also follow Allcott & Taubinsky (2015) and Brockmeyer *et al.* (2023) to express the marginal disutility of inequity in money-metric terms. To see this, note that

$$\begin{aligned}
\varepsilon &\equiv -\frac{\partial c_{Lh}}{\partial T_h}\frac{T_h}{c_{Lh}} = \frac{f\left(\gamma^\star_{L,h}\right)}{1-F\left(\gamma^\star_{Lh}\right)}\frac{\partial \gamma^\star_{Lh}}{\partial T_h}T_h = \frac{f\left(\gamma^\star_{Lh}\right)}{1-F\left(\gamma^\star_{Lh}\right)}u'\left(y_L - T_h\right)T_h \\
\eta &\equiv -\frac{\partial c_{Lh}}{\partial \sigma}\frac{\sigma}{c_{Lh}} = \frac{f\left(\gamma^\star_{Lh}\right)}{1-F\left(\gamma^\star_{Lh}\right)}\frac{\partial \gamma^\star_{Lh}}{\partial \sigma}\sigma = \frac{f\left(\gamma^\star_{Lh}\right)}{1-F\left(\gamma^\star_{Lh}\right)}d'\left(\sigma\right)\sigma \\
&\Leftrightarrow d'\left(\sigma\right) = \frac{\eta}{\varepsilon}u'\left(y_L - T_h\right)T_l
\end{aligned}$$

Mistagged households have higher marginal utility for two reasons. First, they face higher taxes, reducing consumption and raising marginal utility T_h/y_L (the $\rho\frac{T_l}{y_L}\sigma$ term in the square brackets). Second, they experience disutility from inequity, with money-metric equivalent $(\eta/\varepsilon)\,u'T_l$. Increases in T_h aggravate both of these forces, so $dV_{Lh}/dT_h < 0$. However, even though mistagged households don't face the tax T_l, increases in T_l reduce inequity σ, improving their welfare: $dV_{Lh}/dT_l > 0$.

Combining these elements, we can see that the (normalized) marginal social welfare effects are:

$$\begin{aligned}
\frac{dW}{dT_l}\frac{1}{b\left(r\right)} &= \frac{\omega_L}{b\left(r\right)}\psi\frac{dV_{L,h}}{dT_l} + \frac{\omega_L}{b\left(r\right)}\left(1-\psi\right)\frac{dV_{L,l}}{dT_l} + \frac{dr}{dT_l} \\
&\simeq g_L\psi c_{L,h}\left[1+\rho\frac{T_l}{y_L}\sigma\right]\frac{\eta}{\varepsilon}\sigma - g_L\left(1-\psi\right)c_{L,l}\left[1+\rho\frac{T_l}{y_L}\right] + \left[\psi c_{L,h}\eta\sigma + \left(1-\psi\right)c_{L,l}\left(1-\varepsilon\right)\right]
\end{aligned} \tag{F.5}$$

$$\begin{aligned}
\frac{dW}{dT_h}\frac{1}{b\left(r\right)} &= \frac{\omega_L}{b\left(r\right)}\psi\frac{dV_{L,h}}{dT_h} + \frac{\omega_H}{b\left(r\right)}\frac{dV_{H,h}}{dT_h} + \frac{dr}{dT_h} \\
&\simeq -g_L\psi c_{L,h}\left[1+\rho\frac{T_h}{y_L}\right]\left(1+\frac{\eta}{\varepsilon}\right) - g_H c_{H,h}\left[1+\rho\frac{T_h}{y_H}\right] + \left[\psi c_{L,h}\left(1-\varepsilon-\eta\right) + c_{H,h}\left(1-\varepsilon\right)\right]
\end{aligned} \tag{F.6}$$

Dividing (F.5) and (F.6) by the number of taxpayers of each tax, these can be written as

$$\frac{dW}{dT_l}\frac{1}{b\left(r\right)}\frac{1}{\left(1-\psi\right)c_{Ll}} \simeq g_L\varphi_l\left[1+\rho\frac{T_l}{y_L}\sigma\right]\frac{\eta}{\varepsilon}\sigma - g_L\left[1+\rho\frac{T_l}{y_L}\right] + \varphi_l\eta\sigma + \left(1-\varepsilon\right) = 0 \tag{F.7}$$

$$\begin{aligned}
\frac{dW}{dT_h}\frac{1}{b\left(r\right)}\frac{1}{\psi c_{Lh}+c_{Hh}} &\simeq -g_L\varphi_h\left[1+\rho\frac{T_h}{y_L}\right]\left(1+\frac{\eta}{\varepsilon}\right) - g_H\left(1-\varphi_h\right)\left[1+\rho\frac{T_h}{y_H}\right] \\
&\quad + \varphi_h\left(1-\varepsilon-\eta\right) + \left(1-\varphi_h\right)\left(1-\varepsilon\right) = 0
\end{aligned} \tag{F.8}$$

where $\varphi_l = \psi c_{Lh}/(1-\psi)c_{Ll}$ is the number of mistagged L households relative to the number of l-tax taxpayers; and $\varphi_h = \psi c_{Lh}/\left(\psi c_{Lh} + c_{Hh}\right)$ is the number of mistagged L households relative to the number of h-tax taxpayers.

Rearranging (F.7) and (F.8) yields the expressions in equation (3) for the optimal tax schedule in proposition 2. Applying the implicit function theorem to the system of equations (F.7) and (F.8) yields the comparative static statements in proposition 2. □

G Model with Undertagging and Overtagging

This appendix presents the details of the model briefly discussed in section 3.3.1.

We generalize the model in section 3.2 in two ways. First, we allow for a fraction $\psi_{Hl} \geq 0$ of H-type households to be undertagged with the l tag (in addition to the fraction ψ_{Lh} of overtagged L-types). This creates a fourth group of households whose compliance and marginal welfare effects we need to incorporate into the analysis. Second, we allow undertagged and overtagged households to have different elasticities of compliance with respect to inequity. Undertagged households' elasticity is η_{Hl} while overtagged households' elasticity is η_{Lh}. This is important since our empirical evidence in section 5.3 suggests that undertagged households do not respond to inequity ($\eta_{Hl} = 0$), only overtagged households do.

Undertagged households' compliance responds to both T_h and T_l. Specifically,

$$\begin{aligned}
\frac{dc_{Hl}}{dT_h} &= \frac{\partial c_{Hl}}{\partial \sigma_{Hl}}\frac{\partial \sigma_{Hl}}{\partial T_h} = \frac{c_{Hl}}{\sigma_{Hl}}\eta_{Hl}\frac{T_l}{T_h^2} = \frac{c_{Hl}}{T_h}\eta_{Hl} \\
\frac{dc_{Hl}}{dT_l} &= \frac{\partial c_{Hl}}{\partial T_l} + \frac{\partial c_{Hl}}{\partial \sigma_{Hl}}\frac{\partial \sigma_{Hl}}{\partial T_l} = -\varepsilon\frac{c_{Hl}}{T_l} - \eta_{Hl}\frac{c_{Hl}}{\sigma_{Hl}}\frac{1}{T_h} = -\frac{c_{Hl}}{T_l}\left(\varepsilon + \eta_{Hl}\right)
\end{aligned}$$

We can also connect the marginal disutility of inequity and the marginal utility of consumption for this fourth group:

$$\begin{aligned}
\gamma^\star_{Hl} &= u\left(y_H\right) - u\left(y_H - T_l\right) + d\left(\sigma_{Hl}\right) \qquad \frac{\partial \gamma^\star_{Hl}}{\partial T_l} = u'\left(y_H - T_l\right) \qquad \frac{\partial \gamma^\star_{Hl}}{\partial \sigma_{Hl}} = d'\left(\sigma_{Hl}\right) \\
\varepsilon &\equiv -\frac{\partial c_{Hl}}{\partial T_l}\frac{T_l}{c_{Hl}} = \frac{f\left(\gamma^\star_{Hl}\right)}{1 - F\left(\gamma^\star_{Hl}\right)}\frac{\partial \gamma^\star_{Hl}}{\partial T_l}T_l \qquad \eta_{Hl} \equiv -\frac{\partial c_{Hl}}{\partial \sigma_{Hl}}\frac{\sigma_{Hl}}{c_{Hl}}\frac{f\left(\gamma^\star_{Hl}\right)}{1 - F\left(\gamma^\star_{Hl}\right)}\frac{\partial \gamma^\star_{Hl}}{\partial \sigma_{Hl}}\sigma_{Hl} \\
\leftrightarrow d'\left(\sigma_{Hl}\right) &= \frac{\eta_{Hl}}{\varepsilon}u'\left(y_H - T_l\right)T_h
\end{aligned}$$

Incorporating the undertagged housholds, the revenue from taxation now becomes:

$$r = \psi_{Lh}c_{Lh}T_h + (1-\psi_{Lh})c_{Ll}T_l + \psi_{Hl}c_{Hl}T_l + (1-\psi_{Hl})c_{Hh}T_h$$

and the effects of tax changes are:

$$\begin{aligned}
\frac{dr}{dT_h} &= \psi_{Lh}\left(c_{Lh} + \frac{dc_{Lh}}{dT_h}T_h\right) + \psi_{Hl}\frac{dc_{Hl}}{dT_h}T_l + (1-\psi_{Hl})\left(c_{H,h} + \frac{dc_{Hh}}{dT_h}T_h\right) \\
&= \psi_{Lh}c_{Lh}\left(1 - \varepsilon - \eta_{Lh}\right) + \psi_{Hl}c_{Hl}\eta_{Hl}\frac{1}{\sigma} + (1-\psi_{Hl})c_{Hh}\left(1-\varepsilon\right) \\
\frac{dr}{dT_l} &= \psi_{Lh}\frac{dc_{Lh}}{dT_l}T_h + (1-\psi_{Lh})\left(c_{Lh} + \frac{dc_{Ll}}{dT_l}T_l\right) + \psi_{Hl}\left(c_{Hl} + \frac{dc_{Hl}}{dT_l}T_l\right) \\
&= \psi_{Lh}c_{Lh}\eta\sigma + (1-\psi_{Lh})c_{Ll}(1-\varepsilon) + \psi_{Hl}c_{Hl}(1-\varepsilon-\eta_{Hl})
\end{aligned}$$

where $\sigma = T_h/T_l$ is the extent of inequity (but note that $\sigma_{Hl} = 1/\sigma$ while $\sigma_{Lh} = \sigma$).

The undertagged H-type households have private welfare:

$$V_{Hl} = \int_{-\infty}^{\gamma^\star_{Hl}}\left[u\left(y_H\right) - \gamma\right]dF\left(\gamma\right) + \int_{\gamma^\star_{Hl}}^{\infty}\left[u\left(y_H - T_l\right) - d\left(\sigma_{Hl}\right)\right]dF\left(\gamma\right)$$

with marginal welfare effects:

$$\frac{dV_{Hl}}{dT_l} = \int_{\gamma^\star_{Hl}}^{\infty} \left[-u'\left(y_H - T_l\right) - d'\left(\sigma_{Hl}\right)\frac{\partial \sigma_{Hl}}{\partial T_l}\right] dF\left(\gamma\right) = -c_{Hl}\left[u'\left(y_H - T_l\right) + d'\left(\sigma_{Hl}\right)\frac{1}{T_h}\right]$$
$$\simeq -c_{Hl}u'\left(y_H - T_l\right)\left(1 + \frac{\eta_{Hl}}{\varepsilon}\right) \simeq -c_{Hl}u'\left(y_H\right)\left[1 + \rho\frac{T_l}{y_H}\right]\left(1 + \frac{\eta_{Hl}}{\varepsilon}\right)$$
$$\frac{dV_{Hl}}{dT_h} = \int_{\gamma^\star_{Hl}}^{\infty} -d'\left(\sigma_{Hl}\right)\frac{\partial \sigma_{Hl}}{\partial T_h} dF\left(\gamma\right) = c_{Hl}d'\left(\sigma_{Hl}\right)\frac{T_l}{T_h^2}$$
$$\simeq c_{Hl}u'\left(y_H - T_l\right)\frac{\eta_{Hl}}{\varepsilon}\frac{T_l}{T_h} \simeq c_{Hl}u'\left(y_H\right)\left[1 + \rho\frac{T_l}{y_H}\right]\frac{\eta_{Hl}}{\varepsilon}\frac{1}{\sigma}$$

Combining these elements, we can see that the marginal social welfare effects are:

$$W = \omega_L\psi_{Lh}V_{Lh} + \omega_L\left(1-\psi_{Lh}\right)V_{Ll} + \omega_H\psi_{Hl}V_{Hl} + \omega_H(1-\psi_{Hl})V_{Hh} + B\left(r\right)$$
$$\frac{dW}{dT_l}\frac{1}{b\left(r\right)} = \omega_L\psi_{Lh}\frac{dV_{Lh}}{dT_l} + \omega_L\left(1-\psi_{Lh}\right)\frac{dV_{Ll}}{dT_l} + \omega_H\psi_{Hl}\frac{dV_{Hl}}{dT_l} + \frac{dr}{dT_l}$$
$$\simeq g_L\psi_{Lh}c_{Lh}\left[1+\rho\frac{T_h}{y_L}\right]\frac{\eta_{Lh}}{\varepsilon}\sigma - g_L\left(1-\psi_{Lh}\right)c_{Ll}\left(1+\rho\frac{T_l}{y_L}\right)$$
$$- g_H\psi_{Hl}c_{Hl}\left[1+\rho\frac{T_l}{y_H}\right]\left(1+\frac{\eta_{Hl}}{\varepsilon}\right)$$
$$+ \left[\psi_{Lh}c_{Lh}\eta_{Lh}\sigma + (1-\psi_{Lh})c_{Ll}(1-\varepsilon) + \psi_{Hl}c_{Hl}(1-\varepsilon-\eta_{Hl})\right]$$
$$\frac{dW}{dT_h}\frac{1}{b\left(r\right)} = \omega_L\psi_{Lh}\frac{dV_{Lh}}{dT_h} + \omega_H\psi_{Hl}\frac{dV_{Hl}}{dT_h} + \omega_H(1-\psi_{Hl})\frac{dV_{Hh}}{dT_h} + \frac{dr}{dT_h}$$
$$\simeq -g_L\psi_{Lh}c_{Lh}\left[1+\rho\frac{T_h}{y_L}\right]\left(1+\frac{\eta_{Lh}}{\varepsilon}\right) + g_H\psi_{Hl}c_{Hl}\left[1+\rho\frac{T_l}{y_H}\right]\frac{\eta_{Hl}}{\varepsilon}\frac{1}{\sigma}$$
$$- g_H(1-\psi_{Hl})c_{Hh}\left(1+\rho\frac{T_h}{y_H}\right)$$
$$+ \left[\psi_{Lh}c_{Lh}\left(1-\varepsilon-\eta_{Lh}\right) + \psi_{Hl}c_{Hl}\eta_{Hl}\frac{1}{\sigma} + (1-\psi_{Hl})c_{Hh}\left(1-\varepsilon\right)\right]$$

Rearranging these yields the expressions for the optimal tax schedule:

$$\frac{T_l}{y_L} = \frac{1-\varepsilon-\bar{g}_l + \varphi_{Ll}\frac{\eta_{Lh}}{\varepsilon}\sigma\left(g_L+\varepsilon\right) - \varphi_{Hl}\frac{\eta_{Hl}}{\varepsilon}\left(g_H+\varepsilon\right)}{\rho\left(\bar{g}_l + g_H\varphi_{Hl}\left[\left(1+\frac{\eta_{Hl}}{\varepsilon}\right)\frac{y_L}{y_H}-1\right] - g_L\varphi_{Ll}\frac{\eta_{Lh}}{\varepsilon}\sigma^2\right)} \tag{G.1}$$
$$\frac{T_h}{y_H} = \frac{1-\varepsilon-\bar{g}_h + \varphi_{Hh}\frac{\eta_{Hl}}{\varepsilon}\frac{1}{\sigma}\left(g_H+\varepsilon\right) - \varphi_{Lh}\frac{\eta_{Lh}}{\varepsilon}\left(g_L+\varepsilon\right)}{\rho\left(\bar{g}_h + g_L\varphi_{Lh}\left[\left(1+\frac{\eta_{Lh}}{\varepsilon}\right)\frac{y_H}{y_L}-1\right] - g_H\varphi_{Hh}\frac{\eta_{Hl}}{\varepsilon}\frac{1}{\sigma^2}\right)} \tag{G.2}$$

where $\sigma = T_h/T_l$; $\bar{g}_l = \frac{(1-\psi_{Lh})c_{Ll}g_L + \psi_{Hl}c_{Hl}g_H}{(1-\psi_{Lh})c_{Ll} + \psi_{Hl}c_{Hl}}$ is the average social marginal welfare weight of l-tax taxpayers, and analogously $\bar{g}_h = \frac{\psi_{Lh}c_{Lh}g_L + (1-\psi_{Hl})c_{Hh}g_H}{\psi_{Lh}c_{Lh} + (1-\psi_{Hl})c_{Hh}}$ is the average social marginal welfare weight of h-tax taxpayers; and the $\varphi_{\theta\phi}$ terms are the number of mistagged θ-types as a fraction of the number of ϕ-tax taxpayers (e.g., $\varphi_{Lh} = \frac{\psi_{Lh}c_{Lh}}{\psi_{Lh}c_{Lh}+(1-\psi_{Hl})c_{Hh}}$ and $\varphi_{Hh} = \frac{\psi_{Hl}c_{Hl}}{\psi_{Lh}c_{Lh}+(1-\psi_{Hl})c_{Hh}}$).

The three forces discussed in proposition 2 in the context of the baseline model with only mistagging of L-types are present now also for the mistagged H-types. First, the l-tag group now includes mistagged H-types, and the h-tag group includes fewer H-types. This lowers the marginal welfare cost of taxing the l-tag group ($\bar{g}_l < g_L$) and further increases the marginal welfare cost of taxing the h-tag group ($\bar{g}_h > g_H$), driving the planner to increase T_l relative to T_h, thereby reducing progressivity.

Second, the $\varphi_{\theta\phi}$ terms in the numerators account for direct utility losses and the fiscal externality. The $\varphi_{L\phi}$ terms push towards less progressive taxes while the $\varphi_{H\phi}$ terms push towards more progressive taxes. Third, the $\varphi_{\theta\phi}$ terms in the denominators account for the higher marginal utility of consumption of overtagged households and the lower marginal utility of undertagged households. Again, the $\varphi_{L\phi}$ terms push towards less progressive taxes while the $\varphi_{H\phi}$ terms will tend to imply more progressive taxes.[52]

This suggests that the overall effect on the tax schedule is ambiguous and depends on the magnitudes of the parameters (the extent of mistagging of the two types $\psi_{\theta\phi}$, the elasticities $\eta_{\theta\phi}$, and the property values y_θ). However, for reasonable parameter values (e.g. if we consider $\eta_{Lh} \geq \eta_{Hl}$ and $\varphi_{Lh} = \varphi_{Hl}$), all three forces are weaker for the mistagged H-types than for the mistagged L-types, suggesting that the net effects will still be in the directions highlighted by proposition 2.[53] Moreover, as we show in section 5.3, our empirical evidence suggests that the elasticity of compliance with respect to undertagging, η_{Hl} is zero, in which case the net effect is unambiguously towards more progressive taxes. In this case, (G.1) and (G.2) become

$$\begin{aligned} \frac{T_l}{y_L} &= \frac{1 - \varepsilon - \bar{g}_l + \varphi_{Ll} \frac{\eta_{Lh}}{\varepsilon} \sigma \left(g_L + \varepsilon \right)}{\rho \left(\bar{g}_l + g_H \varphi_{Hl} \left(\frac{y_L}{y_H} - 1 \right) - g_L \varphi_{Ll} \frac{\eta_{Lh}}{\varepsilon} \sigma^2 \right)} \\ \frac{T_h}{y_H} &= \frac{1 - \varepsilon - \bar{g}_h - \varphi_{Lh} \frac{\eta_{Lh}}{\varepsilon} \left(g_L + \varepsilon \right)}{\rho \left(\bar{g}_h + g_L \varphi_{Lh} \left[\left(1 + \frac{\eta_{Lh}}{\varepsilon} \right) \frac{y_H}{y_L} - 1 \right] \right)} \end{aligned}$$

and we see that now all the additional terms push towards less progressive taxes.

[52] The term including φ_{Hl} can be negative (pushing towards less progressive taxes) if η_{Hl}/ε or y_L/y_H are small.

[53] To see this, consider the case of the $\varphi_{\theta\phi}$ terms in the numerator of equation (G.1) for T_l. These push towards a less progressive tax (as in the baseline case in proposition 2) whenever the φ_{Lh} term is larger than the φ_{Hl} term. This is likely because first, the positive φ_{Lh} term is multiplied by $\sigma \geq 1$ while the negative φ_{Hl} term is not; and second, because the φ_{Lh} term depends on the social marginal welfare weight of the L-types, g_L, which is larger than the social marginal welfare weight of the H-types, g_H, appearing in the negative φ_{Hl}. As a result, for the force from the mistagged H-types to dominate, it would need to be the case that they are a large group (large φ_{Hl}) and/or that they are much more sensitive to inequity than the mistagged L-types ($\eta_{Hl} > \eta_{Lh}$). Analogous reasoning applies to the numerator of (G.2) and to the $\varphi_{\theta\phi}$ terms in the denominators of (G.1) and (G.2).

H Model with Location Choice and Endogenous House Prices

This appendix presents the details of the model briefly discussed in section 3.3.2. In section H.1 we present a micro-founded model of residential location choice, while in section H.2 we study the welfare implications and optimal policy.

H.1 Location Choice

We consider an extension of the model in section 3.2, in which households first choose where to live and then whether to pay the corresponding property tax. Households are still characterized by similar traits as in section 3.2. They have an evasion cost γ that governs how much utility they lose from evading the tax, and they are of the L-type living in L-type houses with value of housing services v_L or of the H-type living in H-type houses with value of housing services $v_H > v_L$. The key difference is that L-type households can choose to live in L-type houses located in areas with the l tag or the h tag, and they have idiosyncratic preferences for the two types of area ξ_l and ξ_h. For simplicity, we assume that H-type households all live in H-type houses located in areas with the h tag,[54] so that there is again only overtagging in this model.

A L-type household living in a L-type house tagged ϕ paying its property tax receives utility

$$u_{L\phi}^{\text{pay}} = u\left(v_L - p_{L\phi} - T_\phi\right) - d\left(\tilde{\sigma}\right) + \xi_\phi \tag{H.1}$$

where $p_{L\phi}$ is the (annualized) market price of a house of type L with a tag of ϕ. These prices do not depend on whether taxes are paid (they are market prices), but of course, households who anticipate to evade their property tax would have a higher willingness to pay for a house than those who plan to pay. The disutility from inequity now reflects only the portion of inequity that is not capitalized into house prices: $\tilde{\sigma} = \left(T_h + p_{Lh} - p_{Ll}\right)/T_l$. At the extreme, when tax differences are fully capitalized into house prices, we have $p_{Lh} - p_{Ll} = T_l - T_h$ and $\tilde{\sigma} = 1$, so that households no longer experience inequity. However, whenever tax differences are less than fully capitalized into house prices, mistagging still generates inequity and shapes optimal policy schedules. If, on the other hand, households don't pay their property tax, they receive utility

$$u_{L\phi}^{\text{evade}} = u\left(v_L - p_{L\phi}\right) - \gamma + \xi_\phi \tag{H.2}$$

Households pay their property tax whenever this makes them better off:

$$\begin{aligned}
u_{Ll}^{\text{pay}} > u_{Ll}^{\text{evade}} &\leftrightarrow \gamma > \gamma_l^* = u\left(v_L - p_{Ll}\right) - u\left(v_L - p_{Ll} - T_l\right) \\
u_{Lh}^{\text{pay}} > u_{Lh}^{\text{evade}} &\leftrightarrow \gamma > \gamma_h^* = u\left(v_L - p_{Lh}\right) - u\left(v_L - p_{Lh} - T_h\right) + d\left(\tilde{\sigma}\right)
\end{aligned}$$

Assuming there is no over-capitalization of taxes into house prices (i.e., $p_{Ll} - p_{Lh} \leq T_h - T_l$), we can see that this means that $\gamma_h^* > \gamma_l^*$, where γ_h^* and γ_l^* are area-specific cutoffs.

The thresholds γ_l^*, γ_h^* define three types of households, and we can characterize the location choice of each type in turn. First, for households with $\gamma > \gamma_h^*$, who pay their taxes regardless of

[54] For instance, v_H is sufficiently high compared than v_L, so that H-type households never want to live in L-type houses, and H-type houses are sufficiently more expensive than L-type houses, so that L-type households cannot afford to live in H-type houses.

which location they choose, they prefer the high-tag area to the low-tag area whenever

$$\begin{aligned} u\left(v_L - p_{Lh} - T_h\right) - d\left(\tilde{\sigma}\right) + \xi_h &> u\left(v_L - p_{Ll} - T_l\right) + \xi_l \\ \Delta\xi \equiv \xi_h - \xi_l &> u\left(v_L - p_{Ll} - T_l\right) - u\left(v_L - p_{Lh} - T_h\right) + d\left(\tilde{\sigma}\right) \equiv \Delta\xi_h^* \geq 0 \end{aligned} \tag{H.3}$$

Second, for households with $\gamma < \gamma_l^*$, who evade the tax regardless of which location they choose, they prefer the high-tag area whenever

$$\begin{aligned} u\left(v_L - p_{Lh}\right) + \xi_h &> u\left(v_L - p_{Ll}\right) + \xi_l \\ \Delta\xi \equiv \xi_h - \xi_l &> u\left(v_L - p_{Ll}\right) - u\left(v_L - p_{Lh}\right) \equiv \Delta\xi_l^* \geq 0 \end{aligned} \tag{H.4}$$

Finally, the third group has intermediate values of γ: $\gamma_l^* < \gamma \leq \gamma_h^*$. These households evade their property tax if they live in the high-tag area, but pay their tax if they live in the low-tag area. They prefer to locate in the high-tag area (and evade the property tax) whenever

$$\begin{aligned} u\left(v_L - p_{Lh}\right) - \gamma + \xi_h &> u\left(v_L - p_{Ll} - T_l\right) + \xi_l \\ \gamma &< u\left(v_L - p_{Lh}\right) - u\left(v_L - p_{Ll} - T_l\right) + \xi_h - \xi_l \equiv \bar{\gamma}\left(\Delta\xi\right) \end{aligned} \tag{H.5}$$

Combining conditions (H.3), (H.4), and (H.5) we can characterize the location ϕ and compliance $\in \{\textsf{pay}, \textsf{evade}\}$ decisions of all L-type households i as follows:

$$\{\phi^i, \textsf{compliance}^i\} = \begin{cases} \{l, \textsf{evade}\}, & \text{if } \gamma^i \leq \gamma_l^* \ \&\ \Delta\xi^i \leq \Delta\xi_l^*; \\ \{l, \textsf{pay}\}, & \text{if } (\gamma^i > \gamma_l^* \ \&\ \Delta\xi^i \leq \Delta\xi_l^*) \text{ or } (\gamma^i > \bar{\gamma}\left(\Delta\xi^i\right) \ \&\ \Delta\xi_l^* < \Delta\xi^i \leq \Delta\xi_h^*); \\ \{h, \textsf{evade}\}, & \text{if } (\gamma^i \leq \bar{\gamma}\left(\Delta\xi^i\right) \ \&\ \Delta\xi_l^* < \Delta\xi^i \leq \Delta\xi_h^*) \text{ or } (\gamma^i \leq \gamma_h^* \ \&\ \Delta\xi^i > \Delta\xi_h^*); \\ \{h, \textsf{pay}\}, & \text{if } \gamma^i > \gamma_h^* \ \&\ \Delta\xi^i > \Delta\xi_h^*. \end{cases} \tag{H.6}$$

Figure H.1 illustrates these four types of households and the boundaries dividing them.

Equation (H.6) characterizes households' decisions taking taxes T_ϕ and prices $p_{L\phi}$ as given. To pin down prices, we need the demand for each type of house to equal the supply. If the joint distribution of $\gamma, \Delta\xi$ is given by $J\left(\gamma, \Delta\xi\right)$, then the demand for houses in the low-tag area is

$$Q_l^D = \int_{-\infty}^{\Delta\xi_l^*} \int_{-\infty}^{\infty} j\left(\gamma, \Delta\xi\right) d\gamma d\Delta\xi + \int_{\Delta\xi_l^*}^{\Delta\xi_h^*} \int_{\bar{\gamma}(\Delta\xi)}^{\infty} j\left(\gamma, \Delta\xi\right) d\gamma d\Delta\xi$$

Similarly demand for houses in the high-tag area is

$$Q_h^D = \int_{\Delta\xi_l^*}^{\Delta\xi_h^*} \int_{-\infty}^{\bar{\gamma}(\Delta\xi)} j\left(\gamma, \Delta\xi\right) d\gamma d\Delta\xi + \int_{\Delta\xi_h^*}^{\infty} \int_{-\infty}^{\infty} j\left(\gamma, \Delta\xi\right) d\gamma d\Delta\xi$$

And prices adjust to equilibrate the market such that

$$Q_l^D = Q_l^S \equiv 1 - \psi \quad \& \quad Q_h^D = Q_h^S \equiv \psi \tag{H.7}$$

These pin down the equilibrium prices and hence define the cutoffs $\gamma_l^*, \gamma_h^*, \Delta\xi_l^*, \Delta\xi_h^*$ and the function $\bar{\gamma}(\Delta\xi)$. Given these, the compliance rates in each area are given by

$$c_{Ll} = \frac{1}{1-\psi}\left(\int_{-\infty}^{\Delta\xi_l^*}\int_{\gamma_l^*}^{\infty} j(\gamma,\Delta\xi)\, d\gamma d\Delta\xi + \int_{\Delta\xi_l^*}^{\Delta\xi_h^*}\int_{\bar{\gamma}(\Delta\xi)}^{\infty} j(\gamma,\Delta\xi)\, d\gamma d\Delta\xi\right) \tag{H.8}$$

$$c_{Lh} = \frac{1}{\psi}\int_{\Delta\xi_h^*}^{\infty}\int_{\gamma_h^*}^{\infty} j(\gamma,\Delta\xi)\, d\gamma d\Delta\xi \tag{H.9}$$

In this model, changes in taxes affect the compliance of L-type households through three channels. For example, a small increase in the high-tag tax T_h affects compliance through

1. A direct effect shown in Figure H.2: A higher T_h leads to a higher γ_h^* (holding house prices fixed), reducing compliance.

2. A housing demand effect shown in Figure H.3: A higher T_h (holding house prices fixed) makes living in the high-tag area less attractive to those who pay it, raising $\Delta\xi_h^*$ and causing an increase in demand for houses in the low-tag area among compliant households in the high-tag area. This lowers compliance among h-tag households since those affected were compliant while the non-compliant are unaffected, and raises compliance among l-tag households since the affected households become compliant l-tag taxpayers.

3. A house-price effect shown in Figure H.4: To equilibrate demand and supply, the price of houses in the high-tag area p_{Lh} falls and the price of houses in the low-tag area p_{Ll} rises. This affects compliance decisions by lowering the marginal utility of consumption of paying T_h and dampening the increase in effective inequity $\tilde{\sigma}$ from the increase in T_h. These price changes decrease γ_h^* (increasing h-tag compliance), increase γ_l^* (reducing l-tag compliance), decrease $\Delta\xi_h^*$ (increasing h-tag compliance and lowering l-tag compliance), and decrease $\Delta\xi_l^*$ (lowering h-tag compliance and raising l-tag compliance).

Since these effects do not all push in the same direction, their net effect on compliance with each tax is ambiguous, but naturally adding a margin through which households can respond to taxation makes the overall tax base more elastic, so the fiscal externalities of taxes are at least as big as in the model without household location choices.

H.2 Welfare and Optimal Policy

Our empirical analysis shows no evidence of price (see appendix P) or mobility (see appendix Q) responses to tax changes. Our preferred specification (in section 5.2) thus looks at within-property changes in compliance — so that the main response captured is the direct effect — to highlight the potential compliance responses induced by mistagging. Nevertheless, the framework above highlights two key implications of household location choices, which could matter in other settings. First, house price changes can have first-order effects on households' welfare, even if they do not move. Second, mobility responses would affect equilibrium compliance rates and hence have fiscal externalities. These two implications can affect the welfare effects of tax policy and the shape of the optimal tax schedule. This section thus explores these issues in more detail. Moreover, although our empirical work suggests that these two implications are not first-order in our setting, we shed light on their potential impacts in our simulation exercise in Appendix R.

To explore how these two implications can shape the optimal tax schedule, we generalize the model slightly, and instead of committing to a specific model of household residential choice, we capture the reduced form effect of taxes on prices through the expression $p_\theta(T_\phi) = p_\theta^0 - \kappa T_\phi$ where the parameter κ governs the degree of capitalization of taxes into house prices.

In this model, the private welfare of the three types of households is given by[55]

$$V_{Ll} = \int_{-\infty}^{\gamma_{Ll}^\star} \left[u\left(v_L - p_L\left(T_l\right)\right) - \gamma\right] dF(\gamma) + \int_{\gamma_{Ll}^\star}^{\infty} \left[u\left(v_L - p_L\left(T_l\right) - T_l\right)\right] dF(\gamma)$$
$$V_{Lh} = \int_{-\infty}^{\gamma_{Lh}^\star} \left[u\left(v_L - p_L\left(T_h\right)\right) - \gamma\right] dF(\gamma) + \int_{\gamma_{Lh}^\star}^{\infty} \left[u\left(v_L - p_L\left(T_h\right) - T_h\right) - d\left(\tilde{\sigma}\right)\right] dF(\gamma)$$
$$V_{Hh} = \int_{-\infty}^{\gamma_{Hh}^\star} \left[u\left(v_H - p_H\left(T_h\right)\right) - \gamma\right] dF(\gamma) + \int_{\gamma_{Hh}^\star}^{\infty} \left[u\left(v_H - p_H\left(T_h\right) - T_h\right)\right] dF(\gamma)$$

Starting with the correctly tagged households, the marginal private welfare effects are now

$$\begin{aligned}
\frac{\partial V_{Ll}}{\partial T_l} &= \left(1 - c_{Ll}\right) u'\big(y_L\left(T_l\right)\big)\kappa - c_L u'\big(y_L\left(T_l\right) - T_l\big)\left(1-\kappa\right) \\
&\simeq \left(1 - c_L\right) u'\left(y_L\left(T_l\right)\right)\kappa - c_{Ll} u'\left(y_L\left(T_l\right)\right)\left(1 + \rho\frac{T_l}{y_L\left(T_l\right)}\right)\left(1-\kappa\right) \\
&= \kappa u'\left(y_L\left(T_l\right)\right)\left(1 + c_{Ll}\rho\frac{T_l}{y_L\left(T_l\right)}\right) - c_{Ll} u'\left(y_L\left(T_l\right)\right)\left(1 + \rho\frac{T_l}{y_L\left(T_l\right)}\right) \qquad \text{(H.10)}
\end{aligned}$$
$$\frac{\partial V_{Hh}}{\partial T_h} = \kappa u'\left(y_H\left(T_h\right)\right)\left(1 + c_{Hh}\rho\frac{T_h}{y_H\left(T_h\right)}\right) - c_{Hh} u'\left(y_H\left(T_h\right)\right)\left(1 + \rho\frac{T_h}{y_H\left(T_h\right)}\right) \qquad \text{(H.11)}$$

where we introduced the notation that $y_\theta(T_\phi) = v_\theta - p_\theta(T_\phi)$ and we used the approximation to marginal utility that $u'\left(y_\theta\left(T_\phi\right) + x\right) \simeq u'\left(y_\theta\left(T_\phi\right)\right)\left(1 - \rho\frac{x}{y_\theta\left(T_\phi\right)}\right)$.

We get two extra effects beyond those in (E.2):

1. All households have higher utility from the capitalization of tax liabilities into house prices. This is the $\kappa u'\big(\tilde{y}_{\theta\phi}\big) \times 1$ term. This also applies to the households that don't pay the tax since we assume it affects the market price of houses and that there is no price discrimination by tax evasion. We note that our model does not include sellers of houses, only home buyers paying house prices. Since house price changes are merely transfers between buyers and sellers, if we extended the model to include sellers, the change in home buyers' welfare would only impact overall welfare to the extent that home buyers have higher social marginal utility than home sellers. If they had equal welfare weights this extra effect would have impacts of equal sizes but opposite signs on the private welfare of buyers and sellers, respectively, and thus no net impact on overall welfare.

2. The lower house prices also dampen the utility loss from paying the tax due to the concavity of the utility function (governed by ρ), i.e., the marginal disutility of paying taxes is lower. This is the $\kappa u'\big(\tilde{y}_{\theta\phi}\big) \times c_{\theta\phi}\rho\frac{T_\phi}{\tilde{y}_{\theta\phi}}$ term.

Turning to the mistagged households, as before, we will want to express their marginal disutility from inequity $d'(\tilde{\sigma})$ in dollar terms and we use the responsiveness of compliance to inequity and the tax liability to do so. To do this, we use the definitions of the elasticities ε and η

[55] In the specific model of household location decision outlined above, the expressions below hold conditional on location taste $\Delta\xi^i$, and the overall welfare integrates across location tastes to yield expressions like the ones below.

(which in this setting hold location fixed):

$$\eta \equiv -\frac{\partial c}{\partial \sigma}\frac{\sigma}{c} = \frac{\partial c}{\partial \gamma^\star}\frac{\partial \gamma^\star}{\partial \sigma}\frac{\sigma}{c} = (1-\kappa)\, d'(\tilde{\sigma})\, \frac{f(\gamma^\star)}{1-F(\gamma^\star)}\sigma \tag{H.12}$$

$$\begin{aligned}
\varepsilon &\equiv -\frac{\partial c}{\partial T_\phi}\frac{T_\phi}{c} = \frac{\partial c}{\partial \gamma^\star}\frac{\partial \gamma^\star}{\partial T_\phi}\frac{T_\phi}{c} \\
&= \left[-u'(y_\theta(T_\phi))\frac{\partial p_\theta(T_\phi)}{\partial T_\phi} + u'(y_\theta(T_\phi) - T_\phi)\left(1 + \frac{\partial p_\theta(T_\phi)}{\partial T_\phi}\right)\right]\frac{f(\gamma^\star)}{1-F(\gamma^\star)}T_\phi \\
&= \left[u'(y_\theta(T_\phi))\,\kappa + u'(y_\theta(T_\phi) - T_\phi)(1-\kappa)\right]\frac{f(\gamma^\star)}{1-F(\gamma^\star)}T_\phi
\end{aligned} \tag{H.13}$$

Where we see that now the elasticity with respect to the tax liability will be stronger since $u(\cdot)$ is strictly concave and $y'_\theta < 0$. More importantly, (H.12) shows that with capitalization ($\kappa > 0$) we expect a smaller elasticity with respect to inequity η since capitalization dampens the experienced inequity $\tilde{\sigma}$.

It also changes how we use the relationship between the two elasticities to express $d(\tilde{\sigma})$ in terms of elasticities. Combining (H.12) and (H.13), gives us

$$d'(\tilde{\sigma}) = \frac{\eta}{\varepsilon}\left[u'(y_L(T_h) - T_h) + u'(y_L(T_h))\frac{\kappa}{1-\kappa}\right]T_l \tag{H.14}$$

Combining these expressions we can see that the effect of marginal changes in the low-tag tax T_l is

$$\begin{aligned}
\frac{\partial V_{Lh}}{\partial T_l} &= \int_{\gamma^\star_{Lh}}^{\infty} -d'((1-\kappa)\sigma)(1-\kappa)\frac{\partial \sigma}{\partial T_l}dF(\gamma) = c_{Lh}d'(\tilde{\sigma})(1-\kappa)\frac{\sigma}{T_l} \\
&= c_{Lh}\frac{\eta}{\varepsilon}\sigma\left[u'(y_L(T_h) - T_h)(1-\kappa) + \kappa u'(y_L(T_h))\right] \\
&\simeq c_{L,h}\frac{\eta}{\varepsilon}\sigma u'(y_L(T_l))\left(1 + \rho\left[\kappa(1-\sigma) + \sigma(1-\kappa)\right]\frac{T_l}{y_L(T_l)}\right)
\end{aligned} \tag{H.15}$$

while the effect of a marginal change in the high-tag tax T_h is

$$\begin{aligned}
\frac{\partial V_{Lh}}{\partial T_h} &= \int_{-\infty}^{\gamma^\star_{Lh}} u'\left(y_L\left(T_h\right)\right)\frac{\partial y_L}{\partial T_h}dF\left(\gamma\right) + \int_{\gamma^\star_{Lh}}^{\infty}\left[u'\left(y_L\left(T_h\right)-T_h\right)\left(\frac{\partial p_L}{\partial T_h}-1\right)-d'\left(\tilde{\sigma}\right)\left(1-\kappa\right)\frac{\partial \sigma}{\partial T_h}\right]dF\left(\gamma\right)\\
&\simeq \left(1-c_{Lh}\right)u'\left(y_L\left(T_h\right)\right)\kappa + c_{L,h}\left[u'\left(y_L\left(T_h\right)-T_h\right)\left(\kappa-1\right)-d'\left(\tilde{\sigma}\right)\left(1-\kappa\right)\frac{1}{T_l}\right]\\
&= \left(1-c_{Lh}\right)u'\left(y_L\left(T_h\right)\right)\kappa - c_{Lh}u'\left(y_L\left(T_h\right)-T_h\right)\left(1-\kappa\right)\\
&\quad - c_{Lh}\left(1-\kappa\right)\frac{\eta}{\varepsilon}\left[u'\left(y_L\left(T_h\right)-T_h\right)+u'\left(y_L\left(T_h\right)\right)\frac{\kappa}{1-\kappa}\right]\\
&= u'\left(y_L\left(T_h\right)\right)\kappa\left[1-c_{Lh}\left(1+\frac{\eta}{\varepsilon}\right)\right] - c_{Lh}u'\left(y_L\left(T_h\right)-T_h\right)\left(1-\kappa\right)\left(1+\frac{\eta}{\varepsilon}\right)\\
&\simeq u'\left(y_L\left(T_l\right)\right)\left[1-\rho\kappa\left(1-\frac{1}{\sigma}\right)\frac{y_H}{y_L}\frac{T_h}{y_L\left(T_l\right)}\right]\kappa\left[1-c_{Lh}\left(1+\frac{\eta}{\varepsilon}\right)\right]\\
&\quad - c_{Lh}u'\left(y_L\left(T_l\right)\right)\left[1+\rho\frac{y_H}{y_L}\left[1-\kappa\left(1-\frac{1}{\sigma}\right)\right]\frac{T_h}{y_H\left(T_h\right)}\right]\left(1-\kappa\right)\left(1+\frac{\eta}{\varepsilon}\right)\\
&= u'\left(y_L\left(T_l\right)\right)\kappa\left[1-\rho\kappa\left(1-\frac{1}{\sigma}\right)\frac{y_H}{y_L}\frac{T_h}{y_H\left(T_h\right)}\right]\\
&\quad - c_{Lh}u'\left(y_L\left(T_l\right)\right)\left(1+\rho\left[\left(1-\kappa\right)-\left(1-\frac{1}{\sigma}\right)\kappa\right]\frac{y_H}{y_L}\frac{T_h}{y_H\left(T_h\right)}\right)\left(1+\frac{\eta}{\varepsilon}\right)
\end{aligned} \tag{H.16}$$

While the expressions are more involved, the same two additional forces appear in (H.15) and (H.16) relative to (F.3) and (F.4) for mistagged households as in (H.10) and (H.11) relative to (E.2) for correctly tagged households. First, the first term in (H.16) captures the fact that taxes lower house prices and this increases the utility of their occupants regardless of whether they pay taxes. Second, the terms in square brackets in (H.15) and (H.16) involving κ multiplying $c_{Lh}u'\left(y_L\left(T_l\right)\right)$ capture the fact that the marginal disutility of paying taxes is lowered for taxpayers due to their lower house prices.

Marginal Welfare Effects and Optimal Taxes Turning to the social welfare effects and optimal taxation, the equations get uglier, but the intuition is very much the same. Social welfare, as before, is given by

$$W = \omega_L\left[\psi V_{Lh} + \left(1-\psi\right)V_{Ll}\right] + \omega_H V_{Hh} + B\left(r\right) \tag{H.17}$$

By the envelope theorem, households who move in response to marginal changes in taxes do not experience any first-order welfare effects from moving. However, moves can have fiscal externalities if they affect compliance rates in l-tag and h-tag areas through composition effects (e.g., compliant taxpayers moving from paying T_h to paying T_l and non-compliant taxpayers moving from evading T_l to evading T_h). These effects are conceptually distinct from the η and ε elasticities above, which capture behavioral responses holding fixed location. To allow for sorting to affect compliance and draw out the implications for welfare, we define the composition elasticities $\mu_{\phi\phi'}$ — where ϕ indicates the area whose compliance is being considered and ϕ' indicates the tax being varied — to isolate compliance effects that are driven by compositional changes. Note that, as discussed in section H.1 above, these elasticities can in principle be either positive or negative.

With these we can see that the marginal revenue effects are now

$$\begin{aligned}
r &= \psi c_{Lh} T_h + (1-\psi) c_{Ll} T_l + c_{Hh} T_h \\
\frac{dr}{dT_h} &= \psi \left(c_{Lh} + \frac{dc_{Lh}}{dT_h} T_h \right) + (1-\psi) \frac{dc_{Ll}}{dT_h} T_l + c_{Hh} + \frac{dc_{Hh}}{dT_h} T_h \\
&= \psi c_{Lh} (1 - \varepsilon - \eta - \mu_{hh}) - (1-\psi) c_{Ll} \mu_{lh} \frac{1}{\sigma} + c_{Hh} (1-\varepsilon) \\
\frac{dr}{dT_l} &= \psi \frac{dc_{Lh}}{dT_l} T_h + (1-\psi) \left(c_{Ll} + \frac{dc_{Ll}}{dT_l} T_l \right) \\
&= \psi \sigma (\eta - \mu_{hl}) c_{Lh} + (1-\psi) c_{Ll} (1 - \varepsilon - \mu_{ll})
\end{aligned}$$

This means that the normalized marginal welfare effect of the low-tag tax T_l is

$$\begin{aligned}
\frac{\partial W}{\partial T_l} \frac{1}{b(r)} &= \frac{\omega_L}{b(r)} \left[\psi \frac{\partial V_{Lh}}{\partial T_l} + (1-\psi) \frac{\partial V_{Ll}}{\partial T_l} \right] + \frac{\omega_H}{b(r)} \frac{\partial V_{Hh}}{\partial T_l} + \frac{\partial r}{\partial T_l} \\
&= \psi g_L c_{Lh} \frac{\eta}{\varepsilon} \sigma \left(1 + \rho \left[(1-\sigma) \kappa + \sigma (1-\kappa) \right] \frac{T_l}{y_L(T_l)} \right) \\
&\quad + (1-\psi) g_L \left[\kappa \left(1 + c_{Ll} \rho \frac{T_l}{y_L(T_l)} \right) - c_{Ll} \left(1 + \rho \frac{T_l}{y_L(T_l)} \right) \right] \\
&\quad + \psi c_{Lh} (\eta - \mu_{hl}) \sigma + (1-\psi) c_{Ll} (1 - \varepsilon - \mu_{ll})
\end{aligned} \tag{H.18}$$

and the normalized marginal welfare effect of the high-tag tax T_h is

$$\begin{aligned}
\frac{\partial W}{\partial T_h} \frac{1}{b(r)} &= \frac{\omega_L}{b(r)} \left[\psi \frac{\partial V_{Lh}}{\partial T_h} + (1-\psi) \frac{\partial V_{Ll}}{\partial T_h} \right] + \frac{\omega_H}{b(r)} \frac{\partial V_{Hh}}{\partial T_h} + \frac{\partial r}{\partial T_h} \\
&= \psi g_L \left(\kappa \left[1 - \rho \kappa \left(1 - \frac{1}{\sigma} \right) \frac{y_H}{y_L} \frac{T_h}{y_H} \right] - c_{Lh} \left[1 + \rho \left[(1-\kappa) - \left(1 - \frac{1}{\sigma} \right) \kappa \right] \frac{y_H}{y_L} \frac{T_h}{y_H} \right] \left(1 + \frac{\eta}{\varepsilon} \right) \right) \\
&\quad + g_H \left[\kappa \left(1 + c_{Hh} \rho \frac{T_h}{y_H} \right) - c_{Hh} \left(1 + \rho \frac{T_h}{y_H} \right) \right] \\
&\quad + \psi c_{Lh} (1 - \varepsilon - \eta - \mu_{hh}) - (1-\psi) c_{Ll} \mu_{lh} \frac{1}{\sigma} + c_{Hh} (1-\varepsilon)
\end{aligned} \tag{H.19}$$

Setting (H.18) and (H.19) to zero and rearranging, the modified optimal tax formulas are given by equations (H.20) and (H.21):

$$\frac{T_l}{y_L(T_l)} = \frac{1 - \varepsilon - g_L + \varphi_l \frac{\eta}{\varepsilon} \sigma (g_L + \varepsilon) + \kappa \frac{g_L}{c_{Ll}} - \varphi_l \sigma \mu_{hl} - \mu_{ll}}{\rho g_L (1-\kappa) \left[1 - \varphi_l \frac{\eta}{\varepsilon} \sigma^2 (1 - \tilde{\kappa}) \right]} \tag{H.20}$$

$$\frac{T_h}{y_H(T_h)} = \frac{1 - \varepsilon - \tilde{g}_h - \varphi_h \frac{\eta}{\varepsilon} (g_L + \varepsilon) + \kappa \frac{\tilde{g}_h}{\tilde{c}_h} - \varphi_h \left(\mu_{hh} + \frac{\mu_{lh}}{\varphi_l \sigma} \right)}{\rho (1-\kappa) \left[\tilde{g}_h + \varphi_h g_L \left(\frac{y_H(T_h)}{y_L(T_l)} \left(1 + \frac{\eta}{\varepsilon} \right) (1 - \tilde{\kappa}) - 1 \right) + \varphi_h g_L \frac{\kappa}{c_{Lh}} \tilde{\kappa} \frac{y_H(T_h)}{y_L(T_l)} \right]} \tag{H.21}$$

where $\tilde{\kappa} = \frac{\kappa}{1-\kappa} \left(1 - \frac{1}{\sigma} \right)$ measures the increase in marginal utility from the lower prices households have to pay for their homes due to being taxed at T_h rather than T_l; $\tilde{g}_h = (g_H + \psi g_L) / (1 + \psi)$ is the average marginal social welfare weight of those asked to pay the h tax (note this is not the same as the average social marginal welfare weight of those who *do* pay the h-tax $\bar{g}_h$); and $\tilde{c}_h = (c_{Hh} + \psi c_{Lh}) / (1 + \psi)$ is the fraction of those asked to pay the h tax who comply.

The equations look much as before, but with three important changes. First, tax-induced reductions in house prices increase households' private welfare in this model and decrease their marginal utility. The terms including κ/c capture the implications for the optimal tax schedule. As mentioned above, since house price changes are merely transfers between buyers and sellers, if we extended the model to include sellers, the change in home buyers' welfare would only impact policy to the extent that they have higher social marginal utility than home sellers. If they had equal welfare weights the κ/c terms in the numerators would disappear.[56]

Second, since household location changes may create fiscal externalities, the $\mu_{\phi\phi'}$ elasticities appear in the numerators to account for these effects. Our empirical work suggests that there are no first-order effects on mobility in our setting, but they may be meaningful in other settings. We highlight their potential impacts in our simulation exercise in Appendix R.

Third, and more importantly for our study of the impacts of mistagging and inequity aversion, house price changes reduce experienced inequity and dampens the forces towards less progressivity that inequity generates in two ways. First, as noted above, equation (H.12) suggests that we should expect the elasticity of compliance with respect to inequity, η, to be smaller in the presence of capitalization. Second, the marginal disutility of paying (inequitable) taxes is lower since households pay less for their houses, which the $(1-\tilde{\kappa})$ terms in the denominators account for. These two effects dampen, but do not eliminate, the second and third impacts of overtagging and inequity aversion highlighted in proposition 2 on the optimal tax schedule, which made taxes less progressive. Our empirical work in appendix P suggests that there are no first-order effects on prices in our setting, but they may be meaningful in other settings. We highlight their potential impacts in our simulation exercise in Appendix R.

[56]The term in the denominator of H.21 would remain since it captures the change in the marginal disutility of paying taxes — thus mitigating the effect of inequity — and only home buyers pay taxes.

FIGURE H.1: LOCATION AND COMPLIANCE CHOICES

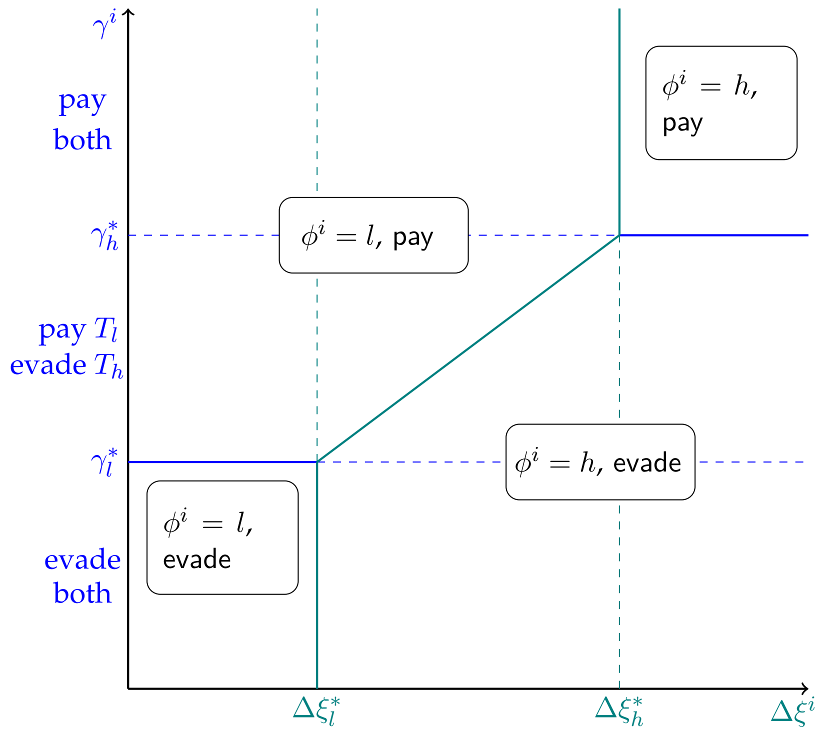

FIGURE H.2: LOCATION AND COMPLIANCE CHOICES: DIRECT EFFECT

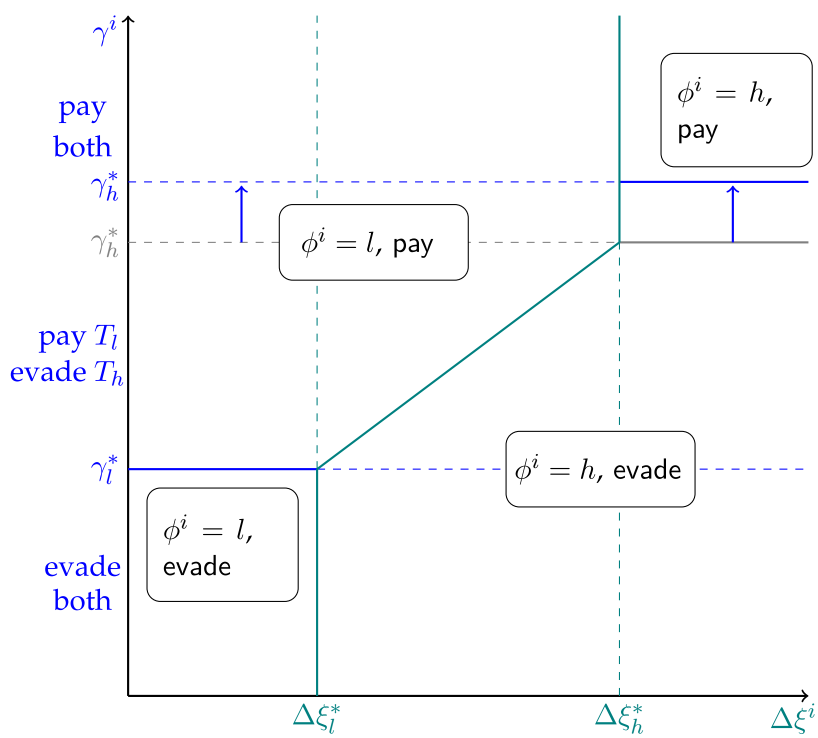

FIGURE H.3: LOCATION AND COMPLIANCE CHOICES: HOUSING DEMAND EFFECT

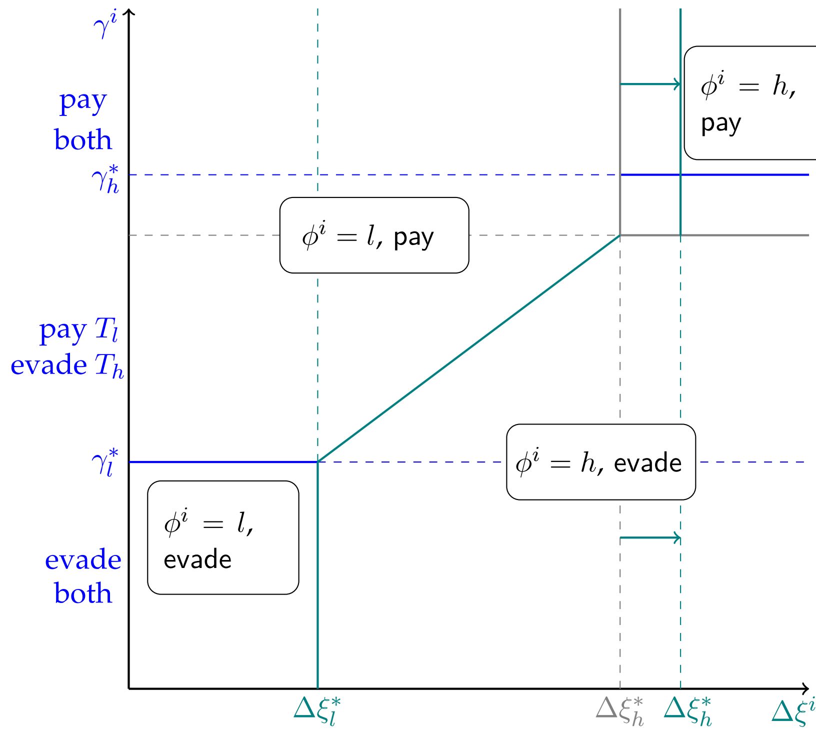

FIGURE H.4: LOCATION AND COMPLIANCE CHOICES: HOUSE PRICE EFFECT

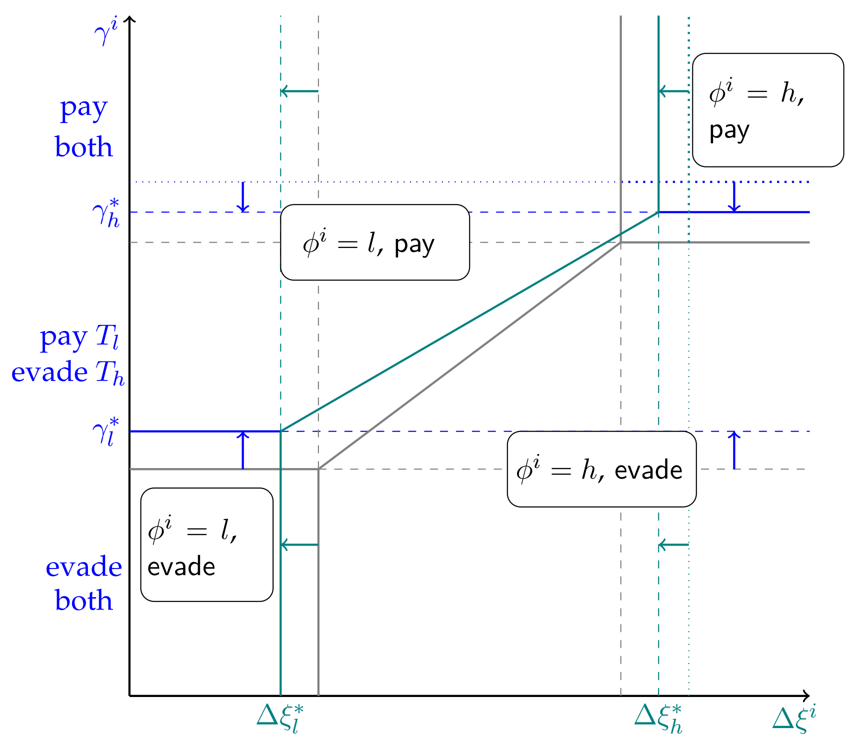

I Boundary Discontinuity Design Controlling for Tax Liability

This appendix presents an augmented boundary discontinuity design that extends the boundary discontinuity design in section 4 to hold properties' tax liabilities fixed. The assumptions required for this to identify the impact of inequity and the identification proof are in section I.1, and the results are presented in section I.2.

I.1 Identification

We seek assumptions under which an extension of the standard boundary discontinuity design in section 4 that also controls for properties' tax liabilities identifies the impact of inequity. The assumptions required are stronger versions of the assumptions presented in section 4.2 and the proof of their sufficiency follows the line of argument of the proof of proposition 6.

Our approach builds on the advances in Frölich & Huber (2019) and Dong *et al.* (2023) who adapt the regression discontinuity design to settings with controls, and continuous treatments, respectively. We denote our compliance outcome $C \in [0,1]$ as the fraction of a taxpayer's liability that they pay in response to the treatment we are interested in: inequity $\sigma \in \mathbb{R}^+$. The running variable in our regression discontinuity design is distance to the boundary of a tax sector $D \in \mathcal{D} \subset \mathbb{R}$. Compliance is determined by potential outcomes given by $C = G(\sigma, \tau, D, \nu)$ where τ is the (log) tax liability, and ν are other, potentially unobserved, determinants of compliance.[57]

It is useful to think of crossing the boundary as an instrument $Z = \mathbf{1}[D > 0]$ giving properties potential treatments when Z is exogenously set to z of $\sigma_z \equiv q_z(E_z) = (-1)^{1-z} \log\left(\frac{1+p_H E_z}{1+p_L E_z}\right)$, where E_z is a property's potential exposure when the instrument is $Z = z$. Since we will invoke a rank invariance assumption, it is convenient to study quantiles of the treatment distribution.[58] Our first assumption allows us to map 1-to-1 between quantiles of exposure to mistagging and inequity:

Assumption 1 (Quantile representation)**.** *The conditional distribution of E_z given distance $D = d$ and tax liability $\tau = t$ is continuous with a strictly increasing CDF $F_{E_z|\tau,D}(e,t,d)$.*

This assumption allows us to define the inequity faced by the property at the uth conditional quantile of exposure as[59]

$$q_z(d,u,t) = (-1)^{1-z} \log\left(\frac{1 + p_H F^{-1}_{E_z|t,d}(u)}{1 + p_L F^{-1}_{E_z|t,d}(u)}\right)$$

More substantively, we make a set of four smoothness assumptions:

Assumption 2 (Smoothness)**.** *$q_z(d,u,t)$, $z = 0,1$, is continuous in $d \in \mathcal{D}$ for any $u \in [0,1]$ and $t \in \mathcal{T} \subset \mathbb{R}^+$. Either $G(\sigma,\tau,D,\nu)$ is continuous in all its arguments, or it is a.e. continuous and bounded. $f_{\nu|U_z,\tau,D}(v,u,t,d)$ is continuous in $d \in \mathcal{D}$ for any $u \in [0,1]$, $t \in \mathcal{T}$, and $v \in \mathcal{V}$, where $\mathcal{V}$ is compact. $f_{D|\tau}(d,t)$ is continuous and strictly positive around $d = 0$.*

This assumption requires that inequity, taxes, distance, and unobservables all generate smooth impacts on compliance. It also assumes that for a given rank in the exposure distribution, the

[57] We allow these determinants $\nu \in \mathcal{V} \subset \mathbb{R}^{\dim_\nu}$ to have arbitrary dimension.

[58] This is also convenient since it offers a natural way to pool across tax sector boundaries.

[59] Note that while the reduced form only depends on e_i, it now depends on τ also because the distribution of e_i we are using to normalize with is conditional on distance and τ.

distribution of unobservables is smooth near the boundaries. These are strong assumptions, and in sections 4.2 and 4.3 we show how we can relax both of them while still achieving identification. The assumption that distance has a smooth effect on potential treatments is easily satisfied as long as assumption 2 holds. The assumption that distance is continuous and has positive density at the boundary is standard in BDD designs.

Our final assumption requires that properties stay at approximately the same rank in the potential exposure distribution on either side of the tax sector boundaries.[60] Formally,

Assumption 3 (Local exposure rank invariance or similarity)**.** *Conditional on $D = 0$ and $\tau = t \in \mathcal{T}$, 1. $U_0 = U_1$; or, more generally, 2. $U_0|\nu \sim U_1|\nu$*

Assumption 3 implies that crossing the boundary (our instrument) does not affect properties' rank in the distribution of exposure to mistagging.[61] Notably, this assumption does not require properties to have the same potential exposure to mistagging on either side of the boundary. The relative, after-tax price of land a is higher on the high-tag side of the boundary and so we might expect property owners to substitute towards built structure. Assumption 3 allows this, but requires that the unobservables are not correlated with the elasticity of substitution between land a and built structure b in such a way that it would reverse the ranks in the potential distribution.

Together with the smoothness of the distribution of ν in assumption 2, assumption 3 means that at the boundary, we can use U as a control variable (Imbens & Newey, 2009) — conditional on U, the change in inequity at the tax sector boundary is exogenous (unrelated to ν) (Dong *et al.*, 2023).

With these assumptions we can show that a boundary regression discontinuity design that conditions on tax liability identifies the treatment effect of inequity:

Proposition 3 (Identification of LATEs conditional on U and τ)**.** *Define the Qτ-LATE:*

$$\begin{aligned}\eta(u,t) &\equiv \int \frac{G(\sigma_1(u,t),t,0,v) - G(\sigma_0(u,t),t,0,v)}{\sigma_1(u,t) - \sigma_0(u,t)} F_{\nu|U,\tau,D}(dv,u,t,0) \\ &= \mathbb{E}\left[\left.\frac{C_{\sigma_1(u,t)} - C_{\sigma_0(u,t)}}{\sigma_1(u,t) - \sigma_0(u,t)}\right| U = u, \tau = t, D = 0\right]\end{aligned}$$

This is the average causal effect of inequity for taxpayers with exposure to mistagging rank $U = u$ and tax liability $\tau = t$.

Under Assumptions 1, 2 & 3, for any $u \in \mathcal{U}$, the set of u for which there is a first stage (non-zero exposure), and for any $t \in \mathcal{T}$, Qτ-LATE $\eta(u,t)$ is identified and is given by

$$\eta(u,t) = \frac{m^+(u,t) - m^-(u,t)}{q^+(u,t) - q^-(u,t)} \tag{I.1}$$

where the limits in the denominator are defined by $q^+(u,t) \equiv \lim_{d\to 0^+} q(d,u,t)$ and $q^-(u,t) \equiv \lim_{d\to 0^-} q(d,u,t)$. Also let $m(s,t,d) \equiv \mathbb{E}[C|\sigma = s, \tau = t, D = d]$, and define $m^+(u,t) \equiv \lim_{d\to 0^+} m(q^+(u,t),t,d)$ and $m^-(u,t) \equiv \lim_{d\to 0^-} m(q^-(u,t),t,d)$. All of these can be consistently estimated from the data.

Further, the W-LATE $\bar{\eta}(w) = \int_{\mathcal{U}}\int_{\mathcal{T}} \eta(u,t)\, w(t,u)\, dtdu$ is identified for any known or estimable weighting function $w(t,u)$ such that $w(t,u) \geq 0$ and $\int_{\mathcal{U}}\int_{\mathcal{T}} w(t,u)\, dtdu = 1$.

[60] Note that this does not require properties to have the same exposure to mistagging, only that their rank is similar.

[61] The more general formulation of the assumption permits random slippages from a property's rank in the exposure distribution just on either side of the boundary (Chenozhukov & Hansen, 2005; Dong *et al.*, 2023).

Proof. The proof of proposition 3 is a relatively straightforward application of theorem 1 in Dong *et al.* (2023). We proceed in three steps. First, we show that potential changes in inequity when $D \to 0$ are independent of ν. Second, we show that the reduced form effect of crossing the boundary is identified. And third, we combine these results to show the proposition.

Our first lemma shows that crossing the boundary can be thought of as an excludable instrument conditional on the mistagging exposure rank U and the tax labiltiy τ:

Lemma 4 (Excludability)**.** *Let Assumptions 1, 2 & 3 hold. Then for any $u \in [0,1]$,*

$$\lim_{d\to 0^-} f_{\nu|\sigma,\tau,D}\left(v, q_0\left(d,u,t\right), t, d\right) = \lim_{d\to 0^+} f_{\nu|\sigma,\tau,D}\left(v, q_1\left(d,u,t\right), t, d\right) = \lim_{d\to 0} f_{\nu|U,\tau,D}\left(v,u,t,d\right) \quad \text{(I.2)}$$

for $v \in \mathcal{V}$ and $\tau \in \mathcal{T}$

Proof. By Bayes' rule, assumption 3, that $U_0|\left(\nu, D=0, \tau=t\right) \sim U_1|\left(\nu, D=0,\tau=t\right)$, where we now make explicit the conditioning on distance $D=0$ and tax liability τ, implies that $\nu|\left(U_0=u, D=0, \tau=t\right) \sim \nu|\left(U_1=u, D=0, \tau=t\right)$, i.e. that $f_{\nu|U_1,D,\tau} = f_{\nu|U_0,D,\tau}$. By invoking our smoothness assumption 2 and the definition relating observed to potential exposure ranks $U \equiv U_1\mathbf{1}\left[D>0\right] + U_0\mathbf{1}\left[D<0\right]$, we can show that their limits are the same from both sides:

$$\lim_{D\to 0^+} f_{\nu|U_1,D,\tau}\left(\nu,u,t\right) = \lim_{D\to 0^-} f_{\nu|U_0,D,\tau}\left(\nu,u,t\right) = \lim_{D\to 0} f_{\nu|U,D,\tau}\left(\nu,u,t\right)$$

Finally, we exploit the fact that under Assumption 1, for a given $D=d$ and $\tau=t$, whenever $d>0$ there is a one-to-one mapping between u and $q_1\left(d,u,t\right)$ and whenever $d<0$ there is a one-to-one mapping between u and $q_0\left(d,u,t\right)$ so that the same limits apply to the distributions conditional on inequity levels as the distributions conditional on exposure ranks

$$\lim_{D\to 0^+} f_{\nu|\sigma,D,\tau}\left(\nu, q_1\left(d,u,t\right), t\right) = \lim_{D\to 0^-} f_{\nu|\sigma,D,\tau}\left(\nu, q_0\left(d,u,t\right), t\right) = \lim_{D\to 0} f_{\nu|U,D,\tau}\left(\nu,u,t\right)$$

□

Lemma 4 thus show that given an exposure rank $U=u$ and a tax liability $\tau=t$, all potential changes in inequity σ when $D\to 0$ are independent of the unobservables ν. Our second lemma shows that the reduced-form impact of crossing the boundary on compliance is identified:

Lemma 5. *Let Assumptions 1, 2 & 3 hold. Then for any $u \in [0,1]$,*

$$\begin{aligned}
&\lim_{d\to 0^+} \mathbb{E}\left[C|U=u,\tau=t,D=d\right] - \lim_{d\to 0^-} \mathbb{E}\left[C|U=u,\tau=t,D=d\right] \\
&= \int \big(G\left(\sigma_1\left(u,t\right),t,0,v\right) - G\left(\sigma_0\left(u,t\right),0,t,v\right)\big) F_{\nu|U,\tau,D}\left(dv,u,t,0\right) \qquad \text{(I.3)}
\end{aligned}$$

Proof. By assumption 1, we can map from the exposure quantiles U to the treatment levels one-to-one:

$$\begin{aligned}
&\lim_{D\to 0^+} \mathbb{E}\left[C|U=u,D=d,\tau=t\right] - \lim_{D\to 0^-} \mathbb{E}\left[C|U=u,D=d,\tau=t\right] \\
&= \lim_{D\to 0^+} \mathbb{E}\left[C|\sigma=q_1\left(d,u,t\right), U_1=u, D=d, \tau=t\right] - \lim_{D\to 0^-} \mathbb{E}\left[C|\sigma=q_0\left(d,u,t\right), U_0=u, D=d,\tau=t\right]
\end{aligned}$$

And we can substitute in the definition of the potential outcome $C = G(\sigma, \tau, D, \nu)$

$$
\begin{aligned}
&\lim_{D\to 0^+} \mathbb{E}\left[C|\sigma = q_1(d,u,t), U_1 = u, D = d, \tau = t\right] - \lim_{D\to 0^-} \mathbb{E}\left[C|\sigma = q_0(d,u,t), U_0 = u, D = d, \tau = t\right] \\
&= \lim_{D\to 0^+} \mathbb{E}\left[G(q_1(d,u,t), t, d, \nu)|\sigma = q_1(d,u,t), U_1 = u, D = d, \tau = t\right] \\
&\quad - \lim_{D\to 0^-} \mathbb{E}\left[G(q_0(d,u,t), t, d, \nu)|\sigma = q_0(d,u,t), U_0 = u, D = d, \tau = t\right]
\end{aligned}
$$

By the smoothness assumption 2 and the compact support of ν, we can exchange the order of the limit and the expectation integral and the expectation above is continuous in D so that

$$
\begin{aligned}
&\lim_{D\to 0^+} \mathbb{E}\left[G(q_1(d,u,t), t, d, \nu)|\sigma = q_1(d,u,t), U_1 = u, D = d, \tau = t\right] \\
&\quad - \lim_{D\to 0^-} \mathbb{E}\left[G(q_0(d,u,t), t, d, \nu)|\sigma = q_0(d,u,t), U_0 = u, D = d, \tau = t\right] \\
&= \mathbb{E}\left[G(\sigma_1(u), t, 0, \nu)|U_1 = u, D = 0, \tau = t\right] - \mathbb{E}\left[G(\sigma_0(u), t, 0, \nu)|U_0 = u, D = 0, \tau = t\right]
\end{aligned}
$$

Finally, by assumption 3 and lemma 4 the two expectations are integrating over the same distribution f_ν so we have that

$$
\begin{aligned}
&\mathbb{E}\left[G(\sigma_1(u), t, 0, \nu)|U_1 = u, D = 0, \tau = t\right] - \mathbb{E}\left[G(\sigma_0(u), t, 0, \nu)|U_0 = u, D = 0, \tau = t\right] \\
&= \int \big(G(\sigma_1(u), t, 0, v) - G(\sigma_0(u), t, 0, v)\big) F_{\nu|U,\tau,D}(dv, u, t, 0)
\end{aligned}
$$

$\square$

For the third step to complete the proof of proposition 3, note that by definition $\sigma = q(d,t,u) = q_0(d,t,u)(1-Z) + q_1(d,t,u)Z$. Assumption 2 implies that $q_z(d,t,u),\ \ z = 0,1$ is smooth and so the right and left limits at $D = 0$ exist: $\lim_{D\to 0^+} q(d,t,u) = q_1(0,t,u) \equiv \sigma_1(t,u)$ and $\lim_{D\to 0^-} q(d,t,u) = q_0(0,t,u) \equiv \sigma_0(t,u)$. Combining this with lemmas 4 and 5 shows that equation (I.1) holds.

To see that the weighted W-LATE also holds note three things. First, the Qτ-LATEs $\eta(u,t)$ are identified. Second, the weighting function $w(t,u)$ is assumed to be known or estimable. Third, the set $\mathcal{U} \equiv \{u \in [0,1] : |\sigma_1(u) - \sigma_0(u)| > 0\}$ is identified given that the potential treatments $q_z(d,t,u),\ z = 0,1$ are identified (and in fact correspond to the quantiles such that $F^{-1}_{E_z|t,d}(u) > 0$).

$\square$

I.2 Results

Proposition 3 shows that we can estimate weighted averages of the causal effects of inequity on compliance at different exposure quantiles and tax liabilities. To implement this in practice, we use regression weights and estimate the following regression:

$$c_i = \lambda_{r(i)} + g(\tau_i, e_i) + f_0(d_i) + \beta_0 HTS_i + f_1(d_i) \times HTS_i + \varepsilon_i \tag{I.4}$$

where $\lambda_{r(i)}$ are fixed effects for 500-meter segments along the boundaries to ensure we are comparing properties who are nearby each other; $g(\tau_i, e_i)$ are flexible controls for property i's (log) tax liability τ_i and exposure to mistagging e_i (our baseline estimates use τ splines and fifty quantiles of exposure fixed effects); $f_0(d_i)$ and $f_1(d_i)$ control flexibly for distance to the boundary on the low- and high-tag sides of the boundary respectively; and HTS_i is an indicator for properties on the high-tag side of the boundary ($d_i > 0$). We estimate the equation using our main sample as described in 2.4.

Panel A of Figure I.1 shows the results of estimating equation (I.4) with (log) inequity σ as the outcome. The figure is constructed analogously to the baseline BDD in figure 3A discussed in section 4.1. It shows that we have a strong first-stage impact on inequity of 0.554 (down from 0.625 in figure 3C) even after controlling flexibly for the tax liability and exposure to mistagging (using cubic splines of the tax liability and fixed effects for fifty quantiles of exposure). Similarly, Panel B of figure I.1 shows the results of estimating equation (6) with compliance as the outcome. It shows that there is a strong impact of inequity on compliance. Compliance is 8.7 percentage points lower on the high-tag side of the boundaries even after controlling flexibly flexibly for the tax liability and exposure to mistagging.

Table I.1 shows the results of estimating equation (I.4) using a variety of approaches to controlling flexibly for the tax liability and exposure. In column (1) we control for cubic splines of the tax liability and fixed effects for fifty quantiles of exposure to mistagging. In column (2) we replace the exposure quantiles with cubic splines of exposure while column (3) replaces the splines of the tax liability with fixed effects for quantiles of tax liability. Columns (4)–(6) additionally interact the tax liability controls with the exposure controls. At the bottom of the table, we also present the first stage results and the compliance elasticity the results imply. The table shows remarkably consistent results: the implied elasticity of compliance with respect to inequity ranges from 0.19 to 0.23.

FIGURE I.1: AUGMENTED BOUNDARY DISCONTINUITY DESIGN

A: FIRST STAGE

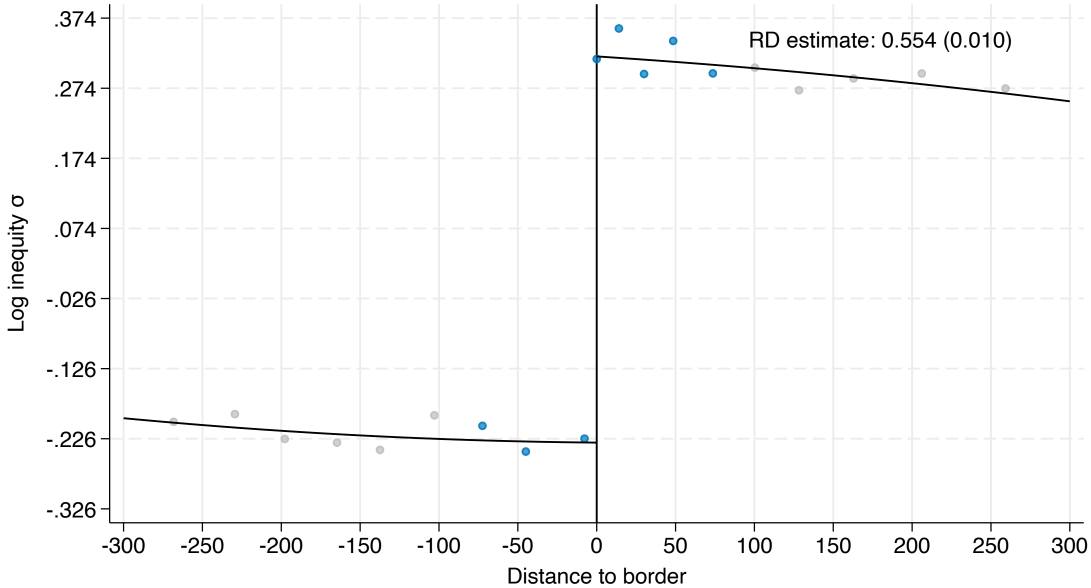

B: COMPLIANCE EFFECTS

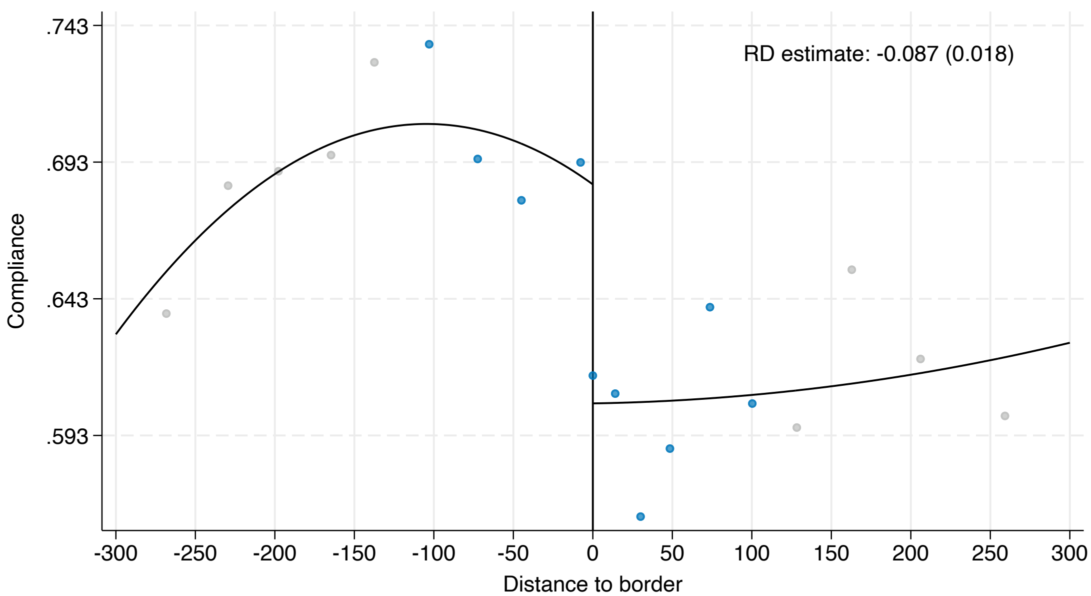

Notes: The figure shows the first stage impact on inequity from the estimation of equation (I.4): $y_i = \lambda_{r(i)} + g(\tau_i, e_i) + f_0(d_i) + \beta_0 HTS_i + f_1(d_i) \times HTS_i + \varepsilon_i$, where $\lambda_{r(i)}$ are fixed effects for 500-meter segments along the boundaries to ensure we are comparing properties who are nearby each other; $g(\tau_i, e_i)$ are flexible controls for property i's (log) tax liability τ_i and exposure to mistagging e_i (our baseline estimates use τ splines and fifty quantiles of exposure fixed effects); $f_0(d_i)$ and $f_1(d_i)$ control flexibly for distance to the boundary on the low- and high-tag sides of the boundary respectively; and HTS_i is an indicator for properties on the high-tag side of the boundary ($d_i > 0$). Panel A uses inequity $\log(\sigma_i)$ as the outcome variable, and panel B uses compliance c_i as the outcome. Overlaid on the figure, we show the point estimate of the discontinuity in the outcome estimated using local linear distance controls, the MSE-minimizing bandwidth, and triangular kernel weights in distance. The dots in the figure show the coefficients from estimating (I.4) with fixed effects for decile-spaced bins of distance, using the same triangular kernel weights but censoring them at their tenth percentile to give non-zero weights to distances outside the optimal bandwidth. The bins in the optimal bandwidth are shown in blue while those outside are shown in gray. The black line is a global cubic polynomial fit in the same way.

TABLE I.1: AUGMENTED BOUNDARY DISCONTINUITY DESIGN: COMPLIANCE EFFECTS

	(1)	(2)	(3)	(4)	(5)	(6)
RD estimate	-0.08***	-0.07***	-0.08***	-0.07***	-0.08***	-0.09***
	(0.02)	(0.02)	(0.02)	(0.02)	(0.02)	(0.02)
R^2						
Distance controls	✓	✓	✓	✓	✓	✓
Segment FEs	✓	✓	✓	✓	✓	✓
τ splines	✓	✓	✓	✓	✗	✗
exp dec FEs	✓	✗	✓	✗	✗	✓
τ decile FEs	✗	✗	✗	✗	✓	✓
exp splines	✗	✓	✗	✓	✗	✗
τ splines $\times$ exp dec FEs	✗	✗	✓	✗	✗	✗
τ splines $\times$ exp splines	✗	✗	✗	✓	✗	✗
τ dec FEs $\times$ exp dec FEs	✗	✗	✗	✗	✗	✓
First-stage	0.538***	0.507***	0.551***	0.524***	0.537***	0.551***
	(0.010)	(0.010)	(0.010)	(0.010)	(0.010)	(0.010)
Elasticity	0.216***	0.194***	0.222***	0.196***	0.220***	0.227***
	(0.050)	(0.055)	(0.049)	(0.055)	(0.052)	(0.051)
N	9236	9235	9236	9235	9236	9236

Notes: The table shows the results of estimating the augmented BDD equation (I.4): $c_i = \lambda_{r(i)} + g(\tau_i, e_i) + f_0(d_i) + \beta_0 HTS_i + f_1(d_i) \times HTS_i + \varepsilon_i$, where $\lambda_{r(i)}$ are fixed effects for 500-meter segments along the boundaries to ensure we are comparing properties who are nearby each other; $g(\tau_i, e_i)$ are flexible controls for property i's (log) tax liability τ_i and exposure to mistagging e_i; $f_0(d_i)$ and $f_1(d_i)$ control flexibly for distance to the boundary on the low- and high-tag sides of the boundary respectively; and HTS_i is an indicator for properties on the high-tag side of the boundary ($d_i > 0$). The columns use a variety of approaches to controlling flexibly for the tax liability and exposure to mistagging. In column (1) we control for cubic splines of the tax liability and fixed effects for fifty quantiles of exposure. In column (2) we replace the exposure quantiles with cubic splines of exposure while column (3) replaces the splines of the tax liability with fixed effect for fifty quantiles. Columns (4)–(6) additionally interact the tax liability controls with the exposure controls. The table shows remarkably consistent results: the implied elasticity of compliance with respect to inequity ranges from 0.25 to 0.27.

J Difference in Boundary Discontinuities Design

We build heavily on the methods developed by Frölich & Huber (2019) to incorporate covariates into Regression Discontinuity Designs (RDD), and by Dong *et al.* (2023) to adapt the RDD to settings with continuous treatments. We denote the distance to the boundary of a tax sector — the running variable — as $D \in \mathcal{D} \subset \mathbb{R}$. Potential compliance outcomes are given by $C = G(\sigma, \tau, D, \nu) = G_0(\tau, D, \nu_0) + G_1(\sigma, \tau, D, \nu_1)$ where inequity $\sigma \in \mathbb{R}$ is our treatment of interest, τ is the (log) tax liability, and ν are other, potentially unobserved, determinants of compliance.[62] We separate the potential outcomes into an untreated component G_0 capturing potential compliance at different tax liabilities τ in the absence of inequity, and a treatment effect G_1 capturing the impact of inequity on compliance. We partition the unobserved determinants of compliance ν into those that influence the treatment effect ν_1 and those that only affect the untreated potential outcomes ν_0. As assumption 5 makes precise, we allow unobservable drivers of the untreated potential outcomes ν_0 to vary arbitrarily around the boundaries, but we maintain smoothness assumptions about the unobservables ν_1 that can interact with inequity.

It is useful to think of crossing the boundary as an instrument $Z = \mathbf{1}[D > 0]$ giving properties potential treatments when Z is exogenously set to z of $\sigma_z \equiv q_z(E_z) = (-1)^{1-z} \log\left(\frac{1+p_H E_z}{1+p_L E_z}\right)$, where E_z is a property's potential exposure when $Z = z$. One of our identifying assumptions relies on properties' rank invariance at the boundaries, so it will be convenient to express treatment exposure in terms of quantiles of the treatment distribution.[63] Our first assumption allows us to map one-to-one between quantiles u of exposure e to mistagging and inequity:

Assumption 4 (Quantile representation)**.** *The conditional distribution of exposure E_z given distance $D = d$ and tax liability $\tau = t$ is continuous with a strictly increasing CDF $F_{E_z|\tau,D}(e, t, d)$.*

Assumption 4 allows us to define the inequity faced by the property at the uth conditional quantile of exposure as[64]

$$q_z(u, t, d) = (-1)^{1-z} \log\left(\frac{1 + p_H F^{-1}_{E_z|t,d}(u)}{1 + p_L F^{-1}_{E_z|t,d}(u)}\right)$$

The next assumption specifies what is required to vary smoothly at the boundaries and what can feature discontinuities at the boundaries:

Assumption 5 (Smoothness)**.** *$q_z(d, u, t)$, $z = 0, 1$, is continuous in $d \in \mathcal{D}$ at all quantiles of potential exposure $U_z = u \in [0, 1]$ and $t \in \mathcal{T} \subset \mathbb{R}^+$. $G_0(\tau, D, \nu_0)$ is right and left continuous in D at $D = 0$ for any $t \in \mathcal{T}$ and $\nu_0 \in \mathcal{V}_0$. $f_{\nu_0|U_z,\tau,D}(v_0, u, t, d) = f_{\nu_0|\tau,D}(v_0, t, d)$ for any $u \in [0, 1]$. $f_{\nu_0|\tau,D}(v_0, t, d)$ is left and right continuous at $D = 0$ for any $t \in \mathcal{T}$ and $v_0 \in \mathcal{V}_0$ where $\mathcal{V}_0$ is compact. Either $G_1(\sigma, \tau, D, \nu_1)$ is continuous in all its arguments or it is a.e. continuous and bounded. $f_{\nu_1|U_z,\tau,D}(v_1, u, t, d)$ is continuous in D for any $u \in [0, 1]$, $t \in \mathcal{T}$ and $v_1 \in \mathcal{V}_1$ where $\mathcal{V}_1$ is compact. x $f_{D|\tau}(d, t)$ is continuous and strictly positive around $d = 0$.*

Assumption 5 requires that inequity, taxes, distance, and unobservables ν_1 all generate smooth impacts on the G_1 component of potential outcomes. It allows for taxes, distance, and the unobservables ν_0 to have a discontinuous effect on compliance at the boundary ($D = 0$), but only

[62]We allow these determinants $\nu \in \mathcal{V} \subset \mathbb{R}^{\dim_\nu}$ to have arbitrary dimension.

[63]This is also convenient since it offers a natural way to pool across tax sector boundaries.

[64]Note that while the reduced form only depends on e_i, it now depends on τ also because the distribution of e_i we are using to normalize with is conditional on distance and τ.

for reasons that are unrelated to inequity. Our final assumption requires that properties stay at approximately the same rank in the potential exposure distribution on either side of the tax sector boundaries. Formally,

Assumption 6 (Local exposure rank invariance or similarity). *Conditional on $D = 0$, 1. $U_0 = U_1$; or more generally, 2. $U_0|\nu_1 \sim U_1|\nu_1$*

Assumption 6 implies that a property would be at roughly the same rank in the distribution of exposure to mistagging if it were exogenously moved across the boundary.[65] This does not require properties to have the same potential exposure to mistagging on either side of the boundary. The relative after-tax price of land a is higher on the high-tag side of the boundary and so we might expect property owners to substitute towards built structure. Assumption 6 allows this, but requires that the unobservables are not correlated with the elasticity of substitution between land a and built structure b in such a way that it would reverse ranks in the exposure distribution when crossing the boundary.

With these assumptions, we can show that the difference in the LATEs between any pair of levels of exposure are identified:

Proposition 6 (Identification of Differences in LATEs). *Define the QDBDD-LATE:*

$$\begin{aligned}\eta\left(\underline{u},\bar{u},t\right) &\equiv \frac{\begin{array}{c}\int G\left(\sigma_1\left(\bar{u},t\right),t,0,v\right)-G\left(\sigma_0\left(\bar{u},t\right),t,0,v\right)F_{\nu|U,\tau,D}\left(dv,\bar{u},t,0\right)\\ -\int G\left(\sigma_1\left(\underline{u},t\right),t,0,v\right)-G\left(\sigma_0\left(\underline{u},t\right),t,0,v\right)F_{\nu|U,\tau,D}\left(dv,\underline{u},t,0\right)\end{array}}{\left[\sigma_1\left(\bar{u},t\right)-\sigma_0\left(\bar{u},t\right)\right]-\left[\sigma_1\left(\underline{u},t\right)-\sigma_0\left(\underline{u},t\right)\right]}\\ &= \frac{\mathbb{E}\left[C_{\sigma_1(\bar{u},t)}-C_{\sigma_0(\bar{u},t)}|U=\bar{u},\tau=t,D=0\right]-\mathbb{E}\left[C_{\sigma_1(\underline{u},t)}-C_{\sigma_0(\underline{u},t)}|U=\underline{u},\tau=t,D=0\right]}{\left[\sigma_1\left(\bar{u},t\right)-\sigma_0\left(\bar{u},t\right)\right]-\left[\sigma_1\left(\underline{u},t\right)-\sigma_0\left(\underline{u},t\right)\right]}\end{aligned} \tag{J.1}$$

This is the difference in the average causal effect of inequity for taxpayers with tax liability $\tau = t$ between taxpayers with exposure rank $U = \bar{u}$ and taxpayers with exposure rank $U = \underline{u}$. Under Assumptions 4, 5 & 6, for any $\bar{u}, \underline{u} \in \mathcal{U}$, and for any $t \in \mathcal{T}$, QDBDD-LATE $\eta\left(\underline{u},\bar{u},t\right)$ is identified and is given by

$$\eta\left(\underline{u},\bar{u},t\right)=\frac{\left[m^+\left(\bar{u},t\right)-m^-\left(\bar{u},t\right)\right]-\left[m^+\left(\underline{u},t\right)-m^-\left(\underline{u},t\right)\right]}{\left[q^+\left(\bar{u},t\right)-q^-\left(\bar{u},t\right)\right]-\left[q^+\left(\underline{u},t\right)-q^-\left(\underline{u},t\right)\right]} \tag{J.2}$$

where the limits in the denominator are defined by $q^+\left(u,t\right) \equiv \lim_{d\to 0^+} q\left(d,u,t\right)$ and $q^-\left(u,t\right) \equiv \lim_{d\to 0^-} q\left(d,u,t\right)$. Also let $m\left(s,t,d\right) \equiv \mathbb{E}\left[C|\sigma = s, \tau = t, D = d\right]$, and define $m^+\left(u,t\right) \equiv \lim_{d\to 0^+} m\left(q^+\left(u,t\right),t,d\right)$ and $m^-\left(u,t\right) \equiv \lim_{d\to 0^-} m\left(q^-\left(u,t\right),t,d\right)$. All of these can be consistently estimated from the data.

Further, the weighted DBDD-LATE $\bar{\eta}_{QDD}\left(w\right) = \int_{\mathcal{U}}\int_{\mathcal{U}}\int_{\mathcal{T}} \eta\left(\underline{u},\bar{u},t\right) w\left(\underline{u},\bar{u},t\right) dt d\bar{u} d\underline{u}$ is identified for any known or estimable weighting function $w\left(\underline{u},\bar{u},t\right)$ such that $w\left(\underline{u},\bar{u},t\right) \geq 0$ and $\int_{\mathcal{U}}\int_{\mathcal{U}}\int_{\mathcal{T}} w\left(\underline{u},\bar{u},t\right) dt d\bar{u} d\underline{u} = 1$.

Proof. Our proof proceeds similarly to the proof of proposition 3. We proceed in five steps. Our first lemma shows that crossing the boundary can be thought of as an excludable instrument conditional on the mistagging exposure rank U and the tax liabiltiy τ:

[65] The more general formulation of the assumption permits random slippages from a property's rank in the exposure distribution just on either side of the boundary (Chenozhukov & Hansen, 2005; Dong *et al.*, 2023).

Lemma 7 (Excludability). *Let Assumptions 4, 5 & 6 hold. Then for any $u \in [0,1]$,*

$$\lim_{d\to 0^-} f_{\nu_1|\sigma,\tau,D}\left(v_1, q_0\left(d,u,t\right), t, d\right) = \lim_{d\to 0^+} f_{\nu_1|\sigma,\tau,D}\left(v_1, q_1\left(d,u,t\right), t, d\right) = \lim_{d\to 0} f_{\nu_1|U,\tau,D}\left(v_1, u, t, d\right) \tag{J.3}$$

for $v_1 \in \mathcal{V}_1$ and $\tau \in \mathcal{T}$

Proof. By Bayes' rule, assumption 6, that $U_0|\left(\nu_1, D=0, \tau=t\right) \sim U_1|\left(\nu_1, D=0, \tau=t\right)$, where we now make explicit the conditioning on distance $D=0$ and tax liability τ, implies that $\nu_1|\left(U_0=u, D=0, \tau=t\right) \sim \nu_1|\left(U_1=u, D=0, \tau=t\right)$, i.e. that $f_{\nu_1|U_1,D,\tau} = f_{\nu_1|U_0,D,\tau}$. By invoking our smoothness assumption 5 and the definition relating observed to potential exposure ranks $U \equiv U_1 \mathbf{1}\left[D>0\right] + U_0 \mathbf{1}\left[D<0\right]$, we can show that their limits are the same from both sides:

$$\lim_{D\to 0^+} f_{\nu_1|U_1,D,\tau}\left(v_1,u,t\right) = \lim_{D\to 0^-} f_{\nu_1|U_0,D,\tau}\left(v_1,u,t\right) = \lim_{D\to 0} f_{\nu_1|U,D,\tau}\left(v_1,u,t\right)$$

Finally, we exploit the fact that under Assumption 4, for a given $D=d$ and $\tau=t$, whenever $d>0$ there is a one-to-one mapping between u and $q_1\left(d,u,t\right)$ and whenever $d<0$ there is a one-to-one mapping between u and $q_0\left(d,u,t\right)$ so that the same limits apply to the distributions conditional on inequity levels as the distributions conditional on exposure ranks

$$\lim_{D\to 0^+} f_{\nu_1|\sigma,D,\tau}\left(v_1, q_1\left(d,u,t\right), t\right) = \lim_{D\to 0^-} f_{\nu_1|\sigma,D,\tau}\left(v_1, q_0\left(d,u,t\right), t\right) = \lim_{D\to 0} f_{\nu_1|U,D,\tau}\left(v_1,u,t\right)$$

□

Lemma 7 thus show that given an exposure rank $U=u$ and a tax liability $\tau=t$, all potential changes in inequity σ when $D\to 0$ are independent of the unobservables ν_1.

Second, our smoothness assumptions mean that we cannot apply lemma 7 to the distribution of ν_0. Instead, the limits are given by the following lemma:

Lemma 8 (ν_0 Limits). *Let Assumptions 4 & 5 hold, Then for any $u \in [0,1]$, The limiting conditional distributions of ν_0 as $D \to 0$ from above and from below exist and are given by*

$$\lim_{D\to 0^+} f_{\nu_0|\sigma,\tau,D}\left(v_0, q_1\left(d,u,t\right), t, d\right) = \lim_{d\to 0^+} f_{\nu_0|U_1,\tau,D}\left(v_0,u,t,d\right) = f_1\left(v_0,t\right)$$
$$\lim_{D\to 0^-} f_{\nu_0|\sigma,\tau,D}\left(v_0, q_0\left(d,u,t\right), t, d\right) = \lim_{d\to 0^-} f_{\nu_0|U_0,\tau,D}\left(v_0,u,t,d\right) = f_0\left(v_0,t\right)$$

Proof. The proof proceeds in two steps. First, by Assumption 4, we can relate observed treatment σ to the potential exposure rank U_z on either side of the boundary. For a given $D=d$ and $\tau=t$, whenever $d>0$ there is a one-to-one mapping between U_1 and $q_1\left(d,U_1,t\right)$ and whenever $d<0$ there is a one-to-one mapping between U_0 and $q_0\left(d,U_0,t\right)$ so that for any $d>0$, $f_{\nu_0|U_1,\tau,D}\left(v_0,u,t,d\right) = f_{\nu_0|\sigma,\tau,D}\left(v_0,q_1\left(d,u,t\right),t,d\right)$ and for any $d<0$, $f_{\nu_0|U_0,\tau,D}\left(v_0,u,t,d\right) = f_{\nu_0|\sigma,\tau,D}\left(v_0,q_0\left(d,u,t\right),t,d\right)$.

Second, note that by Assumption 5, the distribution of ν_0 is independent of a taxpayer's potential mistagging exposure rank, and has both left- and right-limits at $D=0$, though they need not be the same, as indicated by the substricts at the end of the equalities. □

Third, we establish the limiting values of the conditional expectations of compliance.

Lemma 9 (Compliance Limits)**.** *Let Assumptions 4, 5, & 6 hold. Then, for any $u \in [0,1]$,*

$$\lim_{d\to 0^+} \mathbb{E}\left[C|U=u,\tau=t,D=d\right] = \int_{\mathcal{V}_0} G_0\left(t,0,v_0\right) dF_1\left(dv_0,t\right)$$
$$+\int_{\mathcal{V}_1} G_1\left(\sigma_1\left(u,t\right),t,0,v_1\right) F_{\nu_1|U,\tau,D}\left(dv_1,u,t,0\right) \tag{J.4}$$
$$= m_0^+\left(t\right)+m_1^+\left(u,t\right)$$
$$\lim_{d\to 0^-} \mathbb{E}\left[C|U=u,\tau=t,D=d\right] = \int_{\mathcal{V}_0} G_0\left(t,0,v_0\right) dF_0\left(dv_0,t\right)$$
$$+\int_{\mathcal{V}_1} G_1\left(\sigma_1\left(u,t\right),t,0,v_1\right) F_{\nu_1|U,\tau,D}\left(dv_1,u,t,0\right) \tag{J.5}$$
$$= m_0^-\left(t\right)+m_1^-\left(u,t\right)$$
$$\tag{J.6}$$

Proof. We present the proof for the limit from above in equation (J.4). Exactly analogous steps establish the statement for the limit from below in equation (J.5). By assumption 4, we can map from the exposure quantiles U to the treatment levels one-to-one:

$$\lim_{D\to 0^+} \mathbb{E}\left[C|U=u,D=d,\tau=t\right] = \lim_{D\to 0^+} \mathbb{E}\left[C|\sigma=q_1\left(d,u,t\right),U_1=u,D=d,\tau=t\right]$$

And we can substitute in the definition of the potential outcome $C=G\left(\sigma,\tau,D,\nu\right)=G_0\left(D,\tau,\nu_0\right)+G_1\left(\sigma,\tau,D,\nu_1\right)$

$$\lim_{D\to 0^+} \mathbb{E}\left[C|\sigma=q_1\left(d,u,t\right),U_1=u,D=d,\tau=t\right]$$
$$=\lim_{D\to 0^+} \mathbb{E}\left[G_0\left(d,t,\nu_0\right)+G_1\left(q_1\left(d,u,t\right),t,d,\nu_1\right)|\sigma=q_1\left(d,u,t\right),D=d,\tau=t\right]$$

By the smoothness in Assumption 5 with the compact supports of ν_1 and ν_2, we can exchange the order of the limit and the expectation and the expectation has a right-limit in D at $D=0$ so that

$$\lim_{D\to 0^+} \mathbb{E}\left[G_0\left(D,\tau,\nu_0\right)+G_1\left(\sigma,\tau,D,\nu_1\right)|\sigma=q_1\left(d,u,t\right),D=d,\tau=t\right]$$
$$=\mathbb{E}_{\nu_0}\left[G_0\left(0,t,\nu_0\right)|D=0,\tau=t\right]+\mathbb{E}_{\nu_1}\left[G_1\left(\sigma_1\left(u\right),t,0,\nu_1\right)|U_1=u,D=0,\tau=t\right]$$

Finally, applying lemmas 7 and 8, these are

$$\mathbb{E}_{\nu_0}\left[G_0\left(0,t,\nu_0\right)|D=0,\tau=t\right]+\mathbb{E}_{\nu_1}\left[G_1\left(\sigma_1\left(u\right),t,0,\nu_1\right)|U_1=u,D=0,\tau=t\right]$$
$$=\int_{\mathcal{V}_0} G_0\left(t,0,v_0\right) F_{\nu_0|U_1,\tau,D}\left(dv_1,u,t,0\right)+\int_{\mathcal{V}_1} G_1\left(\sigma_1\left(u,t\right),t,0,v_1\right) F_{\nu_1|U_1,\tau,D}\left(dv_1,u,t,0\right)$$
$$=\int_{\mathcal{V}_0} G_0\left(t,0,v_0\right) F_1\left(dv_0,t\right)+\int_{\mathcal{V}_1} G_1\left(\sigma_1\left(u,t\right),t,0,v_1\right) F_{\nu_1|U,\tau,D}\left(dv_1,u,t,0\right)$$

□

Fourth, we combine these elements to establish equation (J.2). For the denominator, note that by definition $\sigma=q\left(d,t,u\right)=q_0\left(d,t,u\right)\left(1-Z\right)+q_1\left(d,t,u\right)Z$. Assumption 2 implies that $q_z\left(d,t,u\right),\ z=0,1$ is smooth and so the right and left limits at $D=0$ exist: $\lim_{D\to 0^+} q\left(d,t,u\right)=$

$q_1(0,t,u) \equiv \sigma_1(t,u)$ and $\lim_{D\to 0^-} q(d,t,u) = q_0(0,t,u) \equiv \sigma_0(t,u)$. Applying lemma 9 to the terms in the numerator, we have

$$\lim_{d\to 0^+} \mathbb{E}\left[C|U=\bar{u},\tau=t,D=d\right] = m_0^+(t) + m_1^+(\bar{u},t)$$
$$\lim_{d\to 0^-} \mathbb{E}\left[C|U=\bar{u},\tau=t,D=d\right] = m_0^-(t) + m_1^-(\bar{u},t)$$
$$\lim_{d\to 0^+} \mathbb{E}\left[C|U=\underline{u},\tau=t,D=d\right] = m_0^+(t) + m_1^+(\underline{u},t)$$
$$\lim_{d\to 0^-} \mathbb{E}\left[C|U=\underline{u},\tau=t,D=d\right] = m_0^+(t) + m_1^+(\underline{u},t)$$

And inserting these into the definition of $\eta(\underline{u},\bar{u},t)$ completes the proof.

Fifth, to see that the weighted WDD-LATE is also identified, note three things. First, the QτDD-LATEs $\eta(\underline{u},\bar{u},t)$ are identified. Second, the weighting function $w(\underline{u},\bar{u},t)$ is assumed to be known or estimable. Third, the set $\mathcal{U} \equiv \{u \in [0,1] : |\sigma_1(u) - \sigma_0(u)| > 0\}$ is identified given that the potential treatments $q_z(d,t,u)$, $z = 0,1$ are identified (and in fact correspond to the quantiles such that $F^{-1}_{E_z|t,d}(u) > 0$). □

Proposition 6 shows that we can identify the difference in the treatment effects of crossing the boundary experienced by properties at any pair of levels of exposure to mistagging ranks $\underline{u}$ and $\bar{u}$ — and hence between any pair of levels of inequity since by assumption 4 there is a one-to-one mapping between exposure ranks u and potential treatments $q_z(d,u,t)$. Since we permit discontinuities in compliance at the boundary, neither the treatment effect experienced by properties with exposure rank $\underline{u}$ nor the treatment effect at $\bar{u}$ is identified. However, the difference between the two, and hence the shape of the relationship between inequity and treatment effects, is identified. In section 5.1 we present our estimates of such weighted LATEs.

K Sample Selection and Robustness Checks

In this appendix, we detail the sampling procedures undertaken to construct the final datasets used in our empirical analyses. Specifically, we outline each subsampling step and document the number of properties excluded at each stage.

For our cross-sectional boundary discontinuity analysis, we focus on properties located within 300 meters of the tax sector boundaries. Additionally, we exclude properties exempt from taxation, properties without construction, and those not designated as residential. Properties located on sector boundaries overlapping neighborhood boundaries were also excluded to prevent potential differences in municipal public goods provision. Table K.1 summarizes these sequential subsampling steps and provides the resulting sample sizes at every stage:

TABLE K.1: SUBSAMPLING STEPS - CROSS SECTIONAL SAMPLE

Subsampling step	N left in 2010	N left 04-18
Initial data	368,828	6,595,279
Drop properties beyond 300 meters from boundaries	178,767	3,011,054
Drop exempted properties	104,746	2,343,319
Drop properties on neighborhood borders	51,041	1,132,079
Drop non-residential properties	41,536	927,390
Drop lots without properties in 2010	41,536	626,076
Drop very large lots	33,500	509,486
Drop properties with no high tag side in 2010	25,098	382,249

We applied similar subsampling steps to construct the sample used for analyzing responses to the tax reform. The primary difference is that we reincorporate tax sector boundaries overlapping neighborhood boundaries, since our empirical design can control for boundary-specific characteristics that remain constant over time, such as differences between neighborhoods.

Table K.2 summarizes these steps and shows the corresponding sample sizes at each stage:

TABLE K.2: SUBSAMPLING STEPS - TAX REFORM SAMPLE

Subsampling step	N left in 2010	N left 04-18
Initial data	368,828	6,595,279
Drop properties beyond 300 meters from boundaries	178,767	3,011,054
Drop exempted properties	104,746	2,343,319
Drop non-residential properties	84,869	1,915,943
Drop lots without properties in 2010	84,869	1,284,321
Drop very large lots	68,735	1,055,587
Drop properties with no high tag side in 2010	53,685	825,865

To assess the robustness of our results to different sampling decisions, the following subsections replicate the main analyses under alternative subsampling criteria. Each figure and table explicitly references the corresponding results presented in the main sections of the paper.

Specifically, we check the robustness of our findings in the following alternative samples:

1. The sample including properties on neighborhood borders in section K.1
2. The sample excluding properties on neighborhood borders in our analysis of the 2011 reform in section K.2

3. The sample including non-residential properties in section K.3
4. The sample using a relaxed "large lots" definition in K.4
5. The sample using a stringent "large lots" definition in K.5
6. Using alternative definitions of a non-trivial degree of inequity in section K.6

K.1 Sample including properties on neighborhood borders

In the main analysis, we excluded properties located on neighborhood boundaries from the cross-sectional sample but retained them in the tax reform analysis. In this subsection, we re-estimate the cross-sectional specifications after including these properties.

FIGURE K.1: CROSS-SECTIONAL ANALYSIS INCLUDING PROPERTIES ON NEIGHBORHOOD BORDERS

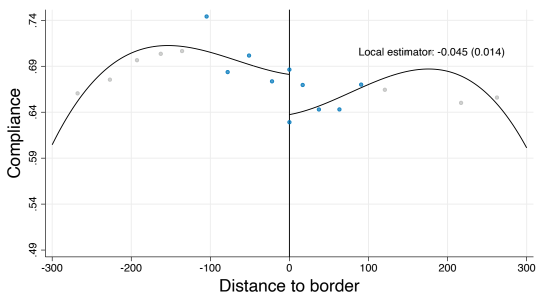

A: PANEL A OF FIGURE 3

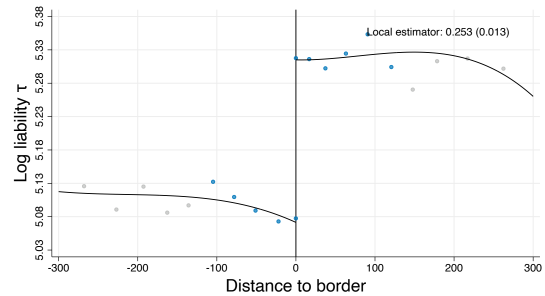

B: PANEL B OF FIGURE 3

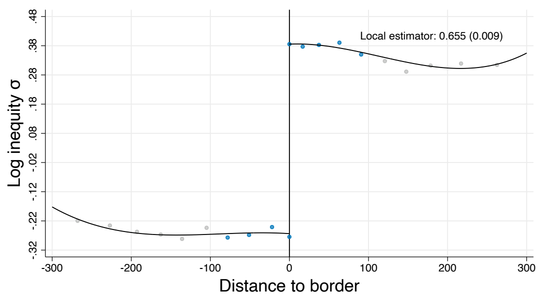

C: PANEL C OF FIGURE 3

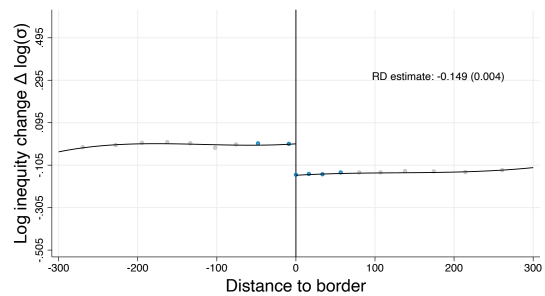

D: PANEL A OF FIGURE 4

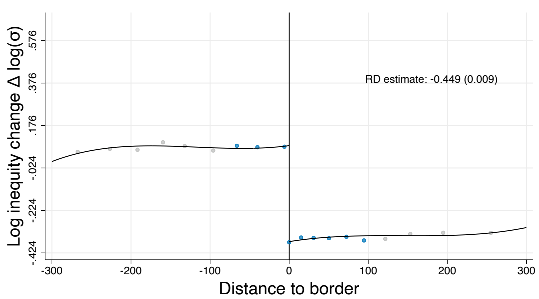

E: PANEL B OF FIGURE 4

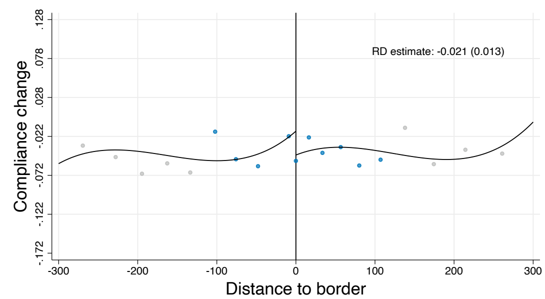

F: PANEL C OF FIGURE 4

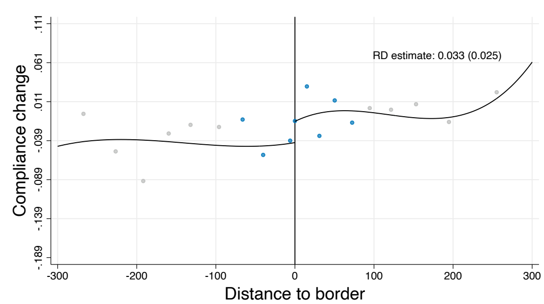

G: PANEL D OF FIGURE 4

Notes: This figure replicates the main cross-sectional analysis from the paper, but additionally includes properties located on neighborhood boundaries. Panels A-C replicate the analysis from panels A-C of figure 3, panel D-G replicate the analysis from panel A-D of figure 4.

TABLE K.3: DIFFERENCE IN BOUNDARY DISCONTINUITY DESIGN: COMPLIANCE EFFECTS

	(1)	(2)	(3)	(4)	(5)	(6)	(7)
1(high tag side) $\times\lvert\log(\sigma)\rvert$	-0.15***	-0.14***	-0.17***	-0.15***	-0.15***	-0.16***	-0.15***
	(0.02)	(0.02)	(0.02)	(0.02)	(0.02)	(0.02)	(0.02)
R^2	0.109	0.110	0.107	0.112	0.118	0.109	0.196
Distance controls	✓	✓	✓	✓	✓	✓	✓
Segment fixed effects	✓	✓	✓	✓	✓	✓	✓
τ splines	✓	✓	✓	✗	✓	✓	✗
τ deciles	✗	✗	✗	✓	✗	✗	✓
Exposure deciles	✓	✓	✗	✓	✓	✗	✓
Exposure splines	✗	✗	✓	✗	✗	✓	✗
τ splines $\times$ HTS	✗	✓	✓	✗	✓	✓	✗
τ deciles $\times$ HTS	✗	✗	✗	✓	✗	✗	✓
Exposure deciles $\times$ HTS	✗	✓	✗	✓	✓	✗	✓
Exposure splines $\times$ HTS	✗	✗	✓	✗	✗	✓	✗
τ splines $\times$ exp deciles	✗	✗	✗	✗	✓	✗	✗
τ splines $\times$ exp splines	✗	✗	✗	✗	✗	✓	✗
τ deciles $\times$ exp deciles	✗	✗	✗	✗	✗	✗	✓
τ splines $\times$ HTS $\times$ exp deciles	✗	✗	✗	✗	✓	✗	✗
τ splines $\times$ HTS $\times$ exp splines	✗	✗	✗	✗	✗	✓	✗
τ deciles $\times$ HTS $\times$ exp deciles	✗	✗	✗	✗	✗	✗	✓
Elasticity η	0.238***	0.225***	0.263***	0.228***	0.238***	0.245***	0.238***
	0.027	0.030	0.028	0.030	0.031	0.029	0.033
N	53643	53643	53643	53643	53643	53643	53534

Notes: This table replicates the analysis from table 1, but additionally includes properties located on neighborhood boundaries. The table shows the results of estimation of equation (7): $c_i = \lambda_{r(i)} + g_0(\tau_i, e_i) + f(d_i) + HTS_i \times [\beta_0 + \eta \log(\sigma) + h(d_i) + g_1(\tau_i, e_i)] + \varepsilon_i$ where terms are as defined above in the notes to table 1. In column (1), we control for cubic splines of the tax liability and fixed effects for fifty quantiles of exposure. In column (2) we control separately for the tax liability and exposure to mistagging on either side of the boundary. Column (3) replaces the exposure quantiles with cubic splines in exposure while column (4) replaces the tax liability cubic splines with fixed effects for fifty quantiles. Columns (5)–(7) replicate the specifications in columns (2)–(4), respectively, but additionally include interactions between the tax liability controls and the exposure controls.

K.2 Sample excluding properties on neighborhood borders

In the main analysis, we excluded properties located on neighborhood boundaries from the cross-sectional analysis but retained them in the tax reform analysis. In this subsection, we re-estimate the tax reform specifications after excluding properties located on neighborhood boundaries.

FIGURE K.2: TAX REFORM ANALYSIS EXCLUDING PROPERTIES ON NEIGHBORHOOD BORDERS

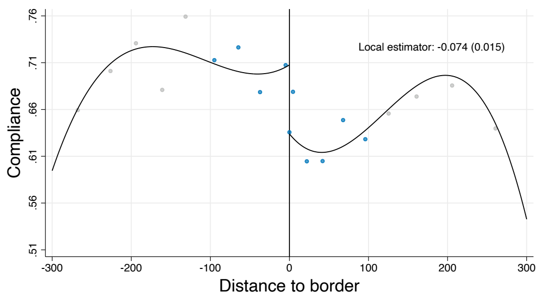

A: PANEL A OF FIGURE 6

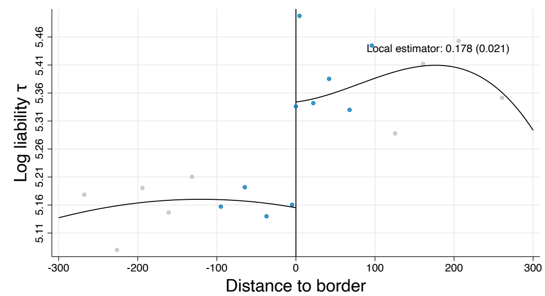

B: PANEL B OF FIGURE 6

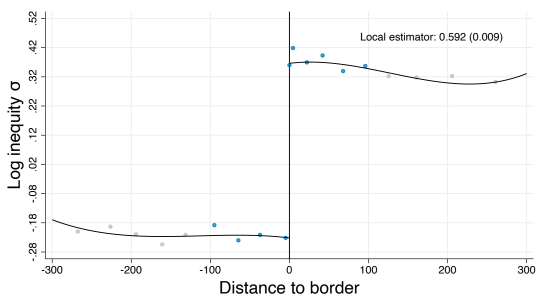

C: PANEL C OF FIGURE 6

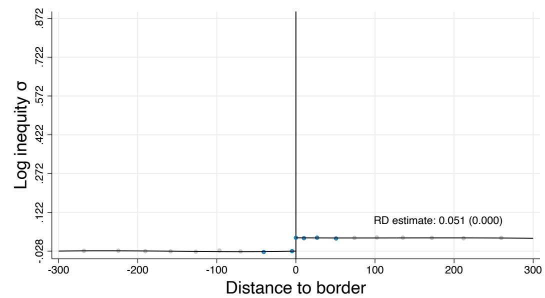

D: PANEL D OF FIGURE 6

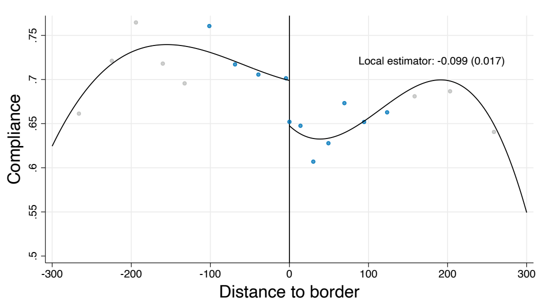

E: PANEL A OF FIGURE 7

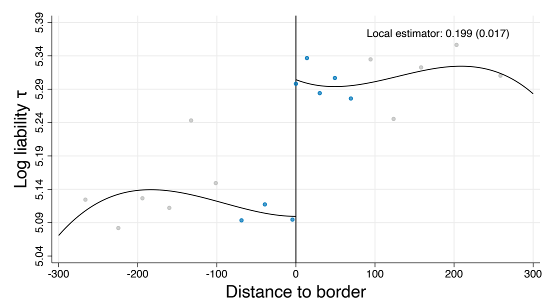

F: PANEL B OF FIGURE 7

Notes: This figure replicates the main tax reform specifications from the paper, but excluding properties located on neighborhood boundaries. Panels A-D replicate the analysis from panel A-D of figure 6, panels E-F replicate the analysis from panel A-B of figure 7.

Table K.4: Dynamic Difference in Boundary Discontinuity Design

	(1)	(2)	(3)	(4)	(5)	(6)	(7)
1(high tag side) X $\Delta\log(\sigma)$	-0.101**	-0.094**	-0.102**	-0.088**	-0.101**	-0.090**	-0.141***
	(0.040)	(0.044)	(0.042)	(0.044)	(0.045)	(0.045)	(0.050)
R^2	0.037	0.039	0.035	0.042	0.055	0.036	0.206
Distance controls	✓	✓	✓	✓	✓	✓	✓
Segment FEs	✓	✓	✓	✓	✓	✓	✓
$\Delta\tau$ splines	✓	✓	✓	✗	✓	✓	✗
$\Delta\tau$ deciles	✗	✗	✗	✓	✗	✗	✓
Exposure deciles	✓	✓	✗	✓	✓	✗	✓
Exposure splines	✗	✗	✓	✗	✗	✓	✗
$\Delta\tau$ splines $\times$ HTS	✗	✓	✓	✗	✓	✓	✗
$\Delta\tau$ deciles $\times$ HTS	✗	✗	✗	✓	✗	✗	✓
Exposure deciles $\times$ HTS	✗	✓	✗	✓	✓	✗	✓
Exposure splines $\times$ HTS	✗	✗	✓	✗	✗	✓	✗
$\Delta\tau$ splines $\times$ exp deciles	✗	✗	✗	✗	✓	✗	✗
$\Delta\tau$ splines $\times$ exp splines	✗	✗	✗	✗	✗	✓	✗
$\Delta\tau$ deciles $\times$ exp deciles	✗	✗	✗	✗	✗	✗	✓
$\Delta\tau$ splines $\times$ HTS $\times$ exp deciles	✗	✗	✗	✗	✓	✗	✗
$\Delta\tau$ splines $\times$ HTS $\times$ exp splines	✗	✗	✗	✗	✗	✓	✗
$\Delta\tau$ deciles $\times$ HTS $\times$ exp deciles	✗	✗	✗	✗	✗	✗	✓
Elasticity η	0.156**	0.146**	0.158**	0.137**	0.156**	0.139**	0.218***
	(0.062)	(0.067)	(0.065)	(0.068)	(0.070)	(0.069)	(0.078)
N	24902	24902	24902	24902	24902	24902	24374

Notes: This table replicates the analysis from table 2, but excluding properties located on neighborhood boundaries. It table shows the results of estimating equation (9) derived in section 4.3 and discussed in section 5.2: $\Delta c_i = \lambda_{r(i)} + g_0(\Delta\tau_i, e_i) + f_0(d_i) + HTS_i \times [\delta_0 + \tilde{\eta}\Delta\log(\sigma_i) + g_1(\Delta\tau_i, e_i) + f_1(d_i)] + \varepsilon_i$ where all terms are as defined above in the notes to table 1. Column (1) controls for cubic splines of the changes in tax liability and fixed effects for fifty quantiles of exposure. Column (2) controls separately for the changes in tax liability and exposure to mistagging on either side of the boundary. Column (3) replaces the exposure quantiles with splines, while column (4) replaces the changes in tax liability splines with fixed effects for fifty quantiles of the changes in tax liability. Columns (5)–(7) replicate the specifications in columns (2)–(4), respectively, but additionally include interactions between the changes in tax liability controls and the exposure controls.

K.3 Sample with non-residential properties

In this subsection, we re-estimate the main specifications after including non-residential properties, which are excluded in the main text.

FIGURE K.3: MAIN ANALYSIS INCLUDING NON-RESIDENTIAL PROPERTIES

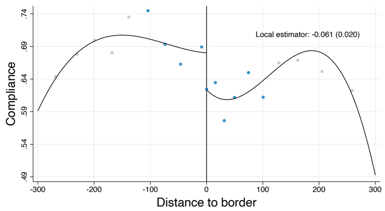

A: PANEL A OF FIGURE 3

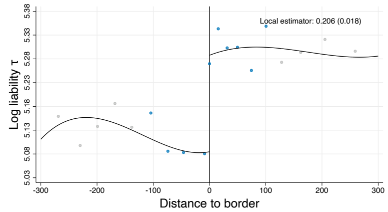

B: PANEL B OF FIGURE 3

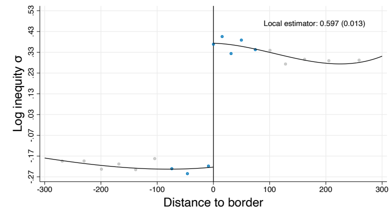

C: PANEL C OF FIGURE 3

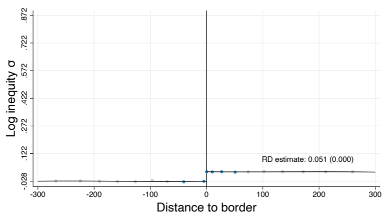

D: PANEL A OF FIGURE 4

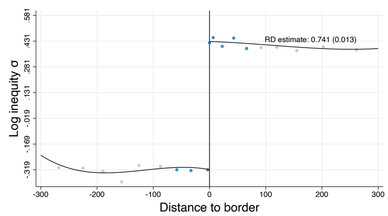

E: PANEL B OF FIGURE 4

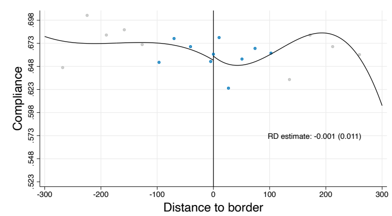

F: PANEL C OF FIGURE 4

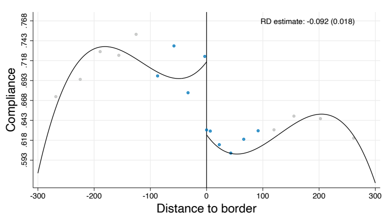

G: PANEL D OF FIGURE 4

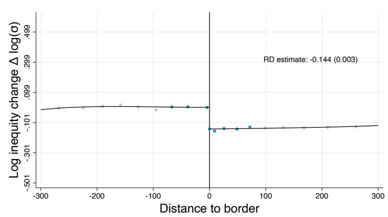

H: PANEL A OF FIGURE 6

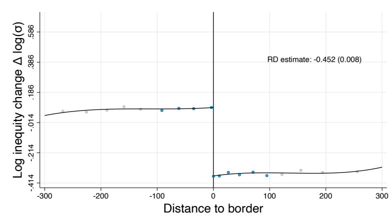

I: PANEL B OF FIGURE 6

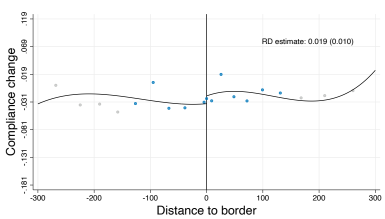

J: PANEL C OF FIGURE 6

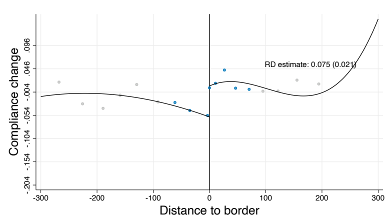

K: PANEL D OF FIGURE 6

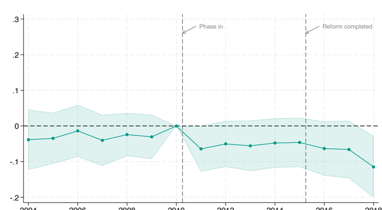

L: PANEL A OF FIGURE 7

M: PANEL B OF FIGURE 7

Notes: This figure replicates the main tax reform specifications from the paper, but after including non-residential properties. Panels A-C replicate the analysis from panels A-C of figure 3, panels D-G replicate the analysis from panels A-D of figure 4, panels H-K replicate the analysis from panel A-D of figure 6, panels L-M replicate the analysis from panels A-B of figure 7.

TABLE K.5: DIFFERENCE IN BOUNDARY DISCONTINUITY DESIGN: COMPLIANCE EFFECTS

	(1)	(2)	(3)	(4)	(5)	(6)	(7)
1(high tag side) $\times \lvert \log(\sigma) \rvert$	-0.15***	-0.13***	-0.16***	-0.13***	-0.14***	-0.15***	-0.14***
	(0.02)	(0.02)	(0.02)	(0.02)	(0.03)	(0.02)	(0.03)
R^2	0.136	0.139	0.135	0.142	0.152	0.136	0.276
Distance controls	✓	✓	✓	✓	✓	✓	✓
Segment fixed effects	✓	✓	✓	✓	✓	✓	✓
τ splines	✓	✓	✓	✗	✓	✓	✗
τ deciles	✗	✗	✗	✓	✗	✗	✓
Exposure deciles	✓	✓	✗	✓	✓	✗	✓
Exposure splines	✗	✗	✓	✗	✗	✓	✗
τ splines $\times$ HTS	✗	✓	✓	✗	✓	✓	✗
τ deciles $\times$ HTS	✗	✗	✗	✓	✗	✗	✓
Exposure deciles $\times$ HTS	✗	✓	✗	✓	✓	✗	✓
Exposure splines $\times$ HTS	✗	✗	✓	✗	✗	✓	✗
τ splines $\times$ exp deciles	✗	✗	✗	✗	✓	✗	✗
τ splines $\times$ exp splines	✗	✗	✗	✗	✗	✓	✗
τ deciles $\times$ exp deciles	✗	✗	✗	✗	✗	✗	✓
τ splines $\times$ HTS $\times$ exp deciles	✗	✗	✗	✗	✓	✗	✗
τ splines $\times$ HTS $\times$ exp splines	✗	✗	✗	✗	✗	✓	✗
τ deciles $\times$ HTS $\times$ exp deciles	✗	✗	✗	✗	✗	✗	✓
Elasticity η	0.224***	0.189***	0.234***	0.194***	0.212***	0.232***	0.213***
	0.033	0.036	0.033	0.036	0.038	0.035	0.042
N	31585	31585	31585	31585	31585	31585	31238

Notes: This table replicates the analysis from table 1, but additionally includes non-residential properties. It shows the results of estimation of equation (7) derived in section 4.2 and discussed in section 5.1: $c_i = \lambda_{r(i)} + g_0(\tau_i, e_i) + f_0(d_i) + HTS_i \times [\beta_0 + \tilde{\eta}\log(\sigma) + f_1(d_i) + g_1(\tau_i, e_i)] + \varepsilon_i$ where $\lambda_{r(i)}$ are boundary segment fixed effects, HTS_i is an indicator for being on the high-tag side of the boundary ($d_i > 0$); $f_0(d_i)$ and $f_1(d_i)$ control for distance to the boundary on the low- and high-tag sides of the boundary, respectively; $g_0(\tau_i, e_i)$ and $g_1(\tau_i, e_i)$ control for the tax liability and exposure on the low- and high-tag sides of the boundary, respectively; and ε_i is the residual. In column (1), we control for cubic splines of the tax liability and fixed effects for fifty quantiles of the exposure distribution. In column (2) we control separately for the tax liability and exposure to mistagging on either side of the boundary. Column (3) replaces the exposure quantiles with cubic splines in exposure while column (4) replaces the tax liability cubic splines with fixed effects for fifty quantiles. Columns (5)–(7) replicate the specifications in columns (2)–(4), respectively, but additionally include interactions between the tax liability controls and the exposure controls.

TABLE K.6: DYNAMIC DIFFERENCE IN BOUNDARY DISCONTINUITY DESIGN

	(1)	(2)	(3)	(4)	(5)	(6)	(7)
1(high tag side) X Δ $\log(\sigma)$	-0.087**	-0.084**	-0.089**	-0.080**	-0.079**	-0.082**	-0.118***
	(0.035)	(0.038)	(0.036)	(0.038)	(0.038)	(0.037)	(0.042)
R^2	0.033	0.034	0.031	0.037	0.047	0.032	0.171
Distance controls	✓	✓	✓	✓	✓	✓	✓
Segment FEs	✓	✓	✓	✓	✓	✓	✓
$\Delta\tau$ splines	✓	✓	✓	✗	✓	✓	✗
$\Delta\tau$ deciles	✗	✗	✗	✓	✗	✗	✓
Exposure deciles	✓	✓	✗	✓	✓	✗	✓
Exposure splines	✗	✗	✓	✗	✗	✓	✗
$\Delta\tau$ splines $\times$ HTS	✗	✓	✓	✗	✓	✓	✗
$\Delta\tau$ deciles $\times$ HTS	✗	✗	✗	✓	✗	✗	✓
Exposure deciles $\times$ HTS	✗	✓	✗	✓	✓	✗	✓
Exposure splines $\times$ HTS	✗	✗	✓	✗	✗	✓	✗
$\Delta\tau$ splines $\times$ exp deciles	✗	✗	✗	✗	✓	✗	✗
$\Delta\tau$ splines $\times$ exp splines	✗	✗	✗	✗	✗	✓	✗
$\Delta\tau$ deciles $\times$ exp deciles	✗	✗	✗	✗	✗	✗	✓
$\Delta\tau$ splines $\times$ HTS $\times$ exp deciles	✗	✗	✗	✗	✓	✗	✗
$\Delta\tau$ splines $\times$ HTS $\times$ exp splines	✗	✗	✗	✗	✗	✓	✗
$\Delta\tau$ deciles $\times$ HTS $\times$ exp deciles	✗	✗	✗	✗	✗	✗	✓
Elasticity η	0.130**	0.126**	0.133**	0.120**	0.119**	0.123**	0.176***
	(0.052)	(0.056)	(0.053)	(0.056)	(0.058)	(0.056)	(0.063)
N	31294	31294	31294	31294	31294	31294	30921

Notes: This table replicates the analysis from table 2, but additionally includes non-residential properties. It shows the results of estimating equation (9) derived in section 4.3 and discussed in section 5.2: $\Delta c_i = \lambda_{r(i)} + g_0(\Delta\tau_i, e_i) + f_0(d_i) + HTS_i \times [\delta_0 + \tilde{\eta}\Delta\log(\sigma_i) + g_1(\Delta\tau_i, e_i) + f_1(d_i)] + \varepsilon_i$ where all terms are as defined above in the notes to table 1. Column (1) controls for cubic splines of the changes in tax liability and fixed effects for fifty quantiles of the exposure distribution. Column (2) controls separately for the changes in tax liability and exposure to mistagging on either side of the boundary. Column (3) replaces the exposure quantiles with splines, while column (4) replaces the changes in tax liability splines with fixed effects for fifty quantiles of the changes in tax liability. Columns (5)–(7) replicate the specifications in columns (2)–(4), respectively, but additionally include interactions between the changes in tax liability controls and the exposure controls.

K.4 Relaxed "large lots" Definition: Drop the top 0.1% in terms of land area

In the main analysis, we exclude lots in the top 0.5 percent of the land area distribution because they introduce measurement error. In this subsection, we re-estimate the main specifications after excluding only the top 0.1 percent of lots by land area.

Figure K.4: Main Analysis Using the Relaxed "Large Lots" Definition

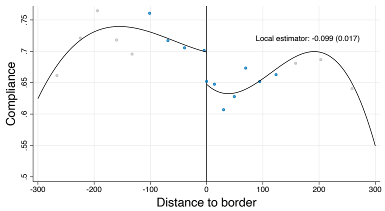

A: Panel A of figure 3

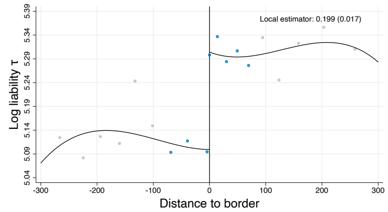

B: Panel B of figure 3

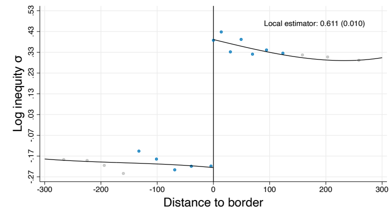

C: Panel C of figure 3

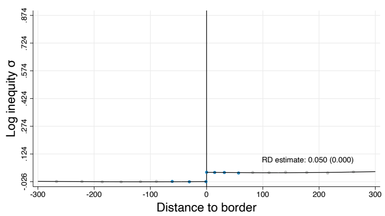

D: Panel A of figure 4

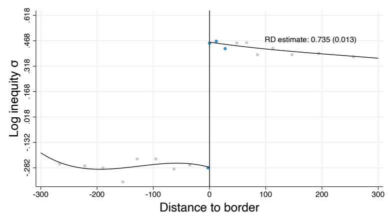

E: Panel B of figure 4

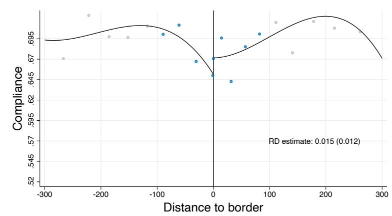

F: Panel C of figure 4

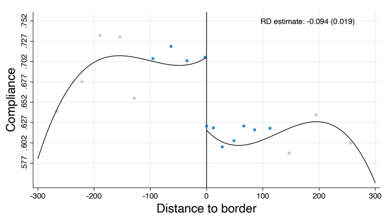

G: Panel D of figure 4

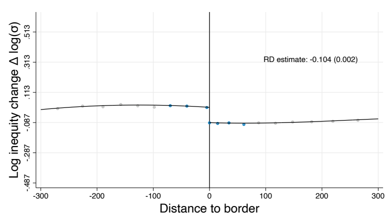

H: Panel A of figure 6

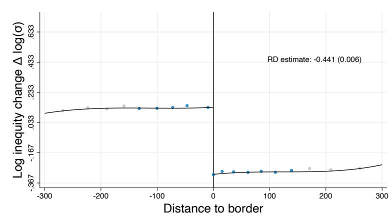

I: Panel B of figure 6

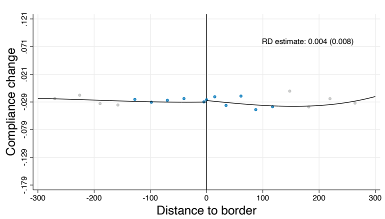

J: Panel C of figure 6

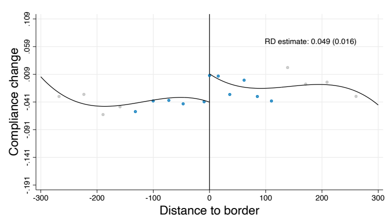

K: Panel D of figure 6

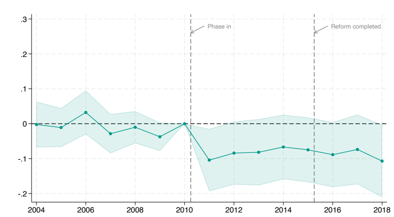

L: Panel A of figure 7

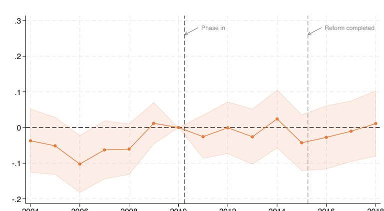

M: Panel B of figure 7

Notes: This figure replicates the main tax reform specifications from the paper, but dropping only the top 0.1%, rather than 0.5%, of lots in terms of land area. Panels A-C replicate the analysis from panels A-C of figure 3, panels D-G replicate the analysis from panel A-D of figure 4, panel H-K replicate the analysis from panels A-D of figure 6, panels L-M replicate the analysis from panel A-B of figure 7.

TABLE K.7: DIFFERENCE IN BOUNDARY DISCONTINUITY DESIGN: COMPLIANCE EFFECTS

	(1)	(2)	(3)	(4)	(5)	(6)	(7)
1(high tag side) $\times \lvert \log(\sigma) \rvert$	-0.15***	-0.14***	-0.15***	-0.14***	-0.15***	-0.15***	-0.13***
	(0.02)	(0.03)	(0.03)	(0.03)	(0.03)	(0.03)	(0.03)
R^2	0.140	0.143	0.138	0.146	0.160	0.140	0.290
Distance controls	✓	✓	✓	✓	✓	✓	✓
Segment fixed effects	✓	✓	✓	✓	✓	✓	✓
τ splines	✓	✓	✓	✗	✓	✓	✗
τ deciles	✗	✗	✗	✓	✗	✗	✓
Exposure deciles	✓	✓	✗	✓	✓	✗	✓
Exposure splines	✗	✗	✓	✗	✗	✓	✗
τ splines $\times$ HTS	✗	✓	✓	✗	✓	✓	✗
τ deciles $\times$ HTS	✗	✗	✗	✓	✗	✗	✓
Exposure deciles $\times$ HTS	✗	✓	✗	✓	✓	✗	✓
Exposure splines $\times$ HTS	✗	✗	✓	✗	✗	✓	✗
τ splines $\times$ exp deciles	✗	✗	✗	✗	✓	✗	✗
τ splines $\times$ exp splines	✗	✗	✗	✗	✗	✓	✗
τ deciles $\times$ exp deciles	✗	✗	✗	✗	✗	✗	✓
τ splines $\times$ HTS $\times$ exp deciles	✗	✗	✗	✗	✓	✗	✗
τ splines $\times$ HTS $\times$ exp splines	✗	✗	✗	✗	✗	✓	✗
τ deciles $\times$ HTS $\times$ exp deciles	✗	✗	✗	✗	✗	✗	✓
Elasticity η	0.232***	0.205***	0.235***	0.209***	0.220***	0.232***	0.199***
	0.038	0.041	0.038	0.041	0.044	0.040	0.049
N	27969	27969	27969	27969	27969	27969	27467

Notes: This table replicates the analysis from table 1, but dropping only the top 0.1%, rather than 0.5%, of lots in terms of land area. It shows the results of estimation of equation (7) derived in section 4.2 and discussed in section 5.1: $c_i = \lambda_{r(i)} + g_0(\tau_i, e_i) + f_0(d_i) + HTS_i \times [\beta_0 + \tilde{\eta}\log(\sigma) + f_1(d_i) + g_1(\tau_i, e_i)] + \varepsilon_i$ where $\lambda_{r(i)}$ are boundary segment fixed effects, HTS_i is an indicator for being on the high-tag side of the boundary ($d_i > 0$); $f_0(d_i)$ and $f_1(d_i)$ control for distance to the boundary on the low- and high-tag sides of the boundary, respectively; $g_0(\tau_i, e_i)$ and $g_1(\tau_i, e_i)$ control for the tax liability and exposure on the low- and high-tag sides of the boundary, respectively; and ε_i is the residual. In column (1), we control for cubic splines of the tax liability and fixed effects for fifty quantiles of the exposure distribution. In column (2) we control separately for the tax liability and exposure to mistagging on either side of the boundary. Column (3) replaces the exposure quantiles with cubic splines in exposure while column (4) replaces the tax liability cubic splines with fixed effects for fifty quantiles. Columns (5)–(7) replicate the specifications in columns (2)–(4), respectively, but additionally include interactions between the tax liability controls and the exposure controls.

TABLE K.8: DYNAMIC DIFFERENCE IN BOUNDARY DISCONTINUITY DESIGN

	(1)	(2)	(3)	(4)	(5)	(6)	(7)
1(high tag side) X Δ $\log(\sigma)$	-0.089**	-0.092**	-0.110***	-0.098**	-0.096**	-0.096**	-0.097**
	(0.037)	(0.039)	(0.042)	(0.039)	(0.040)	(0.044)	(0.040)
R^2	0.032	0.033	0.032	0.033	0.035	0.033	0.039
Distance controls	✓	✓	✓	✓	✓	✓	✓
Segment FEs	✓	✓	✓	✓	✓	✓	✓
$\Delta\tau$ splines	✓	✓	✓	✗	✓	✓	✗
$\Delta\tau$ deciles	✗	✗	✗	✓	✗	✗	✓
Exposure deciles	✓	✓	✗	✓	✓	✗	✓
Exposure splines	✗	✗	✓	✗	✗	✓	✗
$\Delta\tau$ splines $\times$ HTS	✗	✓	✓	✗	✓	✓	✗
$\Delta\tau$ deciles $\times$ HTS	✗	✗	✗	✓	✗	✗	✓
Exposure deciles $\times$ HTS	✗	✓	✗	✓	✓	✗	✓
Exposure splines $\times$ HTS	✗	✗	✓	✗	✗	✓	✗
$\Delta\tau$ splines $\times$ exp deciles	✗	✗	✗	✗	✓	✗	✗
$\Delta\tau$ splines $\times$ exp splines	✗	✗	✗	✗	✗	✓	✗
$\Delta\tau$ deciles $\times$ exp deciles	✗	✗	✗	✗	✗	✗	✓
$\Delta\tau$ splines $\times$ HTS $\times$ exp deciles	✗	✗	✗	✗	✓	✗	✗
$\Delta\tau$ splines $\times$ HTS $\times$ exp splines	✗	✗	✗	✗	✗	✓	✗
$\Delta\tau$ deciles $\times$ HTS $\times$ exp deciles	✗	✗	✗	✗	✗	✗	✓
Elasticity η	0.135*	0.139*	0.166**	0.148*	0.145*	0.145*	0.147*
	(0.057)	(0.059)	(0.064)	(0.059)	(0.061)	(0.066)	(0.061)
N	27805	27805	27805	27805	27805	27805	27805

Notes: This table replicates the analysis from table 2, but but dropping only the top 0.1%, rather than 0.5%, of lots in terms of land area. It shows the results of estimating equation (9) derived in section 4.3 and discussed in section 5.2: $\Delta c_i = \lambda_{r(i)} + g_0(\Delta\tau_i, e_i) + f_0(d_i) + HTS_i \times [\delta_0 + \tilde{\eta}\Delta\log(\sigma_i) + g_1(\Delta\tau_i, e_i) + f_1(d_i)] + \varepsilon_i$ where all terms are as defined above in the notes to table 1. Column (1) controls for cubic splines of the changes in tax liability and fixed effects for fifty quantiles of the exposure distribution. Column (2) controls separately for the changes in tax liability and exposure to mistagging on either side of the boundary. Column (3) replaces the exposure quantiles with splines, while column (4) replaces the changes in tax liability splines with fixed effects for fifty quantiles of the changes in tax liability. Columns (5)–(7) replicate the specifications in columns (2)–(4), respectively, but additionally include interactions between the changes in tax liability controls and the exposure controls.

K.5 Stringent "Large Lots" Definition: Drop thee top 1% in terms of land area

In the main analysis, we exclude lots in the top 0.5 percent of the land area distribution because they introduce measurement error. In this subsection, we re-estimate the main specifications after excluding the top 1 percent of lots by land area.

Figure K.5: Main Analysis Using the Stringent "Large Lots" Definition

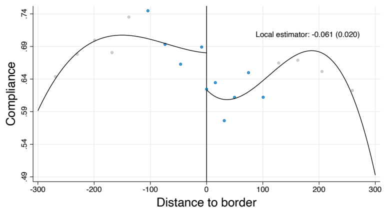

A: Panel A of figure 3

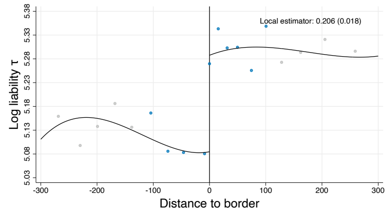

B: Panel B of figure 3

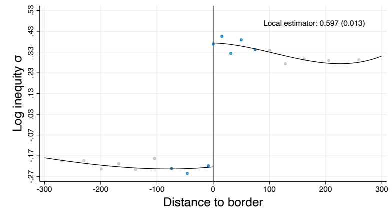

C: Panel C of figure 3

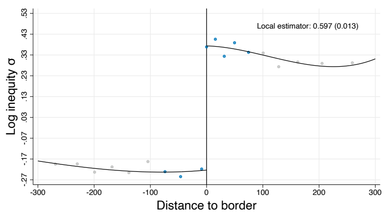

D: Panel A of figure 4

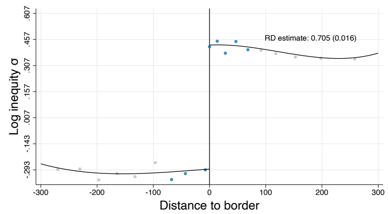

E: Panel B of figure 4

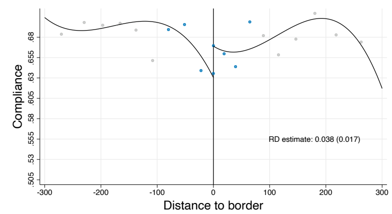

F: Panel C of figure 4

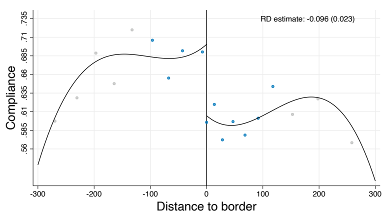

G: Panel D of figure 4

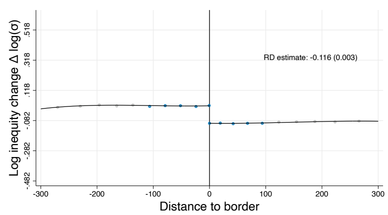

H: Panel A of figure 6

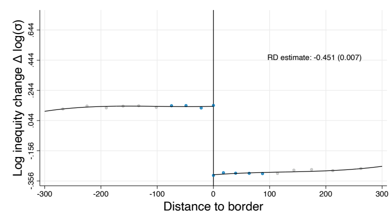

I: Panel B of figure 6

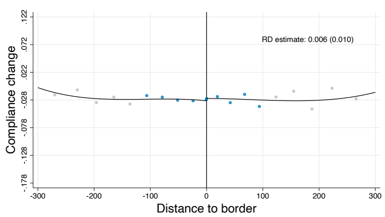

J: Panel C of figure 6

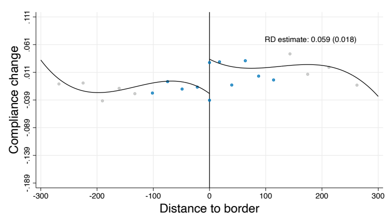

K: Panel D of figure 6

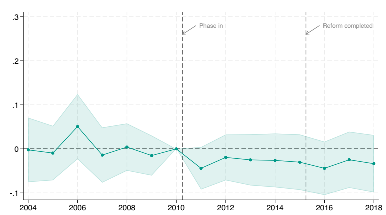

L: Panel A of figure 7

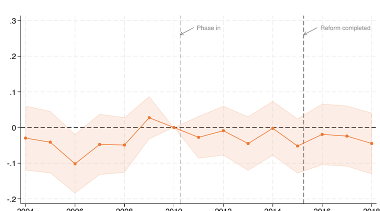

M: Panel B of figure 7

Notes: This figure replicates the main tax reform specifications from the paper, but dropping the top 1%, rather than 0.5%, of lots in terms of land area. Panels A-C replicate the analysis from panels A-C of figure 3, panels D-G replicate the analysis from panels A-D of figure 4, panels H-K replicate the analysis from panels A-D of figure 6, panels L-M replicate the analysis from panel A-B of figure 7.

TABLE K.9: DIFFERENCE IN BOUNDARY DISCONTINUITY DESIGN: COMPLIANCE EFFECTS

	(1)	(2)	(3)	(4)	(5)	(6)	(7)
1(high tag side) $\times \lvert \log(\sigma) \rvert$	-0.16***	-0.14***	-0.18***	-0.14***	-0.16***	-0.19***	-0.18***
	(0.03)	(0.03)	(0.03)	(0.03)	(0.03)	(0.03)	(0.04)
R^2	0.126	0.129	0.125	0.133	0.145	0.126	0.292
Distance controls	✓	✓	✓	✓	✓	✓	✓
Segment fixed effects	✓	✓	✓	✓	✓	✓	✓
τ splines	✓	✓	✓	✗	✓	✓	✗
τ deciles	✗	✗	✗	✓	✗	✗	✓
Exposure deciles	✓	✓	✗	✓	✓	✗	✓
Exposure splines	✗	✗	✓	✗	✗	✓	✗
τ splines $\times$ HTS	✗	✓	✓	✗	✓	✓	✗
τ deciles $\times$ HTS	✗	✗	✗	✓	✗	✗	✓
Exposure deciles $\times$ HTS	✗	✓	✗	✓	✓	✗	✓
Exposure splines $\times$ HTS	✗	✗	✓	✗	✗	✓	✗
τ splines $\times$ exp deciles	✗	✗	✗	✗	✓	✗	✗
τ splines $\times$ exp splines	✗	✗	✗	✗	✗	✓	✗
τ deciles $\times$ exp deciles	✗	✗	✗	✗	✗	✗	✓
τ splines $\times$ HTS $\times$ exp deciles	✗	✗	✗	✗	✓	✗	✗
τ splines $\times$ HTS $\times$ exp splines	✗	✗	✗	✗	✗	✓	✗
τ deciles $\times$ HTS $\times$ exp deciles	✗	✗	✗	✗	✗	✗	✓
Elasticity η	0.252***	0.217***	0.285***	0.219***	0.247***	0.299***	0.280***
	0.042	0.046	0.046	0.046	0.050	0.050	0.057
N	23869	23869	23869	23869	23869	23869	23274

Notes: This table replicates the analysis from table 1, but dropping the top 1%, rather than 0.5%, of lots in terms of land area. It shows the results of estimation of equation (7) derived in section 4.2 and discussed in section 5.1: $c_i = \lambda_{r(i)} + g_0(\tau_i, e_i) + f_0(d_i) + HTS_i \times [\beta_0 + \tilde{\eta}\log(\sigma) + f_1(d_i) + g_1(\tau_i, e_i)] + \varepsilon_i$ where $\lambda_{r(i)}$ are boundary segment fixed effects, HTS_i is an indicator for being on the high-tag side of the boundary ($d_i > 0$); $f_0(d_i)$ and $f_1(d_i)$ control for distance to the boundary on the low- and high-tag sides of the boundary, respectively; $g_0(\tau_i, e_i)$ and $g_1(\tau_i, e_i)$ control for the tax liability and exposure on the low- and high-tag sides of the boundary, respectively; and ε_i is the residual. In column (1), we control for cubic splines of the tax liability and fixed effects for fifty quantiles of the exposure distribution. In column (2) we control separately for the tax liability and exposure to mistagging on either side of the boundary. Column (3) replaces the exposure quantiles with cubic splines in exposure while column (4) replaces the tax liability cubic splines with fixed effects for fifty quantiles. Columns (5)–(7) replicate the specifications in columns (2)–(4), respectively, but additionally include interactions between the tax liability controls and the exposure controls.

TABLE K.10: DYNAMIC DIFFERENCE IN BOUNDARY DISCONTINUITY DESIGN

	(1)	(2)	(3)	(4)	(5)	(6)	(7)
1(high tag side) X $\Delta\log(\sigma)$	-0.061**	-0.062**	-0.062**	-0.059**	-0.064**	-0.061**	-0.061**
	(0.027)	(0.029)	(0.028)	(0.029)	(0.029)	(0.029)	(0.031)
R^2	0.028	0.029	0.027	0.031	0.037	0.027	0.123
Distance controls	✓	✓	✓	✓	✓	✓	✓
Segment FEs	✓	✓	✓	✓	✓	✓	✓
$\Delta\tau$ splines	✓	✓	✓	✗	✓	✓	✗
$\Delta\tau$ deciles	✗	✗	✗	✓	✗	✗	✓
Exposure deciles	✓	✓	✗	✓	✓	✗	✓
Exposure splines	✗	✗	✓	✗	✗	✓	✗
$\Delta\tau$ splines $\times$ HTS	✗	✓	✓	✗	✓	✓	✗
$\Delta\tau$ deciles $\times$ HTS	✗	✗	✗	✓	✗	✗	✓
Exposure deciles $\times$ HTS	✗	✓	✗	✓	✓	✗	✓
Exposure splines $\times$ HTS	✗	✗	✓	✗	✗	✓	✗
$\Delta\tau$ splines $\times$ exp deciles	✗	✗	✗	✗	✓	✗	✗
$\Delta\tau$ splines $\times$ exp splines	✗	✗	✗	✗	✗	✓	✗
$\Delta\tau$ deciles $\times$ exp deciles	✗	✗	✗	✗	✗	✗	✓
$\Delta\tau$ splines $\times$ HTS $\times$ exp deciles	✗	✗	✗	✗	✓	✗	✗
$\Delta\tau$ splines $\times$ HTS $\times$ exp splines	✗	✗	✗	✗	✗	✓	✗
$\Delta\tau$ deciles $\times$ HTS $\times$ exp deciles	✗	✗	✗	✗	✗	✗	✓
Elasticity η	0.097**	0.098**	0.098**	0.094**	0.101**	0.097**	0.097**
	(0.043)	(0.046)	(0.044)	(0.046)	(0.046)	(0.047)	(0.049)
N	50889	50889	50889	50889	50889	50889	50778

Notes: This table replicates the analysis from table 2, but dropping the top 1%, rather than 0.5%, of lots in terms of land area. It shows the results of estimating equation (9) derived in section 4.3 and discussed in section 5.2: $\Delta c_i = \lambda_{r(i)} + g_0(\Delta\tau_i, e_i) + f_0(d_i) + HTS_i \times [\delta_0 + \tilde{\eta}\Delta\log(\sigma_i) + g_1(\Delta\tau_i, e_i) + f_1(d_i)] + \varepsilon_i$ where all terms are as defined above in the notes to table 1. Column (1) controls for cubic splines of the changes in tax liability and fixed effects for fifty quantiles of the exposure distribution. Column (2) controls separately for the changes in tax liability and exposure to mistagging on either side of the boundary. Column (3) replaces the exposure quantiles with splines, while column (4) replaces the changes in tax liability splines with fixed effects for fifty quantiles of the changes in tax liability. Columns (5)–(7) replicate the specifications in columns (2)–(4), respectively, but additionally include interactions between the changes in tax liability controls and the exposure controls.

K.6 Alternative Definitions of Non-Trivial Degree of Inequity

In section 4.1, we restrict our sample to properties that face a non-trivial degree of inequity, defined as having $|\sigma_i| > 0.05$. In this appendix, we assess the robustness of our results by varying the threshold used to define a "non-trivial degree of inequity."

In section 4.1, we develop a boundary discontinuity design that that estimates the overall effect on compliance from facing a tax schedule based on a high land-price assessment rather than a lower-priced schedule. Specifically, we estimate the equation for compliance c_i:

$$c_i = \lambda_{r(i)} + f_0(d_i) + \beta_0 HTS_i + f_1(d_i) \times HTS_i + \mathbf{X}_i\boldsymbol{\beta} + \varepsilon_i \tag{K.1}$$

where $\lambda_{r(i)}$ are boundary-segment fixed effects, HTS_i is an indicator for being on the high-tag side of the boundary ($d_i > 0$); $f_0(d_i)$ and $f_1(d_i)$ control for distance to the boundary on the low- and high-tag sides of the boundary, respectively; $\mathbf{X}_i$ are the properties' effective land area a_i and assessed built structure value b_i; and ε_i is the residual.

Figure K.6 presents robustness checks in which we systematically vary the definition of the "non-trivial degree of inequity" threshold. For each alternative cutoff of $|\sigma_i|$, we re-estimate equation (K.1). The vertical axis plots the estimated elasticity from the discontinuity in compliance as a solid blue line, along with its corresponding 95% confidence interval (shaded area). The horizontal axis shows the chosen threshold for "non-trivial inequity." Gray bars indicate the proportion of properties retained in each estimation. The figure demonstrates that the results from figure 3A remain stable for thresholds ranging between 0.02 and 0.2.

FIGURE K.6: OVERALL ELASTICITY OF COMPLIANCE AT TAX SECTOR BOUNDARIES

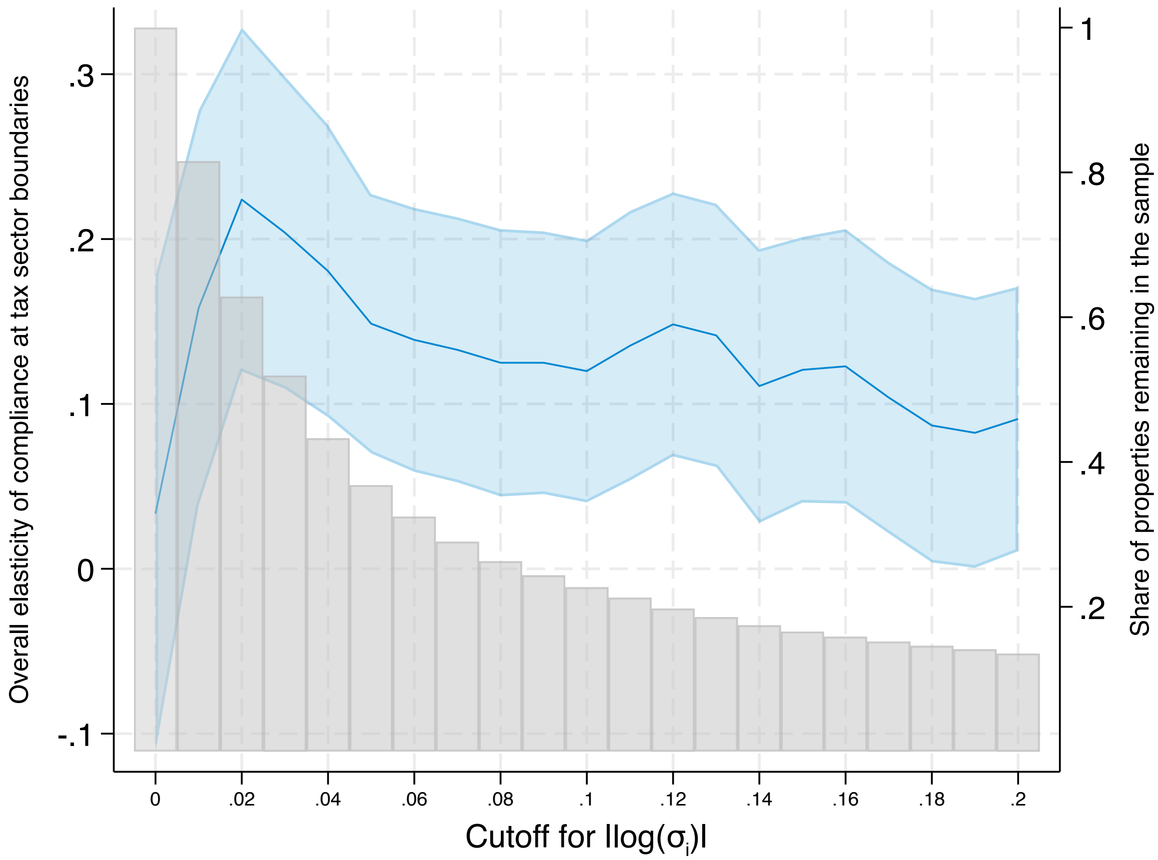

Notes: This figure replicates the analysis from Figure 3A, varying the threshold of $|\log(\sigma_i)|$ used to define a non-trivial degree of inequity" for sample inclusion. Specifically, we repeatedly estimate the following equation for compliance (K.1): c_i by taxpayer i: $c_i = \lambda_{r(i)} + f_0(d_i) + \beta_0 HTS_i + f_1(d_i) \times HTS_i + \mathbf{X}_i\boldsymbol{\beta} + \varepsilon_i$ where $\lambda_{r(i)}$ are boundary-segment fixed effects, HTS_i is an indicator for being on the high-tag side of the boundary ($d_i > 0$); $f_0(d_i)$ and $f_1(d_i)$ control for distance to the boundary on the low- and high-tag sides of the boundary, respectively; $\mathbf{X}_i$ are the properties' effective land area a_i and assessed built structure value b_i; and ε_i is the residual. The estimation is repeated twenty-one times, each with a different cutoff defining "non-trivial inequity." The vertical axis plots the estimated elasticity from the discontinuity in compliance as a solid blue line, along with its corresponding 95% confidence interval (shaded area). The horizontal axis shows the chosen threshold for "non-trivial inequity." Gray bars indicate the proportion of properties retained in each estimation. The figure demonstrates that the results from figure 3A remain stable for thresholds ranging between 0.02 and 0.2.

L Robustness to Alternative Definitions of Compliance

In section 2.3, we introduced compliance—defined as the proportion of a household's property tax bill paid within 18 months of issuance—as our main outcome for analyzing behavioral responses to mistagging. In this appendix, we revisit our core analyses while adjusting two key choices related to our outcome variable. First, we explore the extensive margin response to mistagging. Second, we vary the payment time frame used in our compliance definition.

L.1 Extensive Margin Response

In the main text, we combine both extensive and intensive margin behavioral responses to mistagging in our definition of compliance. Figure A.3 illustrates that compliance is driven almost entirely on the extensive margin, with households typically settling their entire tax bill when they choose to pay. In this section, we refine our analysis by focusing solely on the extensive margin of compliance. Specifically, we redefine our outcome variable such that it equals one if a household makes any payment within 18 months of receiving their bill, and zero otherwise. The figures and tables below reproduce the main evidence with this new outcome variable. Each figure and table references the corresponding result from the main sections of the paper.

appendixL1a appendixL1b appendixL1c appendixL1d appendixL1e appendixL1f appendixL1g

Figure L.1: Main Evidence Using the Extensive Margin of Compliance

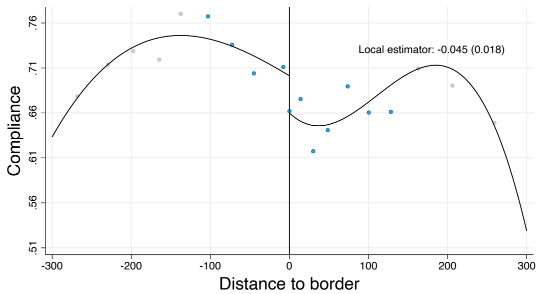

A: Panel A of figure 3

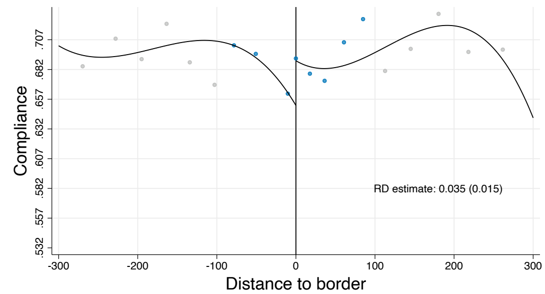

B: Panel C of figure 4

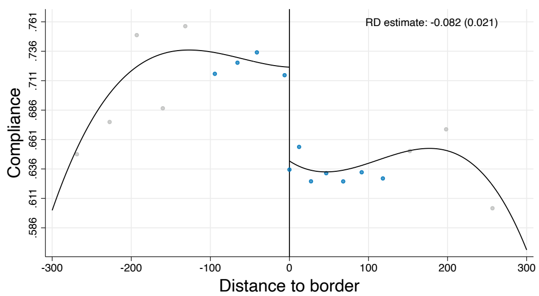

C: Panel D of figure 4

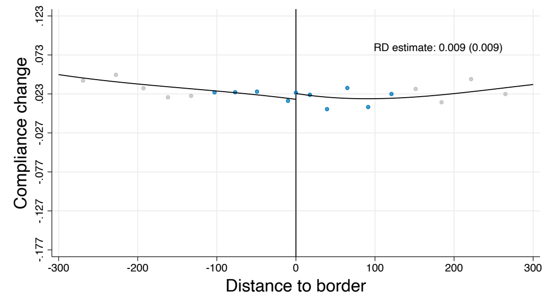

D: Panel C of figure 6

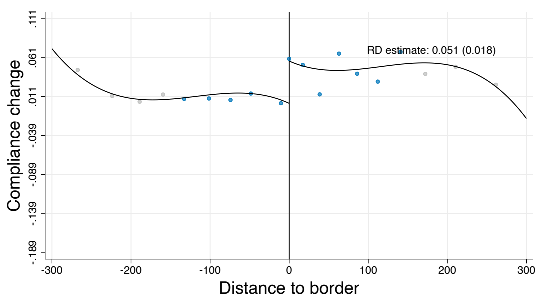

E: Panel D of figure 6

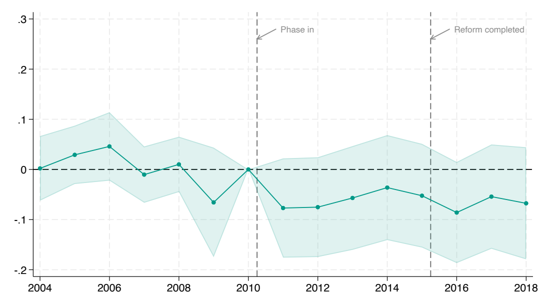

F: Panel A of figure 7

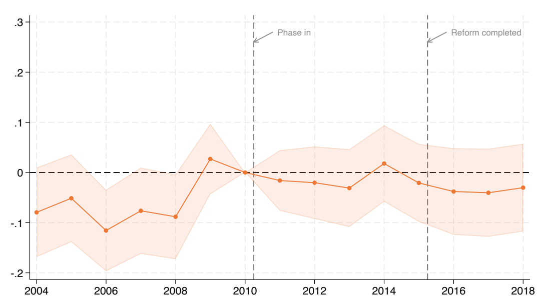

G: Panel B of figure 7

Notes: This figure replicates the main evidence from the paper, but using only the extensive margin of compliance. Panel A replicates the analysis from panel A of figure 3, panels B-C replicate the analysis from panels C-D of figure 4, panels D-E replicate the analysis from panels C-D of figure 6, and panels F-G replicate the analysis from panels A-B of figure 7.

TABLE L.1: DIFFERENCE IN BOUNDARY DISCONTINUITY DESIGN: COMPLIANCE EFFECTS

	(1)	(2)	(3)	(4)	(5)	(6)	(7)
1(high tag side) $\times \lvert \log(\sigma) \rvert$	-0.16***	-0.14***	-0.18***	-0.14***	-0.16***	-0.19***	-0.14***
	(0.03)	(0.03)	(0.03)	(0.03)	(0.03)	(0.03)	(0.03)
R^2	0.134	0.137	0.133	0.140	0.152	0.134	0.298
Distance controls	✓	✓	✓	✓	✓	✓	✓
Segment fixed effects	✓	✓	✓	✓	✓	✓	✓
τ splines	✓	✓	✓	✗	✓	✓	✗
τ deciles	✗	✗	✗	✓	✗	✗	✓
Exposure deciles	✓	✓	✗	✓	✓	✗	✓
Exposure splines	✗	✗	✓	✗	✗	✓	✗
τ splines $\times$ HTS	✗	✓	✓	✗	✓	✓	✗
τ deciles $\times$ HTS	✗	✗	✗	✓	✗	✗	✓
Exposure deciles $\times$ HTS	✗	✓	✗	✓	✓	✗	✓
Exposure splines $\times$ HTS	✗	✗	✓	✗	✗	✓	✗
τ splines $\times$ exp deciles	✗	✗	✗	✗	✓	✗	✗
τ splines $\times$ exp splines	✗	✗	✗	✗	✗	✓	✗
τ deciles $\times$ exp deciles	✗	✗	✗	✗	✗	✗	✓
τ splines $\times$ HTS $\times$ exp deciles	✗	✗	✗	✗	✓	✗	✗
τ splines $\times$ HTS $\times$ exp splines	✗	✗	✗	✗	✗	✓	✗
τ deciles $\times$ HTS $\times$ exp deciles	✗	✗	✗	✗	✗	✗	✓
Elasticity η	0.239***	0.213***	0.272***	0.218***	0.242***	0.279***	0.214***
	0.039	0.043	0.040	0.043	0.046	0.041	0.052
N	25061	25061	25061	25061	25061	25061	24515

Notes: This table replicates the analysis from table 1, but focuses on the extensive margin response of compliance. It shows the results of estimation of equation (7) derived in section 4.2 and discussed in section 5.1: $c_i = \lambda_{r(i)} + g_0(\tau_i, e_i) + f_0(d_i) + HTS_i \times [\beta_0 + \tilde{\eta} \log(\sigma) + f_1(d_i) + g_1(\tau_i, e_i)] + \varepsilon_i$ where $\lambda_{r(i)}$ are boundary segment fixed effects, HTS_i is an indicator for being on the high-tag side of the boundary ($d_i > 0$); $f_0(d_i)$ and $f_1(d_i)$ control for distance to the boundary on the low- and high-tag sides of the boundary, respectively; $g_0(\tau_i, e_i)$ and $g_1(\tau_i, e_i)$ control for the tax liability and exposure on the low- and high-tag sides of the boundary, respectively; and ε_i is the residual. In column (1), we control for cubic splines of the tax liability and fixed effects for fifty quantiles of the exposure distribution. In column (2) we control separately for the tax liability and exposure to mistagging on either side of the boundary. Column (3) replaces the exposure quantiles with cubic splines in exposure while column (4) replaces the tax liability cubic splines with fixed effects for fifty quantiles. Columns (5)–(7) replicate the specifications in columns (2)–(4), respectively, but additionally include interactions between the tax liability controls and the exposure controls.

Table L.2: Dynamic Difference in Boundary Discontinuity Design

	(1)	(2)	(3)	(4)	(5)	(6)	(7)
1(high tag side) X $\Delta\log(\sigma)$	-0.086***	-0.087***	-0.081***	-0.087***	-0.092***	-0.093***	-0.093***
	(0.027)	(0.029)	(0.028)	(0.029)	(0.029)	(0.029)	(0.031)
R^2	0.025	0.026	0.024	0.027	0.034	0.025	0.116
Distance controls	✓	✓	✓	✓	✓	✓	✓
Segment FEs	✓	✓	✓	✓	✓	✓	✓
$\Delta\tau$ splines	✓	✓	✓	✗	✓	✓	✗
$\Delta\tau$ deciles	✗	✗	✗	✓	✗	✗	✓
Exposure deciles	✓	✓	✗	✓	✓	✗	✓
Exposure splines	✗	✗	✓	✗	✗	✓	✗
$\Delta\tau$ splines $\times$ HTS	✗	✓	✓	✗	✓	✓	✗
$\Delta\tau$ deciles $\times$ HTS	✗	✗	✗	✓	✗	✗	✓
Exposure deciles $\times$ HTS	✗	✓	✗	✓	✓	✗	✓
Exposure splines $\times$ HTS	✗	✗	✓	✗	✗	✓	✗
$\Delta\tau$ splines $\times$ exp deciles	✗	✗	✗	✗	✓	✗	✗
$\Delta\tau$ splines $\times$ exp splines	✗	✗	✗	✗	✗	✓	✗
$\Delta\tau$ deciles $\times$ exp deciles	✗	✗	✗	✗	✗	✗	✓
$\Delta\tau$ splines $\times$ HTS $\times$ exp deciles	✗	✗	✗	✗	✓	✗	✗
$\Delta\tau$ splines $\times$ HTS $\times$ exp splines	✗	✗	✗	✗	✗	✓	✗
$\Delta\tau$ deciles $\times$ HTS $\times$ exp deciles	✗	✗	✗	✗	✗	✗	✓
Elasticity η	0.131***	0.132***	0.122***	0.132***	0.139***	0.141***	0.140***
	(0.040)	(0.043)	(0.042)	(0.044)	(0.044)	(0.043)	(0.046)
N	53267	53267	53267	53267	53267	53267	53137

Notes: This table replicates the analysis from table 2, but focuses on the extensive margin response of compliance. It shows the results of estimating equation (9) derived in section 4.3 and discussed in section 5.2: $\Delta c_i = \lambda_{r(i)} + g_0(\Delta\tau_i, e_i) + f_0(d_i) + HTS_i \times [\delta_0 + \tilde{\eta}\Delta\log(\sigma_i) + g_1(\Delta\tau_i, e_i) + f_1(d_i)] + \varepsilon_i$ where all terms are as defined above in the notes to table 1. Column (1) controls for cubic splines of the changes in tax liability and fixed effects for fifty quantiles of the exposure distribution. Column (2) controls separately for the changes in tax liability and exposure to mistagging on either side of the boundary. Column (3) replaces the exposure quantiles with splines, while column (4) replaces the changes in tax liability splines with fixed effects for fifty quantiles of the changes in tax liability. Columns (5)–(7) replicate the specifications in columns (2)–(4), respectively, but additionally include interactions between the changes in tax liability controls and the exposure controls.

L.2 Timeframe for Payments in the Definition of Compliance

In section 2.3, we introduced compliance—defined as the proportion of a household's property tax bill paid within 18 months of issuance—as our main outcome for analyzing behavioral responses to mistagging. In this appendix, we vary the time frame considered for payments in the definition of compliance, and replicate the main analyses with each definition.

When evaluating the results presented in this section, two considerations are worth noting. First, our payments data is complete only up to the year 2020. Therefore, time frames extending beyond four years should be approached with caution when analyzing compliance data from 2016 onward. Second, there are constant amnesties of debt, which incentivize back payments. Consequently, time frames extending multiple years should also be treated with caution for any year.

The figures below reproduce three of the main analyses, repeating each exercise eight times. In each time, we vary the time horizon considered to define compliance. We then plot on the vertical coordinate the estimated parameter of interest of each analysis, and in the the horizontal coordinate the time horizon considered for payments. Each figure references the corresponding result from the main sections of the paper.

FIGURE L.2: DIFFERENCE IN BOUNDARY DISCONTINUITY DESIGN: COMPLIANCE EFFECTS

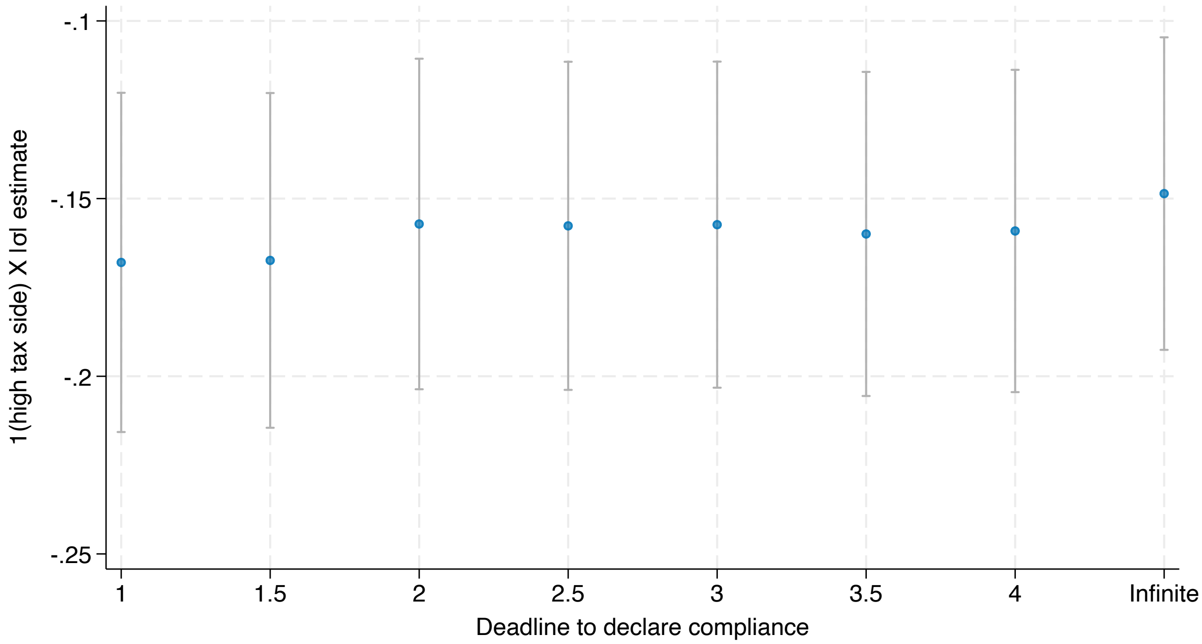

Notes: This figure presents the same analysis as depicted in column one of table 1, but varies the timeline we consider of payments for the definition of compliance. The figure shows shows the results of estimation of equation (7): $c_i = \lambda_{r(i)} + g_0(\tau_i, e_i) + f_0(d_i) + HTS_i \times [\beta_0 + \tilde{\eta}\log(\sigma) + f_1(d_i) + g_1(\tau_i, e_i)] + \varepsilon_i$ where $\lambda_{r(i)}$ are boundary segment fixed effects, HTS_i is an indicator for being on the high-tag side of the boundary ($d_i > 0$); $f_0(d_i)$ and $f_1(d_i)$ control for distance to the boundary on the low- and high-tag sides of the boundary, respectively; $g_0(\tau_i, e_i)$ and $g_1(\tau_i, e_i)$ control for the tax liability and exposure on the low- and high-tag sides of the boundary, respectively; and ε_i is the residual. We estimate equation (7) separately eight times, where we vary the time horizon considered to define compliance. The vertical coordinate of each dot and the vertical gray bars show the estimated η and its 95% confidence interval. The horizontal coordinate of each dot shows the time horizon considered.

FIGURE L.3: DYNAMIC DIFFERENCE IN BOUNDARY DISCONTINUITY DESIGN

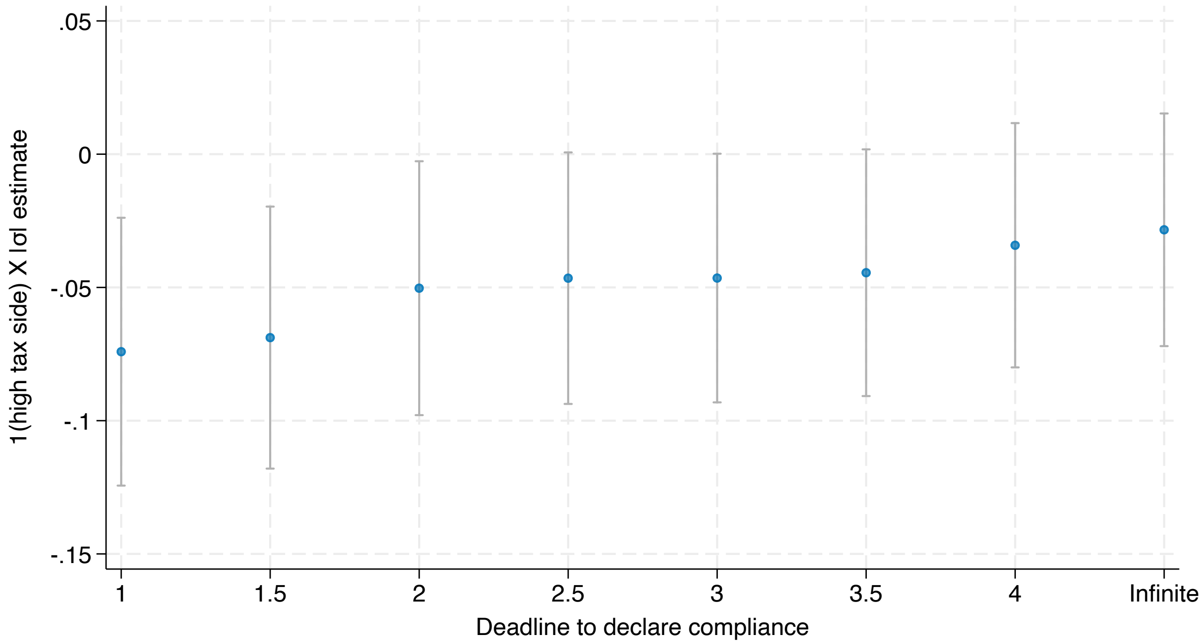

Notes: This figure presents the same analysis as depicted in column one of table 2, but varies the timeline we consider of payments for the definition of compliance. The figure shows shows the results of shows the results of estimating equation (9) discussed in section 5.2: $\Delta c_i = \lambda_{r(i)} + g_0(\Delta\tau_i, e_i) + f_0(d_i) + HTS_i \times [\delta_0 + \tilde{\eta}\Delta\log(\sigma_i) + g_1(\Delta\tau_i, e_i) + f_1(d_i)] + \varepsilon_i$ where all terms are as defined above in the notes to table 1. We estimate (9) separately eight times, where we vary the time horizon considered to define compliance. The vertical coordinate of each dot and the vertical gray bars show the estimated η and its 95% confidence interval. The horizontal coordinate of each dot shows the time horizon considered.

M Salience of inequity

In this appendix, we describe the two methodologies we use for constructing measures of the salience of tax inequity faced by each property. We then use this measure in figure 5, discussed in section 5.1, to argue that our results from the difference in boundary discontinuity design are driven by households for whom the inequity of the property tax is salient.

Our first measure of salience–the density measure–builds on the notions of similarity used in Auerbach & Hassett (2002) to study horizontal inequity of taxation among similar taxpayers. Intuitively, salience is higher when a property's counterfactual tax liability is similar to the actual tax liability of properties located immediately across the tax boundary. Specifically, for each property i, we first calculate a counterfactual tax liability, $\hat{\tau}_i$. We then define our salience measure as the density of $\hat{\tau}_i$ evaluated in the distribution of tax liabilities of properties situated directly on the opposite side of the boundary they face.

To construct our density-measure of salience, we take the following steps:

1. Calculate the counterfactual tax liability ($\hat{\tau}_i$) for every property in 2010.

2. For each street segment $r \in R$ and tax-side $h \in 0, 1$:

    - Identify properties located directly across the boundary (on the opposite tag side within the same street segment).
    - If there are fewer than two properties on the opposite side, assign a salience value of zero to all properties on side h within segment r.
    - Otherwise, for properties on side h within segment r, denote the set of their counterfactual tax liabilities by V.
    - Estimate the kernel density (using an Epanechnikov kernel) of each value in V, based on the distribution of observed tax liabilities on the opposite side of the boundary within the same segment.
    - Assign the estimated density to each corresponding property as its salience measure.

Figure M.1 displays the resulting distribution of our constructed salience measure across properties:

FIGURE M.1: DISTRIBUTION OF OUR DENSITY MEASURE OF SALIENCE

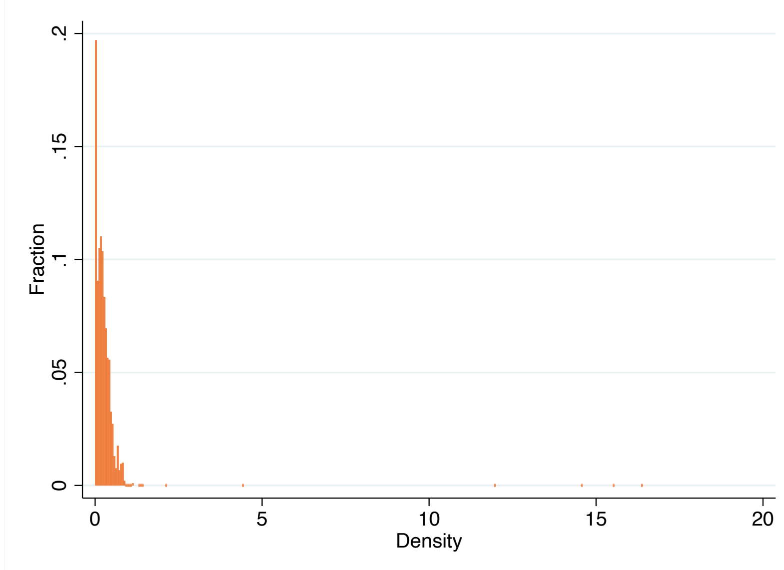

Next, we divide our sample into four groups according to the quartiles of the salience measure distribution. Within each quartile group, we estimate the difference in boundary discontinuity design specification from equation 6

$$c_i = \lambda_{r(i)} + g\left(\tau_i, e_i\right) + f_0\left(d_i\right) + \beta_0 HTS_i + f_1\left(d_i\right) \times HTS_i + \varepsilon_i$$

where terms are as defined in equation (4) and we add flexible controls for property i's (log) tax liability τ_i and exposure to mistagging e_i in the term $g\left(\tau_i, e_i\right)$. Specifically, we control for property i's (log) tax liability τ_i using cubic splines and exposure to mistagging e_i using fixed effects for fifty quantiles of exposure.

Panel A of Figure 5 summarizes the estimated results, displaying the implied elasticity of compliance with respect to inequity in each quartile. The figure shows that our results are increasing in the salience of the property tax. In the bottom quartile the estimated effect is zero, but the elasticity is positive in the higher quintiles of salience.

Our second measure of salience–the type measure–defines similarity between properties using their types (house or apartment). Intuitively, salience for property i is higher when most properties on the other side of the boundary are of the same type as i's. Specifically, for each property, we first measure their type. Then, we define our type measure of salience as the share of properties with the same type that are directly on the opposite side of the boundary they face.

Figure M.2 displays the resulting distribution of our constructed salience measure across properties:

FIGURE M.2: DISTRIBUTION OF OUR TYPE MEASURE OF SALIENCE

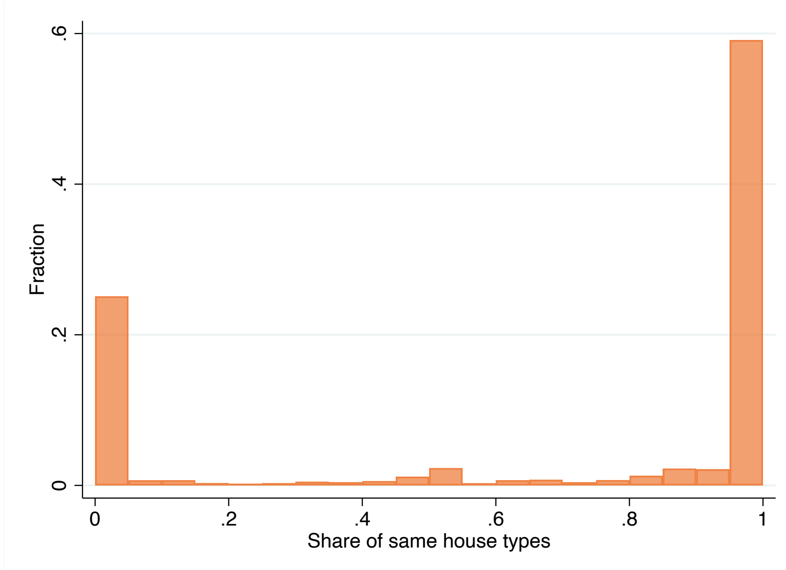

Given that the distribution of the type measure of salience is concentrated between 0 and 1, we divide our sample into two groups: above and below 0.5. Within each group, we once again estimate the difference in boundary discontinuity design specification from equation 6.

Panel B of Figure 5 summarizes the estimated results, displaying the implied elasticity of compliance with respect to inequity in each group. The figure shows that our results are increasing in the salience of the property tax.

N Placebo Test for Difference in Boundary Discontinuities Design

In Section 4.2, we introduce a Difference-in-Boundary Discontinuities Design that permits discontinuities in the untreated potential outcomes, G_0, and allows for the distribution of unobservables, ν_0, to vary discontinuously at sector boundaries. Specifically, our design accommodates the possibility that the left and right limits of the conditional expectation $\mathbb{E}\left[G_0\left(t, d, \nu_0\right)|\tau = t, D = d\right]$ at $D = 0$ differ. However, we assume that this discontinuity remains constant across potential treatment intensities σ_z. That is, we assume that while households on the high-tag side may be differentially compliant to households on the low-tag side, this difference is constant across households with different levels of exposure to mistagging.

To empirically assess the validity of this assumption, we implement a placebo test using boundaries separating sectors with identical rates, where no actual tax difference exists ($\sigma_i = 0$ for all properties). We construct a placebo dataset by pairing properties along such boundaries with properties located at the nearest boundary with a different sector rate. For example, in Figure N.1, the boundary between sectors 31-32 is matched to the boundary between sectors 28-29.[66] We classify each boundary as either a "high-tag boundary" or a "low-tag boundary," based on their relative sector rates. In the given example, sectors 31-32 form the "low-tag boundary" (sector rate 0.02), while sectors 28-29 form the "high-tag boundary" (sector rate 0.03).

FIGURE N.1: ILLUSTRATION OF BOUNDARY MATCHING FOR PLACEBO TEST

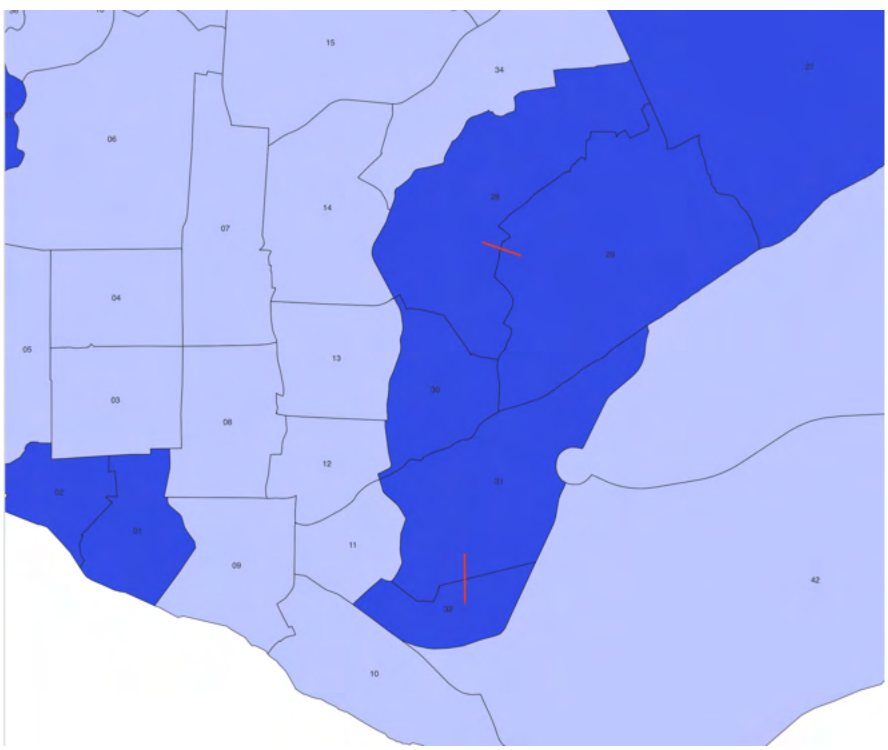

This approach enables us to construct simulated values of σ that represent placebo tax-rate differences faced by each property if it were located at the paired boundary:

[66]We avoid linking sectors 31-32 with sectors 30-31 because both share the same sector rate of 0.02.

$$\tilde{\sigma_i} = \frac{T_h}{T_l} = \frac{1 + p_{d(i)} \frac{a_i}{b_i}}{1 + \hat{p}_{d(i)} \frac{a_i}{b_i}} \tag{N.1}$$

where $d(i)$ denotes the boundary segment of property i, $p_{d(i)}$ represents the sector rate at the actual boundary $d(i)$, and $\hat{p}_{d(i)}$ denotes the sector rate at the matched placebo boundary. Importantly, the true inequity measure, σ_i, remains zero for all properties, since genuine inequities are defined within actual boundaries rather than across matched placebo boundaries. Using this simulated variable, we estimate the following placebo Difference-in-Boundary Discontinuities specification:

$$c_i = \gamma_{b(i)} + g_0 (\tau_i, e_i) + f (d_i) + HTS_i \times [\beta_0 + \tilde{\eta} \log (\tilde{\sigma}) + h (d_i) + g_1 (\tau_i, e_i)] + \varepsilon_i \tag{N.2}$$

where $\gamma_{b(i)}$ are fixed effects for the placebo boundary matches; $g (\tau_i, e_i)$ are flexible controls for property i's (log) tax liability τ_i and exposure to mistagging e_i (our baseline estimates use τ splines and fixed effects for fifty quantiles of exposure); $f (d_i)$ and $h (d_i)$ control flexibly for distance to the true boundary on the low- and high-tag sides of the boundary respectively; and HTS_i is an indicator for properties on the high-tag side of the boundary match ($d_i > 0$).

Table N.1 summarizes the estimated results. Reassuringly, none of the specifications show evidence that compliance gaps are correlated with exposure to mistagging as measured through the placebo tax-rate differences, providing support for our identifying assumption.

TABLE N.1: DIFFERENCE IN BOUNDARY DISCONTINUITY DESIGN: COMPLIANCE EFFECTS AND PLACEBO INEQUITY

	(1)	(2)	(3)	(4)	(5)	(6)	(7)
1(high tag side) $\times \lvert\log(\sigma)\rvert$	-0.04	-0.09	0.04	-0.08	-0.02	-0.06	-0.03
	(0.07)	(0.07)	(0.13)	(0.07)	(0.08)	(0.16)	(0.08)
R^2	0.048	0.057	0.046	0.073	0.114	0.048	0.395
Distance controls	✓	✓	✓	✓	✓	✓	✓
Segment fixed effects	✓	✓	✓	✓	✓	✓	✓
τ splines	✓	✓	✓	✗	✓	✓	✗
τ deciles	✗	✗	✗	✓	✗	✗	✓
Exposure deciles	✓	✓	✗	✓	✓	✗	✓
Exposure splines	✗	✗	✓	✗	✗	✓	✗
τ splines $\times$ HTS	✗	✓	✓	✗	✓	✓	✗
τ deciles $\times$ HTS	✗	✗	✗	✓	✗	✗	✓
Exposure deciles $\times$ HTS	✗	✓	✗	✓	✓	✗	✓
Exposure splines $\times$ HTS	✗	✗	✓	✗	✗	✓	✗
τ splines $\times$ exp deciles	✗	✗	✗	✗	✓	✗	✗
τ splines $\times$ exp splines	✗	✗	✗	✗	✗	✓	✗
τ deciles $\times$ exp deciles	✗	✗	✗	✗	✗	✗	✓
τ splines $\times$ HTS $\times$ exp deciles	✗	✗	✗	✗	✓	✗	✗
τ splines $\times$ HTS $\times$ exp splines	✗	✗	✗	✗	✗	✓	✗
τ deciles $\times$ HTS $\times$ exp deciles	✗	✗	✗	✗	✗	✗	✓
Elasticity η	0.067	0.161	-0.076	0.140	0.036	0.103	0.047
	0.128	0.131	0.226	0.132	0.139	0.282	0.136
N	12304	12304	12304	12304	12304	12304	11827

Notes: This table replicates the analysis from table 1, but using placebo boundaries and inequities $\tilde{\sigma}$ rather than true inequities σ. The table shows the results of estimation of equation (N.2): $c_i = \gamma_{b(i)} + g_0(\tau_i, e_i) + f(d_i) + HTS_i \times [\beta_0 + \eta \log(\tilde{\sigma}) + h(d_i) + g_1(\tau_i, e_i)] + \varepsilon_i$ where $\gamma_{b(i)}$ are fixed effects for the placebo boundary matches; $g(\tau_i, e_i)$ are flexible controls for property i's (log) tax liability τ_i and exposure to mistagging e_i; $f(d_i)$ and $h(d_i)$ control flexibly for distance to the true boundary on the low- and high-tag sides of the boundary respectively; and HTS_i is an indicator for properties on the high-tag side of the boundary match ($d_i > 0$). In column (1), we control for cubic splines of the tax liability and fixed effects for fifty quantiles of the exposure distribution. In column (2) we control separately for the tax liability and exposure to mistagging on either side of the boundary. Column (3) replaces the exposure quantiles with cubic splines in exposure while column (4) replaces the tax liability splines with fixed effects for fifty quantiles. Columns (5)–(7) control for these separately on either side of the boundary.

O Tax Enforcement

This appendix provides some additional background on the way that the property tax is enforced to assist in interpreting our findings. We touch upon these issues briefly in describing the context in section 2 and raise the potential issue of differential enforcement on either side of the tax sector boundaries in section 4.1. Here we expand upon the tax enforcement procedures in place and investigate empirically whether there is evidence that tax enforcement is indeed less stringent on the high-tag side.

In contrast to many low- and middle-income countries, tax enforcement in Manaus is predominantly automated and involves minimal discretion. The municipal finance and technology authority (SEMEF; *Secretaria Municipal de Finanças e Tecnologia da Informaç ao*) notifies households of their tax liabilities by mail in mid-January each tax year. These tax notices contain the tax liability calculated automatically by a computer using the statutory formula and the properties' data in the cadaster.

If a household does not settle its tax bill, fines and interest are automatically applied, and legal actions may be initiated. The application of these fines and interest occurs automatically for any household that remains delinquent as of January 1 of the year following the bill issuance, without any discretion on the part of SEMEF officials.[67]

While the fines and interest are automatically applied and carry the force of law, if the debt remains unpaid, the municipality must actively pursue it in order to collect the debt. Under federal law N. 6.830, municipalities are required to secure a "certification of debt" prior to pursuing judicial enforcement. This raises the possibility that SEMEF, internalizing the inequity of the jump in tax liabilities at the sector boundaries, may pursue delinquent taxpayers on the high-tag side of the tax sector boundaries less aggressively than cases on the low-tag side, and that it is this difference in enforcement that accounts, at least in part, for the jump in compliance at the boundaries.

To explore this concern empirically, we use the same sample of properties used in the analysis of the overall compliance responses in section 4.1, focusing on properties that remained delinquent on their 2010 tax bills by the end of 2011. We then tracked whether these properties had received a "certified debt" status by the end of 2011. Of these, 62% were certified, while 38% were not. To determine if the likelihood of certification varied according to tag side, we applied the same BDD model used in Equation (4), reformulated as follows to assess certification status:

$$\mathbf{1}[\text{debt certified}]_i = \lambda_{r(i)} + f_0\left(d_i\right) + \beta_0 HTS_i + f_1\left(d_i\right) \times HTS_i + \varepsilon_i \tag{O.1}$$

where $\lambda_{r(i)}$ are boundary-segment fixed effects, HTS_i is an indicator for being on the high-tag side of the boundary ($d_i > 0$); $f\left(d_i\right)$ and $h\left(d_i\right)$ control for distance to the boundary on the low- and high-tag sides of the boundary, respectively; and ε_i is the residual.

Figure O.1 displays the outcomes of estimating Equation (O.1). This figure provides our point estimate for the change in the probability of having debt certified at the boundary, calculated using local linear controls for distance, the MSE-minimizing bandwidth, and triangular weighting kernels (Calonico *et al.*, 2014, 2020). To help visualize the design, the figure also shows an estimated conditional expectation over the full -300 meter – +300 meter window, estimated using decile-spaced bins of distance on either side of the boundary and the triangular kernel used to estimate the point estimate, censoring the kernel at its tenth percentile to still give positive weight to observations outside the MSE-optimal bandwidth. Bins containing the optimal bandwidth are shown in blue while bins outside the optimal bandwidth are shown in gray.

[67] See `https://www.manaus.am.gov.br/pgm/divida-ativa-servico/`, accessed 2025-03-12.

FIGURE O.1: CHANGE IN DEBT CERTIFICATION PROBABILITY AT TAX SECTOR BOUNDARIES

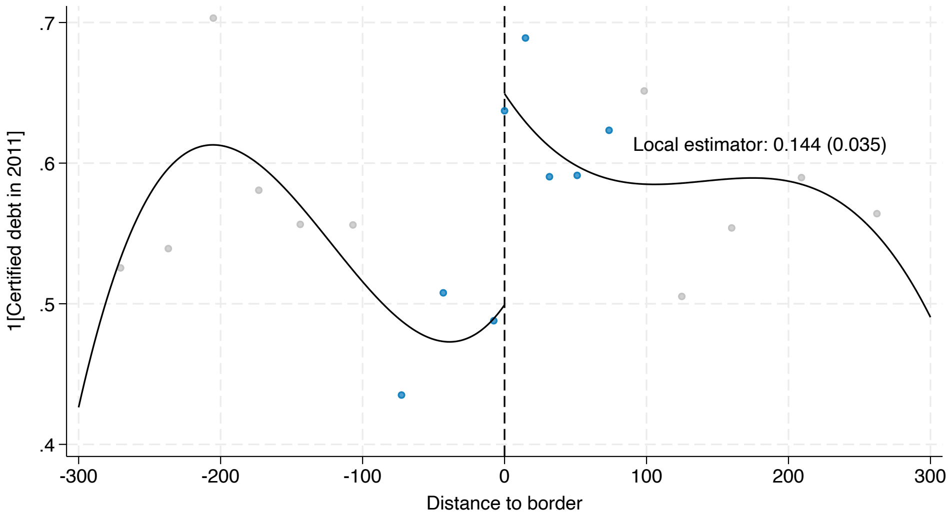

Notes: The figure shows the change in the probability of having a debt certified at tax sector boundaries. Specifically, we show the results of estimating the following equation (O.1): $1[\text{debt certified}]_i = \lambda_{r(i)} + f(d_i) + \beta_0 HTS_i + h(d_i) \times HTS_i + \varepsilon_i$ where $\lambda_{r(i)}$ are boundary-segment fixed effects, HTS_i is an indicator for being on the high-tag side of the boundary ($d_i > 0$); $f(d_i)$ and $h(d_i)$ control for distance to the boundary on the low- and high-tag sides of the boundary, respectively; and ε_i is the residual. Overlaid on the figure, we show the point estimate of the discontinuity in the probability to be certified estimated using local linear distance controls, the MSE-minimizing bandwidth, and triangular kernel weights in distance. The dots in the figure show the coefficients from estimating (O.1) with fixed effects for decile-spaced bins of distance, using the same triangular kernel weights but censoring them at their tenth percentile to give non-zero weights to distances outside the optimal bandwidth. The bins in the optimal bandwidth are shown in blue while those outside are shown in gray. The black line is a global cubic polynomial fit in the same way. The results indicate a 13.8 percentage point higher likelihood of certification on the high-tag side of the boundary, which allows us to confidently dismiss the possibility of lesser enforcement on the high-tag side. Consequently, we interpret our main BDD results as lower bounds on the effect with identical enforcement on each side.

The results indicate that, among 2010 delinquent taxpayers, the likelihood of debt certification is 14.4 percentage points *higher* on the high-tag side of the boundary. The jump is precisely estimated, so we can confidently reject the possibility that certification — and hence enforcement at this stage — is weaker on the high-tag side. If anything, enforcement appears stronger precisely where compliance is lower, which could mean that our boundary estimates of the compliance response understate the true behavioral effect rather than reflecting laxer enforcement. Because the certification procedure is centralized and uniform across the boundary, the gap is unlikely to reflect differential treatment of the two sides; instead, it is consistent with high-tag-side properties entering delinquency with larger or longer-standing unpaid balances, given their lower overall compliance across years.

P House Prices and Property Tax: Evidence from Property Listings

As we discuss in section 2.5, capitalization of the property tax into house prices may dampen the inequity taxpayers feel when making tax compliance decisions. In Section 3.3.2 and Appendix H, we introduce a modified model that allows households to select properties based on their preferences, which includes a consideration of tax differences and a distaste for tax inequities. This model suggests that, beyond compliance elasticities, a critical sufficient statistic for assessing welfare and shaping optimal policy is $\kappa \equiv -\partial p_{L\phi}/\partial T_{\phi}$. This parameter represents the degree to which property taxes are reflected in house prices. In this appendix, we empirically explore the extent of this tax capitalization.

We gathered data on housing market asking prices by scraping the online real estate platform Viva Real, collecting details such as addresses and property features (e.g., number of rooms). Figure P.1 shows an example of a property listing. It is one of the minority of 43% that do include a value for the IPTU, suggesting that the IPTU is of only modest salience when people search for houses to buy.

To merge the market prices from Viva Real with our administrative data, research assistants manually overlaid SEFAZ's geographic map of Manaus onto Google Maps addresses. Through manual inspection, the RAs matched properties between the two sources and rated their confidence in each match. This exercise yielded a dataset comprising 2,553 properties, with asking prices, tax liabilities, and other attributes. Nearly 43% of the observations included information on the IPTU for the listed property. Figure P.2 presents a scatter plot of log tax liability against log asking price for these properties, indicating that assessed property values serve only as an approximate proxy for actual market values.

To investigate the extent to which property taxes are capitalized into house prices, we perform two exercises. First, using the properties where the match was classified as "confident" by the RAs, we estimated the following equation:

$$\log(p)_i = e_\kappa \tau_i + \beta X_i + \varepsilon_i \tag{P.1}$$

where $\log(p)_i$ is the log of the asking market price for property i, τ_i is the log of tax liability, X_i are several characteristics of the property collected, and ε_i is the residual. We estimated this equation using a double-selection lasso linear regression. Our coefficient of interest is $e_\kappa = \kappa \frac{T_i}{p_i}$, the elasticity of the asking price with respect to the tax liability.

Next, we used a boundary discontinuity design akin to section 4.1. Specifically, we estimated the equation

$$y_i = \gamma_{b(i)} + f(d_i) + \beta_0 HTS_i + h(d_i) \times HTS_i + \varepsilon_i \tag{P.2}$$

where $\gamma_{b(i)}$ are boundary fixed effects, HTS_i is an indicator for being on the high-tag side of the boundary ($d_i > 0$); $f(d_i)$ and $h(d_i)$ control for distance to the boundary on the low- and high-tag sides of the boundary, respectively; and ε_i is the residual. The outcome variable, y_i, is the log of tax liability for property i in the first stage, and the log of the asking market price for property i in the reduced form. Both stages are estimated using local linear controls for distance, the same MSE minimizing bandwidth, and triangular weighting kernels (Calonico *et al.*, 2014, 2020).

The results of both exercises are displayed in table P.1. The results show no evidence of any meaningful capitalization of the propety tax into listing prices.

FIGURE P.1: EXAMPLE OF A VIVA REAL LISTING

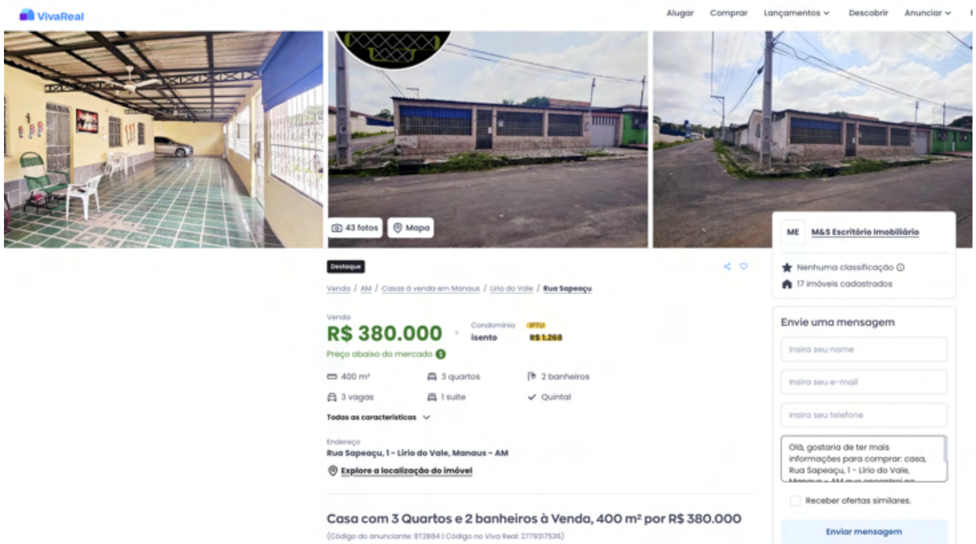

Notes: This is an example of a listing for a house sale on Viva Real, with the listed IPTU highlighted in yellow.

FIGURE P.2: DISTRIBUTION OF LOG LIABILITY AND LOG ASKING PRICE

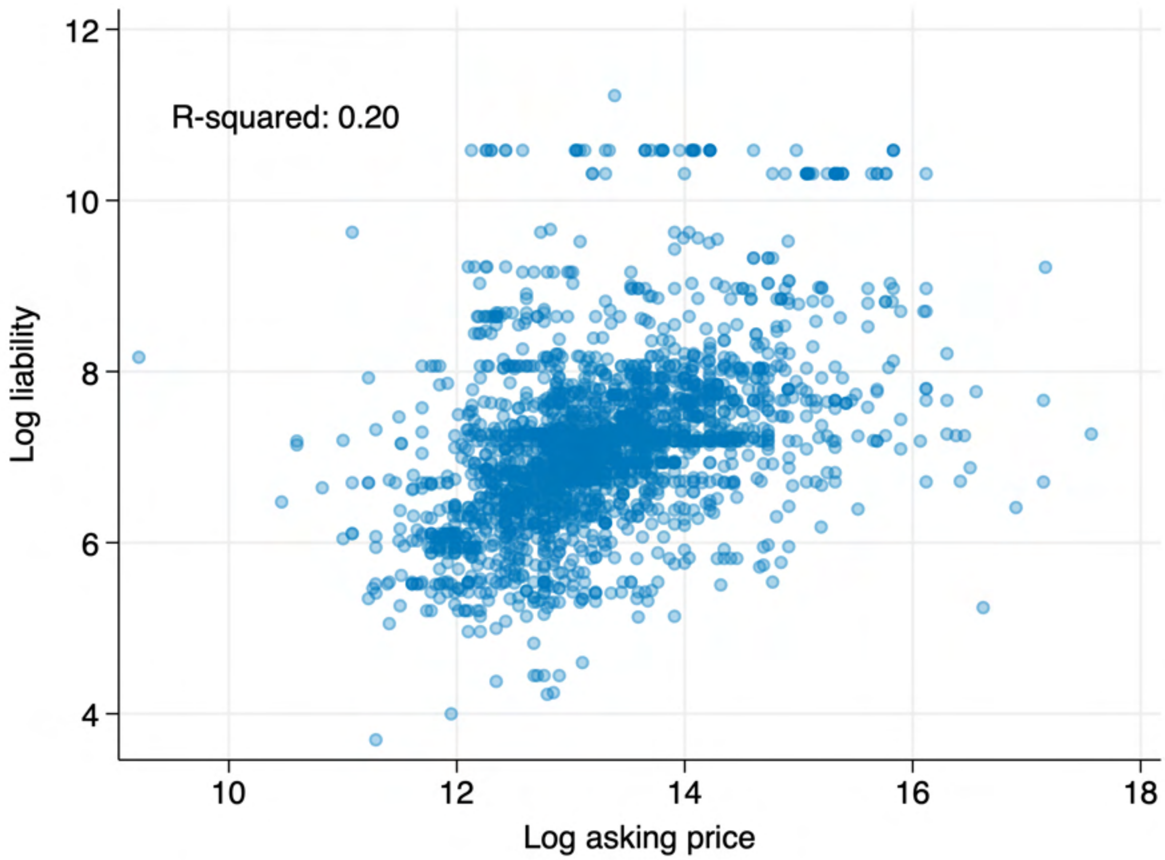

Notes: The figure shows the scatter plot of the log liability and the log asking price. We gathered data on housing market asking prices by scraping the online real estate platform Viva Real, collecting details such as addresses. To integrate these market prices with our administrative data, research assistants overlaid SEFAZ's geographic map of Manaus onto Google Maps addresses and matched properties between the two sources. This exercise yielded a dataset comprising 2,553 properties, with asking prices, tax liabilities, and other attributes.

TABLE P.1: HOUSING PRICE RESPONSE TO PROPERTY TAXES

	(1)	(2)
Elasticity estimate	0.04	-0.06
	(0.05)	(0.18)
Admin controls	✓	✗
VivaReal controls	✓	✗
RD specification	✗	✓
N	930	1014

Notes: The table shows estimates of the elasticity of the asking price of properties with respect to the tax liability. Column (1) shows the results of estimating equation (P.1): $\log(P)_i = e_\kappa \tau_i + \beta X_i + \varepsilon_i$ where $\log(p)_i$ is the log of the asking market price for property i, τ_i is the log of tax liability, X_i are several characteristics of the property collected, and ε_i is the residual. Column (2) shows the implied elasticity from estimating the first stage and the reduced form from equation (P.2): $y_i = \gamma_{b(i)} + f(d_i) + \beta_0 HTS_i + h(d_i) \times HTS_i + \varepsilon_i$ where $\gamma_{b(i)}$ are boundary fixed effects, HTS_i is an indicator for being on the high-tag side of the boundary ($d_i > 0$); $f(d_i)$ and $h(d_i)$ control for distance to the boundary on the low- and high-tag sides of the boundary, respectively; and ε_i is the residual. The outcome variable, y_i, is the log of tax liability for property i in the first stage, and the log of the asking market price for property i in the reduced form.

Q Information on Historical Property Sales Using ITBI Data

While data from listings on the Viva Real platform (see appendix P) can shed light on house prices in recent years, we are not able to use it to study historical property sales. To look at property sales since 2007, we use data provided by SEMEF on the land transaction tax (ITBI: *Imposto sobre a Transmissão de Bens Imóveis*). This tax is imposed on all land sales in the municipality, with the buyer of the property required to pay a bill equal to two percent of the property's value. The ITBI must be paid to the municipal government before the sale can be finalized and registered at a notary's office. Given this legal requirement of the sale, the ITBI data provides the universe of property transactions for the years 2007-2020, with 101,867 transactions.[68]

The ITBI data is useful to understand the number of property sales over time, but not necessarily the implied market value for a given property. This is because the "property value" used to calculate the ITBI bill is not entirely straightforward. Legally the ITBI is calculated as two percent of the *max(market value, sales price)* for a given property. This is to ensure the parties do not have an incentive to significantly under-report the sales price to avoid a larger tax bill. However, discussions with SEMEF detailed that the "market value" is based on an evaluation of the property by SEMEF, and does not follow a presumptive formula similar to the IPTU.

Despite this drawback, we can use the ITBI data to see if there was any first-order effects of tax changes brought on by the 2011 reform on mobility–that is, people selling their houses to move to a lower tax sector. Figure Q.1 plots the cumulative annual property sales in Manaus from 2007-2020. We do not see a spike in house sales around the implementation of the reform, rather property sales during the five years of the reform appear to be continuing the trend of year-over-year increases in property sales since 2007. While there is a subsequent decrease in housing sales to pre-2009 levels, this may be partially attributed to a discount on ITBI bills in the first half of 2015.[69] The lower housing sales in the years after 2015 may also be partly attributed to the effects of the 2014-2016 economic crisis, which was one of the largest recessions in Brazilian economic history, with GDP shrinking by over 3.5% in both 2015 and 2016.

[68] Note that these observations do not necessarily represent unique properties, as it is possible for a given property to be sold multiple times during this period.

[69] Law 1956/2014 provided for a discount of up to 50% on ITBI payments and was passed in December 2014 and valid for 180 days in the last year of Artur Neto's mayoral term. https://d24am.com/noticias/publicada-a-lei-que-concede-desconto-na-quitacao-do-itbi/

FIGURE Q.1: YEARLY PROPERTY SALES IN MANAUS, 2007-2020

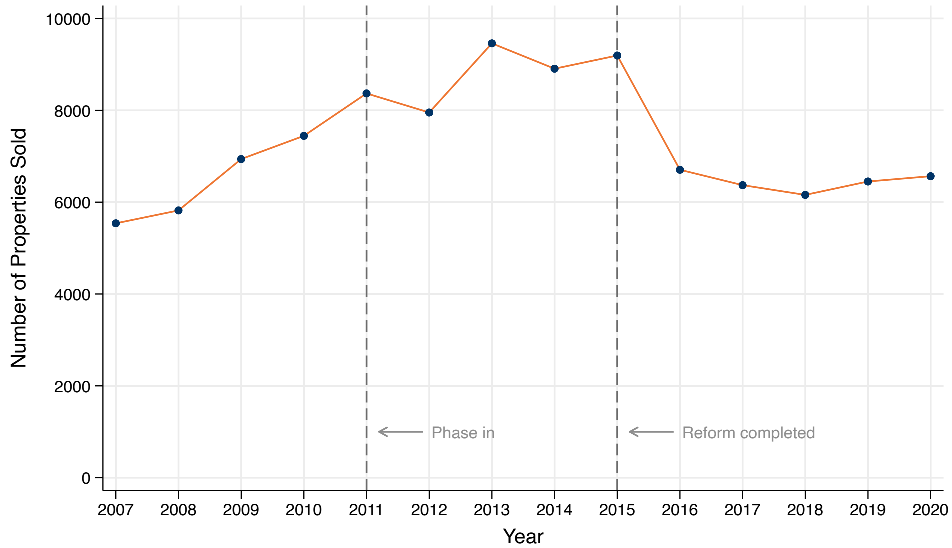

To see whether there is a differential impact on housing sales based on tagging, we replicate the results equation (10), with the outcome variable of interest being whether property i was sold in year y. In particular, we are interested in observing whether there are any direct first-order effects from tax changes ($\Delta\tau$). Figure Q.2 shows the results separately for over-tagged and under-tagged properties. We find little to no evidence that increasing tax burdens led to increases in the likelihood of selling a house after the 2011 reform.

FIGURE Q.2: DIFFERENCE IN DIFFERENCE ESTIMATES OF TAX CHANGES ON HOUSE SALES

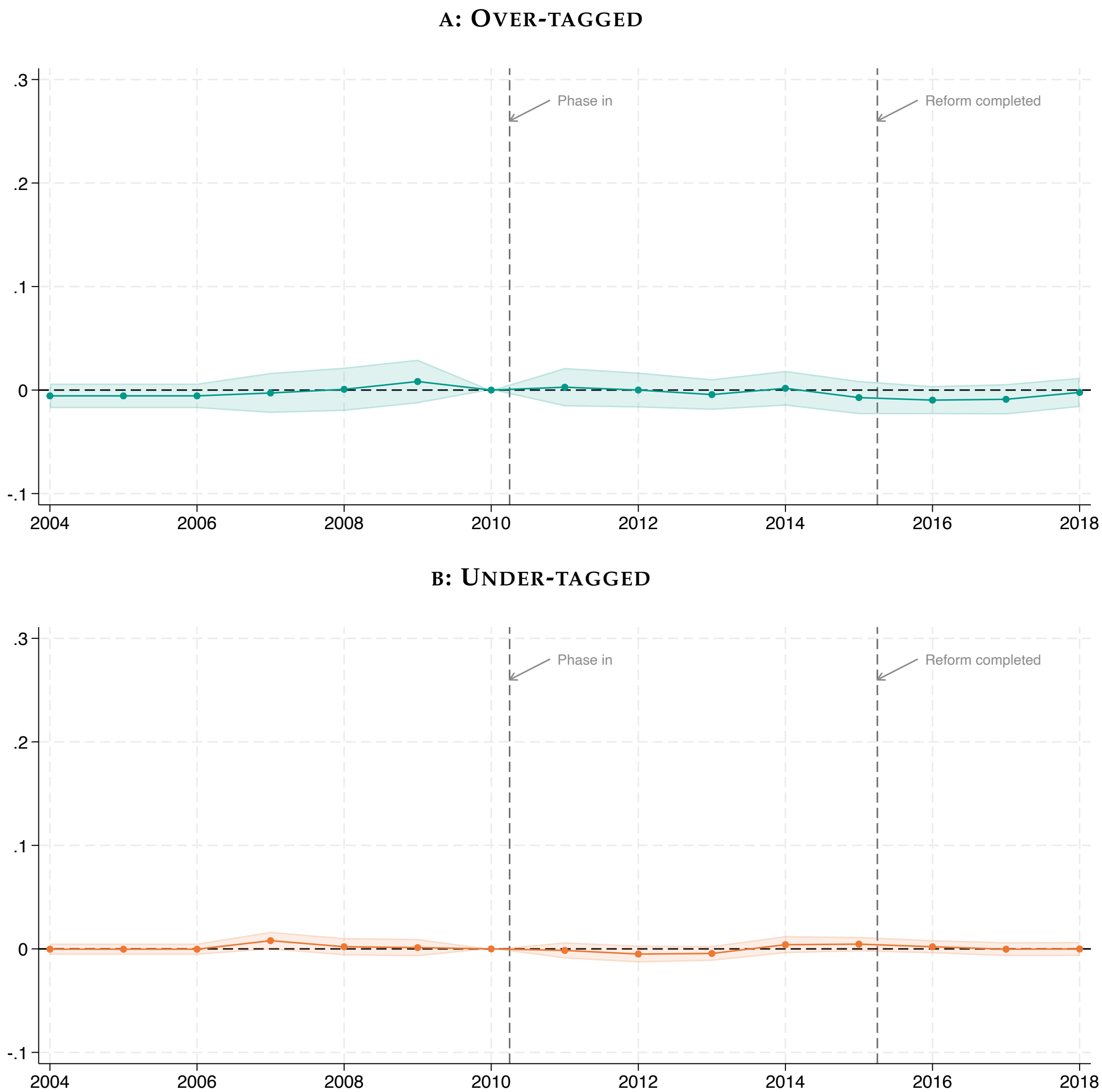

Notes: The figure shows the results of the estimation of equation (10) as discussed in section 5.3, with an indicator for whether property i was sold in year y as the outcomes variable. The coefficients of interest relate to the direct effect of tax increases ($\Delta\tau$) before and after the 2011 reform. Panel A shows the estimated $\eta_{0j} + \eta_{1j}$ coefficients along with their 95% confidence intervals. Panel B shows the estimated η_{0j} coefficients along with their 95% confidence intervals.

R Optimal Tax Simulations

This appendix performs a series of simulations of our conceptual framework in section 3. We use the optimal tax expressions from the model with both under- and over-tagging in appendix G and set the extent of under- and over-tagging equal, but the response to inequity from the undertagged equal to zero, consistent with our empirical results. To calibrate the model, we need to make a parametric assumption about compliance rates. In particular, we will assume that compliance takes the iso-elastic form

$$c_{\theta\phi} = c_0 \left(\frac{T_\phi}{y_\theta}\right)^{-\varepsilon} \sigma^{-\eta} \tag{R.1}$$

R.1 Share of Overall Response from Inequity

As discussed in section 6, the model can be used to study the implications for tax policy of different decompositions of the overall compliance response at the tax sector boundaries into the part that comes from responses to inequity and the part that comes from responses to the tax liability. Figure 8 shows the results of that calibration.

Here, we also study how the optimal tax schedule's progressivity varies with the share of the overall response due to inequity as we make different assumptions about welfare weights. To do this, we hold the welfare weight on the occupants of low-value houses, g_L, fixed and vary the ratio g_L/g_H between 1.4 and 1.8. For each of these, in Figure R.1, we report the progressivity of the optimal tax schedule with our baseline estimate of the share of the overall response due to inequity (42%) relative to the progressivity of the optimal tax schedule with no responses to inequity. Our baseline calibration suggests that the progressivity at our baseline estimates is 61% of the progressivity absent inequity responses. This ratio ranges from 58% when $g_L/g_H = 1.8$ to 65% when $g_L/g_H = 1.4$, suggesting that this result is quite insensitive to the strength of redistributive preferences used.

R.2 Comparative Statics

The model that we simulate has a number of parameters. Table R.1 lists the parameters, what they are, and the values we set them to. The table also displays the range of the parameters over which we perform comparative statics. For the social marginal welfare weights, our comparative statics exercises hold the average social marginal weight fixed at its baseline value $\frac{1}{2}\left(0.5 + \frac{0.5}{1.6}\right)$, and then vary the ratio of the social marginal welfare weights g_L/g_H between 1.4 and 1.8. Similarly when studying inequality we hold the average property value fixed at its baseline value $\frac{1}{2}(6,630.8 + 4,911.5)$ and vary the ratio y_H/y_L between 1.25 and 1.45. Figure R.2 shows the results of these comparative statics exercises. The figures confirm the comparative statics highlighted in proposition 2 and add new comparative statics also.

The model in Appendix G also permits differential mistagging (undertagging $\psi_{Hl} \neq$ overtagging ψ_{Lh}) and differential behavioral responses to inequity (elasticity wrt undertagging $\eta_{Hl} \neq$ elasticity wrt overtagging η_{Lh}). In our baseline simulations we set $\psi_{Hl} = \psi_{Lh} = 0.05$ and $\eta_{Hl} = 0$. Here we reintroduce these forces. First, in panel A of figure R.3, we hold fixed the extent of mistagging of both house types $\psi_{Lh} = \psi_{Lh} = 0.05$ and the strength of the behavioral response to overtagging $\eta_{Lh} = 0.11$ and vary the strength of the behavioral response to undertagging $\eta_{Hl} \in [-0.05, 0.15]$. In Panel B we hold fixed the strength of the behavioral response to mistagging $\eta_{Lh} = \eta_{Hl} = 0.11$ and the extent of overtagging $\psi_{Lh} = 0.05$ and vary the extent of undertagging $\psi_{Hl} \in [0, 0.15]$. Panel A shows that the progressivity of the tax schedule changes only marginally across the range of η_{Hl} values considered. In panel B progressivity is decreasing in the fraction of undertagged households ψ_{Hl}, though not dramatically so.

R.3 Location Choice and Endogenous House Prices

We now turn to simulating the optimal tax schedule in the extended model that allows for location choice and endogenous house prices discussed in section 3.3.2 and Appendix H. The key additional sufficient statistic is now $\kappa \equiv -dp_{\theta\phi}/dT_{\phi}$. Our analysis in Appendix P finds no evidence in support of a non-zero value for κ, but nevertheless we consider a range of values for κ between -0.15 and 0.15. Figure R.4 shows the results, suggesting that one needs to see quite substantial amounts of capitalization before the progressivity of the tax schedule is very much affected.

A second set of additional statistics concern how the composition of taxpayers resulting from their mobility affects their responsiveness to taxation. In figure R.5, we vary these impacts (governed by the statistics $\mu_{\phi\phi'}$, where ϕ is the tax whose compliance elasticity is affected by changes in the tax ϕ'). The results suggest that the progressivity of the tax schedule is not particularly sensitive to the $\mu_{h\phi'}$ elasticities. Rather, the elasticities that have some bearing are μ_{ll} and μ_{lh}. These elasticities govern the extent to which changes in taxes reduce compliance in the l-tag areas through mobility responses. These occur for two reasons. First, compliant taxpayers may leave the l-tag area; and second, non-compliant taxpayers may move to the l-tag area. When these happen due to increases in T_h (which would increase progressivity), this increases the efficiency cost of differentiating between the H and the L types, pushing towards less progressivity. When these happen due to increases in T_l, they reduce the burden of the l-tag tax since fewer households pay it, strengthening the case for progressivity. However, these effects would need to be quite strong to have meaningful impacts on our conclusions.

Table R.1: Baseline Model Parameters

	Parameter	Value	Justification	Simulation Range
ε	Elasticity of compliance wrt tax liability	0.2	consistency with reduced form: $-\frac{dc}{c} = \varepsilon\frac{dT}{T} + \eta\frac{d\sigma}{\sigma}$ and $\hat{\eta} = 0.11$	0.12 – 0.38
$\eta = \eta_{Hl}$	Elasticity of compliance wrt inequity	0.11	Dynamic boundary discontinuity design	0 – 0.2
η_{Lh}	Elasticity of undertagged compliance wrt inequity	0	Difference in Differences Design	
ψ_{Lh}	Fraction of L types with h tag	0.05	$\sim 10\%$ of properties are near boundaries	0 – 0.15
ψ_{Hl}	Fraction of H types with l tag	0.05	$\sim 10\%$ of properties are near boundaries	
ρ	Coefficient of relative risk aversion	2	Standard in literature (Elminejad *et al.*, 2025)	1.5 – 4
λ	marginal value of public good $b(r)$	1	Normalization	
g_H	marginal social welfare weight: $g_H \equiv \omega_H u'(y_H)/b(r)$	$0.5/1.6$	baseline	$g_L/g_H \in [1.4, 1.8]$
g_L	marginal social welfare weight: $g_L \equiv \omega_L u'(y_L)/b(r)$	0.5	baseline	
y_H	value from high-value house	6,630.8	$E[T\|LTS] = 172.4$ and 2.6% of income	$y_H/y_L \in [1.25, 1.45]$
y_L	value from high-value house	4,911.5	$E[T\|HTS] = 127.7$ and 2.6% of income	
c_0	coefficient in compliance equation (R.1)	0.339	Make baseline compliance of 0.7 consistent with y_H, y_L, baseline taxes and equation (R.1).	

FIGURE R.1: INEQUITY AND PROGRESSIVITY UNDER DIFFERENT REDISTRIBUTIVE PREFERENCES

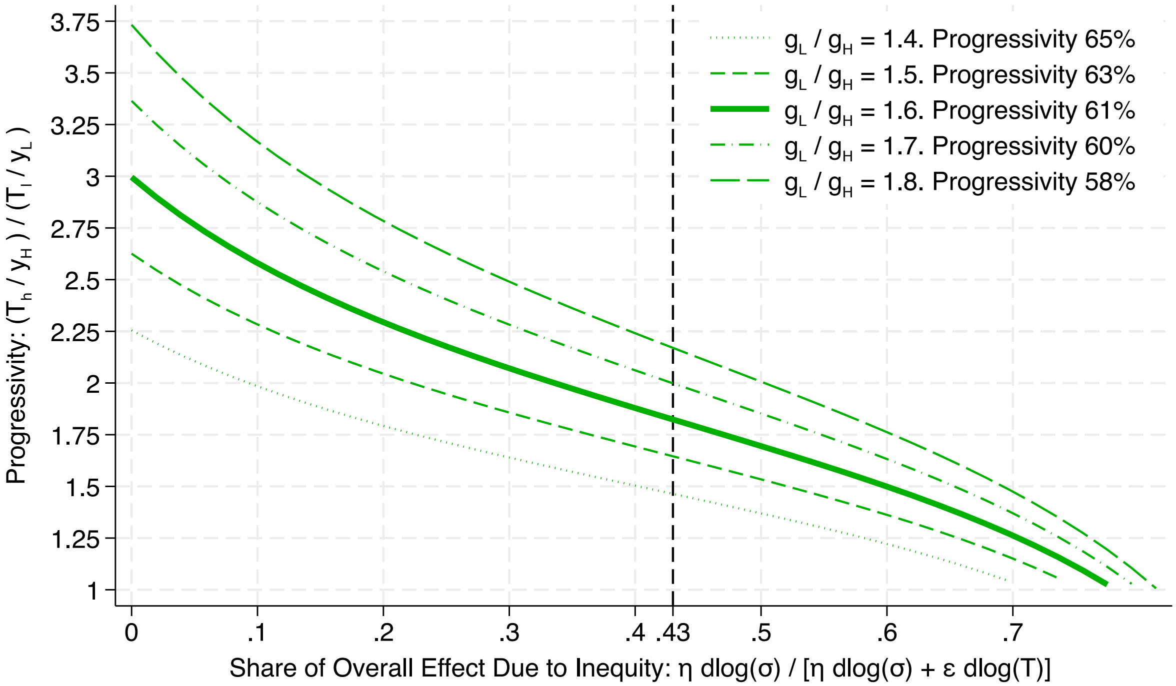

Notes: The figure shows the progressivity of the optimal tax schedule in proposition 2 as a function of the share of the overall response at the tax sector boundaries that is driven by responses to inequity. Each line is drawn for a different strength of redistributive preferences g_L/g_H between 1.4 and 1.8 (our baseline value is 1.6). For each simulation, we compute the progressivity of the tax schedule at our baseline estimates (which suggest that inequity responses account for 42% of the overall response) relative to the progressivity of the optimal tax schedule absent inequity responses.

FIGURE R.2: SIMULATIONS OF BASELINE MODEL COMPARATIVE STATICS

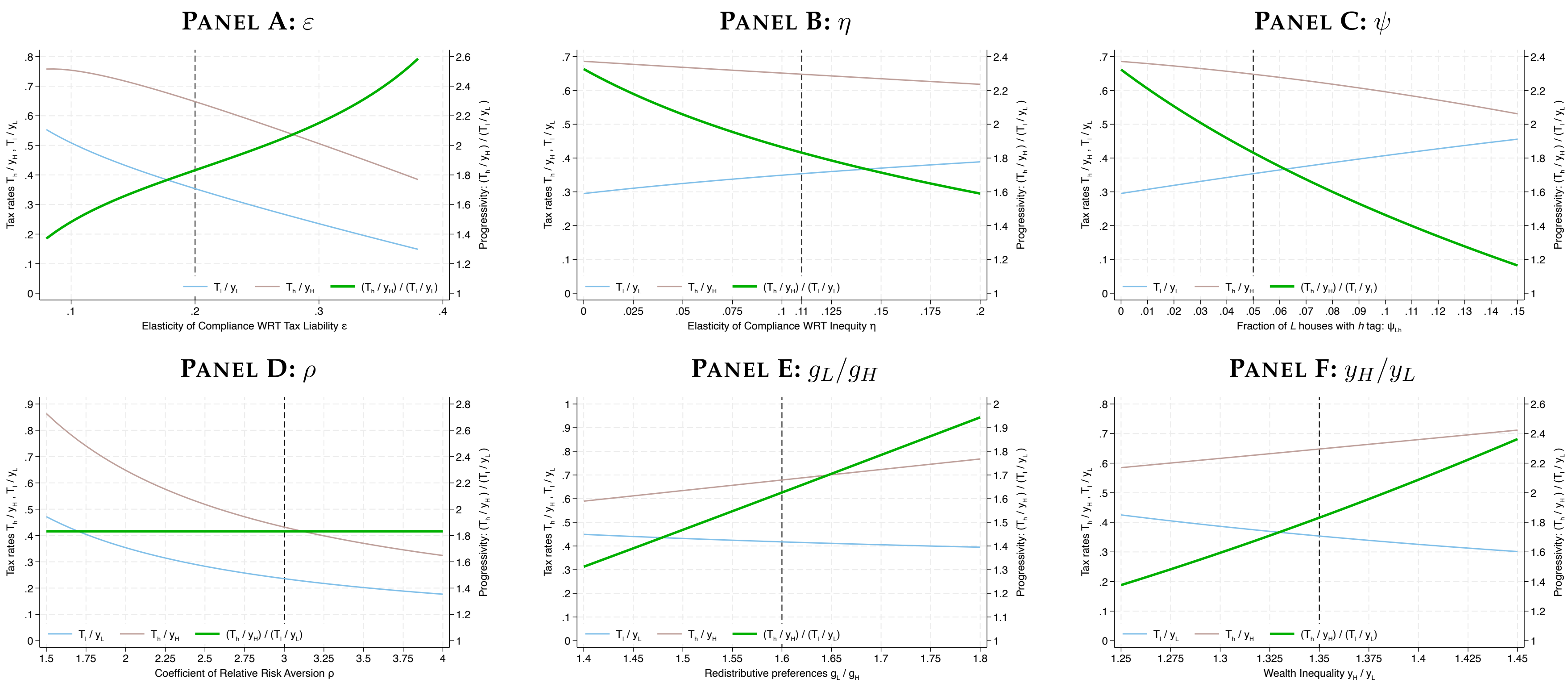

FIGURE R.3: OPTIMAL TAX SCHEDULE WITH MISTAGGING OF BOTH HOUSE TYPES

PANEL A: BEHAVIORAL RESPONSE TO UNDERTAGGING: η_{Hl}

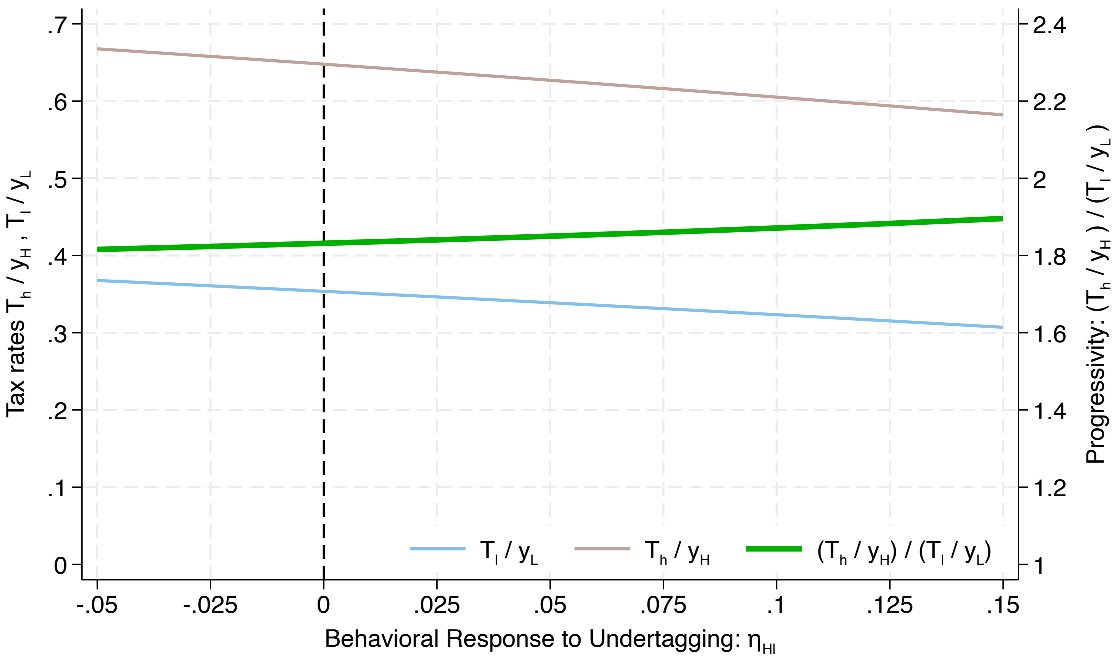

PANEL B: EXTENT OF UNDERTAGGING: ψ_{Hl}

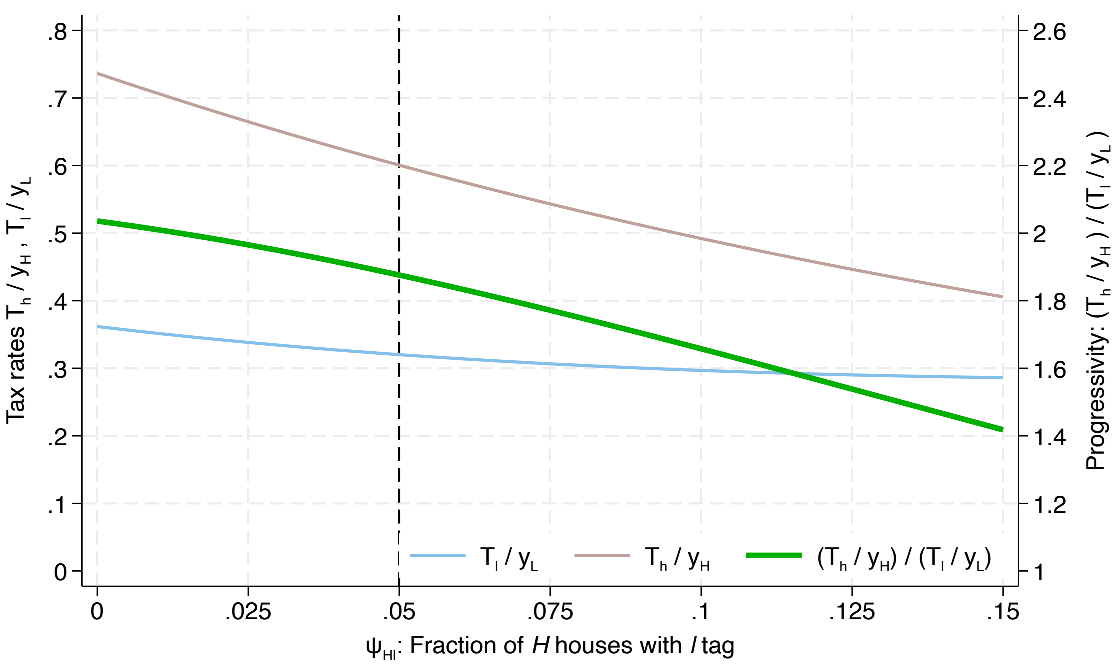

Notes: The figure shows the optimal tax schedule in the extended model allowing for mistagging of both types of households, discussed in section 3.3.1 and Appendix G. In Panel A we hold fixed the extent of mistagging of both house types $\psi_{Lh} = \psi_{Lh} = 0.05$ and the strength of the behavioral response to overtagging $\eta_{Lh} = 0.11$ and vary the strength of the behavioral response to undertagging $\eta_{Hl} \in [-0.05, 0.15]$. In Panel B we hold fixed the strength of the behavioral response to mistagging $\eta_{Lh} = \eta_{Hl} = 0.11$ and the extent of overtagging $\psi_{Lh} = 0.05$ and vary the extent of undertagging $\psi_{Hl} \in [0, 0.15]$.

FIGURE R.4: OPTIMAL TAX SCHEDULE WITH ENDOGENOUS HOUSE PRICES

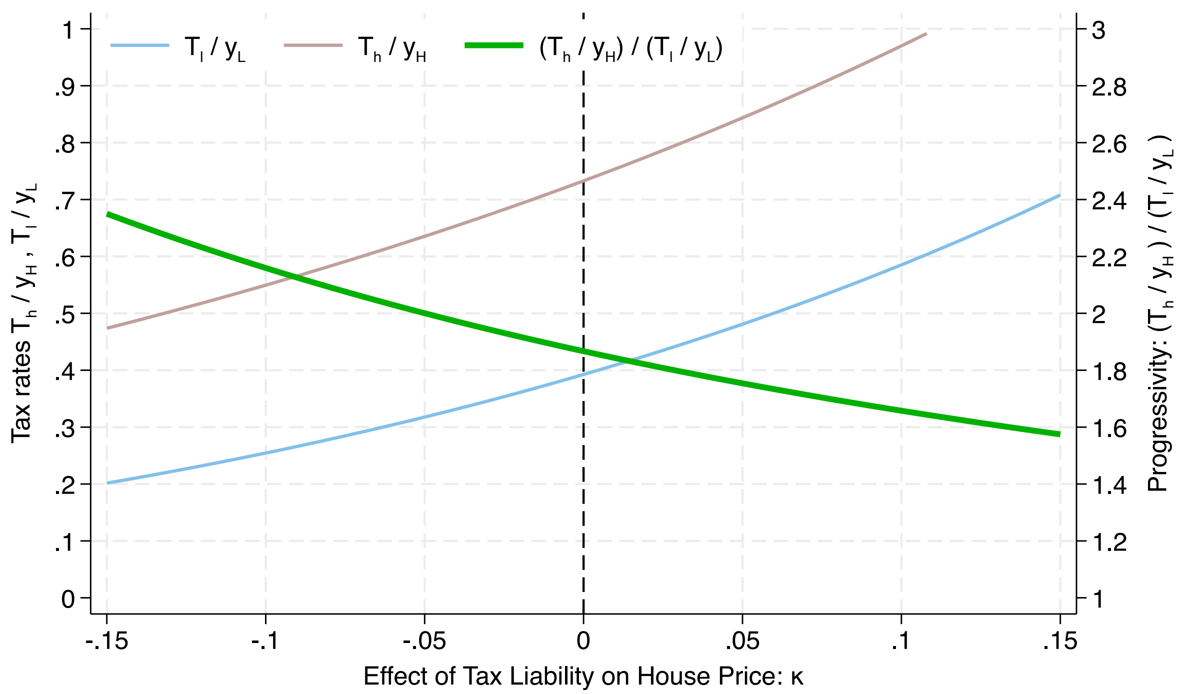

Notes: The figure shows the optimal tax schedule in the extended model allowing for location choices and endogenous house prices, discussed in section 3.3.2 and Appendix H. We vary the responsiveness of house prices to property taxes $\kappa = -dp_{\theta\phi}/dT_\phi$ between -0.15 and 0.15.

Figure R.5: Optimal Tax Schedule with Composition Effects on Responsiveness

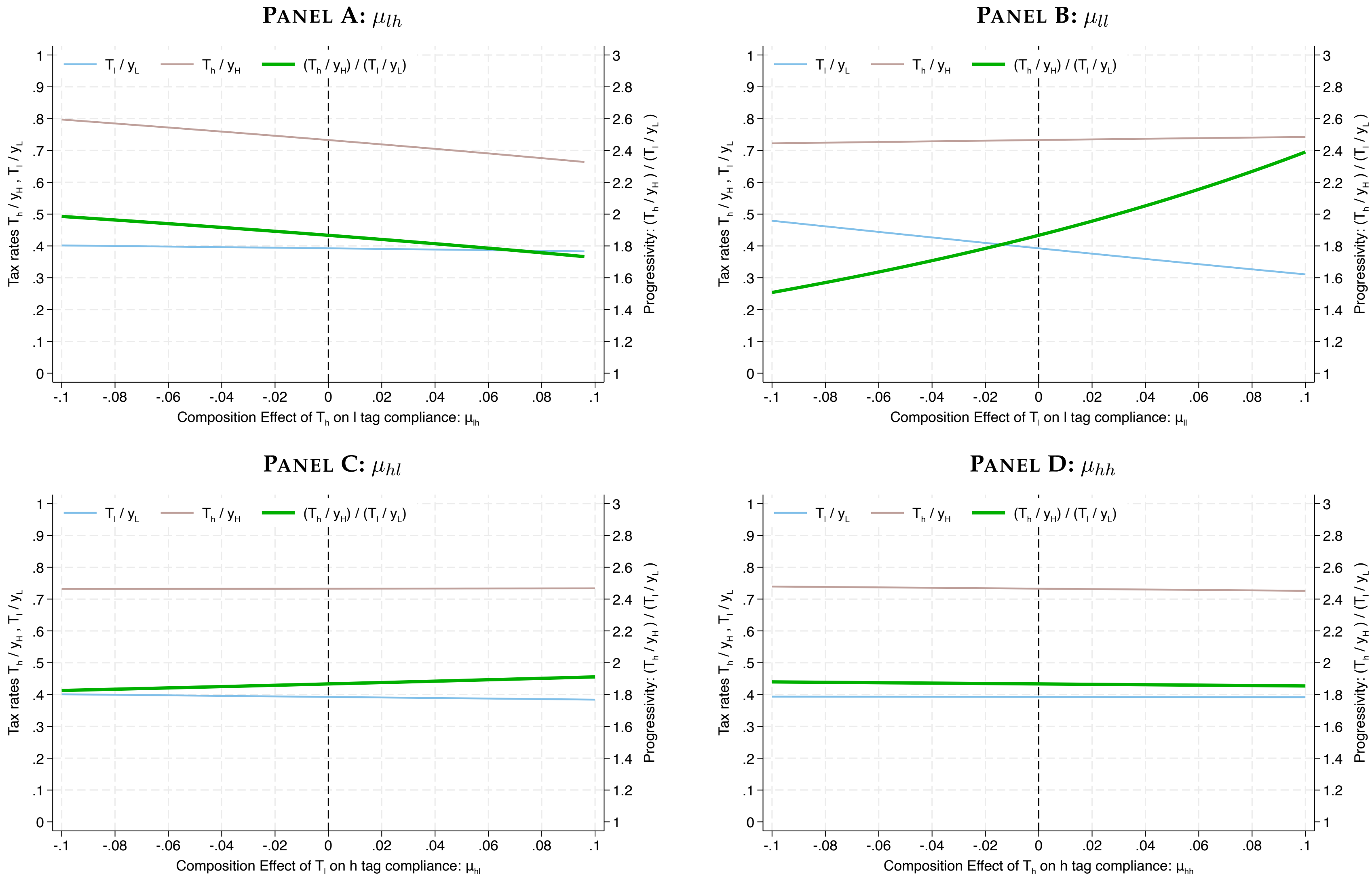

Notes: The figure shows the optimal tax schedule in the extended model allowing for location choices and endogenous house prices, discussed in section 3.3.2 and Appendix H. We vary the impact of composition effects on the responsiveness of compliance to property taxes $\mu_{\phi\phi'}$ (where ϕ is compliance by properties facing tax ϕ and ϕ' is the tax being varied) between -0.1 and 0.1.

S Fiscal Capacity Counterfactuals

As discussed in Section 6, the finding that taxpayers respond strongly to inequities in the tax schedule implies substantial returns to investments in fiscal capacity—specifically, the ability to differentiate between high- and low-value properties. In this appendix, we use data on housing market asking prices from the online real estate platform Viva Real to quantify the potential gains from three counterfactual improvements in the property assessment system that would enable more accurate valuations.

As a benchmark, we first measure the implied assessed market price from the current presumptive formula, highlighting that assessed values often diverge substantially from market asking prices. We then consider three counterfactual improvements to the assessment system. First, we recalibrate the coefficients in the existing tax formula using the asking price data. Second, we evaluate a more flexible estimation of assessed values based on the same set of attributes currently used in the presumptive formula. Third, we assess the gains from incorporating additional property characteristics available in the Viva Real data but not presently observed by the tax authority.

We collected data on housing market asking prices by scraping the online real estate platform Viva Real, which includes property addresses and physical characteristics (the complete list of characteristics can be read in table S.1). To link this data to the administrative tax records, research assistants manually georeferenced properties by overlaying SEFAZ's cadastral maps onto Google Maps and matching properties across the two sources. This process yielded 2,553 properties with matched asking prices, tax liabilities, and physical attributes. To ensure consistency across counterfactual exercises, we restrict the sample to the 1,659 properties with complete information in both the administrative cadaster and the Viva Real dataset.

As a benchmark, we compute the implied assessed market value for each property based on its tax liability. Since all properties in our sample are subject to a uniform tax rate of 0.9%, the assessed market value, $\hat{y}_i$, is given by

$$\hat{y}_i = \frac{T_i}{0.009} = \left[b_i + p_{s(i)} a_i\right]$$

where T_i is the tax liability for property i, b_i is the assessed building value, a_i is the land value, and $p_{s(i)}$ is the sector-specific price per unit of land. To evaluate the prediction accuracy of the assessed market value, we calculate the mean squared error (MSE) between $\hat{p}_i$ and the observed asking price y_i, the root mean squared error (RMSE), and the mean absolute error (MAE). Table S.3 shows the corresponding results. Given that the average asking price is 856,322.34, the RMSE and the MAE are quite large, which imply that the current formula frequently mistakes the market price.

We next evaluate how recalibrating the coefficients in the existing property tax formula improves prediction accuracy relative to market prices. The presumptive tax formula can be expressed as a nonlinear function of property characteristics and administrative coefficients. Specifically, note that the assessed market value of property i is given by

$$a_i = \text{land area}_i \times \text{share constructed}_i \prod_{A_j \in A} \alpha_j^{1[A_j]_i}$$

where while $A_j \in A$ denote binary attributes with associated coefficients α_j. For example, consider a property with 100 square meters of land, of which 50 percent is constructed. Suppose the property is located on a corner ($A_1 = 1$ with $\alpha_1 = 1.1$), has flat topography ($A_7 = 0$ with

$\alpha_7 = 1$), and normal pedology ($A_{11} = 1$ with $\alpha_{11} = 1$). The assessed land value in this case is given by $10000 \times 0.5 \times 1.1 = 5500$.

Similarly, both the sector-specific land price $p_{s(i)}$ and the assessed building value are determined as functions of binary property attributes with associated coefficients. In total, the presumptive formula contains 371 coefficients, which are estimable with sufficiently data. Given our limited sample from Viva Real, we estimate 51 of the coefficients from the presumptive using nonlinear least squares estimation. The remaining coefficients correspond to attributes that are either universally zero in the sample or exhibit insufficient variation (e.g., sectors with a single observation), in which case we aggregate them with related categories where appropriate. Using the recalibrated formula, we predict the associated asking prices. The results show that, relative to the current formula, we are able to improve the MSE, the RMSE and the MAE by 35%, 20%, and 28% respectively.

We next evaluate how much the government could improve assessment accuracy using a more flexible, yet readily implementable, prediction model. Specifically, we estimate a random forest model to predict asking prices based on the same set of property attributes used in the presumptive property tax formula. We conduct a grid search over hyperparameters—the number of features considered at each split and the number of trees in the forest—and select the combination that minimizes the out-of-bag (OOB) mean squared error (MSE). Model performance is evaluated by predicting asking prices and computing the same accuracy measures used in previous exercises. As shown in Table S.3, the random forest achieves substantial improvements relative to the current presumptive formula: MSE declines by 66 percent, RMSE by 41 percent, and MAE by 52 percent.

Finally, we analyze what would be the benefits of also incorporating additional property attributes available in the Viva Real data but not in the cadaster. We repeat the same exercise to train the random forest model and we use it to predict the asking prices. The results highlight the large returns to investing in fiscal capacity. Relative to the current presumptive formula, we are able to improve the MSE, the RMSE and the MAE by 93%, 74%, and 83% respectively.

TABLE S.1: PROPERTY ATTRIBUTES AVAILABLE IN THE VIVA REAL DATA BUT NOT IN THE CADASTER

Property Attribute	Property Attribute	Property Attribute
24-hour concierge	Accessibility access	Acoustic insulation
Adult pool	Air conditioning	Alarm system
Aluminum windows	Aquarium	Armored guardhouse
Artesian well	Backyard	Balcony
Balcony barbecue	Bar	Barbecue area
Bathtub	Beauty center	Bicycle parking
Breakfast nook	Breakfast room	Built-in closets
Cable TV	Cafeteria	Caretaker's house
Children's playroom	Children's pool	Clay soil
Coffee shop	Concrete slab roof	Convention hall
Convertible extra room	Corner lot	Corral
Coworking space	Custom cabinetry	Deck
Decorative ceiling molding	Detached annex	Dining room
Digital lock	Drywall	East-facing

Continued on next page

Table S.1 – Continued from previous page

Property Attribute	Property Attribute	Property Attribute
Electricity	Elevated front lot	Electronic gate
Elevator	Enclosed glass balcony	Entrance hall
Entire floor	Fence	Fireplace
Flat lot	Freezer	Fruit trees
Furnished	Game room	Garage
Garden	Gas shower	Gated community
Glass shower enclosure	Gourmet area	Gourmet balcony
Gourmet kitchen	Gravel surface	Green area / Park
Guardhouse	Gym	Half bathroom
Half floor	Hammock area	Hardwood flooring
Heating system	High ceilings	Home theater
Indoor soccer court	Internet connection	Intercom
Jacuzzi	Japanese hot tub	Jogging track
Kennel	Kitchen	Kitchen cabinets
Lake view	Laminate flooring	Large kitchen
Large living room	Laundry room	Lawn
Library	Locker room	Maid's quarters
Main house	Marina	Massage room
Meeting room	Mezzanine	Multi-sport court
Natural ventilation	North-facing	Number of bathrooms
Number of rooms	Ocean view	Office
Open-concept layout	Open-plan kitchen	Orchard
Panoramic view	Pantry	Parking
Party room	Partition walls	Paved street
Pay-per-use services	Pet area	Pets allowed
Piped gas	Pizza oven	Playground
Plaza	Poolside bar	Porcelain tile flooring
Private pool	Ramp	Rear house
Reception	Recreation area	Recycling collection
Reflecting pools	Restaurant	River view
Sand court	Sandy soil	Sauna
Security cameras	Security guard	Security patrol
Security system	Service bathroom	Service entrance
Service room	Shared rooftop terrace	Side entrance
Skate park	Sloping rear lot	Small living room
Soccer field	South-facing	Spa
Squash court	Staircase	Staff changing room
Storage room	Stove	Sun deck
Swimming pool	Teen lounge	Tennis court
Thermal insulation	Tile flooring	Tree-top adventure course
Truck access	Utility area	Vegetable garden
Visitor parking	Vinyl flooring	Walk-in closet
Wall and fence	Water and sewer connection	Water reservoir
Well	West-facing	Zen space

TABLE S.2: PREDICTION ACCURACY ACROSS MODELS

TABLE S.3: PREDICTION ACCURACY ACROSS MODELS

Model	**Accuracy Measure**	**Prediction Error**
Current presumptive formula	MSE	1,853,381,610,800
Updated formula	MSE	1,196,531,776,658
Random forest	MSE	637,163,296,788
Random forest with additional attributes	MSE	122,630,026,334
Current presumptive formula	RMSE	1,361,390
Updated formula	RMSE	1,093,861
Random forest	RMSE	798,225
Random forest with additional attributes	RMSE	350,186
Current presumptive formula	MAE	735,637
Updated formula	MAE	532,152
Random forest	MAE	328,255
Random forest with additional attributes	MAE	126,342